NPo-forskning
fra Miljøstyrelsen

Nr. A10 1990

DAISY - Soil Plant Atmosphere System Model

Miljøministeriet **Miljøstyrelsen**

Danish Research Programme on Nitrogen, Phosphorus and Organic Matter (NPO)

The aim of the NPO Research Programme is to gather knowledge on the decomposition of Nitrogen (N), Phosporus (P) and organic matter (o) in the soil, and on their impact on lakes, watercourses, inlets, groundwater and the sea.

This report is one of a total of about 50 reports to be issued in connection with the implementation of the NPO Research Programme. The National Agency of Environmental Protection (NAEP) is responsible for the programme, under which about 70 NPO projects have been launched, carried out at 25-30 institutions.

In the 1970's and the beginning of the 1980's there was a growing awareness of the threats to life in watercourses etc. presented by discharges of nutrients – and of the risk of nitrate contamination of groundwater. In 1984 a report was prepared, synthesising existing knowledge in this field. The report, known by the name of NPO Report, was published by the NAEP.

To follow up this report the Dansih Parliament took the first steps in 1985 to reduce pollution with nutrients – laying down requirements for storage and application of farm yard manure in the agricultural sector.

For the purpose of improving our knowledge on the impact of nutrients in nature, the Danish Parliament also reserved 50 million DKK for the research programme, running from 1985 to the end of 1990.

The significance of the NPO Research Programme was further underlined with the Danish Parliament's adoption of the Action Plan on the Aquatic Environment in 1987. The results of the NPO Research Programme will play a vital role in the evaluation of the effects of the Action Plan.

To safeguard the technical and economic interests relating to the research activities a steering group was set up, having the overall responsibility for the implementation of the NPO Research Programme. Furthermore, three coordination groups were formed, each of them responsible for one of the three fields: soil and air, groundwater, and surface water.

The reports are published in the series »NPo-forskning fra Miljøstyrelsen« (NPo Research in the NAEP), divided into three sections:

A: reports on soil and air
B: reports on groundwater
C: reports on watercourses, lakes and marine waters.

The NAEP has been secretariat for the research programme. The reports published in this series are edited by the Agency with the assistance of the coordination groups.

NPo-forskning fra Miljøstyrelsen
Nr. A10 1990

DAISY - Soil Plant Atmosphere System Model

Søren Hansen, Henry E. Jensen, Niels Erik Nielsen og Henrik Svendsen

The Royal Veterinary and Agricultural University

Miljøministeriet
Miljøstyrelsen

This project is partly financed
through the European Communities'
Environmental Research Programme
by participation in the project
EV-4V-0098 »Nitrate in Soils«.

CONTENTS

PREFACE

The present research report contains the result of a research project performed at the Section of Soil and Water and Plant Nutrition, Department of Agricultural Sciences, The Royal Veterinary and Agricultural University, Copenhagen. The research project has been performed within the framework of the Danish NPO Research Programme conducted by the National Agency of Environmental Protection.

The main objective of the research project has been to develop a mathematical simulation model for the soil plant system to enable simulation of crop production, water dynamics, and nitrogen dynamics in crop production at various agricultural management practices and strategies. Thus the final result presented in this report represents an integration of substantial knowledge from various disciplines including soil science and crop science. Within the framework of the present project comprehensive literature reviews were performed by Ole Jensen and Herluf Nielsen who were temporarily associated to the research group. The result has been published in five minor research reports (Jensen, 1988 a, b, c, d; Nielsen, 1988).

The present work has involved cooperation with a number of research groups abroad as well as with several research groups performing related research projects within the Danish NPO Research Programme. Secretary functions during the course of the project were attended by Mrs. Marie Louise Langkjær and Mrs. Jette Youden who also carefully typed this report. The research project was financed in part by the National Agency of Environmental Protection and The Royal Veterinary and Agricultural University, Copenhagen. We greatly acknowledge all assistance received during the course of the project.

Copenhagen, July 1, 1990

S. Hansen, H.E. Jensen, N.E. Nielsen, H. Svendsen

SUMMARY

Objectives

The objectives of the present research project has been to develop and validate a mathematical model for simulation of crop production, soil water dynamics, and nitrogen dynamics in crop production at various agricultural management practices and strategies. The aim has been a comprehensive dynamic explanatory simulation model for the soil plant system. The particular processes considered include transformation and transport processes involving water, heat, carbon, and nitrogen. For some of the processes theories and mechanisms are well established while for other processes existing knowledge is limited. The various processes considered have been described and modelled in accordance with existing knowledge.

Hydrological processes

The hydrological processes considered in the model include snow accumulation and melting, interception of precipitation by the crop canopy, evaporation from crop and soil surfaces, infiltration, water uptake by plant roots, transpiration, and vertical movement of water in the soil profile. In the model snow melting is influenced by incident radiation, and soil and air temperatures. Interception is determined either by precipitation or by the crop canopy. Description of evapotranspiration is based on a climatical determined potential evapotranspiration and the availability of water. Modelling of water uptake by plant roots is based on a quasi steady state solution of the differential equation for radial water flow to the root surfaces, and the plant root density in the soil profile. The vertical movement of water in the soil profile is modelled by means of a nummerical solution of the Richards equation.

Soil temperature

Soil temperature is modelled by solving the heat flow equation taking into account heat transfer by conduction and convection, and changes in heat content by freezing and melting processes. The freezing process induces water flow in the soil as ice formation is assumed to take place in the large soil

pores extracting water from small soil pores resulting in water flow towards the freezing zone.

Organic matter pools

Organic matter turnover is modelled by dividing the organic matter conceptually into three main pools viz. added organic matter which includes organic matter in plant residues and in manure, microbial biomass which includes organic matter in living microorganisms, and soil organic matter which includes non living native organic matter in the soil. Each main pool of organic matter is subdivided into two subpools each one being characterized by a particular carbon nitrogen ratio and by a particular turnover time. For each subpool of soil organic matter and added organic matter carbon turnover is modelled by applying first order kinetics assuming the rate coefficient to be influenced by soil temperature and soil water content. In the case of subpools of soil organic matter the rate coefficients are assumed also to be influenced by the clay content of the soil.

Biomass growth and decay

The biomass utilizes organic matter as substrate. Each subpool of biomass is characterized by a substrate utilization efficiency, a maintenance respiration coefficient, and a death rate coefficient. The maintenance respiration and the death rate are assumed to be influenced by soil temperature and soil water content, and in the case of the resistant biomass subpool also by the clay content of the soil. Carbon is lost as carbon dioxide due to the biomass respiration processes.

Nitrogen mineralization

During biomass growth and decay carbon is translocated between the various subpools of organic matter during which processes mineral nitrogen is released or immobilized depending on the carbon nitrogen ratio of the organic matter being utilized as substrate and the carbon nitrogen ratio in the microorganisms being synthesized. The overall result of all the organic matter turnover processes is net mineralization of nitrogen which may be positive in which case ammonium is released or negative in which case ammonium or nitrate is immobilized.

Nitrification

The soil mineral nitrogen processes in the model include nitrification, denitrification, uptake by plant roots, and vertical movement in the soil profile. Nitrification is simulated by applying first order kinetics assuming the rate coefficient to be influenced by soil temperature and soil water content.

Denitrification

Denitrification is simulated by defining a potential denitrification rate assumed to be related to the carbon dioxide evolution rate in the soil and the soil temperature. The potential denitrification rate is reduced according to the oxygen status of the soil expressed as a function of soil water content. The actual denitrification rate is either determined as the reduced potential denitrification rate or as the rate at which nitrate in soil is available for denitrification.

Nitrogen uptake

The nitrogen uptake model is based on the concept of a potential nitrogen demand simulated by the crop model, and the availability of nitrogen in the soil for plant uptake. Modelling of the uptake of nitrogen by plants is actually based on a quasi steady state solution of the differential equation for diffusive and convective radial transfer of nitrogen to the plant root surfaces, and the plant root density in the soil profile. Ammonium is taken up by plant roots in preference to nitrate.

Nitrogen movement

The mobility of the ammonium in soil is considered less than that of nitrate due to adsorption of ammonium to soil colloids which is described by an adsorption desorption isotherm. The vertical movement of nitrogen is modelled by means of a nummerical solution of the convection dispersion equation for ammonium as well as for nitrate. The source sink term in the convection dispersion equation integrates the transformation processes in the case of ammonium as well as in the case of nitrate.

Canopy development

The crop model is based on the concept that the physiological age of a crop can be described as the thermal age in terms of a temperature sum. The crop canopy is described in terms of total crop area index and green crop area index simulated as functions of crop thermal age, and accumulated top dry matter.

Root development

Root penetration rate is simulated as a function of the soil temperature at the root tip, while root density is simulated as a function of the amount of accumulated root dry matter, and the rooting depth.

Crop production

Simulation of crop dry matter production is based on calculation of canopy gross photosynthesis and partitioning of assimilates between the various parts of the crop. Canopy gross photosynthesis is determined by the amount of photosynthetically active radiation absorbed by the crop canopy and the efficiency by which the absorbed radiation is converted into carbohydrates. Partitioning of assimilates from gross photosynthesis between crop parts, i.e. top, roots, and for some crops storage organs, is simulated as a function of the crop thermal age. Respiration comprises growth respiration and a temperature dependent maintenance respiration.

Production levels

The gross photosynthesis of the crop canopy may be limited due to water or nitrogen deficiency. In the case of water deficiency gross photosynthesis is reduced by the ratio of actual and potential transpiration. At high and extremely low nitrogen supply the nitrogen concentration in the dry matter is assumed to reach an upper and a lower limit, respectively, both of which are dependent of the crop thermal age. Between these limits a nitrogen concentration in dry matter at just ample nitrogen supply exists also depending on the crop thermal age. The limitation of gross photosynthesis due to nitrogen deficiency is assumed proportional to the deviation of the actual nitrogen concentration in dry matter from the nitrogen concentration in dry matter at just ample nitrogen supply.

Management strategies	The system management model allows for various agricultural management practices and strategies including different soil tillage, crop sowing, fertilization, irrigation, and crop harvest.
Driving variables	Required meteorological variables to run the simulation model are daily values of global radiation, air temperature, and precipitation. Furthermore a number of parameters characterizing the system is required.
Model validation	Model validation has included experimental data on soil water content concentration of nitrate in soil, concentration of ammonium in soil, crop yield, nitrogen in top dry matter, denitrification, and leaching of nitrogen from the soil. It is concluded that basicly the overall performance of the model is satisfactory, although some adjustments may prove to be necessary.
Model application	An example of predictive application of the model is given in form of a simulation of the effects of straw incorporation in soil during twenty years. Before extensive predictive application of the model further validation including data from more combinations of soil, crop, climate, and management would be useful.

1. INTRODUCTION

Farming productivity

Agricultural crop production is the human activities by which food and useful organic material is produced by plants with the sun as the primary source of energy. For many soil types and climates, farming systems have been developed that enable subsistence. However, to sustain a substantial non farming population, the productivity of the farmers has to be much higher than their own subsistence level. This is only possible if the means of crop production available are yield increasing, crop protecting, and labour saving, respectively.

Production level

During the past century and in particular during the recent four decades crop production per unit area has increased substantially. In general terms this persistent yield increase can be attributed to simultaneous effects of soil amelioration by soil tillage, control of crop growth factors by irrigation and fertilization, crop protection against diseases by application of pesticides as well as introduction of varieties that were able to benefit from the increased input to the crop production system.

Production systems

In addition to higher input the structure of agricultural crop production systems has changed considerably during the recent decades. Thus in response to prevailing political and economical conditions and developments in technology bigger farm units, bigger herds of cattle and pigs per farm unit, less mixed farming and highly specialized practice of crop production have been developed in many countries.

Environmental impacts

The impact of agricultural crop production on the environment, e.g. in terms of losses of nitrogen to surface waters and ground water, may be related to the input level of fertilizer as well as to the structure of the cropping system. Thus it is well known that e.g. high application rates of farmyard manure and in particular cropping systems without crop cover during periods in which mineral nitrogen is released from organic matter in the soil may result in increased losses of nitrogen by lea-

Sustainable systems

ching from the soil in subsequent periods with water discharge. Due to the fact that losses of nitrogen from agricultural arable land to the aquatic environment have increased in many areas, in particular during the recent four decades, great concern has arisen as to how an economically and environmentally sustained agricultural crop production can be developed. This includes sustained crop yield and crop quality, sustained natural ressources for crop production, high ressource use efficiency in crop production and limitation of the impact of crop production on environmental quality.

Nitrogen losses

Agricultural crop production as well as losses of matter, e.g. loss of nitrogen to the environment, is determined by a number of physical, chemical and biological processes in the soil plant atmosphere continuum which interact simultaneously in a complex way. In the nitrogen cycle in the soil plant system which is an integral part of the overall nitrogen cycle in nature the path way of nitrogen is a complex series of transformation and transport processes all of which are affected by a number of external factors. Thus it is difficult to predict how modified management practices will affect crop production, nitrogen use efficiency, and nitrogen losses from the soil plant system.

Conventional approach

In the conventional scientific approach field experiments have been used extensively to explore possibilities for appropriate system management practices in agricultural crop production. This type of research which has limitations due to the complexity of the system often requires a wide range of experiments to establish how different management practices affect crop production and impacts on the environment.

Simulation models

Simulation models are increasingly used to support experimental research. The value of simulation models seems substantial. Simulation models draw on knowledge from various diciplines and may contribute to our understanding of the system because models can help us to integrate the relevant processes and to bridge areas and levels of knowledge.

Integration of knowledge

Thus modelling the soil plant system including the behaviour of nitrogen in the system is of substantial interest. A soil plant system model will enable us to integrate current knowledge and to simulate the performance of the system in terms of interrelationships between the energy, water, and nitrogen cycles in the system under various external conditions.

Model applications

The potential areas of application of a soil plant system model are numerous. A simulation model can be used to explore and predict how various system management practices and strategies will affect the nitrogen cycle including losses of nitrogen in agricultural crops production. In addition the knowledge of the behaviour of nitrogen in the soil plant system integrated in a simulation model may be essential in our improvement of expert systems that are being developed to assess appropriate amounts of fertilizer nitrogen for crop production under various soil and climate conditions. Furthermore, a soil plant system model would be useful in matching the nitrogen supply to the nitrogen demand of the crop during the growing season making allowance for crop development, weather conditions, and previous nitrogen application. Hence a simulation model of the soil plant system can be considered as an essential management tool to secure efficient nitrogen utilization and limitation of nitrogen losses in agricultural crop production.

Objectives of study

The objective of the present study has been to develop a comprehensive simulation model for transformation and transport of matter and energy in the soil plant atmosphere system. The particular simulation model which is described in the present research report has been developed to enable simulation of crop production, water balance, and nitrogen balance for various agricultural management practices including crop follow, fertilization, irrigation, and soil tillage. The simulation model has been developed to facilitate application at the farm level as a management tool as well as at higher level, e.g. regionally, as a basic part of a model system for administrative purposes.

2. SYSTEM AND MODELLING CONCEPTS

2.1 Introduction

Pioneering work

Since the pioneering work by de Wit (1959, 1965) in the early sixties much scientific effort has been devoted to agricultural system analysis and simulation. Thus system analysis and simulation have been used in agricultural research for more than a quater of a century.

In the present chapter some basic principles and concepts of system modelling are briefly described. Furthermore within the framework of the soil plant atmosphere continuum the system has been defined for which the present model has been developed. Finally the basic structure of the model is outlined.

2.2 Basic principles and concepts

Modelling concepts

The modelling approach is characterized by terms such as system, model and simulation. According to de Wit (1982) a system is a limited part of reality that contains interrelated elements, a model is a simplified representation of a system while simulation may be defined as the art of building mathematical models and the study of their properties in reference to those of the system. Ideally the boundaries of a system are chosen such that the environment influences processes within the system, but that the system itself does not modify its environment.

Model characterization

Mathematical models may be descriptive or explanatory. A descriptive model reflects little or none of the mechanisms and processes that are the cause of the behaviour of the system. Descriptive models often consist of one or more mathematical equations. Explanatory models consist of a quantitative description of the mechanisms and processes that cause the behaviour of the system. These descriptions are explicit state-

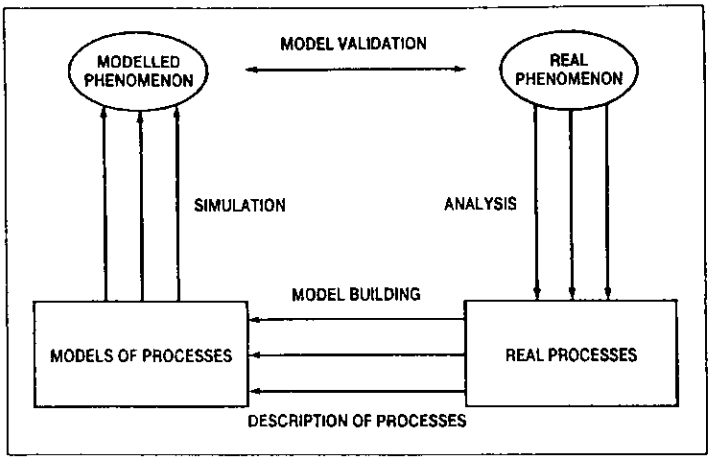

Fig. 2-1 Analysis and integration of real system observations into an explanatory model.

ments of the scientific theory or hypotheses. To create an explanatory model the real phenomenon of the system is analyzed and the causal processes in the system are identified, described and modelled to be integrated into a model for the entire system, Fig. 2-1. Simulation may be performed to give a modelled picture of the phenomenon which then can be evaluated against the real phenomenon.

Static and dynamic models

Models may be of the static or dynamic type, the latter of which includes the dimension of time which allows simulation of the temporal behaviour of the system. Static models often form part of a dynamic model. Dynamic explanatory models are based on the assumption that the state of the system at any given moment can be quantified and that changes of the state of the system can be described by mathematical equations. This leads to the concept of system state, rate, and driving variables. The rate variables describe the rate of change of the state variables while the driving variables characterize the effect of the environment on the system at the boundaries of the system.

Comprehensive models

During development a model moves gradually from one phase into the next. Preliminary models may be defined as models with a structure that reflects current scientific knowledge which may be limited at the explanatory level. A comprehensive model is a model of a system whose essential elements are thoroughly understood and in which much knowledge is incorporated. Summary models which may be considered as abstracts of comprehensive models contain essential aspects of the comprehensive models formulated in less detail than is possible.

Preliminary models

Such a division of dynamic models into three classes is obviously an oversimplification. In particular those models that have been developed over a long period of time and that are still being improved consist of submodels of which some are in fact summary models, others are comprehensive in nature and still others are preliminary submodels. The characteristics given for the three phases of development of models apply then to the individual submodels of the overall model.

Model validation

Validation of a model is the process by which the behaviour of the model is compared with that of the real system, i.e. modelled and real phenomena of the system are compared. If the behaviour of the model matches qualitatively with that of the real system a quantitative comparison and evaluation of the predictive performance of the model is to be made. At this stage statistical tools may be usefull. However, it should be realized that even when sufficient and accurate data are available a model can not be proved to be correct.

2.3 System and structure of model

Soil plant system

Within the framework of the soil plant atmosphere continuum and in terms of the concepts outlined previously a system is defined which includes the soil and plant part of the continuum. It is noted that in the present context the term soil refers to the

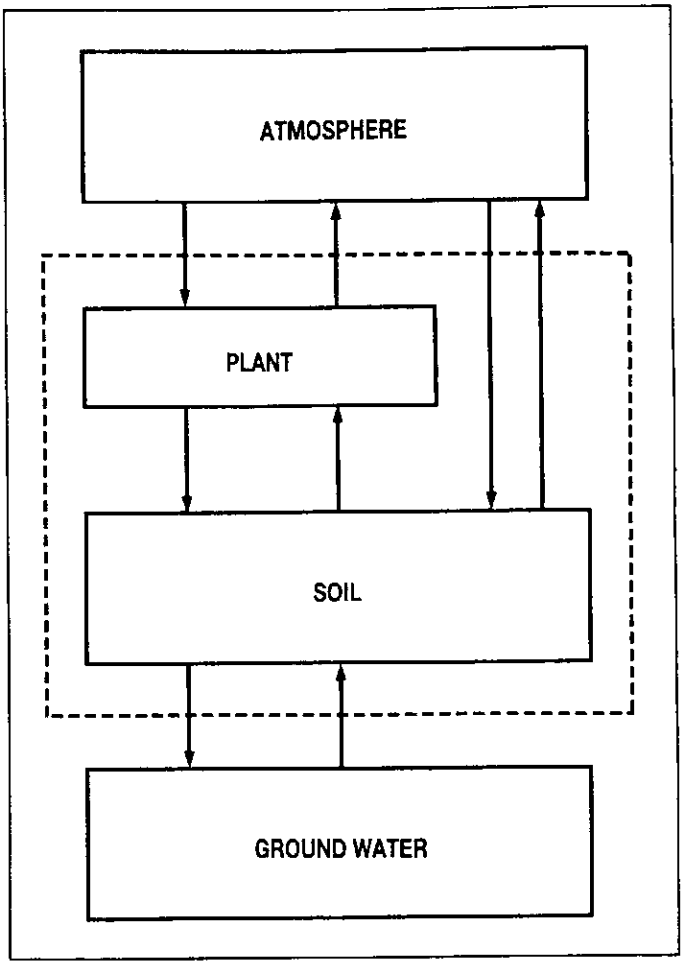

Fig. 2–2 Soil plant system defined within the framework of the soil plant atmosphere continuum. Boundary to system environment indicated as a broken line. Arrows indicate flows of energy and matter.

unsaturated zone. The atmosphere and the ground water constitute the system environment which influences the soil plant system at its boundaries in terms of driving variables. A schematic representation of the soil plant system, its boundaries, and the system environment is shown in Fig. 2–2. Thus the soil plant system is conceptualized to be one dimensional

in vertical direction with upper and lower boundaries.

System variables

In order to construct the model the soil plant system is schematized and relevant system variables and processes are identified in accordance with the objectives of the model. In the present conceptualization of the soil plant system the soil is characterized by a number of main system variables viz. soil water content, soil temperature, soil nitrate content, soil ammonium content and soil organic matter content. The organic matter is characterized by a number of pools, including pools of microbial biomass, each of which is described in terms of carbon content, carbon nitrogen ratio and turnover time. In a similar way the crop is characterized by a number of main system variables viz. dry matter content of shoots, dry matter content of storage organs, dry matter content of roots, and nitrogen content of crop.

State of system

The state of the system variables changes due to the influence of a number of processes which take place within the system. These processes include transformation and transport processes involving heat, water, carbon and nitrogen. A particular process may depend on driving variables, state of system variables and other processes taking place within the system. Furthermore system variables as well as processes within the system may be influenced by human manipulation of the system in terms of system management operations.

Overall structure of soil plant system

The over all structure of the conceptualized soil plant system which is basis for the model is shown in Fig. 2–3. Rectangles represent system variables or parts of the system, valve symbols represent processes, ovals represent auxiliary variables while the underlined variables are driving variables. The solid lines represent flows of matter (water, carbon and nitrogen) while the dashed lines represent flows of information. A number of feed back loops may be identified. It should be noted that only the most important system variables and processes are included in Fig. 2–3.

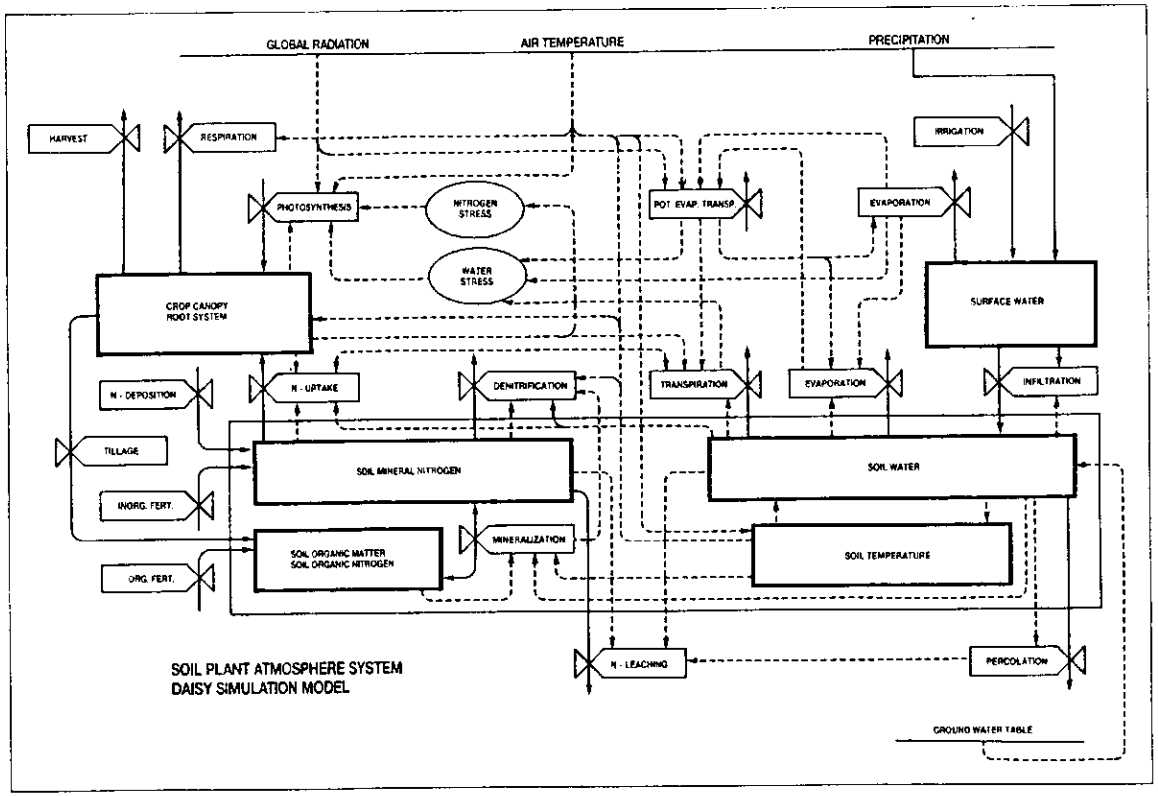

Fig. 2–3 Relational diagram of the soil plant system. Global radiation, air temperature, and precipitation are driving variables. Rectangles represent system state variables, valve symbols represent processes while ovals represent auxiliary variables. Solid lines represent flows of matter while broken lines represent flows of information.

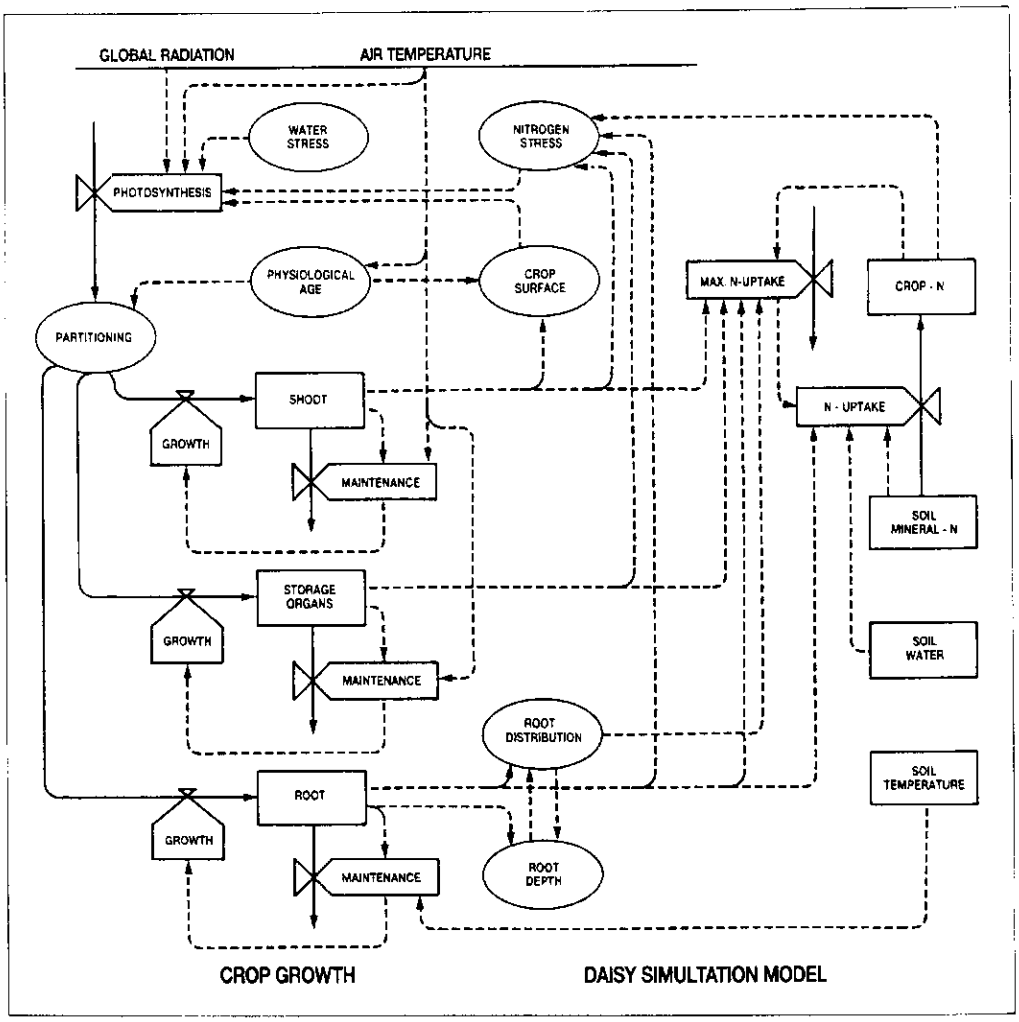

Fig. 2–4 Relational diagram of the crop part of the soil plant system. Rectangles represent system state variables, valve symbols represent processes while ovals represent auxiliary variables. Solid lines represent flows of matter while broken lines represent flows of information.

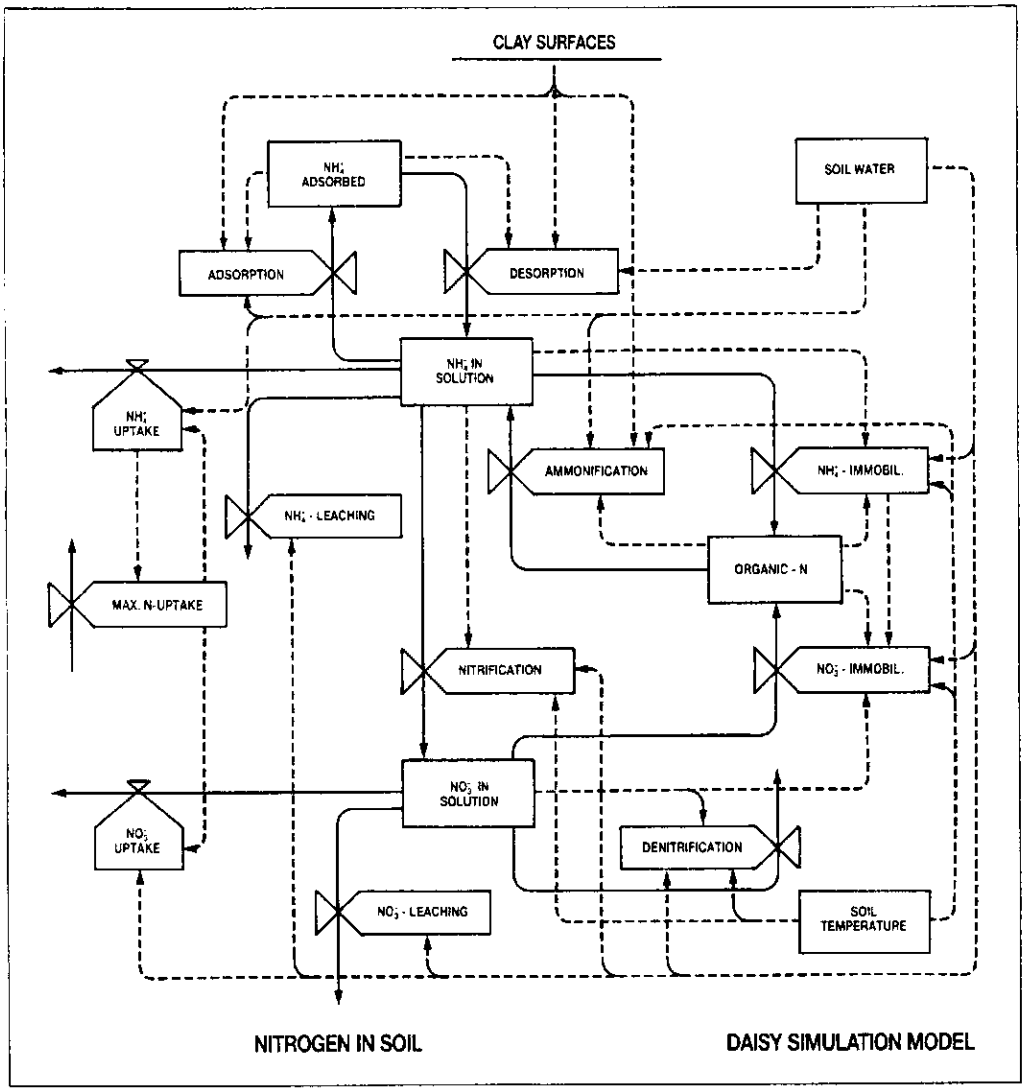

Fig. 2-5 Relational diagram of the nitrogen part of the soil plant system. Rectangles represent system state variables, while valve symbols represent processes. Solid lines represent flows of matter while broken lines represent flows of information.

The crop and soil nitrogen part of the system is shown in more detail in Fig. 2–4 and Fig. 2–5, respectively.

Internal and external processes

The processes illustrated in Fig. 2–3 may be characterized as internal or external processes. Internal processes include processes such as infiltration, evaporation, transpiration, mineralization, denitrification, nitrogen uptake and nitrogen turnover etc. while external processes include processes such as fertilization, irrigation, tillage, and harvest operations.

The various processes considered have been described and modelled in accordance with existing knowledge. For some processes the theories and mechanisms are well established and the processes are modelled accordingly. This applies to such processes as e.g. heat flow and water flow in soil. For other processes theories and knowledge of mechanisms involved are limited. In such cases a conceptual approach has been applied. This is true for e.g. the models for organic matter transformation and net mineralization of nitrogen in soil. Still some parts of the model may be characterized as descriptive, e.g. the assimilate partitioning in the crop model.

Priorities

During development of the model it has been a priority for operational reasons to keep the number of necessary driving variables at a minimum and to limit the requirement of temporal resolution of the driving variables to one day. This has made compromises necessary regarding modelling of some processes. Thus a more refined modelling of e.g. photosynthesis and soil temperature would require more driving variables as well as a higher temporal resolution of the driving variables. However, what the model for such reasons has lost in refinement hopefully is gained as greater sturdiness.

3. ATMOSPHERIC ENVIRONMENT AND SURFACE PHENOMENA

3.1 Introduction

Exchange processes at system boundary

In the soil plant atmosphere continuum the atmospheric environment acts as a source-sink for energy, water, nitrogen and carbon. At the boundary between the atmosphere and the surface of soil and crop several important exchange processes occur. Thus energy is exchanged in terms of radiation, sensible and latent heat, and exchange of water takes place by precipitation and evapotranspiration.

Furthermore exchange of CO_2 takes place as a result of crop photosynthesis and respiration processes in crop and soil. In the crop model it is assumed that the CO_2 concentration in the atmosphere is 330 ppm. Exchange of nitrogen takes place as a result of atmospheric deposition of nitrogen and losses of gaseous nitrogen to the atmosphere by several processes e.g. biological denitrification and votalization of ammonia from plants, slurry and farmyard manure.

Surface phenomena

In this section the meteorological variables nessecary for running the present model are briefly described and the calculation of potential evapotranspiration is outlined. Furthermore a model for interception of precipitation in the crop canopy as well as a model for snow accumulation, melting and freezing at the soil surface is described. Finally a description of a simple rutine for calculation of nitrogen deposition is included.

3.2 Meteorological driving variables

Driving variables

In the present model the required meteorological variables for simulation of transformation and transport of energy and matter in the soil plant atmosphere system are global radiation, air temperature and precipitation.

Potential evapotranspiration

In addition the potential evapotranspiration which is a derived variable is of major importance. Thus the present model requires daily values of

S_i = global radiation [W m^{-2}]
T_a = air temperature [°C]
P = precipitation [mm day^{-1}]

which are used as driving variables in the model. Global radiation is used in the crop model as well as in the snow model whereas air temperature is used in the snow model, the soil temperature model, and the crop model. Furthermore if not available potential evapotranspiration may be derived from global radiation and air temperature. Precipitation is used in the interception model, the snow model, and the soil water model.

3.3 Potential evapotranspiration

Definition of potential evapotranspiration

In the present model potential evapotranspiration is of major importance in the calculation of actual evapotranspiration.

Potential evapotranspiration can be defined as the maximum water loss by evaporation and transpiration from a surface which is amply supplied with water. This definition implies the basic assumption that potential evapotranspiration constitutes the upper limit of evapotranspiration.

Furthermore this definition leads to different rates of potential evapotranspiration for different crops due to the fact that the quantity of energy available for evapotranspiration is influenced by the particular surface properties. Thus netradiation which strongly influences the potential evapotranspiration has been shown to vary considerably among field crops (Aslyng and Hansen, 1985).

Therefore the potential evapotranspiration should be determined for each individual surface or crop under consideration. However, in order to get accurate values of potential evapotranspiration extensive measurements are required. To overcome this problem the concept of a reference surface has been introduced e.g. a crop of short grass. Hansen, Jensen and Aslyng (1981) have shown that under Danish climatic conditions the Penman equation (Penman, 1948) gives an accurate estimate of the potential evapotranspiration from such a reference surface. However, application of the Penman equation still requires extensive measurements of climatic variables.

Estimation of potential evapotranspiration

To be used in the present model potential evapotranspiration may be supplied together with the required meteorological driving variables. However, if measured or calculated values of the potential evapotranspiration are not available, an estimate of the potential evapotranspiration can be obtained from an empirical equation proposed by Makkink (1957), eq. (3-1), which has been shown to give reliable results for a reference surface of short grass (Hansen and Aslyng, 1984).

$$E_p = 0.7 \frac{\Delta}{\Delta+\gamma} \frac{S_i}{\lambda} \qquad (3-1)$$

E_p = potential evapotranspiration [mm day^{-1}]
S_i = global radiation [M J day^{-1}]
Δ = slope of the saturated vapor pressure versus temperature relationship [Pa $°C^{-1}$]
γ = psycrometric constant (66.7 Pa $°C^{-1}$]
λ = latent heat of vaporization (2.47 M J mm^{-1}]

Basic time step

In the soil water model the basic time step is one hour while the potential evapotranspiration is given on a daily basis. Therefore from the daily values potential evapotranspiration has been distributed over the day according to eq. (3-2).

$$E_p'(h) = (E_p - E_s - E_i)[1 + A_m \cos(\frac{2\pi}{24} h) + B_m \sin(\frac{2\pi}{24} h)] \quad (3-2)$$

$E_p'(h)$ = potential evapotranspiration [mm h^{-1}]
E_p = potential evapotranspiration [mm day^{-1}]
E_s = evaporation and sublimation from snowpack [mm day^{-1}]
E_i = evaporation of water intercepted by the vegetation [mm day^{-1}]
h = hour of the day, h = 1, 2, ..,24
A_m, B_m = constants, cf. Table 3-1

It is noted that in eq. (3-2) it is a basic assumption that evaporation from wet surfaces takes place before water is extracted from the soil either by soil evaporation or by transpiration from plants.

The constants A_m and B_m in eq. (3-2) have been determined month by month by a harmonic analysis as the first harmonic in a finite Fourier serie using data from The Climate and Water Balance Station situated (55°40'N; 12°18'N; 28m above mean sea level) 20 km west of Copenhagen (Hansen, Jensen and Aslyng, 1981).

The analysis was based on hourly values of potential evapotranspiration calculated by the Penman equation for the period 1966-1979. The results are shown in Table 3-1.

It is noted that the values of the constants, Table 3-1, are not fixed as other values representative for a particular location may be used.

Table 3-1 Constants entering eq. (3-2) for distribution of potential evapotranspiration over a day.

Month	A_m	B_m
1	-0.92	-0.17
2	-1.69	-0.44
3	-1.68	-0.45
4	-1.47	-0.38
5	-1.39	-0.34
6	-1.38	-0.34
7	-1.39	-0.39
8	-1.52	-0.41
9	-1.63	-0.36
10	-1.63	-0.24
11	-1.33	-0.17
12	-0.90	-0.20

3.4 Interception model

Interception storage

Part of the precipitation reaching the top of the crop is intercepted by the crop canopy which acts as an interception storage. Subsequently the intercepted water is evaporated from the crop canopy surfaces which is assumed to take place at a potential rate.

It is assumed that the amount of intercepted water is determined either by the amount of precipitation or by the interception capacity of the crop canopy. Furthermore it is assumed that the interception capacity of the crop canopy is proportional to the total crop area index, eq. (3-3).

$$I_c = C_i C_{ai} \qquad (3-3)$$

I_c = interception capacity [mm]
C_i = interception capacity coefficient [mm]
C_{ai} = total crop area index [$m^2\ m^{-2}$]

A value of C_i of 0.5 mm was proposed by Jensen (1979). The amount of water stored in the interception storage at any given time is given by eq. (3-4) in which superscript i+1 and i refer to the present and previous time step, respectively.

$$I_s^{i+1} = \text{Min} \left\{ I_c,\ I_s^i + (P + E_I)\ \Delta t \right\} \qquad (3-4)$$

I_s = water stored in interception storage [mm]
P = precipitation [mm day^{-1}]
E_I = evaporation from the interception storage [mm day^{-1}]
Δt = time step (1 day)

The evaporation of water from the interception storage is estimated from eq. (3-5) in which E_p is potential evapotranspiration.

$$E_I = \begin{cases} E_p & E_p \le I_s^i/\Delta t + P \\ I_s^i/\Delta t + P & E_p > I_s^i/\Delta t + P \end{cases} \qquad (3-5)$$

The precipitation which is not intercepted by the crop canopy is allocated to the soil surface for infiltration or ponding depending on the soil conditions.

3.5 Model for snow accumulation and melting

The model for snow accumulation in the present model is basically adopted from Jansson and Haldin (1980). The basic equations in the model, eq. (3-6) and eq. (3-7), express the conservation of mass.

$$S_s^{i+1} = S_s^i + [P_s + P_r - E_s - q_s]\Delta t \qquad (3-6)$$

$$S_w^{i+1} = S_w^i + [P_r - E_s' + M - q_s]\Delta t \qquad (3-7)$$

S_s = snow and water in snow storage expressed in equivalent water [mm]
S_w = water in snow storage [mm]
P_s = precipitation in the form of snow [mm day^{-1}]
P_r = precipitation in the form of rain [mm day^{-1}]
E_s = evaporation plus sublimation from snow storage [mm day^{-1}]
E_s' = evaporation from snow storage [mm day^{-1}]
q_s = percolation from snow storage [mm day^{-1}]
M = snow melting, a negative value indicates freezing [mm day^{-1}]
Δt = time step (1 day)

The superscripts i+1 and i in eq. (3-6) and eq. (3-7) refer to the present and previous time step, respectively.

Precipitation is assumed to fall as snow if the air temperature is below a certain limit (T_1) and as rain if the air temperature is above another limit (T_2). In between these limits the precipitation is assumed to be a mixture of rain and snow, eq. (3-8) and eq. (3-9).

$$P_s = \begin{cases} P & T_a \le T_1 \\ \dfrac{T_2 - T_a}{T_2 - T_1} P & T_2 < T_a < T_1 \\ 0 & T_2 \le T_a \end{cases} \qquad (3-8)$$

$$P_r = P - P_s \qquad (3-9)$$

P = total precipitation [mm day^{-1}]
T_a = air temperature [°C]
T_1, T_2 = empirical constants [°C]

The evaporation plus sublimation from the snow storage is estimated from eq. (3-10) in which E_p is potential evapotranspiration while the evaporation from the snow storage is estimated from eq. (3-11).

$$E_s = \begin{cases} E_p & E_s \leq S_w^i/\Delta t + P \\ S_s^i/\Delta t + P & \text{else} \end{cases} \qquad (3-10)$$

$$E_s' = \begin{cases} E_s & E_s \leq S_s^i/\Delta t + P_r + M \\ S_w^i/\Delta t + P_r + M & \text{else} \end{cases} \qquad (3\text{-}11)$$

The potential snow melting is assumed to be determined by the properties of the snow, the air temperature, the global radiation, and the soil heat flux at the soil surface, eq. (3-12).

$$M^* = (m_t T_a + m_r S_i + q_h/L_m) f \qquad (3-12)$$

M^* = potential snow melting [mm day^{-1}]
S_i = global radiation [J m^{-2} day^{-1}]
q_h = soil heat flux at the surface [J m^{-2} day^{-1}]
L_m = melting heat (3.34 10^5 J kg^{-1})
m_t = parameter [kg J^{-1}]
m_r = parameter [kg J^{-1}]
f = constant (1 mm (H_2O) (kg (H_2O) m^{-2})$^{-1}$)

The influence of temperature on snow melting and freezing in terms of the parameter m_t is expressed in eq. (3-13).

$$m_t = \begin{cases} m_t^* & T_a \geq 0 \\ m_t^* \ \text{Min} \left\{ 1, (\Delta Z_s \, m_f) \right\} & T_a < 0 \end{cases} \qquad (3-13)$$

m_t^* = constant [kg m^{-2} day^{-1} °C]
m_f = constant [m^{-1}]
ΔZ_s = depth of snow storage [m]

The depth of the snow storage is estimated from eq. (3-14) in which the depth of precipitation (ΔZ_p) is estimated from the snow-rain mixture which has fallen the present day.

$$\Delta Z_s^{i+1} = \Delta Z_s^i + \Delta Z_p \qquad (3-14)$$

ΔZ_p = depth of precipitation fallen the present day [m]

The depth of the precipitation is estimated from eq. (3-15) and eq. (3-16).

$$\rho_p = \rho_w + (\rho_s + \rho_w) \frac{P_s}{P} \qquad (3-15)$$

$$\Delta Z_p = \frac{P \, \Delta t}{f \, \rho_P} \qquad (3-16)$$

ρ_p = density of snow-rain mixture [kg m^{-3}]
ρ_w = density of water (10^3 kg m^{-3})
ρ_s = density of newly fallen snow [kg m^{-3}]

The influence of global radiation on snow melting and freesing in terms of the parameter m_r is expressed in eq. (3-17).

$$m_r = m_r^* (1 + m_1(1 - \exp(-m_2 \Delta t_s))) \qquad (3-17)$$

m_r^* = constant [kg J^{-1}]
Δt_s = age of surface snow [days]
m_1 = constant [kg J^{-1}]
m_2 = constant [$days^{-1}$]

The age of the surface snow is counted from the previous date with a snow fall greater than a certain predescribed value. Thus the change in albedo of the snow storage with time is taken into account.

The actual snow melting and freezing is then estimated from eq. (3-18).

$$M = \begin{cases} M_1 & M^* < M_1 \\ M^* & M_1 \le M^* \le M_2 \\ M_2 & M_2 < M^* \end{cases} \qquad (3-18)$$

$$M_1 = -(S_w^i/\Delta t + P_r - E_s')$$

$$M_2 = (S_s^i - S_w^i)/\Delta t + P_s - (E_s - E_s')$$

The snow storage is assumed to possess a certain capacity for retention of liquid water which is expressed by eq. (3-19).

$$S_c = f_c (S_s^i + (P - E_s)/\Delta t) \qquad (3-19)$$

S_c = storage capacity of snow storage for retention of liquid water [mm]
f_c = capacity coefficient of snow storage for retention of liquid water

The percolation of water out of the snow storage is estimated from eq. (3-20) while the depth of the snowpack is calculated from eq. (3-21) in which $\rho_{s,p}$ is density of the snowpack.

$$q_s = \text{Max}\ \{\ 0,\ S_w^i + (P_r - E_s + M)\ \Delta t\ -\ S_c\ \}/\Delta t \qquad (3-20)$$

$$\Delta Z_s^{i+1} = \frac{S_s^{i+1}}{f\ \rho_{s,p}^{i+1}} \qquad (3-21)$$

The density of the snow pack is estimated as follows. Taking compaction of the snow into consideration a new estimate for the density of the snowpack is calculated from eq. (3–22) after which a new value of the depth of the snowpack is calculated from eq. (3–23) in which S_s^i is measured in kg m^{-3}.

$$\rho_{s,p}^{i+\frac{1}{2}} = \text{Max}\ \left\{\rho_{s,p}^i,\ \rho_s + \rho_1\ \frac{S_w^{i+1}}{S_c} + \rho_2\ S_s^i\right\} \qquad (3-22)$$

$$\Delta Z_{s,p}^{i+\frac{1}{2}} = \frac{S_s^i}{f\ \rho_{s,p}^{i+\frac{1}{2}}} \qquad (3-23)$$

$\rho_{s,p}$ = density of snowpack [kg m^{-3}]
ρ_1 = constant [kg m^{-3}]
ρ_2 = constant [m^{-1}]

A new estimate of the density of the snowpack can now be estimated from eq. (3–24).

$$\rho_{s,p}^{i+1} = \frac{(P - E_s)\Delta t + S_s^i}{f\ (\Delta Z)} \qquad (3-24)$$

The new estimate of the density of the snowpack is then used to calculate a new depth of the snowpack by eq. (3–21) and then stored to be used in the next time step.

The nummerical values of the parameters in the present model for snow accumulation and melting assessed for Nordic climatical conditions are shown in Table 3–2.

Table 3-2 Parameters in model for snow accumulation and melting adopted from Jansson and Haldin (1980)

Symbol	Equation	Unit	Parameter Value
T_1	(3- 8)	°C	- 2.0
T_2	(3- 8)	°C	2.0
m_t^*	(3-13)	kg $m^{-2}day^{-1}\cdot C^{-1}$	2.0
m_f	(3-13)	m^{-1}	10.0
ρ_s	(3-15)	kg m^{-3}	100.0
m_r^*	(3-17)	kg J^{-1}	1.5 10^{-7}
m_1	(3-17)	-	2.0
m_2	(3-17)	day^{-1}	0.1
f_c	(3-19)	-	0.07
ρ_1	(3-21)	kg m^{-3}	200.0
ρ_2	(3-21)	m^{-1}	0.5

3.6 Deposition of nitrogen

Atmospheric deposition

Atmospheric deposition of nitrogen constitutes an input of nitrogen to the soil which has to be taken into consideration when modelling the transformation and transport of nitrogen in the soil plant atmosphere system. The nitrogen deposition takes place as wet deposition in the form of NH_4^+-N and NO_3^--N dissolved in the precipitation and as dry deposition in the form of NH_4^+-N and NO_3^--N adsorbed to solid particles. The major sources of nitrogen which is deposited at the soil surface are

- losses of gaseous nitrogen to the atmosphere from ocean and land surfaces e.g. by biological denitrification and by votalization of ammonia from plants, slurry and farmyard manure
- emission of gaseous nitrogen to the atmosphere from industry e.g. by combustion of fossil fuel
- fixation of atmospheric N_2 by photochemical and electrical processes in the atmosphere

Surface storage

In the present model the nitrogen deposited at the soil surface is allocated to a surface storage. When infiltration occurs the nitrogen in the surface storage is released and enters the soil as dissolved $NH_4^+ - N$ and $NO_3^- - N$ in the infiltrating water. The accumulation of nitrogen in a surface storage of $NH_4^+ - N$ and $NO_3^- - N$ is calculated from eq. (3-26) and eq. (3-27), respectively.

$$S^{i+1}_{NH_4^+ - N} = S^{i}_{NH_4^+ - N} + (d_{NH_4^+ - N} + c_{NH_4^+ - N} P)\,\Delta t \qquad (3-26)$$

$$S^{i+1}_{NO_3^- - N} = S^{i}_{NO_3^- - N} + (d_{NO_3^- - N} + c_{NO_3^- - N} P)\,\Delta t \qquad (3-27)$$

$S_{NH_4^+ - N}$ = surface storage of $NH_4^+ - N$ [kg m^{-2}]

$S_{NO_3^- - N}$ = surface storage of $NO_3^- - N$ [kg m^{-2}]

$d_{NH_4^+ - N}$ = dry deposition rate of $NH_4^+ - N$ [kg m^{-2} day^{-1}]

$d_{NO_3^- - N}$ = dry deposition rate of $NO_3^- - N$ [kg m^{-2} day^{-1}]

$c_{NH_4^+ - N}$ = concentration of $NH_4^+ - N$ in precipitation [kg m^{-2} mm^{-1}]

$c_{NO_3^- - N}$ = concentration of $NO_3^- - N$ in precipitation [kg m^{-2} mm^{-1}]

P = precipitation [mm day^{-1}]

Δt = time step (1 day)

In eq. (3-26) and eq. (3-27) subscript i+1 and i refer to the present and previous day, respectively. If snow is present or ponding occurs it is assumed that the nitrogen in the surface storage is dissolved in all the water present at the surface and that the infiltrating water carries that concentration.

During the recent 25 years the average deposition of nitrogen under Danish conditions has almost doubled (Jensen, 1962; Jørgensen, 1979; Grundahl and Hansen, 1990). In the present model $c_{NH_4^+-N} = 0.9\ 10^{-6}$ kg m^{-2} mm^{-1}, $c_{NO_3^--N} = 0.6\ 10^{-6}$ kg m^{-2} mm^{-1}, $d_{NH_4^+-N} = 0.6\ 10^{-6}$ kg m^{-2} day^{-1} and $d_{NO_3^--N} = 0.3\ 10^{-6}$ kg m^{-2} day^{-1} may be used as appropriate values for Danish average conditions.

4. SOIL WATER MODEL

4.1 Introduction

Soil water as a reaction medium and transport agent

Soil water acts as a reaction medium for several transformation processes in the soil. Furthermore soil water is a transport agent by which matter is transported through the soil. In particular such processes as microbial transformation of carbon and nitrogen in soil are strongly influenced by soil water content.

Plant uptake of water and vertical water flow

Soil water flow to root surfaces is a process of great significance for plant water uptake as well as for plant nutrient transport to the root surfaces. Furthermore leaching of chemicals from the root zone is strongly related to vertical soil water flow. Thus a soil water model has been developed to provide values of soil water content and pressure potential of soil water for abiotic functions governing several biological processes described in other submodels of DAISY and for calculating plant uptake of soil water and vertical flow of water in the unsaturated zone.

The concept of soil as a continuum

The soil is considered as a continuum in which no preferential flow occurs. Thus only matrix flow is considered. The hydraulic functions for the soil are expressed in terms of a soil water retention characteristic and a hydraulic conductivity function relating the hydraulic conductivity to the soil water content. The present soil water model is based upon the one dimensional Richards equation including a sink term taking into account plant water uptake. The sink term is calculated assuming radial flow towards the plant roots. In situations in which frost and thaw occur a simple procedure is used in part of the soil profile.

4.2 Soil water retention

Estimation of the soil water retention curve

In order to simulate soil water dynamics in the unsaturated zone a continuous relation between pressure potential and soil water content is required. In the present version of DAISY soil water retention is described by a single valued function connecting the pressure potential with volumetric soil water content. Thus the hysteresis phenomena is neglected.

A mathematical interpolation method proposed by Butland (1980) has been used to obtain a continuous relation between pressure potential and soil water content from the experimental data on soil water retention. In this method parametric piecewise cubics are used to calculate intermediate values in the segments between the data points. Thus the soil water retention characteristic is given piecewise as expressed in eq. (4 – 1).

$$\theta = \theta_i + a_i(x - x_i) + b_i(x - x_i)^2 + c_i(x - x_i)^3 \qquad (4-1)$$

θ = volumetric soil water content [$m^3\ m^{-3}$]

θ_i = volumetric soil water content at the beginning of segment i [$m^3\ m^{-3}$]

x = pressure potential of soil water expressed as pF

x_i = pressure potential of soil water expressed as pF at $\theta = \theta_i$

a_i, b_i, c_i are parameters for segment i

The parameters in eq. (4 – 1) are chosen in such a way that when the segments are joined they form a continuous monotonic curve passing through the data points. The specific water capacity, $C_\theta(\psi)$, is defined in eq. (4 – 2) in which ψ is pressure potential expressed in m H_2O.

$$C_\theta(\psi) = \frac{d\theta}{d\psi} \qquad (4-2)$$

$C_\theta(\psi)$ = specific water capacity [$m^3\ m^{-3}\ (m\ H_2O)^{-1}$]
θ = volumetric water content [$m^3\ m^{-3}$]
ψ = pressure potential of soil water [$m\ H_2O$]

The specific water capacity is easily derived from eq. (4-1) and can be calculated from eq. (4-3).

$$C_\theta(\psi)_i = [a_i + 2b_i(x - x_i) + 3c_i(x - x_i)^2] \frac{dx}{d\psi} \qquad (4-3)$$

$$\frac{dx}{d\psi} = \frac{d[\log(-100\ \psi)]}{d\psi} = \frac{-100}{\psi\ \ln(10)}$$

A number of other methods exists for determination of the course of the retention curve which in some cases may be more feasible.

4.3 Hydraulic conductivity

Estimation of hydraulic conductivity in soil

A number of methods exist for predicting the hydraulic conductivity function of soil. One type of methods utilizes the information found in the soil water retention characteristic. Childs and Collis-George (1950) were the first to show that the hydraulic conductivity of soil is related to the pore-size distribution of the soil. Their model was later modified by Marshall (1958), Millington and Quirk (1960) and Kunze, Uehara and Graham (1968). Basic assumptions of the model are that the soil is a pore system, consisting of pores of various sizes, and that the pore-size distribution is random throughout the soil. Further assumptions are that the pores can be divided in pore classes, that the pores of different pore-classes are connected randomly with pores of other pore classes, and that flow within each pore class can be calculated by the Poiseuelle equation. The formulation as given by Kunze, Uehara and Graham (1968) is expressed in eq. (4-4).

$$K(\psi)_i = \frac{K_m\, 30\, \gamma^2 \theta}{K_c\, \rho_w g \eta n^2} \sum_{j=i}^{n} (2j + 1 - 2i)\, \frac{1}{\psi_j^2} \qquad (4-4)$$

$K(\psi)_i$ = Hydraulic conductivity for pore class i [m s^{-1}]
K_m/K_c = matching factor (measured conductivity/calculated conductivity)
γ = surface tension [N m^{-1}]
ρ_w = density of water [kg m^{-3}]
g = gravitational constant [m s^{-2}]
η = water viscosity [kg $m^{-1}s^{-1}$]
θ = water filled porosity [m^3m^{-3}]
n = total number of pore classes
ψ = pressure potential [m]
i = 1, 2, 3 .. n

In application of eq. (4–4) a value of the matching factor has to be established from measured or estimated values of K_m and calculated values of K_c at a given value of the pressure potential. Several other methods exist for predicting the hydraulic conductivity function of soil. Recently fourteen methods were compared by Alexander and Skaggs (1986).

4.4 Richards equation

Darcy water flow

Flow of water in the unsaturated zone is assumed to be Darcy flow, eq. (4–5), and to take place in one dimension only. The positive direction of flow is assumed to be in the direction of decreasing gravitational potential.

$$q = -K \frac{\partial \varphi}{\partial z} \qquad (4-5)$$

q = Darcy flow velocity [$m^3m^{-2}s^{-1}$]
K = hydraulic conductivity [$m^2(m\ H_2O)^{-1}s^{-1}$]
φ = hydraulic potential $\psi - z$ [m H_2O]
z = distance in flow direction [m]

The hydraulic potential is assumed to consist of a gravitational potential and a pressure potential. Thus vertical flow can be described by eq. (4–6) in which ψ is pressure potential and the number 1 represents the gravitational term the unit of which in the present formulation is m H_2O m^{-1}.

$$q = -K\left(\frac{\partial \psi}{\partial z} - 1\right) \qquad (4-6)$$

For non–deformable soil and incompressible water the conservation of matter in one dimension is given by eq. (4–7).

$$\frac{\partial \theta}{\partial t} = -\frac{\partial q}{\partial z} - S \qquad (4-7)$$

θ = volumetric soil water content [m^3m^{-3}]
q = water flow [$m^3m^{-2}s^{-1}$]
S = volumetric sink term [$m^3m^{-3}s^{-1}$]
t = time [s]

Richards equation

By combination of eq. (4–6) and eq. (4–7) and introducing the specific water capacity eq. (4–8) is obtained which is designated as Richards equation (Richard 1931).

$$C_\theta \frac{\partial \psi}{\partial t} = \frac{\partial}{\partial z}\left[K \frac{\partial \psi}{\partial z}\right] - \frac{\partial K}{\partial z} - S \qquad (4-8)$$

$$C_\theta = \frac{d\theta}{d\psi} \quad \text{(Specific water capacity)}$$

It is noted that eq. (4–8) does not take preferential flow into account. The sink term S is described in section 4.7 in terms of extraction of soil water by plant roots. The influence of frost and thaw on soil water flow is described in section 4.8.

4.5 Evaporation from soil surface

Calculation of evaporation from soil surface

The evaporation from the soil surface is assumed to be determined by either the energy which can be utilized by evaporation or the transport of soil water to the soil surface. The energy which can be utilized by evaporation from soil surface is estimated as a fraction of the potential evapotranspiration (latent heat), eq. (4-9).

$$E_{p,s} = E_p \, e^{-K_c C_{ai}} \qquad (4-9)$$

$E_{p,s}$ = potential evaporation from soil surface [$m^3 \, m^{-2} \, s^{-1}$]
E_p = potential evapotranspiration above the crop canopy [$m^3 \, m^{-2} \, s^{-1}$]
C_{ai} = total crop area index [$m^2 \, m^{-2}$]
K_c = extinction coefficient (0.4-0.5)

The amount of soil water which can be transported to the soil surface is estimated from eq. (4-10). The gradient $\partial\theta/\partial z$ is estimated on the assumption that $\theta = 0$ at $z = 0$. The evaporation from the soil surface is then estimated from eq. (4-11). If ponding on the soil surface occurs then eq. (4-12) is used.

$$q_0^* = - \frac{K}{C_\theta} \frac{\partial\theta}{\partial z} \qquad (4-10)$$

q_0^* = Darcy flow velocity at soil surface [$m^3 m^{-2} s^{-1}$]

$$E_s = \text{Min} \{ E_{p,s}, - q_0^* \} \qquad (4-11)$$

$$E_s = E_{p,s} \qquad (4-12)$$

E_s = evaporation from soil surface [$m^3 m^{-2} s^{-1}$]

4.6 Boundary conditions

Upper boundary

In order to solve the Richards equation an upper as well as a lower boundary condition must be specified.

The upper boundary condition depends on the conditions at the surface. The present model operates with the following situations:

- a specified flux in or out of the soil surface (Neuman condition)
- a specified potential at the soil surface (Dirichlet condition)
- a specified flux at a specified depth (Neuman condition)

The first boundary condition specified is used when rain, irrigation or melting snow cause infiltration that does not exceed the infiltrability of the soil or when evaporation takes place from the surface.

The second boundary condition specified is used when water is ponding on the soil surface. This may occur when rain, irrigation or melting snow provides water at a rate which exceeds the infiltrability of the soil.

The third boundary condition specified is used when the Richards equation is not solved for the whole profile. This is often the case when freezing or thawing takes place.

Lower boundary

The lower boundary condition can be one of two conditions:

- a specified potential at a specified depth
- a specifiec flux at a specified depth

The first of the lower boundary conditions specified is used when the position of the ground water table is known. The second boundary condition specified is a free drainage condition assuming gravity flow.

4.7 Extraction of soil water by plant roots

The sink term in Richards equation

In Richards equation the extraction of soil water by plant roots is entered as a sink term, S, which is given by eq. (4 – 13).

$$S = L\,Q_r \qquad (4-13)$$

S = volumetric sink term [$m^3\ m^{-3}\ s^{-1}$]
L = root density [$m\ m^{-3}$]
Q_r = water uptake rate per unit length of root [$m^3 s^{-1} m^{-1}$]

In calculating Q_r it is assumed that water uptake only takes place where the root surface is in contact with soil water, eq. (4 – 14) and eq. (4 – 15).

$$Q_r = -\int_0^{2\pi} f_c(\omega) r_r v(r_r) d\omega$$

$$= -r_r v(r_r) \int_0^{2\pi} f_c(\omega) d\omega \qquad (4-14)$$

$$f_c(\omega) = \begin{cases} 0 & \text{if no contact} \\ 1 & \text{if contact} \end{cases} \qquad (4-15)$$

r_r = root radius [m]
$-v(r_r)$ = water flow velosity towards the root at the root surface [$m\ s^{-1}$]

It is now assumed that water flow to the root surface takes place as radial flow and that the flow pattern around the root can be estimated as a series of steady states. Hence conservation of mass in a small element located at the distance r from the center of the root is given by eq. (4 – 16).

$$\frac{d(r\Delta\omega v(r))}{dr} = 0 \qquad (4-16)$$

Water flow towards root surfaces

The flow velocity v(r) is estimated by eq. (4 – 17) by taking only the pressure potential into consideration.

$$v(r) = - K \frac{d\psi}{dr} \qquad (4-17)$$

Combining eq. (4 – 16) and eq. (4 – 17) results in eq. (4 – 18).

$$\frac{d}{dr} \left(rK \frac{d\psi}{dr} \right) = 0 \qquad (4-18)$$

This differential equation is solved with the boundary conditions

$\psi = \psi_r$ for $r = r_r$
$\psi = \psi_s$ for $r = r_s$

and the flow velocity is found from eq. (4 – 19).

$$v(r) = -\frac{1}{r} \frac{M(\psi_s) - M(\psi_r)}{\ln(r_s/r_r)} \qquad (4-19)$$

$$M(\psi) = \int_{\psi_0}^{\psi} K d\psi \qquad (4-20)$$

$$r_s = (\pi L)^{-½} \qquad (4-21)$$

$$\psi_s = \psi_z \qquad (4-22)$$

M = matrix flux potential [$m^2 s^{-1}$]

ψ_z = pressure potential of the bulk soil

It is noted that the matrix flux potential just is another hydraulic function characterizing the soil and that it can be calculated from the hydraulic conductivity function.

Estimation of the sink term in Richards equation

Furthermore, it is noted that this approximation of r_s represents the average half distance between roots. The pressure potential of water in the bulk soil, which is the pressure potential ψ_z that occurs in Richards equation, is selected to represent ψ_s because the potential drop which causes water to flow toward the roots for the largest part occurs very close to the root surface.

Combining eq. (4-14), eq. (4-19), and eq. (4-21) and setting $r = r_r$ eq. (4-23) is obtained.

$$Q_r = \frac{M(\psi_z) - M(\psi_r)}{-\frac{1}{2}\ln(r_r^2\pi L)} \int_0^{2\pi} f_c(\omega)d\omega \qquad (4-23)$$

The integral in eq. (4-14) represents a "relative contact area" and it is estimated from eq. (4-24).

$$\int_0^{2\pi} f_c(\omega)d\omega = \frac{\theta(\psi_r)}{\theta_s} \qquad (4-24)$$

$\theta(\psi_r)$ = volumetric water content at ψ_r
θ_s = volumetric water content at water saturation

The sink term is then estimated from eq. (4-25).

$$S = L \frac{\theta(\psi_r)}{\theta_s} \frac{M(\psi_z) - M(\psi_r)}{-\frac{1}{2}\ln(r_r^2\pi L)} \qquad (4-25)$$

It is assumed that L, r_r, ψ_z and hence $M(\psi_z)$ are known, while ψ_r and hence $\theta(\psi_r)$ and $M(\psi_r)$ are not known.

Two different situations can occur

- transpiration at a potential rate
- transpiration at a lower rate than the potential rate

Water uptake determined by climatical conditions

In the first situation it is the climatic conditions that determine the water uptake by the plants. In this situation it is assumed that a common hydraulic potential φ_r exists along the root. The task is then to find the value of the pressure potential ψ_r by iteration so that the condition expressed in eq. (4–26) is fulfilled.

$$E_t = \int_0^{z_r} S dz \qquad (4-26)$$

E_t = transpiration of the crop [m s^{-1}]
z_r = root depth [m]

Water uptake determined by soil water status

In the second situation it is assumed that it is the transport of water from the bulk soil to the root surface that determines the water uptake. In this case a common hydraulic potential along the root is assumed and the value of this common hydraulic potential is assumed to be equal to the pressure potential at the wilting point.

4.8 Water flow under frost or thaw conditions

Freezing induces soil water movement

When the soil begins to freeze ice is formed. It is assumed that the formation of ice takes place in the large pores of the soil resulting in a movement of water from the small to the large pores. This generates a lowering of the pressure potential in the freezing soil, which again often results in a movement of water from beneath the freezing zone. This in combination with the fact that water expands when it is freezing results in a lowering of the air content of the soil.

As long as air still is present in the soil it is assumed that the pressure potential can be found from the soil content of liquid water and vice versa by use of the soil water retention characteristic.

As the ice content of the soil increases the amount of liquid water required to establish a positive or zero pressure potential in the soil gets smaller and smaller because it is assumed that the ice occupies the more large pores in the soil. When the pressure potential in a freezing zone starts to become zero or positive the numerical procedure used in solving the Richards equation is no longer feasible. In this situation the Richards equation is no longer applied in and above the freezing zone instead a simple procedure is used in the upper zones. Eq. (4 – 7) is still used, but q is approximated with gravity flow, eq. (4 – 27).

$$q = K \qquad (4-27)$$

This procedure is then used until the soil is no longer frozen and air has entered the soil. The hydraulic conductivity K in eq. (4 – 27) is estimated as the K at the liquid water content present in the soil.

Below the zone where eq. (4 – 27) is used the Richard equation is solved with a specified flux at a specified depth as upper boundary condition.

4.9 Numerical solution

The finite difference method

The finite difference scheme used in the numerical approximation to the Richards equation (eq 4 – 8) is illustrated in Fig. 4 – 1.

All nodes in the time – distance plan are numbered with the subscript j referring to the depth and the superscript i referring to the time (i = 0 is referring to the time of initialization). The time increments as well as the depth increments may vary. The numeric method used is adopted from Jensen (1983) where it was proved efficient in solving Richards equation.

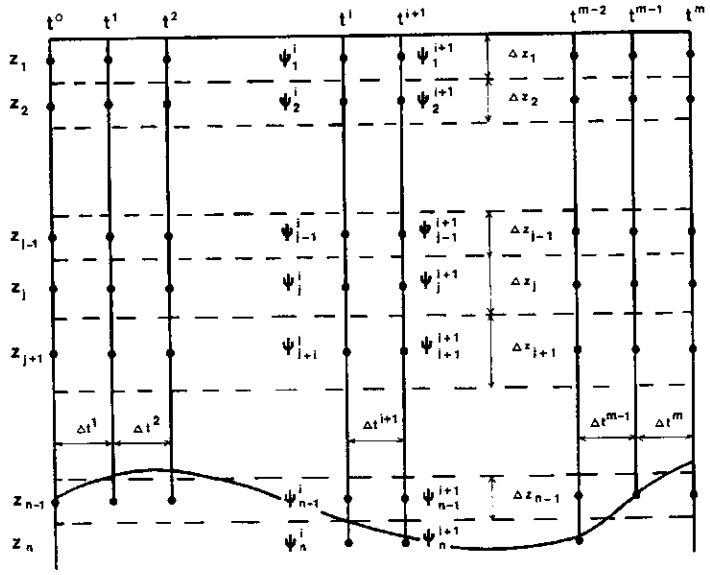

Fig. (4-1) Discretization after the finite difference method.

The Richards equation, eq. (4-8), is approximated by eq. (4-28).

$$C_j^{i+\frac{1}{2}} \frac{\psi_j^{i+1} - \psi_j^i}{\Delta t^{i+1}} =$$

$$\frac{K_{j+\frac{1}{2}}^{i+\frac{1}{2}} \frac{\psi_{j+1}^{i+1} - \psi_j^{i+1}}{z_{j+1} - z_j} - K_{j+\frac{1}{2}}^{i+\frac{1}{2}} - K_{j-\frac{1}{2}}^{i+\frac{1}{2}} \frac{\psi_j^{i+1} - \psi_{j-1}^{i+1}}{z_j - z_{j-1}} + K_{j-\frac{1}{2}}^{i+\frac{1}{2}}}{\Delta z_j} - S_j^i \qquad (4-28)$$

The superscript $i+\frac{1}{2}$ refers to values centered in time and the subscripts $j+\frac{1}{2}$ and $j-\frac{1}{2}$ refer to values centered in space. It is noted only that the coefficients C and K are centered in time while the values of ψ are put forward in time (explicit formulation).

The C and K values are found by iteration. Jensen (1983) found that this formulation resulted in only insignificant deviations from a Crank-Nicolson formulation of the problem (also ψ values centered in time). Furthermore, the explicit formulation resulted in fewer iterations.

Eq. (4-28) can be rearranged to give eq.(4-29) - eq.(4-33)

$$a_j^{i+1}\,\psi_{j-1}^{i+1} + b_j^{i+1}\,\psi_j^{i+1} + c_j^{i+1}\,\psi_{j+1}^{i+1} = d_j^{i+1} \qquad (4-29)$$

$$a_j^{i+1} = -\frac{K_{j-\frac{1}{2}}^{i+\frac{1}{2}}}{(z_j - z_{j-1})\Delta z_j} \qquad (4-30)$$

$$b_j^{i+1} = \frac{C_j^{i+\frac{1}{2}}}{\Delta t^{i+1}} + \frac{K_{j-\frac{1}{2}}^{i+\frac{1}{2}}}{(z_j - z_{j-1})\Delta z_j} + \frac{K_{j+\frac{1}{2}}^{i+\frac{1}{2}}}{(z_{j+1} - z_j)\Delta z_j} \qquad (4-31)$$

$$c_j^{i+1} = -\frac{K_{j+\frac{1}{2}}^{i+\frac{1}{2}}}{(z_{j+1} - z_j)\Delta z_j} \qquad (4-32)$$

$$d_j^{i+1} = \frac{C_j^{i+\frac{1}{2}}}{\Delta t^{i+1}}\,\psi_j^i - \frac{K_{j+\frac{1}{2}}^{i+\frac{1}{2}} - K_{j-\frac{1}{2}}^{i+\frac{1}{2}}}{\Delta z_j} - S_j^i \qquad (4-33)$$

Eq. (4-29) - Eq. (4-33) is valid for the interior nodes in the distance discretization. Special attention must be drawn to the conditions at the uppermost and lowermost node. If ice is present in the soil uppermost node Eq. (4-29) - Eq.(4-33) may be a lower node than node 1. If the upper boundary condition is a flux condition Eq. (4-8) can be approximated by eq. (4-34).

$$C_J^{i+\frac{1}{2}}\,\frac{\psi_J^{i+1} - \psi_J^i}{\Delta t^{i+1}} =$$

$$\frac{K_{J+\frac{1}{2}}^{i+\frac{1}{2}}\,\dfrac{\psi_{J+1}^{i+1} - \psi_J^{i+\frac{1}{2}}}{z_{J+1} - z_J} - K_{J+\frac{1}{2}}^{i+\frac{1}{2}} + q_{J-\frac{1}{2}}^{i+1}}{\Delta z_J} - S_J^i \qquad (4-34)$$

The value of $q_{J-\frac{1}{2}}^{i+1}$ is the flux entering the system. If J = 1, that is at the top of the soil, then $q_{J-\frac{1}{2}}^{i+1}$ can be either the evaporation rate at the surface or the infiltration rate. If J > 1, then $q_{J-\frac{1}{2}}^{i+1}$ is the percolation coming from the node above node J.

Eq. (4-34) can be rearranged to give eq.(4-35) - eq.(4-38).

$$b_J^{i+1}\,\psi_J^{i+1} + c_J^{i+1}\,\psi_{J+1}^{i+1} = d_J^{i+1} \qquad (4-35)$$

$$b_J^{i+1} = \frac{C_J^{i+\frac{1}{2}}}{\Delta t^{i+1}} + \frac{K_{J+\frac{1}{2}}^{i+\frac{1}{2}}}{(z_{J+1} - z_J)\Delta z_J} \qquad (4-36)$$

$$c_J^{i+1} = -\frac{K_{J+\frac{1}{2}}^{i+\frac{1}{2}}}{(z_{J+1} - z_J)\Delta z_J} \qquad (4-37)$$

$$d_J^{i+1} = \frac{C_J^{i+\frac{1}{2}}}{\Delta t^{i+1}}\psi_J^i - \frac{K_{J+\frac{1}{2}}^{i+\frac{1}{2}} - q_{J-\frac{1}{2}}^{i+1}}{(z_{J+1} - z_J)\Delta z_J} - S_J^i \qquad (4-38)$$

If the upper boundary condition is a potential condition, water is ponding at the surface, then eq. (4-39) is applied.

$$\psi_1^{i+1} = z_1 \qquad (4-39)$$

In this case the number of equations to be solved is consequently reduced by one and eq. (4-28) can be solved if the lower boundary condition is known.

If the lower boundary condition is a flux condition, that is gravity flow is assumed at the bottem, then at the lowest computational node N is approximated by eq. (4-40).

$$C_N^{i+\frac{1}{2}} \frac{\psi_N^{i+1} - \psi_N^i}{\Delta t^{i+1}} =$$

$$\frac{-K_N^i - K_{N-\frac{1}{2}}^{i+\frac{1}{2}} \frac{\psi_N^{i+1} - \psi_{N-1}^{i+1}}{z_N - z_{N-1}} + K_{N-\frac{1}{2}}^{i+\frac{1}{2}}}{\Delta z_N} - S_N^i \qquad (4-40)$$

Rearranging eq. (4-40) results in eq. (4-41) - eq. (4-44).

$$a_N^{i+1} \psi_{N-1}^{i+1} + b_N^{i+1} \psi_N^{i+1} = d_N^{i+1} \qquad (4-41)$$

$$a_N^{i+1} = - \frac{K_{N-\frac{1}{2}}^{i+\frac{1}{2}}}{(z_N - z_{N-1})\Delta z_N} \qquad (4-42)$$

$$b_N^{i+1} = \frac{C_N^{i+\frac{1}{2}}}{\Delta t^{i+1}} + \frac{K_{N-\frac{1}{2}}^{i+\frac{1}{2}}}{(z_N - z_{N-1})\Delta z_N} \qquad (4-43)$$

$$d_N^{i+1} = \frac{C_N^{i+\frac{1}{2}}}{\Delta t^{i+1}} \psi_N^i - \frac{K_N^i - K_{N-\frac{1}{2}}^{i+\frac{1}{2}}}{\Delta z_N} - S_N^i \qquad (4-44)$$

If the lower boundary condition is a potential condition, a groundwater condition, then the lowest computational node, N+1, will be the first node below the groundwater table and the potential at this node is estimated as from eq. (4-45).

$$\psi_{N+1}^{i+1} = z_g - z_{N+1} \qquad (4-45)$$

z_g = depth of groundwater below the surface [m]

Also in this case the number or equations to be solved are consequently reduced by one.

The numerical solution of eq. (4-8) can now be formulated as a matrix equation, eq. (4-46).

$$\bar{H} \cdot \bar{\psi} = \bar{D} \tag{4-46}$$

$$\bar{H} = \begin{bmatrix} b_J & c_J & & & & \\ a_{J+1} & b_{J+1} & c_{J+1} & & & \\ & a_{J+2} & b_{J+2} & c_{J+2} & & \\ & & & & & \\ & & & a_{N-1} & b_{N-1} & c_{N-1} \\ & & & & a_N & b_N \end{bmatrix} \tag{4-47}$$

$$\bar{\psi} = \begin{bmatrix} \psi_{J+1}^{i+1} \\ \psi_{J+2}^{i+1} \\ \psi_{J+2}^{i+1} \\ \\ \psi_{N-1}^{i+1} \\ \psi_N^{i+1} \end{bmatrix} \tag{4-48}$$

$$\bar{D} = \begin{bmatrix} d_J \\ d_{J+1} \\ d_{J+2} \\ \\ d_{N-1} \\ d_N \end{bmatrix} \tag{4-49}$$

The elements in the $\bar{H}$ and $\bar{D}$ matrix for the nodes J+1 to N-1 are calculated from eq. (4-30) - eq. (4-33).

For node J the calculations of the elements in the $\bar{H}$ and $\bar{D}$ matrix depend on the type of the upper boundary condition.

If the upper boundary condition is a flux condition then b_j, c_j, and d_j are calculated from eq. (4-36), eq. (4-37), and eq. (4-38), respectively.

If the upper boundary condition is a potential condition then $J=1$ and b_1 and c_1 are calculated from eq. (4-36) and eq. (4-37), respectively, while d_1 is calculated from eq. (4-50).

$$d_1 = d_1^{i+1} - a_1^{i+1} z_1 \qquad (4-50)$$

The values of d_1^{i+1} and a_1^{i+1} in eq. (4-50) are calculated from eq. (4-38) and eq. (4-39), respectively.

If the lower boundary condition is a flux condition then a_N, b_N, and d_N are calculated from eq. (4-42, eq. (4-43), and eq. (4-44), respectively.

If the lower boundary condition is a potential condition then a_N and b_N are calculated from eq. (4-30) and eq. (4-31), respectively, while d_N is calculated from eq. (4-51).

$$d_N = d_N^{i+1} - c_N^{i+1} \psi_{N+1}^{i+1} \qquad (4-51)$$

The values of d_N^{i+1} and c_N^{i+1} are calculated from eq. (4-37) and eq.(4-32), respectively. ψ_{N+1}^{i+1} is given by eq. (4-45).

It appears that $\bar{H}$ constitutes a tridiagonal matrix hence the matrix equation (4-46) can be solved by the double-sweep-method, where the solution involves two calculations in opposite directions.

Introducing two auxiliary variables e_j and f_j the backword subsitution gives

$$e_{j-1} = \frac{a_{j-1}}{b_{j-1} - c_{j-1} e_j} \qquad (4-52)$$

$$f_{j-1} = \frac{d_{j-1} - c_{j-1} f_j}{b_{j-1} - c_{j-1} e_j} \qquad (4-53)$$

In the calculation of e_{j-1} and f_{j-1}

$$a_J^{i+1} = 0,\ c_N^{i+1} = 0,\ e_N = \frac{a_N}{b_N^{i+1}} \text{ and } f_n = \frac{d_n}{b_n}$$

The forward substitution starting with node J gives

$$\psi_j^{i+1} = f_j \qquad (4-54)$$

and for the following nodes

$$\psi_j^{i+1} = f_j - e_j \psi_{j-1}^{i+1} \qquad (4-55)$$

Since $C_j^{i+½}$ and $K_j^{i+½}$ in the finite difference approximation are dependent on the actual value of ψ_j^{i+1} the solution has to be obtained by an iterative procedure.

At the beginning of a time step $C_j^{i+½}$ and $K_j^{i+½}$ assume values corresponding to ψ_j^i. These values are introduced in the finite difference scheme and a new set of ψ_j^{i+1} can be found. A new set of $C_j^{i+½}$ and $K_j^{i+½}$ is estimated and a new set of ψ_j^{i+1} values is found. The procedure is continued until the diviation between new and former solution is small, that is until convergence is found.

Convergence is assumed to occur if one of the following two criteria is fulfilled, eq. (4-56) and eq. (4-57).

$$\left| \frac{\psi_j^{i+1}(M) - \psi_j^{i+1}(M-1)}{\psi_j^{i+1}(M-1)} \right| < \varepsilon_1 \text{ for all j} \qquad (4-56)$$

or

$$\left| \psi_j^{i+1}(M) - \psi_j^{i+1}(M-1) \right| < \varepsilon_2 \text{ for all j} \qquad (4-57)$$

$\psi_j^{i+1}(M)$ represents the solution to the interactive step M and $\psi_j^{i+1}(M-1)$ the solution obtained at the former step.

If convergence is not found within a specified number of iterative steps then the time step Δt^{i+1} is made 4 times shorter and the calculations are restarted.

If convergence still is not found then the time step is once again made 4 times shorter and the calculations are restarted. This procedure is repeated a specified number of times.

If convergence still is not found then the calculation continues without convergence.

A key point in the numeric procedure is how the time averaging of $C_j^{i+½}$ and $K_j^{i+½}$ is done. Jensen (1983) found that the following procedure had a stabilizing effect on the numerical solution

$$C_j^{i+½} = \frac{1}{2}\left[C_\theta\,(\psi_j^{i+1}\,(M)) + \frac{1}{M}\sum_{m=1}^{M} C_\theta\,(\psi_j^{i+1}\,(m)) \right] \qquad (4-58)$$

$$K_j^{i+½} = \frac{1}{2}\left[K_\theta\,(\psi_j^{i+1}\,(M)) + \frac{1}{M}\sum_{m=1}^{M} K_\theta\,(\psi_j^{i+1}\,(m)) \right] \qquad (4-59)$$

M = iterations within the current timestep
$C_\theta\,(\psi)$ = specific water capacity function [$m^3\ m^{-3}\ (m\ H_2O)^{-1}$]
$K_\theta\,(\psi)$ = hydraulic conductivity function [$m\ s^{-1}$]

Another key point in the numeric procedure is how the spatial averaging of $C_{j+½}^{i+½}$ and $K_{j+½}^{i+½}$ is done.

For $C_{j+½}^{i+½}$ a simpel aritmetric mean is used

$$C_{j+½}^{i+½} = ½(C_j^{i+½} + C_{j+1}^{i+½}) \qquad (4-60)$$

Regarding the spatial averaging of $K_{j+½}^{i+1}$ a number of methods can be found in the litterature. Jensen (1983) investigated two different methods, an aritmetric mean and a geometric mean, and he found that when water uptake by plants was included in the model the aritmetric mean was the most appropriate. Because hysteresis is not included in the model it seems that it simulates too large a capillary rise, therefore the value of $K_{j+½}^{i+1}$ may be estimated from eq. (4-61).

$$K_{j+½}^{i+1} = K_j^{i+1} \tag{4-61}$$

However, the artimetric mean can also be used, eq. (4-62)

$$K_{j+½}^{i+1} = ½(K_j^{i+1} + K_{j+1}^{i+1}) \tag{4-62}$$

A major problem in connection with the numerical solution of Richards equation is whether the hydraulic functions used are representative. Often a drying curve is used to characterize soil water retention. However, such a representation may result in too high water contents in a wetting situation and also tend to overestimate capillary rise in the presence of a shallow ground water table. For that reason eq. (4-61) is often used instead of eq. (4-62).

5. SOIL TEMPERATURE MODEL

5.1 Introduction

The importance of soil temperature

Soil temperature is a factor of primary importance for several processes related to transformation and transport of matter in the soil plant atmosphere system. In particular temperature strongly influences biological processes such as root growth and microbial transformation of carbon and nitrogen in soil. Thus a soil temperature model has been developed to provide soil temperature for abiotic functions governing several biological processes described in other submodels of DAISY.

Soil temperature profile

Soil temperature varies in response to changes in the radiant, thermal and latent energy exchange processes which take place primarily through the soil surface. The effects of these phenomena are propagated into the soil profile by a complex series of processes, the rate of which is affected by time-variable and space variable of soil properties. The pertinent soil parameters include heat capacity and thermal conductivity both of which are strongly affected by soil texture, soil mineralogy, soil bulk density and soil water content.

Heat flow by conduction and convection

The present soil temperature model is based upon the one dimensional heat flow equation which takes into account heat flow due to conduction and convection. Furthermore the heat flow equation is expanded to include frost as well as thaw processes. The thermal parameters of soil are calculated on the basis of the composition of the soil and the properties of the individual soil constituents. In this approach it is a basic assumption that each small unit cell of soil contains a representative sample of soil constituents.

5.2 Heat capacity of soil

Heat capacity of soil constituents

The volumetric heat capacity of a unit cell of soil can be found by addition of the heat capacity of the various constituents of the soil.

$$C_s = x_m \rho_m c_m + x_o \rho_o c_o + x_w \rho_w c_w + x_i \rho_i c_i + x_a \rho_a c_a \qquad (5-1)$$

Symbols:

C_s = volumetric heat capacity [K m^{-3} °C^{-1}]
c = specific heat capacity [J kg^{-1} °C^{-1}]
ρ = density [kg m^{-3}]
x = fraction

Subscript:
a = air
m = mineral particles
o = organic particles
w = liquid water
i = ice

$$x_m + x_o + x_w + x_i + x_a = 1$$

The specific heat capacity and the density of different soil constituents are given in Table (5-1).

Most soil minerals have about the same densities and specific heats (de Vries, 1963) therefore the different soil mineral constituents are taken together. From Table 5-1 it is evident that the contribution of air to the volumetric heat capacity of the soil can be neglected.

Table 5 – 1 Density (ρ), specific heat capacity (c), and thermal conductivity (K) of different soil constituents. Water and air at 10°C (de Vries, 1963).

Soil constituent	ρ kg m^{-3}	c J kg^{-1} °C^{-1}	K W m^{-1} °C^{-1}
Quarts	2660	750	8.8
Clay minerals	2650	750	2.9
Organic matter	1300	1920	0.25
Water	1000	4192	0.57
Ice	920	2050	2.2
Air	1.25	1005	0.025

5.3 Thermal conductivity of soil

Thermal conductivity of soil constituents

In Table 5 – 1 the thermal conductivity of various soil constituents is given. It appears that large differences in thermal conductivity exist. The thermal conductivity of a soil depends on its composition, i.e. the fractions of its different constituents, but the dependence is a very complex one. At complete dryness the heat flow passes mainly through the grains, but it has to bridge the air – filled gaps between the grains around their contact points. When water is present it starts to fill these gaps. Because of the large difference in thermal conductivity between air and water the thermal conductivity of the soil depends heavily on the water content of the soil, especially in relative dry situations when bridges are being formed.
De Vries (1952, 1963) has developed a physical based model for calculating the thermal conductivity of a soil on basis of its constituents. The model is based on an analogy to the physical problems of expressing the electric conductivity or the dielectric constant of a granular material as a function of the volume fractions and the respective physical properties of its constituents. This analogous problem was solved mathematically by Burger (1919).

Model for thermal conductivity of soil

The basic ideas of the model shall be outlined here. Consider a volume V consisting of a continous medium, with the volume fraction x_o and the thermal conductivity K_o, in which N different types of granular materials, with the volume fractions x_i and the thermal conductivities K_i are dispersed. The average heat flow through the volume can be calculated from eq. (5-3).

$$\mathbf{q}_h = \frac{1}{V}\int \mathbf{q}dV = \frac{1}{V}\int -K\mathbf{G}dV \qquad (5-3)$$

$\mathbf{q}_h$ = average heat flow vector
$\mathbf{q}$ = local heat flow vector
K = local thermal conductivity
$\mathbf{G}$ = local thermal gradient vector

Assuming that in the same material the same gradient exists throughout the volume then the average heat flux can be calculated from Eq. (5-4).

$$\mathbf{q}_h = \sum_{i=0}^{N} x_i K_i \mathbf{G}_i \qquad (5-4)$$

x_i = volume fraction of material i
K_i = thermal conductivity of material i
$\mathbf{G}_i$ = thermal gradient in material i

Introducing an apparent thermal conductivity K_h the average heat flow through the volume can be calculated from eq. (5-5).

$$\mathbf{q}_h = -K_h \cdot \mathbf{G}_v \qquad (5-5)$$

$\mathbf{G}_v$ = average thermal gradient given by eq. (5-6).

$$\mathbf{G}_v = \frac{1}{V}\int \mathbf{G}dV = \sum_{i=0}^{N} x_i \mathbf{G}_i \qquad (5-6)$$

Combining Eqs. (5–4), (5–5) and (5–6) results in eq. (5–7).

$$K_h \sum_{i=0}^{N} x_i \mathbf{G}_i = \sum_{i=0}^{N} x_i K_i \mathbf{G}_i \qquad (5-7)$$

Considering the flow in the **e** direction ($|\mathbf{e}| = 1$) eq. (5–8) is obtained.

$$K_h \sum_{i=0}^{N} x_i \mathbf{G}_i \cdot \mathbf{e} = \sum_{i=0}^{N} x_i K_i \mathbf{G}_i \cdot \mathbf{e}$$

or

$$K_h = \frac{\sum_{i=0}^{N} x_i K \mathbf{G}_i \cdot \mathbf{e}}{\sum_{i=0}^{N} x_i \mathbf{G}_i \cdot \mathbf{e}} = \frac{x_0 K_0 + \sum_{i=1}^{N} f_i x_i K_i}{x_0 + \sum_{i=1}^{N} f_i x_i} \qquad (5-8)$$

$$f_i = \frac{\mathbf{G}_i \cdot \mathbf{e}}{\mathbf{G}_0 \cdot \mathbf{e}}$$

The value of f_i depends on the ratio (K_i/K_0), on the size and shape of the granules, and on their relative positions. A mathematical expression for f_i can be found under the following restictions

- the granules are of ellipsoidal shape
- the granules are so far apart that they do not interact

For a grain in form of an ellipsoid with principal axes a_1, a_2, a_3 eq. (5–9) and eq. (5–10) are derived for a temperature gradient in the direction a_j (Burger, 1919).

$$f_{ij} = \left[1 + \left(\frac{K_i}{K_0} - 1\right) g_j\right]^{-1} \qquad (5-9)$$

$$g_j = \tfrac{1}{2} a_1 a_2 a_3 \int_0^{\infty} [(a_1^2+u)(a_2^2+u)(a_3^2+u)]^{-\frac{1}{2}} (a_j^2+u)^{-1} du \qquad (5-10)$$

In the theory of the dielectric constant the quantity g_j is called the depolarisation factor of the ellipsoid in the direction of the a_j-axis. In the theory of thermal heat conduction g_j is often called the shape factor (de Vries, 1952, 1953). The value of g_j depends on the ratios of the principal axes (a_j), but not on their absolute value.

$$g_1 + g_2 + g_3 = 1 \qquad (5-11)$$

If the ellipsoidal granulas are randomly orientated then f_i is given by eq. (5-12).

$$f_i = \sum_{j=1}^{3} f_{ij} \qquad (5-12)$$

For a spheroid with the axes $a_1 = a_2 = \alpha a_3$ resulting in eq. (5-13).

$$g_1 = \tfrac{1}{2}\alpha^2 a_3^3 \int_0^\infty ((\alpha a_3)^2+u)^{-2}(a_3^2+u)^{-\frac{1}{2}}du$$

$$= \tfrac{1}{2}\alpha^2 \int_0^\infty \frac{dV}{(\alpha^2+V)^2\,(1+V)^{\frac{1}{2}}} \qquad (5-13)$$

For $\alpha < 1$ (oblate spheroid)

$$g_1 = \tfrac{1}{2}\frac{\alpha^2}{(1-\alpha^2)}\left[\frac{1}{\alpha^2} + \frac{1}{2(1-\alpha^2)^{\frac{1}{2}}}\ln\left(\frac{1-(1-\alpha^2)^{\frac{1}{2}}}{1+(1+\alpha^2)^{\frac{1}{2}}}\right)\right] \qquad (5-14a)$$

For $\alpha = 1$ (spherical granulas)

$$g_1 = 1/3 \qquad (5-14b)$$

For $\alpha > 1$ (prolate spheroid)

$$g_1 = \tfrac{1}{2} \frac{\alpha^2}{(\alpha^2-1)} \left[\frac{\pi}{2(\alpha^2-1)^{1/2}} - \frac{1}{\alpha^2} - \frac{1}{(\alpha^2-1)^{1/2}} \operatorname{arctg}((\alpha^2-1)^{-1/2}) \right] \tag{5-14c}$$

For all three cases:

$$g_2 = g_1 \tag{5-15}$$

$$g_3 = 1 - 2g_1 \tag{5-16}$$

For elongated cylinders with elliptical cross section:

$$a_1 = m\, a_2 \tag{5-17a}$$

$$a_3 = \infty \tag{5-17b}$$

$$g_1 = \frac{1}{m+1} \tag{5-17c}$$

$$g_2 = \frac{m}{m+1} \tag{5-17d}$$

$$g_3 = 0 \tag{5-17e}$$

For flat particles with small thickness, lamellae:

$$a_2 = a_3 = \infty \tag{5-18a}$$

$$g_1 = 1 \tag{5-18b}$$

$$g_2 = g_3 = 0 \tag{5-18c}$$

Use of the model

For solid soil particles the spheroid model with an α–value around 4 often can be used (de Vries, 1963). In moist soils water can be considered as a continous medium in which soil particles and air voids are dispersed. We use water as the continous medium down to the soil water content corresponding to half way between field capacity (pF = 2.0) and wilting point (pF = 4.2). De Vries (1963) states "In moist soils water can be considered as a continous medium, in which soil particles and air voids are dispersed, for moisture contents ranging from saturation to well below the field capacity". In dry soils air can be considered as the continous medium. We use air as the continous medium up to the soil water content at pF = 4.2. In the region between soil water content half way between field capacity and the wilting point, the thermal conductivity is found by interpolation.

In most soils heat transfer in the air filled pore space does not only take place as thermal conduction, but also as latent heat, i.e. transfer of heat by diffusion of water vapour in the soil air. The transfer of energy as latent heat is highly dependent on the soil temperature. At 0°C the transfer of heat by conduction and by vapour diffusion is of the same order of magnitude. The influence on the transfer of heat as latent heat is taken into account by substituting the thermal conductivity of the air by an apparent conductivity, eq. (5–19).

$$K'_a = K_a + K_v \qquad (5-19)$$

K'_a = apparent thermal conductivity of soil air [W m^{-1} $°C^{-1}$]
K_a = thermal conductivity of soil air [W m^{-1} $°C^{-1}$]
K_v = thermal conductivity due to vapour transfer [W m^{-1} $°C^{-1}$]

At moisture contents below the wiltning point the liquid is held by adsorption forces and the relative humidity is becoming

considerably less than 1. Then the transfer of heat by water vapour is restricted. We assume that the thermal conductivity due to vapour diffusion can be estimated from eq. (5–20).

$$K_V = \begin{cases} K_V^S \, \theta/\theta_{wp} & \text{for } \theta < \theta_{wp} \\ K_V^S & \text{for } \theta \geq \theta_{wp} \end{cases} \qquad (5-20)$$

K_V^S = thermal due to vapour diffusion under saturated conditions [W m^{-1} °C]

θ = volumetric soil water content [m^3 m^{-3}]

θ_{wp} = volumetric soil water content at pF = 4.2 [m^3 m^{-3}]

We have used the value 0.04 W m^{-1}°C^{-1} for K_V^S, which is a reasonable value at a temperature around 10°C (de Vries, 1963).

Calculations with water as continuous medium

When the soil is near water saturation soil air forms spherical voids. The influence of the shape factor (g) on the parameter (f) is illustrated in Fig. 5–1. The minimum influence occurs when $g_1 = g_2 = g_3 = 1/3$. As the water content of the soil decreases air replaces water and subsequently the f–values increase. As it may be seen from Fig. 5–1 this occurs at decreasing values of g_1. It is assumed that the g–values assume values which correspond to an oblate spheroid with an α–value of the order of 10 ($g_1 = 0.07$) at a soil water content which corresponds to pF = 4.2. By assuming a linear relation between g_1 and x_a in the region of water content between the saturated condition and pF 4.2 eq. (5–21) is obtained.

$$g_1 = 0.333 - (0.333 - 0.070) \frac{x_a}{\theta_s - \theta_{wp}} \qquad (5-21)$$

θ_s = saturation water content.

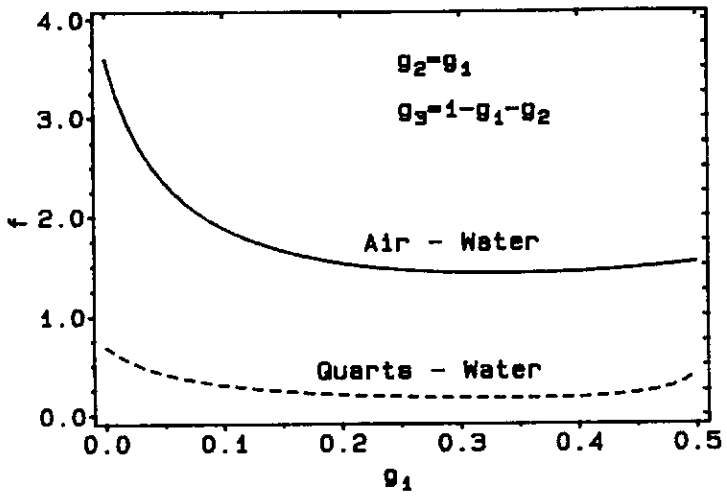

Fig. 5–1 Relationships between the parameter f and the shape factor g_1 for systems with water as the continuous medium and with air and granular of quarts, respectively, as dispersed material.

Furthermore it is assumed that $g_2 = g_1$ and subsequently that $g_3 = 1 - 2g_1$. It is noted that the relation only is used down to a water content corresponding to half way between field capacity (pF = 2) and wilting point (pF = 4.2).

Calculation with air as continuous medium

In the dry situation when air can be considered as the continuous medium the water, which is present, forms a thin film covering the soil particles and forms small water rings around the contact points of the particles and in a way forms bridges for the heat flow. It is assumed that water has a maximum contribution to the heat transfer. This is obtained by setting $g_1 = 1$ and $g_2 = g_3 = 0$ which corresponds to flat particles with small thickness.

Calculations for frozen soil

When the moisture content is below what corresponds to pF 4.2 the same curve is used as in the unfrozen situation. At higher water contents the calculations are performed as in the unfrozen case, but the thermal properties of water is now substituted by the thermal properties of ice. In the frozen situation ice forms the bridges between the solid soil particles instead of liquid water.

De Vries (1952, 1963) has tested the model with good results. He concludes that the accuracy of the estimates is better than 10% in most cases. Kimball et al. (1976) have used de Vries theory in calculating soil–heat fluxes in a field of Avondale loam in Arizona. They compared the calculated values with experimental ones. They concluded that "a fair agreement between measured and computed fluxes was obtained only after modyfying the air shape factor curve and ignoring heat transfer due to water vapour movement". Kimball et al. (1976) included the variation of K_v^s with temperature. They considered water as the continuous medium over the whole range between oven dry soil and water saturated soil and they used the air shape factor proposed by de Vries (1963). We use air as the continuous medium in the dry region (soil water content below the wilting point) and in the intermediate region (soil water content between the wilting point and half way between the wilting point and the field capacity) thermal conductivity is found by interpolation.

Sepaskhah and Boersma (1979) tested de Vries model for loamy sand, loam, and silty clay loam soils. They found that the model could be used satisfactorily to predict the thermal conductivity of the soil. Hopmans and Dane (1986) also found that de Vries model could be used satisfactorily to predict the thermal conductivity of the soil as the calculated and measured values were within 10%.

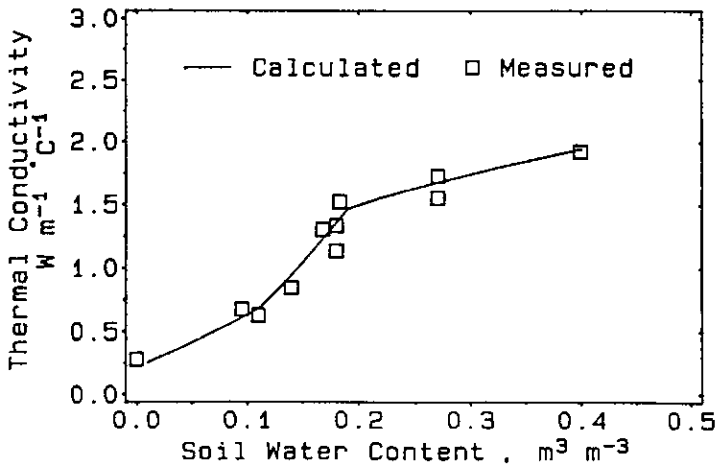

Fig. 5-2 Measured and calculated thermal conductivity of soil related to soil water content.

For comparing calculated and experimental values of thermal conductivity of soil we used the de Vries model assuming a porosity of 40%, a quarts fraction of 30%, a fraction of other minerals 27% and an organic fraction of 3%. We further assumed that the form factor of solid particles (quarts and other minerals) corresponded to spheriodes with an α-value equal to 3.5 (eq. (5-4c)) and that the form factor of the organic material corresponded to elongated cylinders with elliptical cross section (m = 3 in eq. (5-16)). The field capacity is 0.27 and the wilting point is 0.11. The results are shown in Fig. 5-2 together with experimental data obtained by Mogensen (1969).

5.4 Heat flow equations

The one dimensional heat flow equation

One dimensional combined heat flow due to conduction and convection is given by eq. (5-22).

$$q_h = -K_h \frac{\partial T}{\partial z} + c_w T q_w \qquad (5-22)$$

q_h = heat flux density [W m^{-2}]
K_h = thermal conductivity [W m^{-1} °C^{-1}]
T = temperature [°C]
z = depth [m]
c_w = specific heat capacity of water [J kg^{-1} °C^{-1}]
q_w = water flux density [kg m^{-2} s^{-1}]

Conservation of heat is expressed in eq. (5-23)

$$\frac{\partial H}{\partial t} = - \frac{\partial q_h}{\partial z} + S_h \qquad (5-23)$$

H = heat content of soil [J m^{-2}]
t = time [s]
S_h = heat source [J m^{-2} s^{-1}]

When frost and thaw are included the change in heat content can be expressed by eq. (5-24).

$$\frac{\partial H}{\partial t} = \frac{\partial (C_s T)}{\partial t} - L_m \rho_i \frac{\partial x_i}{\partial t}$$

$$= C_s \frac{\partial T}{\partial t} + \frac{\partial C_s}{\partial t} T - L_m \rho_i \frac{\partial x_i}{\partial t} \qquad (5-24)$$

C_s = volumetric heat capacity of soil [J m^{-3} °C^{-1}]
L_m = latent heat of melting [J kg^{-1}]
ρ_i = density of ice [kg m^{-3}]
x_i = volumetric ice content

The change in volumetric heat capacity can be expressed as eq. (5-25).

$$\frac{\partial C_s}{\partial t} = \rho_w c_w \frac{\partial x_w}{\partial t} + \rho_i c_i \frac{\partial x_i}{\partial t} + \rho_a c_a \frac{\partial x_a}{\partial t} \qquad (5-25)$$

Water can be present in soil as liquid water and ice, eq. (5-26).

$$\rho_w \theta = \rho_w x_w + \rho_i x_i \qquad (5-26)$$

$\rho_w \theta$ = amount of water in the soil [kg m^{-3}]

From eq. (5-26) eq. (5-27) is obtained.

$$\frac{\partial \theta}{\partial t} = \frac{\partial x_w}{\partial t} + \frac{\rho_i}{\rho_w} \frac{\partial x_i}{\partial t} \qquad (5-27)$$

Conservation of matter (ice plus liquid water) results in eq. (5-28).

$$\rho_w \frac{\partial \theta}{\partial t} = - \frac{\partial q_w}{\partial z} - \rho_w S_w \qquad (5-28)$$

S_w = volumetric water sink [$m^3\ m^{-3}\ s^{-1}$]

Combining eq. (5-27) and eq. (5-28) results in eq. (5-30).

$$\frac{\partial x_w}{\partial t} + \frac{\rho_i}{\rho_w} \frac{\partial x_i}{\partial t} = - \frac{1}{\rho_w} \frac{\partial q_w}{\partial z} - S_w \qquad (5-30)$$

Neglecting the influence of soil air on the heat capacity and introducing eq. (5-25) and eq. (5-30) in eq. (5-24) eq. (5-31) is obtained.

$$\frac{\partial H}{\partial t} = C_s \frac{\partial T}{\partial t} - [L_m + (c_w - c_i)T] \rho_i \frac{\partial x_i}{\partial t} - c_w \frac{\partial q_w}{\partial z} T - c_w \rho_w S_w \quad (5-31)$$

Since $(c_w - c_i)T \ll L_m$ when soil is freezing or thawing

$$\frac{\partial H}{\partial t} = C_s \frac{\partial T}{\partial t} - L_m \rho_i \frac{\partial x_i}{\partial t} - c_w \frac{\partial q_w}{\partial z} T - c_w \rho_w S_w T \quad (5-32)$$

Assuming that $S_h = -c_w \rho_w S_w T$ and introducing eq. (5-22) and eq. (5-32) in eq. (5-23) eq. (5-33) is obtained.

$$C_s \frac{\partial T}{\partial t} - L_m \rho_i \frac{\partial x_i}{\partial t} - c_w \frac{\partial q_w}{\partial z} + S_h = \frac{\partial q_h}{\partial z} + S_h$$

or

$$C_s \frac{\partial T}{\partial t} - L_m \rho_i \frac{\partial x_i}{\partial t} = K_h \frac{\partial^2 T}{\partial z^2} + \frac{\partial K_h}{\partial z} \frac{\partial T}{\partial z} - c_w q_w \frac{\partial T}{\partial z} \quad (5-33)$$

When neither freezing nor thawing takes place eq. (5-33) can be reduced to eq. (5-34).

$$C_s \frac{\partial T}{\partial t} = K_h \frac{\partial^2 T}{\partial z^2} + \frac{\partial K_h}{\partial z} \frac{\partial T}{\partial z} - c_w q_w \frac{\partial T}{\partial z} \quad (5-34)$$

When freezing or thawing takes place it is assumed that the temperature in the soil can be described by eq. (5-35) as proposed by Miller (1980).

$$T = 273 \frac{\frac{\psi - \pi}{\rho_w} - \frac{P_i}{\rho_i}}{L_m} - 273 \quad (5-35)$$

ψ = pressure potential [Pa]

π = osmotic potential [Pa]

P_i = ice pressure [Pa]

Neglecting all other effects than that of the change in ψ eq. (5-35) can be obtained.

$$\frac{\partial T}{\partial t} = \frac{273}{\rho_w L_m} \frac{\partial \psi}{\partial t}$$

$$= \frac{273}{\rho_w L_m} \frac{d\psi}{dx_w} \frac{\partial x_w}{\partial t}$$

$$= \frac{273}{\rho_w L_m C_\theta} \frac{\partial x_w}{\partial t} \qquad (5-36)$$

C_θ = specific water capacity of the soil [J m^{-3}]

If C_θ is expressed in [m H_2O]$^{-1}$ then the value should be multiplied by 1.019 · 10^{-5} m^3 J^{-1} m H_2O. Combining eq. (5-27) and eq. (5-36) results in eq. (5-37).

$$\frac{\partial T}{\partial t} = \frac{273}{\rho_w L_m} C_\theta^{-1} \left[\frac{\partial \theta}{\partial t} - \frac{\rho_i}{\rho_w} \frac{\partial x_i}{\partial t} \right]$$

or

$$\frac{\partial x_i}{\partial t} = \frac{\rho_w}{\rho_i} \left[-\frac{L_m \rho_w}{273} C_\theta \frac{\partial T}{\partial t} + \frac{\partial \theta}{\partial t} \right] \qquad (5-37)$$

Assuming that S_w = 0 when the soil is freezing or thawing then combining eq. (5-36) and eq. (5-37) results in eq. (5-38).

$$\frac{\partial x_i}{\partial t} = \frac{\rho_w}{\rho_i}\left[-\frac{1}{\rho_w}\frac{\partial q_w}{\partial z} - \frac{\rho_w L_m}{273} C_\theta \frac{\partial T}{\partial t}\right] \qquad (5-38)$$

Eq. (5-38) gives the rate of change of the ice content of the soil (freezing or thawing rate). It is assumed that freezing or thawing are initiated when the temperature passes 0°C. Combining eq. (5-37) and eq. (5-38) results in eq. (5-39).

$$C_s \frac{\partial T}{\partial t} + \rho_w L_m \left[\frac{1}{\rho_w}\frac{\partial q_w}{\partial t} + \frac{\rho_w L_m}{273} C_\theta \frac{\partial T}{\partial t}\right]$$

$$= K_h \frac{\partial^2 T}{\partial z^2} + \frac{\partial K_h}{\partial z}\frac{\partial T}{\partial z} - c_w q_w \frac{\partial T}{\partial z}$$

or

$$\left[C_s + \frac{\rho_w^2 L_m^2}{273} C_\theta\right]\frac{\partial T}{\partial t}$$

$$= K_h \frac{\partial^2 T}{\partial z^2} + \left[\frac{\partial K_h}{\partial z} - c_w q_w\right]\frac{\partial T}{\partial z} - L_m \frac{\partial q_w}{\partial z} \qquad (5-39)$$

When solving the heat equation, eq. (5-34) is used when neither freezing nor thawing takes place while eq. (5-39) is used when freezing or thawing takes place.

5.5 Boundary conditions

Upper boundary

Soil surface temperature is assumed to constitute the upper boundary condition. The soil surface temperature is approximated by the air temperature except when snow is covering the soil surface. If infiltration is due to irrigation it is assumed that the infiltrating water assumes the temperature of the irrigation water.

To include a diurnal variation in the air temperature it is assumed that the maximum temperature occurs at 3 p.m. if the average daily temperature is higher than the temperature of the previous night. If the average daily temperature is lower than the temperature of the previous night it is assumed that the minimum temperature of the day occurs at 9 a.m.

If snow is present and the snow contains liquid water it is assumed that the surface temperature is 0°C. If snow is present and the snow does not contain any liquid water the surface temperature (the temperature at the bottom of the snow) is calculated by assuming steady state heat flow through the snow cover and through the upper soil, that is

$$- K_s \frac{T_{sf} - T_a}{\Delta z_s} = - K_{h1} \frac{T_1 - T_{sf}}{z_1}$$

or

$$T_{sf} = \frac{(K_{h1}/z_1)T_1 + (K_s/\Delta z_s)T_a}{(K_{h1}/z_1) + (K_s/\Delta z_s)} \qquad (5-40)$$

T_{sf} = surface temperature [°C]
T_a = air temperature [°C]
T_1 = soil temperature at z_1 [°C]
z_1 = soil depth [m]
Δz_s = depth of snow cover [m]
K_{h1} = thermal conductivity of soil [W m^{-1} $°C^{-1}$]
K_s = thermal conductivity of snow [W m^{-1} $°C^{-1}$]

The thermal conductivity of the snow is estimated according to Corps of Engineers (1956).

$$K_s = S \rho_s^2 \qquad (5-41)$$

S = emperical parameter [$2.86 \cdot 10^{-6}$ W m^4 kg^{-2}]
ρ_s = density of snowpack [kg m^{-3}]

Lower boundary

Neglecting frost, thaw and transfer of heat by convection and assuming constant C_s and K_h eq. (5-34) is reduced to eq. (5-42).

$$\frac{\partial T}{\partial t} = \frac{K_h}{C_s} \frac{\partial^2 T}{\partial z^2} \qquad (5-42)$$

This equation can be solved analytically with the boundary conditions given by eqs. (5-43a, b).

$$T(t, 0) = T_{av} + A_t \cos(\omega(t - t_0)) \qquad (5-43a)$$

$$T(t, \infty) = T_{av} \qquad (5-43b)$$

The solution is eq. (5-44).

$$T(t, z) = T_{av} + A_t e^{-z/d} \cos(\omega(t - t_0) - z/d) \qquad (5-44)$$

$$d = \left[\frac{2K_h}{C_s \omega} \right]^{1/2}$$

d is the damping depth.

Eq. (5-44) is used as a lower boundary condition with

T_{av} = annual average of air temperature [°C]
A_t = amplitude of the annual variation in air temperature [°C]
ω = $2\pi/365$ [day^{-1}]
t = day in the year [day]
t_0 = day number when $T(t, 0) = T_{av} + A_t$ [day]
K_h = average thermal conductivity of the soil profile [$W\ m^{-1}\ °C^{-1}$]
C_s = average volumetric heat capacity of the soil profile [$J\ m^{-3}$]

z is chosen as the deepest computational point.

5.6 Numerical solution

The finite difference method

The finite difference scheme used in the numerical approximation of the heat flow equation is illustrated in Fig. (5–3).

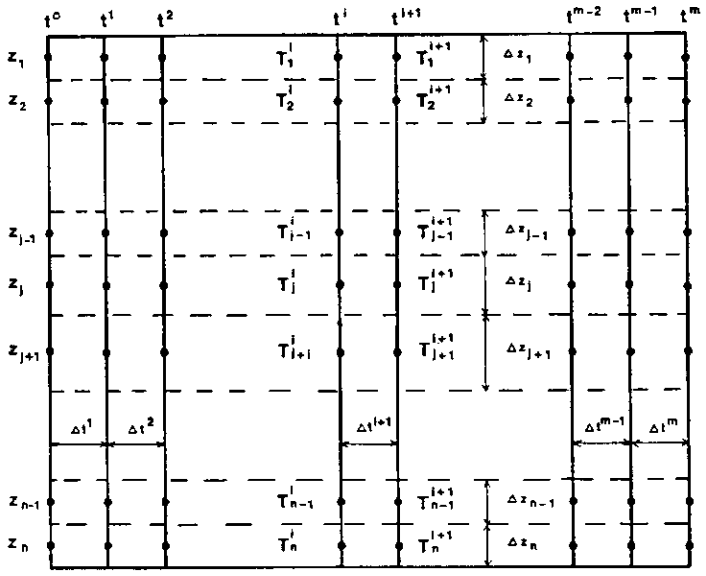

Fig. 5–3 Discretization after the finite difference method.

All nodes in the time–distance plan are numbered with the subscript j referring to the depth and the superscript i is referring to the time (i = 0 is referring to the time of initialization). The time increments are kept constant while the depth increments may vary. The heat flow equations (5–34) and (5–39) may both be approximated by eq. (5–46) in which the superscript i+½ refers to values centered in time.

$$A_j^{i+\frac{1}{2}} \frac{T_j^{i+1} - T_j^i}{\Delta t^{i+1}} =$$

$$K_j^{i+\frac{1}{2}} \frac{\frac{T_{j+1}^{i+1} - T_j^{i+1}}{z_{j+1} - z_j} - \frac{T_j^{i+1} - T_{j-1}^{i+1}}{z_j - z_{j-1}} + \frac{T_{j+1}^i - T_j^i}{z_{j+1} - z_j} - \frac{T_j^i - T_{j-1}^i}{z_j - z_{j-1}}}{2\,½(z_{j+1} - z_{j-1})}$$

$$+ \left(\left[\frac{\partial K}{\partial z} \right]_j^{i+\frac{1}{2}} - c_w q_j^{i+\frac{1}{2}} \right) \frac{(T_{j+1}^{i+1} - T_{j-1}^{i+1}) + (T_{j+1}^i - T_{j-1}^i)}{2(z_{j+1} - z_{j-1})} - B_j^{i+\frac{1}{2}} \qquad (5-46)$$

If eq. (5–46) is an approximation of eq. (5–34), i.e. no frost or thaw, then

$$A_j^{i+\frac{1}{2}} = ½(C_j^i + C_j^{i+1}) \qquad (5-47a)$$

$$B_j^{i+\frac{1}{2}} = 0 \qquad (5-47b)$$

If eq. (5–46) is an approximation of eq. (5–39), i.e. frost or thawing takes place, then

$$A_j^{i+\frac{1}{2}} = ½(C_j^i + C_j^{i+1}) + \frac{\rho_w^2 L_m^2}{273} \bar{C}_\theta \qquad (5-48a)$$

$$B_j^{i+\frac{1}{2}} = L_m \rho_w \frac{q_{j+\frac{1}{2}}^{i+\frac{1}{2}} - q_{j-\frac{1}{2}}^{i+\frac{1}{2}}}{\Delta z_j} \qquad (5-48b)$$

The volumetric heat capacity of the soil is estimated according to eq. (5–1), neglecting the contribution of the soil air. From the solution of the water flow equation (Richards equation) the soil water content is known at the depth z_j at the time t^i and t^{i+1}. These values are used in calculating C_j^i and C_j^{i+1}.

If ice is also present the ice content at the time t^i is used in the calculation of C_j^i as well as of C_j^{i+1}. When freezing or thawing takes place then

$$\frac{\rho_w^2 L_m^2 \bar{C}_\theta}{273} >> \tfrac{1}{2}(C_j^i + C_j^{i+1})$$

and therefore C_j^i as well as C_j^{i+1} are determined with sufficient accuracy.

The apparent thermal conductivity is calculated by using eq. (5-49).

$$K_j^{i+\frac{1}{2}} = \tfrac{1}{2}(K_j^i + K_j^{i+1}) \qquad (5-49)$$

where K_j^i and K_j^{i+1} are taken at the soil water content at t^i and t^{i+1}, respectively. If ice is present the K-values are found by interpolation between curves representing air-water and air-ice, respectively, as continuous medium.

In a similar way the following term is estimated.

$$\left(\frac{\partial K}{\partial z}\right)_j^{i+\frac{1}{2}} = \tfrac{1}{2}\left[\frac{K_{j+1}^i - K_{j-1}^i}{z_{j+1} - z_{j-1}} + \frac{K_{j+1}^{i+1} - K_{j-1}^{i+1}}{z_{j+1} - z_{j-1}}\right] \qquad (5-50)$$

The term

$$q_j^{i+\frac{1}{2}} = \tfrac{1}{2}(q_{j-\frac{1}{2}}^{i+\frac{1}{2}} + q_{j+\frac{1}{2}}^{i+\frac{1}{2}}) \qquad (5-51)$$

as the values of $q_{j-\frac{1}{2}}^{i+\frac{1}{2}}$ and $q_{j+\frac{1}{2}}^{i+\frac{1}{2}}$ are known from the solution of the water flow equation.

The term $B_j^{i+\frac{1}{2}}$ in eq. (5-46) is calculated from eq. (5-47b) in the case of no freezing or thawing or from eq. (5-48b) if freezing or thawing takes place.

Eq. (5-46) can be rearranged to give eq. (5-52) - eq. (5-56).

$$a_j^{i+1} T_{j-1}^{i+1} + b_j^{i+1} T_j^{i+1} + c_j^{i+1} T_{j+1}^{i+1} = d_j^{i+1} \qquad (5-52)$$

For $j > 1$

$$d_j^{i+1} = \frac{A_j^{i+\frac{1}{2}}}{\Delta t^{i+1}} \cdot T_j^i + \frac{K_j^{i+\frac{1}{2}}}{z_{j+1} - z_{j-1}} \left[\frac{T_{j+1}^i - T_j^i}{z_{j+1} - z_j} - \frac{T_j^i - T_{j-1}^i}{z_j - z_{j-1}} \right]$$

$$+ \left(\left[\frac{\partial K}{\partial z} \right]_j^{i+\frac{1}{2}} - c_w q_j^{i+\frac{1}{2}} \right) \frac{T_{j+1}^i - T_{j-1}^i}{2(z_{j+1} - z_{j-1})} - B_j^{i+\frac{1}{2}} \qquad (5-53)$$

$$c_j^{i+1} = -\frac{K_j^{i+\frac{1}{2}}}{z_{j+1} - z_{j-1}} \cdot \frac{1}{z_{j+1} - z_j}$$

$$- \left(\left[\frac{\partial K}{\partial z} \right]_j^{i+\frac{1}{2}} - c_w q_j^{i+\frac{1}{2}} \right) \frac{1}{2(z_{j+1} - z_{j-1})} \qquad (5-54)$$

$$b_j^{i+1} = \frac{A_j^{i+\frac{1}{2}}}{\Delta t^{i+1}} + \frac{K_j^{i+\frac{1}{2}}}{z_{j+1} - z_{j-1}} \left[\frac{1}{z_{j+1} - z_j} + \frac{1}{z_j - z_{j-1}} \right] \qquad (5-55)$$

$$a_j^{i+1} = -\frac{K_j^{i+\frac{1}{2}}}{z_{j+1} - z_{j-1}} \cdot \frac{1}{z_j - z_{j-1}}$$

$$+ \left(\left[\frac{\partial K}{\partial z} \right]_j^{i+\frac{1}{2}} - c_w q_j^{i+\frac{1}{2}} \right) \frac{1}{2(z_{j+1} - z_{j-1})} \qquad (5-56)$$

For j=1 the following approximations are adopted, eq. (5-57) – eq. (5-60).

$$d_j^{i+1} = \frac{A_1^{i+\frac{1}{2}}}{\Delta t^{i+1}} T_1^{i+1} + \frac{K_1^{i+\frac{1}{2}}}{z_2}\left[\frac{T_2^i - T_1^i}{z_2 - z_1} - \frac{T_1^i - T_0^i}{z_1} + \frac{T_0^{i+1}}{z_1}\right] - c_w q_1^{i+\frac{1}{2}} \frac{T_2^i - \tau^i + \tau^{i+1}}{2 z_2} \qquad (5-57)$$

$$c_1^{i+1} = -\frac{K_1^{i+\frac{1}{2}}}{z_2(z_2 - z_1)} + \frac{c_w q_1^{i+\frac{1}{2}}}{2 z_2} \qquad (5-58)$$

$$b_j^{i+1} = \frac{A_j^{i+\frac{1}{2}}}{\Delta t^{i+1}} + \frac{K_1^{i+\frac{1}{2}}}{z_2}\left[\frac{1}{z_2 - z_1} + \frac{1}{z_1}\right] \qquad (5-59)$$

$$a_1^{i+1} = 0 \qquad (5-60)$$

If irrigation occurs τ^i and τ^{i+1} are approximated by the temperature of the irrigation water. Otherwise they are approximated by T_0^i and T_0^{i+1}, respectively. The value of T_0^1 and T_0^{i+1} represent the surface temperature at the timestep i and i+1, respectively.

The nummerical solution of eq. (5-34) or eq. (5-39) can now be formulated as a matrix equation, eq. (5-61).

$$\bar{H} \cdot \bar{T} = \bar{D} \tag{5-61}$$

$$\bar{H} = \begin{bmatrix} b_1^{i+1} & c_1^{i+1} & & & & & \\ a_2^{i+1} & b_2^{i+1} & c_2^{i+1} & & & & \\ & a_3^{i+1} & b_3^{i+1} & c_3^{i+1} & & & \\ & & & & a_{n-1}^{i+1} & b_{n-1}^{i+1} & c_{n-1}^{i+1} \\ & & & & & a_n^{i+1} & b_n^{i+1} \end{bmatrix} \tag{5-62}$$

$$\bar{T} = \begin{bmatrix} T_1^{i+1} \\ T_2^{i+1} \\ T_3^{i+1} \\ \\ T_{n-1}^{i+1} \\ T_n^{i+1} \end{bmatrix} \tag{5-63},$$

$$\bar{D} = \begin{bmatrix} d_1^{i+1} \\ d_2^{i+1} \\ d_3^{i+1} \\ \\ d_{n-1}^{i+1} \\ d_n^{i+1} - c_n^{i+1} T_{n+1}^{i+1} \end{bmatrix} \tag{5-64}$$

In estimating the $\bar{D}$ in eq. (5-61) T_{n+1}^{i+1} represents the lower boundary condition.

As $\bar{H}$ is a tri-diagonal matrix the system can be solved by the double-sweep-method.

A special problem arises when freezing is initiated at a particular node, j, within a timestep. In this case $A_j^{i+½}$ and $B_j^{i+½}$ are recalculated according to eq. (5–47b) and eq. (5–48b), respectively, and new values of b_j^{i+1} and d_j^{i+1} are hereafter calculated from eq. (5–53) and eq. (5–55), respectively. If freezing is not initiated with the new values of b_j^{i+1} and d_j^{i+1}, i.e. $T_j^{i+1} > 0$, it is assumed that $T_j^{i+1} = 0$. When thawing is initiated a similar procedure is adopted.

It is noted that an average value of the specific water capacity is used in the calculation of $A_j^{i+½}$ (eq. (5–48a)). The same average value is used when the freezing or thawing rate is calculated from eq. (5–38).

6. SOIL ORGANIC MATTER MODEL

6.1 Introduction

Forms of nitrogen in soil

Usually more than 90% of the nitrogen (N) in the root zone is organically combined. Most of the remaining part is ammonium ($NH_4^+ - N$) fixed in clay minerals whereas ammonium and nitrate ($NO_3^- - N$) available for plant uptake and extractable with e.g. 1 M KCl seldom come to more than 1% of the total amount of nitrogen present in the root zone. Thus organic forms of nitrogen constitute the main part of the soil nitrogen. Therefore turnover of soil nitrogen involves turnover of soil organic matter.

Microbial turnover of organic matter

The processes of soil organic matter turnover are performed by saprophytic or predatory heterotrophic soil organisms, the soil biomass, that assimilate or utilize nitrogeneous organic substances as a source of e.g. energy, carbon, nitrogen, phosphorus and sulphur. The resulting growth of the soil biomass requires nitrogen and other nutrients for cell synthesis which imply nitrogen immobilization.

Nitrogen mineralization and immobilization

If the content of nitrogen in the assimilated organic substance is higher than that required by the biomass for growth $NH_4^+ - N$ is excreated to the soil solution. If on the other hand the content of nitrogen in the assimilated organic substance is lower than that required by the biomass for growth $NH_4^+ - N$ or $NO_3^- - N$ is assimilated from the soil solution and transformed into nitrogeneous organic compounds. Hence the net production of $NH_4^+ - N$ which is designated net mineralization of nitrogen is the difference between two opposing processes viz. nitrogen mineralization and nitrogen immobilization. The course and extent of net mineralization of nitrogen during the year is of paramount importance for plant nutrition and for the potential of the soil for leaching of $NO_3^- - N$.

Relating mineralization of nitrogen to turnover rate of organic matter

The activity of the soil biomass and hence the turnover of soil organic matter is usually determined by the availability of the soil organic matter for the soil organisms. Hence it seems wise to base the simulation of net mineralization of nitrogen on the simulation of the turnover rate of soil organic matter.

The soil organic matter consists of various products which range from intact plant and animal tissues and organisms that live in the soil to black organic material designated humus which is without traces of the anatomical structure from which it was derived. The soil organic matter is composed of carbon, hydrogen, oxygen, nitrogen, sulphur and phosphorus. The C:N:S:P ratio in soil organic matter is usually about 100:10:1:1. Apart from acid soils and poorly drained soils the C:N ratio in soil organic matter of mineral soil is usually in the range 10 to 12.

Mineral soils of arable land often contain 1 to 3% carbon corresponding to 1.7 to 5.2% organic matter in the top soil. Grassland and forest soils most often contain somewhat more organic matter than arable soils. In general the concentration of organic matter decreases rapidly with soil depth. For that reason and due to the presence of fixed NH_4^+ – N the organic carbon:total nitrogen ratio decreases with soil depth and values of about 5 are not uncommon at a soil depth of 1 m.

Physical-chemical protection of organic matter against decomposition

Soil organic matter and in particular humic substances have long been known to form relatively stable complexes with polyvalent cations, e.g. Al^{3+}, Fe^{3+}, and Ca^{2+}, which by cation bridging can be adsorbed to negatively charged clay surfaces. In this way and by several other mechanisms the soil organic matter as well as microorganisms may be partly protected against microbial decomposition. For that reason the content of easily decomposible soil organic matter and the soil biomass often increase with increasing clay content of the soil.

Abiotic factors

In addition to the availability of soil organic matter for the soil biomass the decomposition rate of organic matter in soil is affected by soil water content, soil temperature, pH, oxygen pressure, and availability of inorganic nutrients. In the pH range 5 to 8 the decomposition rate of organic matter in soil seems unaffected by pH whereas the decomposition rate is limited in acid soils.

In general the decomposition rate of organic matter in soil is unlimited or only slightly limited by oxygen pressure if the oxygen pressure in the soil air is within the range 0.05 to 0.2 bar (Parr and Reuszer, 1959; Kempner, 1937). At low oxygen pressure the rate of decomposition of organic matter is low and the decomposition less complete. However, soil aeration and oxygen supply to oxygen demanding processes in the soil, such as root respiration and microbial decomposition, are closely related to soil water content. Hence the aeration conditions may be expressed in term of the soil water content. Lack of nitrogen seems to be the only nutrient element which may limit the decomposition of organic matter in agricultural soils.

In the present soil organic matter model abiotic factors in terms of soil water content, soil temperature, and clay content are taken into account.

6.2 Organic matter pools

It appears that before nitrogen mineralization can take place the soil organic matter has to be dissolved. The latter process may be considered as the step determining the turnover rate of soil organic matter (Nielsen et al., 1988). Furthermore it appears that inorganic nitrogen ($NH_4^+ - N$) is in a quasi-equilibrium with clay minerals as well as with the soil biomass which implies that the C:N ratio of the soil biomass in part depends on the concentration of $NH_4^+ - N$ in the soil solution.

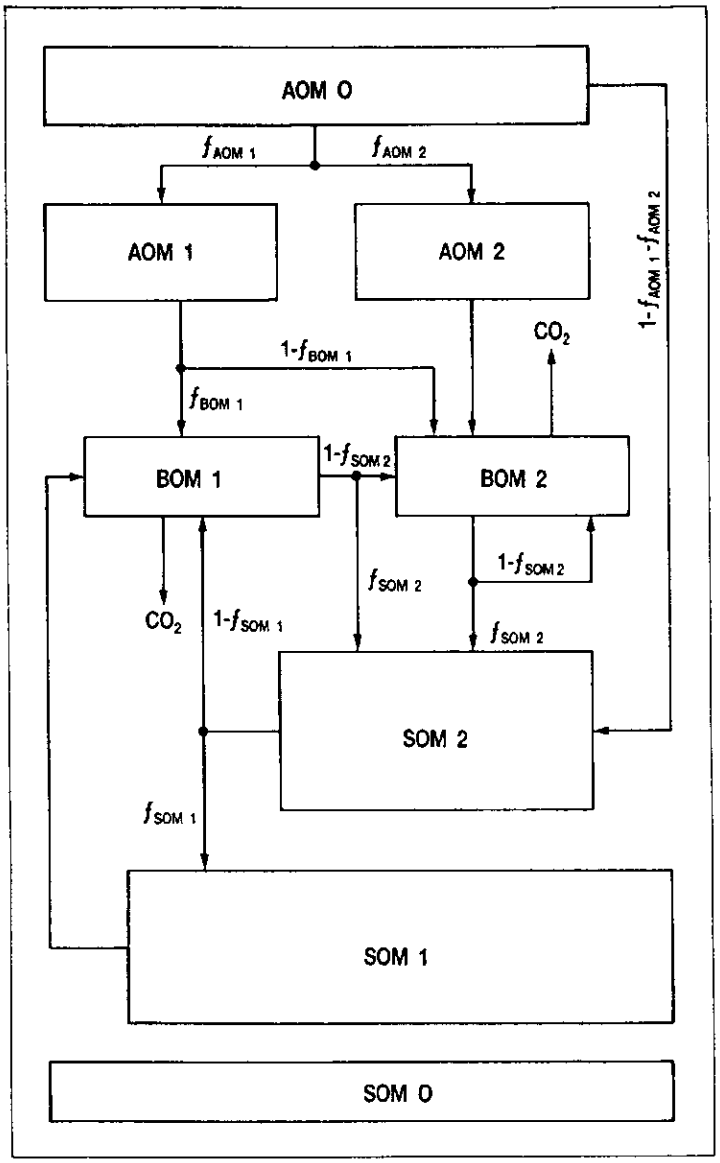

Fig. 6.1 Pools and subpools (1 and 2) of organic matter and related partitioning coefficients (f). AOM: Added organic matter, BOM: Biomass, SOM: Soil organic matter.

Dissolution rate of organic matter

In accordance with assumptions inherent in models suggested by Jenkinson and Rayner (1977), Van Veen and Paul (1981) and Van Veen et al. (1984) it is assumed that the rate of enzymatically catalysed turnover from undissolved to dissolved organic matter usually is determined by the chemical nature as well as physical-chemical protection of the undissolved organic matter in the soil. This implies that microbial activity is depending on the rate of transformation from undissolved to dissolved organic matter.

Organic matter pools

Organic matter in soil can be divided into at least three main pools, i.e. dead native soil organic matter (SOM), microbial biomass (BOM), and added organic matter (AOM), Fig. 6–1. However, in order to apply first order kinetics in modelling the organic matter turnover the three main pools may be subdivided as suggested by Jenkinson and Rayner (1977) and Jenkinson et al. (1987).

Native soil organic matter

In the present model dead native soil organic matter which constitutes the main part of the organic matter in the soil has been subdivided into three subpools designated SOM 0, SOM 1 and SOM 2, Fig. 6–1. The subpool SOM 0 consists of almost inert organic matter having a turnover which can be neglected. The subpool SOM 1 consists of chemically stabilized organic matter which is decomposed at a slow rate whereas the subpool SOM 2 consists of physically stabilized organic matter which is decomposed at a rate about 50 times the rate at which SOM 1 is decomposed.

The rates of decomposition of SOM 1 and SOM 2 are considered to be affected by soil temperature, soil water content, and clay content of the soil. It is assumed that the C:N ratios of SOM 1 and SOM 2 are within the range from 10 to 12. In soils with a high input rate of organic matter SOM 2 will increase more rapid than SOM 1 whereas in soils with a low input rate of organic matter SOM 2 will decrease faster than SOM 1.

Potential nitrogen mineralization

Thus the potential nitrogen mineralization rate from dead native organic matter in soil is highly dependent on the distribution of the dead native soil organic matter between SOM 1 and SOM 2 which in turn is strongly related to the management history of the soil including in particular the previous application of farmyard manure.

Microbial biomass

The microbial biomass in the soil which usually accounts for less than 3% of organic carbon in the soil is of great importance for production of exoenymes and for turnover of dissolved organic matter. In order to have a relatively stable as well as a dynamic microbial biomass organic matter pool the microbial biomass has been subdivided into two subpools designated BOM 1 and BOM 2, Fig. 6–1. The subpool BOM 1 is considered to be the more stable part while BOM 2 is considered to be the more dynamic part of the microbial biomass. The two subpools differ in particular in respect to death rates expressed by first order kinetics and in respect to organic matter pool used as substrate.

The rate of turnover of BOM 1 is considered to be affected by soil temperature, soil water content, and clay content of the soil whereas the turnover of BOM 2 is considered to be affected only by soil temperature and soil water content. The C:N ratio for BOM 1 and BOM 2 is assumed to be 6 and 10, respectively, if not otherwise specified. It follows from the interrelationships described, Fig. 6–1, that the pool size of BOM 1 and BOM 2 is affected considerably by the rate of added organic matter rather than by the pools of dead native organic matter in the soil.

Added organic matter

Added organic matter AOM 0 can be organic fertilizers as farmyard manure, slurry, green crop manure, or crop residues left in the field after harvest. Organic matter input to the soil is allocated to two subpools designated AOM 1 and AOM 2. The subpool AOM 2 consists of organic matter which is decomposed easily while subpool AOM 1 consists of organic matter

which is decomposed slowly. The decomposition rates of AOM 1 and AOM 2 are considered to be affected by soil temperature and soil water content. In case of an organic fertilizer, e.g. farmyard manure, in which some decomposition already has taken place a part of the organic matter is allocated to SOM 2.

6.3 Organic matter transformation

First order kinetics

In the present model the rate of decomposition or decay of organic matter in soil is described by first order reaction kinetics, eq. (6-1).

$$\zeta_x = k_x C_x \qquad (6-1)$$

ζ_x = decomposition or decay rate of pool x [kg C $m^{-3}s^{-1}$]
C_x = carbon concentration in soil of pool x [kg C m^{-3}]
k_x = decomposition or decay rate coefficient for pool x [s^{-1}]

Abiotic functions

The decomposition or decay rate coefficient at the actual condition is derived as a rate coefficient at standard abiotic conditions multiplied by abiotic functions taking into account effects of soil temperature, soil water content, and clay content of the soil. For pools of the soil organic matter, SOM 1 and SOM 2, the decomposition rate coefficient is calculated from eq. (6-2).

$$k_x = k_x^* F_m^c(X_c) F_m^T(T) F_m^{\psi}(\psi) \qquad (6-2)$$

k_x^* = decomposition rate coefficient at standard conditions [s^{-1}]

$F_m^c(X_c)$ = clay content function

$F_m^T(T)$ = temperature function

$F_m^{\psi}(\psi)$ = pressure potential function

X_c = clay content [%]
T = soil temperature [°C]
ψ = pressure potential of soil water [m H_2O]

Standard abiotic conditions

The standard condition related to eq. (6-2) is defined as X_c = 0, T = 10°C and a range of ψ optimal for microbial activity.

For pools of the added organic matter, AOM 1 and AOM 2, the decomposition rate coefficient is calculated from eq. (6-3).

$$k_x = k_x^* F_m^T(T) F_m^{\psi}(\psi) \qquad (6-3)$$

For pools of the microbial biomass, BOM 1 and BOM 2, the decay rate at the standard conditions as specified in relation to eq. (6-2) is assumed to include a specific death rate coefficient and a specific maintenance rate coefficient, eq. (6-4).

$$k_x^* = d^* + m^* \qquad (6-4)$$

d^* = death rate coefficient for microbial biomass at standard conditions [s^{-1}]
m^* = maintenance coefficient for microbial biomass at standard conditions [s^{-1}]

The decay rate coefficients for BOM 1 and BOM 2 at the actual conditions are then calculated from eq. (6-2) and eq. (6-3), respectively. The respective death rates (D_x) are also described by first order kinetics by substituting the decay rate coefficient in eq. (6-1) with the death rate coefficient. The abiotic functions describing the effects of temperature, soil water content, and clay content of the soil on the decomposition or the decay rate of the various pools of organic matter are described in a subsequent section. The formation of organic carbon in the six pools of organic matter defined previously and shown schematically in Fig. 6-1 is described by the following six equations in which the subscripts refer to the various pools of carbon in organic matter.

$$\frac{dC_{AOM\,1}}{dt} = f_{AOM\,1}\, I_D - \zeta_{AOM\,1} \qquad (6-5)$$

$$\frac{dC_{AOM\,2}}{dt} = f_{AOM\,2}\, I_D - \zeta_{AOM\,2} \qquad (6-6)$$

$$\frac{dC_{BOM\,1}}{dt} = E_{BOM\,1}[\zeta_{SOM\,1} + (1 - f_{SOM\,1})\zeta_{SOM\,2} + f_{BOM\,1}\,\zeta_{AOM\,1}] - \zeta_{BOM\,1} \qquad (6-7)$$

$$\frac{dC_{BOM\,2}}{dt} = E_{BOM\,2}[(1 - f_{SOM\,2})(D_{BOM\,1} + D_{BOM\,2}) + (1 - f_{BOM\,1})\zeta_{AOM\,1} + \zeta_{AOM\,2}] - \zeta_{BOM\,2} \qquad (6-8)$$

$$\frac{dC_{SOM\,1}}{dt} = f_{SOM\,1}\,\zeta_{SOM\,2} - \zeta_{SOM\,1} \qquad (6-9)$$

$$\frac{dC_{SOM\,2}}{dt} = f_{SOM\,2}(D_{BOM\,1} + D_{BOM\,2}) - \zeta_{SOM\,2} \qquad (6-10)$$

C = carbon concentration in soil [kg m^{-3}]
ζ = decomposition or decay rate [kg C $m^{-3}s^{-1}$]
E = substrate utilization efficiency
D = death rate [kg C $m^{-3}s^{-1}$]
f = partitioning coefficient
t = time [s]
I_c = organic carbon input [kg C m^{-3}]
I_D = input function, Dirac's Delta function [kg $cm^{-3}s^{-1}$]

$$I_D = \begin{cases} \dfrac{I_c}{\Delta} & t_0 < t < t_0 + \Delta \\ 0 & \text{else} \end{cases}$$

It is noted that the Delta function ensures that the input of added organic matter occurs in short time intervals between the time t_0 and the time $t_0 + \Delta$.

6.4 Abiotic functions

The abiotic functions in the present model are used to adjust the decomposition rate of soil organic matter at standard conditions to the actual conditions of soil temperature, soil water content, and content of clay, respectively.

Effect of clay content

The effect of clay content is associated with a chemical as well as a physical protection of organic matter against decomposition. It is known that polyanionic humic colloids form relatively stable complexes with several polyvalent cations, e.g. Al^{3+}, Fe^{2+}, and Ca^{2+}, which by cation bridging can be adsorbed to negatively charged clay surfaces. Several other chemical adsorption mechanisms may be envisaged in addition to physical adsorption mechanisms, e.g. van der Vaal attraction forces (Emerson, 1959; Harris et al., 1965). In arable soil most of the soil organic matter is incorporated into domains of primary particles which by clustering form soil microaggregates, aggregates, and clods. In the interior of domains and clusters of microaggregates the soil pore system is made up of micropores with diameters in the range of 0.1 – 10 µm, which is comparable to the range of dimensions of bacteria and fungal hyphae (Dexter, 1988). Thus in accordance with e.g. Sørensen (1975) and Anderson (1979) it is realized that protection of organic matter against decomposition or decay varies with the degree of aggregation and the clay content of the soil.

As suggested by van Veen et al.(1984, 1985) it is assumed that soils possess a characteristic capacity to protect soil organic matter as well as microorganisms against decomposition or decay and that protection increases with clay content to a maximum at a certain clay content of the soil. Thus in the present model the function used to account for the effect of clay content of the soil on the rate of decomposition or decay of organic matter is given as eq. (6 – 11) and shown in Fig. 6 – 2.

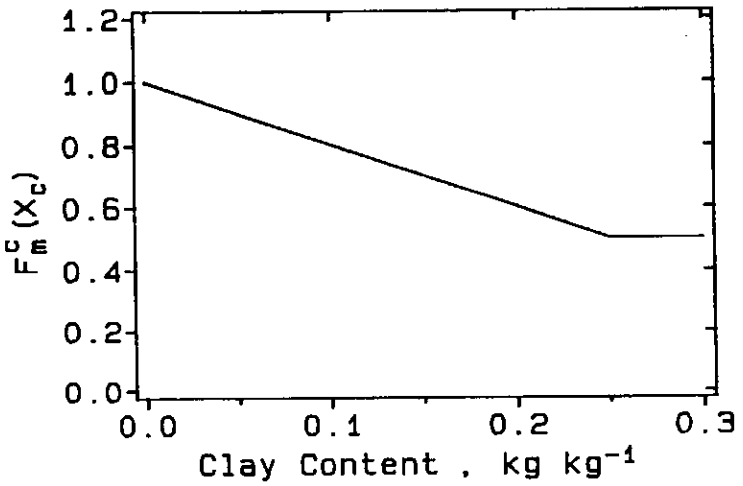

Fig. 6-2 Clay content function for adjustment of the decomposition rate coefficient to actual clay content.

$$F_m^c(X_c) = \begin{cases} 1.0 - a\,X_c & 0 < X_c \leq X_c' \\ 1.0 - a\,X_c' & X > X_c' \end{cases} \qquad (6-11)$$

$F_m^c(X_c)$ = function accounting for effects of clay content

X_c = clay content [kg kg^{-1}]

X_c' = limit for effect of clay content (0.25 kg kg^{-1})

a = parameter (0.02)

Most of the capacity of soil to protect microbial biomass against decay, which might be a protection against predation, is assumed currently to be utilized. The microbial biomass which is formed at a high rate after a heavy input of e.g. stable manure is therefore assumed to be less protected and partly for that reason decomposed at a relatively high rate.

Effect of temperature

The turnover of organic matter is influenced considerably by temperature. Under Danish climatical conditions the soil temperature is often within the range of 0–20°C which is well below the optimum temperature for nitrogen mineralization. The effect of temperature on net mineralization has been considered by several authors. In Table 6–1 are listed a number of references in all of which an Arrhemius type equation to describe the temperature effect has been used, eq. (6–12).

$$F(T) = A\, e^{-B/T} \qquad (6-12)$$

F(T) = function to account for effect of temperature
T = temperature [K]
A = constant
B = constant [K]

The various functions normalized to 1.0 at 10°C are shown in Fig. 6–3. It is noted that good agreement exists between results obtained by Stanford et al. (1973) and Campbell et al. (1981) when measurements in the range of 5–40°C are considered. It is also noted that Campbell et al. (1981) found that net mineralization of nitrogen was less affected by temperature in the subsoil than in the topsoil. Addiscott (1983) found greater temperature effect on net mineralization of nitrogen in arable soil which had received 35 tons $ha^{-1}year^{-1}$ of farmyard manure since 1843 than in arable soil which had received mineral nitrogen fertilizer in the same period of time. Nordmeyer and Richter (1985) found that turnover of the rapid decomposible fraction of added plant residues was affected much more by temperature than turnover of the more resistant fraction of the added plant residues. They also observed that turnover of the more resistant fraction of the added plant residues was depending considerably on the clay content of the soil.

Table 6-1 Temperature effect on net mineralization of nitrogen described by an Arrhenius type equation as suggested in literature.

Reference	Temperature, °C	Comment	Legend[1)]
Campbell et al. (1981)	5-40	5 soils, subsoil	a
Campbell et al. (1981)	5-40	5 soils, topsoil	b
Stanford et al. (1973)	5-35	11 soils	c
Stanford et al. (1973)	15-35	11 soils	e
Addiscott (1983)	5-25	mineral fertilizer	f
Addiscott (1983)	5-25	farmyard manure	g
Nordmeyer and Richter (1985)	10-35	slowly decomposable fraction	h
Nordmeyer and Richter (1985)	10-35	rapid decomposable fraction	i

1) Figure 6-4

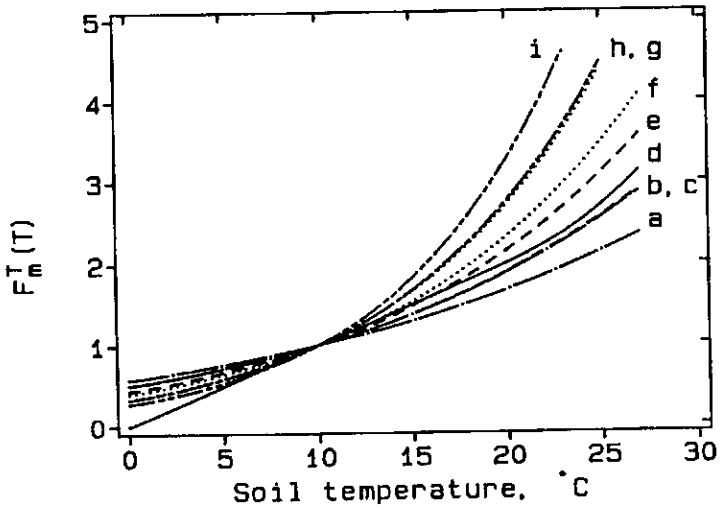

Fig. 6-3 Several soil temperature functions for adjustment of the decomposition rate coefficient to actual soil temperature. Legend explanation, cf. Table 6-1.

Thus the experimental evidence considered suggests that the temperature effect on the turnover rate is related to the nature of the organic matter in the soil. This may explain the considerable differences in experimental results obtained as illustrated by Fig. 6-3.

However, due to lack of sufficient quantitative information it has not been possible to include the lability of the organic matter in modelling the temperature effect on the turnover rates.

Realizing the lack of experimental evidence for conditions below 5°C it is assumed, nevertheless, that the aerobic microbial decomposition rate of soil organic matter approaches zero at 0°C. Furthermore in the present model it is assumed that the effect of soil temperature on the decomposition rate of organic matter increases linearly in the temperature range 0-20°C and exponentially at soil temperatures greater than 20°C, eq. (6-13).

$$F_m^T(T) = \begin{cases} 0 & T \leq 0 \\ 0.1\,T & 0 < T \leq 20 \\ \exp(0.47 - 0.027T + 0.00193T^2) & T > 20 \end{cases} \qquad (6-13)$$

$F_m^T(T)$ = function to account for effect of soil temperature

T = soil temperature [°C]

The function represented by eq. (6-13) is shown in Fig. 6-3 denoted with legend d and in Fig. 6-4. This temperature function corresponds to a Q_{10} value greater than 2 in the temperature range 0-10°C and a Q_{10} value equal to approximately 2 in the temperature range 10-30°C.

Only a small fraction of the organic matter in soil is likely to be in close proximity to microorganisms at any time. Consequently transport processes through the liquid phase of the soil are certainly of importance for the decomposition rate of organic matter in soils. As transport processes in soils are considerably influenced by the soil water content it is realized that the turnover rate of organic matter in soil is strongly related to the corresponding pressure potential of soil water. Miller and Johnson (1964) found from incubation experiments that the evolution of CO_2 was small at low pressure potentials and that the evolution of CO_2 increased to a maximum value at pressure potentials in the range from -5.0 m (H_2O) to -1.5 m (H_2O). Orchard and Cook (1983) and Stott et al. (1986) found that the effect of soil water content on the rate of CO_2 evolution could be expressed as eq. (6-14) and eq. (6-15), respectively.

$$Y = -0.385 \log(-100\,\psi) + 2.5;\ r^2 = 0.98 \qquad (6-14)$$

$$Y = -9.06 \log(-100\,\psi) + 59.6;\ r^2 = 0.87 \qquad (6-15)$$

Y = evolution rate of CO_2 [$\mu l(CO_2)g^{-1}(soil)h^{-1}$]

ψ = pressure potential of soil water [m H_2O]

The pressure potential range applied was from -1000 to -0.5 m H_2O and from -3.3 to -500 m H_2O in the case of eq. (6-14) and eq. (6-15), respectively. When extrapolating to $Y = 0$ a pressure potential corresponding to pF equal to 6.5 and 6.6 is obtained in the case of eq. (6-14) and eq. (6-15), respectively.

Stanford and Epstein (1974) and Miller and Johnson (1964) found that an optimum level of soil water content exists for net mineralization of nitrogen. Jenkinson (1981) states that the decomposition rate of organic matter is slower under anaerobic conditions than under aerobic conditions.

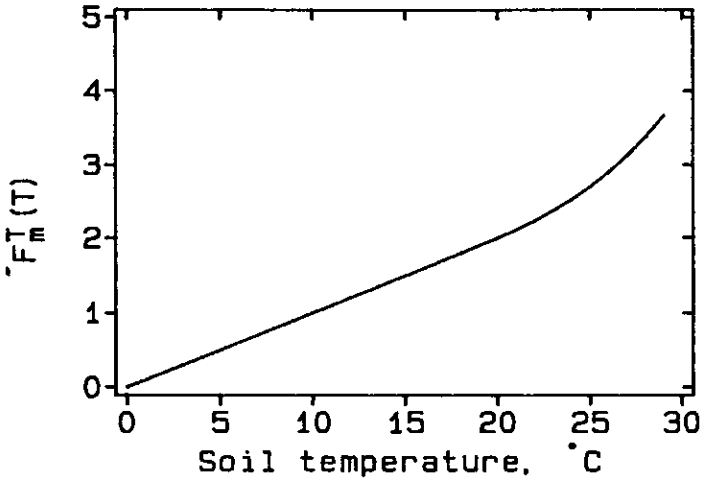

Fig. 6-4 Soil temperature function for adjustment of the decomposition rate coeffficient to actual soil temperature.

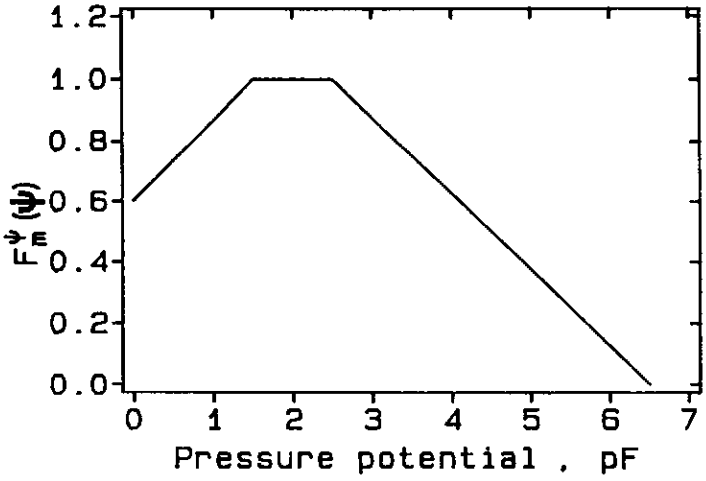

Fig. 6-5 Pressure potential function for adjustment of decomposition rate coefficient to actual soil water pressure potential.

In the present model it is assumed that turnover of soil organic matter approaches zero at pF = 6.5, that optimal conditions exist in the range 1.5 < pF < 2.5. Furthermore it is assumed that the function to account for effect of water content on the turnover rate increases linearly from 0.6 (van Veen and Paul, 1981) at water saturation to 1.0 at pF = 1.5 and that the function decreases linearly from 1.0 at pF = 2.5 to zero at pF = 6.5, eq. (6–16).

$$F_m^{\psi}(\psi) = \begin{cases} 0.6 & \psi \geq -(10^{-2}) \\ 0.6 + 0.4 \log(-100\,\psi)/1.5 & -(10^{-2}) > \psi \geq -(10^{-0.5}) \\ 1.0 & -(10^{-0.5}) > \psi \geq -(10^{0.5}) \\ 1.0 - \log(-100\,\psi)/4.0 & -(10^{0.5}) > \psi \geq -(10^{4.5}) \\ 0 & -(10^{4.5}) > \psi \end{cases} \quad (6-16)$$

$F_m^{\psi}(\psi)$ = function to account for effect of soil water content

ψ = pressure potential of soil water [m H_2O]

The function describing the effect of soil water content on the decomposition rate of organic matter in soil is shown in Fig. 6–5.

6.5 Nitrogen mineralization and immobilization

The concept of net mineralization

Net mineralization of nitrogen, i.e. transformation of organic nitrogen to NH_4^+–N, is a result of two opposite processes viz. nitrogen mineralization and nitrogen immobilization. Therefore the net mineralization of nitrogen is determined by

- the rate by which soil organic matter is dissolved to form substrate for soil microorganisms
- the difference between growth rate and death rate of soil microorganisms

- the efficiency by which soil microorganisms utilize dissolved organic matter as substrate

- the C:N ratio in the various pools of organic matter being decomposed

- the C:N ratio in the microorganisms being synthesized

Thus net mineralization of nitrogen is to a great extent dependent on the reserves of nitrogeneous organic matter in soils, the nature of the organic matter and its C:N ratio. The C:N ratio at which net mineralization of nitrogen approaches zero is often about 25. Thus if the C:N ratio of the organic matter undergoing decomposition is considerably higher than 25 then the concentration of $NH_4^+ - N$ or $NO_3^- - N$ in the soil solution may be limiting for the growth of soil microorganisms.

Thus in the present model the rate of net mineralization of nitrogen is an overall result of the various processes related to the pools of organic matter in soil, eq. (6-17).

$$\xi_m = -\frac{\frac{d\,C_{AOM\,1}}{dt}}{\left[\frac{C}{N}\right]_{AOM\,1}} - \frac{\frac{d\,C_{AOM\,2}}{dt}}{\left[\frac{C}{N}\right]_{AOM\,2}} - \frac{\frac{d\,C_{SOM\,1}}{dt}}{\left[\frac{C}{N}\right]_{SOM\,1}}$$

$$- \frac{\frac{d\,C_{SOM\,2}}{dt}}{\left[\frac{C}{N}\right]_{SOM\,2}} - \frac{\frac{d\,C_{BOM\,1}}{dt}}{\left[\frac{C}{N}\right]_{BOM\,1}} - \frac{\frac{d\,C_{BOM\,2}}{dt}}{\left[\frac{C}{N}\right]_{BOM\,2}} \qquad (6-17)$$

If the net mineralization is negative, i.e. net immobilization occurs, then the upper limit for the immobilization rate is determined by the availability of inorganic nitrogen, eq. (6-18) and eq. (6-19).

In the present model it is assumed that the microorganisms can be supplied with nitrogen from the inorganic pools at a rate which is proportional to the concentration of NH_4^+-N or NO_3^--N in the soil solution, eq. (6-18) and eq. (6-19), respectively.

$$\xi^{im}_{NH_4^+-N} = k^{im}_{NH_4^+-N}\, N_{NH_4^+-N} \qquad (6-18)$$

$$\xi^{im}_{NO_3^--N} = k^{im}_{NO_3^--N}\, N_{NO_3^--N} \qquad (6-19)$$

$\xi^{im}_{NH_4^+-N}$ = rate by which NH_4^+-N can be utilized by microorganisms [kg N m^{-3} s^{-1}]

$\xi^{im}_{NO_3^--N}$ = rate by which NO_3^--N can be used by the microorganisms [kg N m^{-3} s^{-1}]

$N_{NH_4^+-N}$ = concentration of NH_4^+-N in soil [kg N m^{-3}]

$N_{NO_3^--N}$ = concentration of NO_3^--N in soil [kg N m^{-3}]

$k^{im}_{NH_4-N}$ = immobilization rate coefficient for NH_4^+-N [s^{-1}]

$k^{im}_{NO_3-N}$ = immobilization rate coefficient for NO_3^--N [s^{-1}]

If sufficient mineral nitrogen is present in the soil it is assumed the NH_4-N is utilized in preference to NO_3^--N.

6.6 Organic matter input to the soil

Forms of added organic matter

Organic matter input to the soil may be plant residues in the form of roots and above ground parts of the plant such as stalks and leaves, stubble and straw including chaff and other crop residues. In the present model root deposits and rhizodeposition during the growth period are considered to be included in the organic matter input as plant roots. Furthermore organic matter input to the soil may be in the form of farmyard manure, slurry and other forms of added organic matter input.

Distribution of added organic matter in the soil profile

In the case of organic matter input to the soil in the form of plant roots the organic matter is distributed in the soil profile similar to the distribution of root dry matter in the soil, whereas in the case of organic matter input to the soil in the form of above ground plant residues, farmyard manure, and slurry the organic matter or part of it is homogeneously mixed within a layer of soil the thickness and position of which are specified in the system management model.

In accordance with Jenkinson et al. (1987) added organic matter (plant residues and other forms of organic matter which have not been partly humified) is divided into two fractions which are then allocated to two subpools AOM 1 and AOM 2. The division of the organic matter input is made according to its nature and properties. The fraction ($f_{AOM\ 1}$) of the organic matter input allocated to AOM 1 is assumed to be slowly decomposable organic matter with a prediscribed C:N ratio, whereas the fraction ($f_{AOM\ 2}$) allocated to AOM 2 is assumed to be easily decomposable organic matter with a C:N ratio depending on the C:N ratio in the organic matter input and on the partitioning coefficients $f_{AOM\ 1}$ and $f_{AOM\ 2}$.

Partly humified added organic matter

In the case of farmyard manure, slurry and other forms of added organic matter input which during storage have been partly humified the organic matter input is divided into three fractions which are then allocated to AOM 1, AOM 2 and SOM 2. The fraction ($1-f_{AOM\ 1}-f_{AOM\ 2}$) allocated to the SOM 2 depends on the asumed degree of previous humification of the particular organic matter input.

In the case of plant residue, roots and above ground plant parts, the organic matter input is derived from the crop model or stated as initial values. In the case of farmyard manure, slurry, and other forms of added organic matter input the organic matter input is derived from the system management model.

The decomposition rate of organic matter input is described in terms of first order reactions, with decomposition rate constants assumed to be independent of the rate of organic matter input.

6.7 Parameter assessment

The present soil organic matter model is as a conceptual model which implies that a number of parameters are required. Thus in order to assess parameters entering the soil organic matter model, results of several experimental studies have been considered. The experiments considered include long term field experiments with application of farm yard manure and incorporation of plant residues (Jenkinson et al., 1987) as well as short term incubation experiments with incorporation of straw, plant residues from ryegrass, and pig slurry (Lind et al., 1990).

Long term field experiments

The long term field experiments with application of farmyard manure and incorporation of plant residues at Rothemsted Experimental Station (Jenkinson et al., 1987) have been considered.

In the Hoosfield and Broadbalk fields different treatments have been maintained for a very long period of time. The following treatments were considered:

Broadbalk a:	Unmanured since 1839
Broadbalk b:	NPK in fertilizer applied annually since 1843
Broadbalk c:	Farmyard manure applied annually since 1843
Hoosfield a:	Unmanured since 1852
Hoosfield b:	Farmyard manure applied annually since 1852
Hoosfield c:	Farmyard manure applied annually 1852 – 1871, unmanured thereafter.

Table 6–2 Assumed initial values of carbon, kg C ha^{-1}, in various pools of organic matter in the Hoosfield and Broadbalk fields at Rothamsted Experimental Station.

Pool	Broadbalk	Hoosfield
SOM 1	24750	21750
SOM 2	8250	7250
BOM 1	165	145
BOM 2	165	145
AOM 1	0	0
AOM 2	0	0

Table 6–3 Annual application rates of carbon, kg C ha^{-1} $year^{-1}$, in farmyard manure and plant residues to plots in the Hoosfield and Broadbalk fields at Rothamsted Experimental Station.

Field-plot	AOM 0	AOM 1	AOM 2	SOM 2
Broadbalk a	1200	960	240	0
Broadbalk b	1900	1520	380	0
Broadbalk c	4900[1)]	3680	620	600
Hoosfield a	1100	880	220	0
Hoosfield b	4500[2)]	3090	500	900
Hoosfield c	1500[3)]	1200	300	0

[1)] 3000 and 1900 in farmyard manure and plant residues, respectively.

[2)] 3000 and 1500 in farmyard manure and plant residues, respectively.

[3)] As plot b until 1975, then 1500 and 1100 in plant residues for 4 years and the remaining period, respectively.

Table 6-4 Assumed partitioning coefficients for carbon input in plant residues and farmyard manure for long term field experiments in the Hoosfield and Broadbalk fields at Rothamsted Experimental Station.

Carbon source	$f_{AOM\ 1}$	$f_{AOM\ 2}$	$1-(f_{AOM\ 1}+f_{AOM\ 2})$
Plant residues	0.80	0.20	0
Farmyard manure (Broadbalk)	0.72	0.08	0.20
Farmyard manure (Hoosfield)	0.63	0.07	0.30

The parameters for soil organic matter and microbial biomass in the soil organic matter model were assessed by adjustment of the parameters when applying the model to the long term experiments. In Table 6-2 the initial values of carbon in the various pools of organic matter used for the simulations are listed. The annual application rates of carbon and the assumed partitioning coefficients are shown in Table 6-3 and Table 6-4, respectively. The decomposition rate coefficients for AOM 1 and AOM 2 at standard conditions were assumed to be $7.0\ 10^{-3}$ and $7.0\ 10^{-2}$ day^{-1}, respectively, while the partitioning coefficient $f_{BOM\ 1}$ was assumed to be 0.5. Regarding abiotic factors a clay content of 23% was used while a soil water content corresponding to pF = 3.0 was assumed. The soil temperature was assumed to follow an annual course with an amptitude of about 10 °C around an annual mean value of 9.8 °C. The values of parameters for the soil organic matter and the microbial biomass finally selected are shown in Table 6-5.

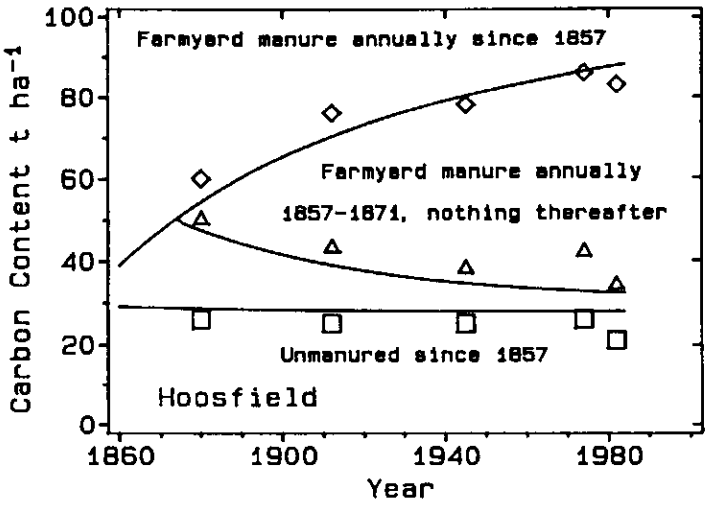

Fig. 6-6 Measured and simulated long term carbon content of soil with different annual applications of fertilizer and manure.

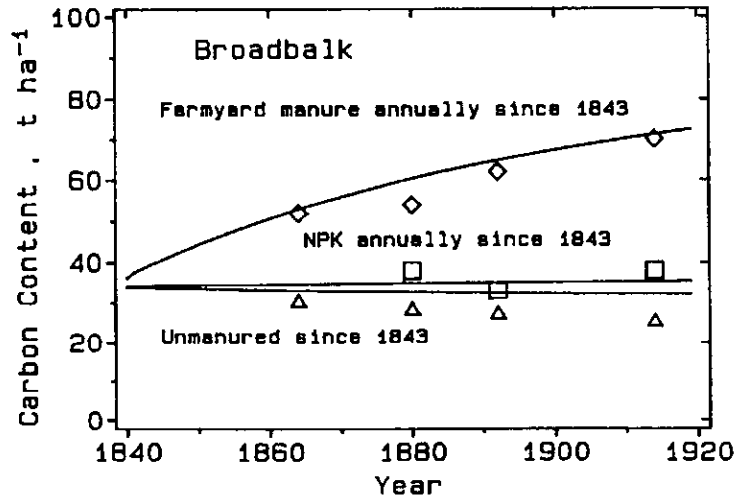

Fig. 6-7 Measured and simulated long term carbon content of soil with different annual applications of fertilizer and manure.

Table 6-5 Values of parameters for soil organic matter and microbial biomas in the soil organic matter model assessed from long term field experiments.

$k^*_{SOM\ 1}$	$= 2.7\ 10^{-6}\ day^{-1}$	$m^*_{BOM\ 1}$	$= 1.0\ 10^{-2}\ day^{-1}$
$k^*_{SOM\ 2}$	$= 1.4\ 10^{-4}\ day^{-1}$	$m^*_{BOM\ 2}$	$= 1.0\ 10^{-2}\ day^{-1}$
$d^*_{BOM\ 1}$	$= 1.0\ 10^{-3}\ day^{-1}$	$E_{BOM\ 1}$	$= 0.60$
$d^*_{BOM\ 2}$	$= 1.0\ 10^{-2}\ day^{-1}$	$E_{BOM\ 2}$	$= 0.60$
$f_{SOM\ 1}$	$= 0.10$	$f_{SOM\ 2}$	$= 0.40$

By using the selected parameters the soil organic matter turnover was simulated for the various treatments in the Hoosfield and Broadbalk fields. The results in terms of carbon content in the topsoil (0-23 cm) versus time are shown in Fig. 6-6 and Fig. 6-7, respectively, for comparison with the experimental results. In general good agreement between simulated and experimental data has been obtained except in the case of the unfertilized plot in the Broadbalk field.

Short term incubation experiments

In addition to the long term experiments at Rothamsted Experimental Station short term incubation experiments described by Lind et al. (1990) have been considered for assessment of parameters entering the soil organic matter model. The two soils considered were Jyndevad (Coarse sand) and Askov (Sandy clay). After application of various rates of straw (0, 2, 4, and 6 t DM ha^{-1}), plant residues of ryegrass (0, 0.5, 1.0, and 2.0 t DM ha^{-1}), and pig slurry (0, 25, 50 and 100 t ha^{-1}) soil samples at various soil water contents (25, 75, 100, and 125% of Field Capacity) were incubated at various temperatures (5, 10, and 20 °C) for about 3 months during which period evolution of CO_2 and the concentrations of NH_4^+ - N and NO_3 - N were currently measured.

Unfortunately the initial values of C and N in the various pools of organic matter were not known. Therefore in order to estimate the initial values an iterative procedure was adobted. For the soil samples without application of organic matter the six pools of organic matter (AOM 1, AOM 2, BOM 1, BOM 2, SOM 1, SOM 2) were considered one of which (AOM 2) was assumed to be zero at the time of soil sampling. Furthermore it was assumed that the pools of microbial biomass (BOM 1 and BOM 2) were in equilibrium with the other pools of organic matter at the time of sampling. Then it was possible to establish 5 equations (viz. equations for total content of carbon, total content of nitrogen in organic matter, steady state of BOM 1 and BOM 2 and initial evolution rate of CO_2) with 5 unknown variables.

For each soil the values of the rate coefficients and partitioning coefficients were adjusted for assumed values of C:N ratios of 100, 6, 10, 10, and 12 for AOM 1, BOM 1, BOM 2, SOM 1, and SOM 2, respectively, to minimize the difference between measured and simulated values of the CO_2 evolution rate and the concentration of inorganic nitrogen in the soil.
Thus after establishing a set of parameters in this way the five equations could be solved for the initial content of C and N in the various pools of organic matter.

Table 6–6 Values of parameters for added organic matter to soil in the soil organic matter model assessed from short term incubation experiments ($f_{BOM\ 1}$ = 0.50 in all cases).

Parameter	Straw	Plant residues	Pig slurry
$k^*_{AOM\ 1}$, day^{-1}	$1.0\ 10^{-2}$	$5.0\ 10^{-3}$	$5.0\ 10^{-3}$
$k^*_{AOM\ 2}$, day^{-1}	$1.0\ 10^{-1}$	$5.0\ 10^{-2}$	$5.0\ 10^{-2}$
$f_{AOM\ 1}$	0.45	0.40	0.90
$f_{AOM\ 2}$	0.55	0.60	0
$1-f_{AOM\ 1}-f_{AOM2}$	0	0	0.10

In the case of application of organic matter to the soil the amount of C and N in the applied organic matter were known. Furthermore the initial differences in the rate of CO_2 evolution rates between the soil with and without application of organic matter were known. Thus in the case of application of straw and plant residues from ryegrass two equations (viz. equations relating the difference in the content of carbon in organic matter and the difference in initial evolution rate of CO_2, respectively, to AOM 1 and AOM 2) with two unknown variables could be established from which AOM 1 and AOM 2 could be calculated. Nitrogen in applied organic matter was then allocated to AOM 1 and AOM 2 using an assumed value of C:N ratio of 100 for AOM 1. In the case of pig slurry which appeared to be considerably decomposed AOM 2 was assumed to be zero. Consequently C and N in the applied organic matter were allocated to AOM 1 and SOM 2 in a similar way as described for allocation of C and N in straw and plant residues of ryegrass to AOM 1 and AOM 2. Finally after assuming an approximate value of the decomposition rate coefficient for AOM 2 simulations of the carbon and nitrogen turnover were performed.

Thus by introducing the parameters assessed from long term experiments described previously and by parameter adjustments including readjustments of initial values of C and N in the various pools of organic matter, a set of parameters was selected, which minimized the differences between measured and simulated values of CO_2 evolution rate and content of inorganic nitrogen in the soil by considering the whole experimental data set.

The resulting parameters in addition to those given in Table 6-5 are given in Table 6-6. In Fig. 6-8 and Fig. 6-9 examples of simulated values of CO_2 evolution rate and nitrogen contents in soils by using the selected set of assessed parameters in the soil organic matter model are shown for comparison with experimental results.

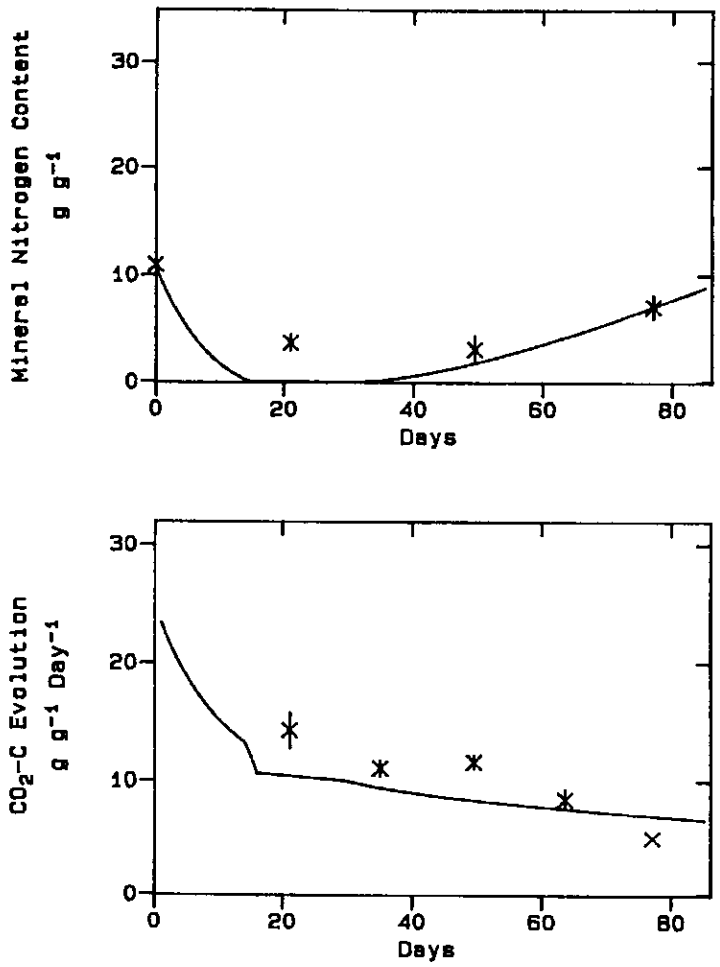

Fig 6-8 Measured and simulated short term mineral nitrogen contents and carbon dioxide evolution rate at field capacity and 10 °C for Askov soil after application of 4 t (DM) ha^{-1} of straw.

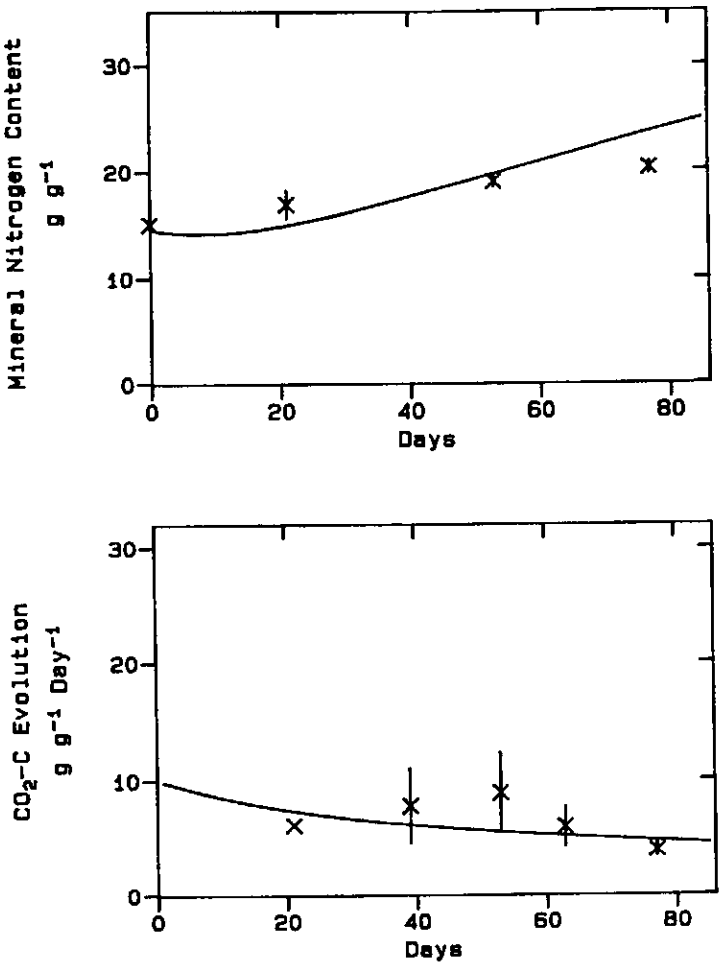

Fig. 6–9 Measured and simulated short term mineral nitrogen contents and carbon dioxide evolution rate at field capacity and 10 °C for Jyndevad soil after application of 1 t (DM) ha ^{1} of plant residues of grass.

It is noted that assessment of the present parameters is based on incubation experiments in which the added organic matter was finely divided which may have resulted in an overestimation of the turnover rates as compared to those expected under usual field conditions. Furthermore it is noted that the added organic matter contains lignin and other resistant constituents. Thus it might have been appropriate to route parts of the added organic matter directly to soil organic matter (SOM 2) as in the case of partly humified slurry or manure. Consequently for subsequent simulations the decomposition rate coefficients for straw are assumed to be similar to those assessed for plant residues and pig slurry, Table 6–6, while $f_{AOM\ 1}$, $f_{AOM\ 2}$, and $1-f_{AOM\ 1}-f_{AOM\ 2}$ are assumed to be 0.73, 0.20, and 0.07, respectively.

7. SOIL MINERAL NITROGEN MODEL

7.1 Introduction

The significance of inorganic nitrogen

In general mineral nitrogen in arable soils constitute only a minor part of soil nitrogen. Nevetheless, transformation and transport processes involving different forms of mineral nitrogen are of great importance in the overall cycle of nitrogen in nature.

The processes relating organic forms of soil nitrogen to mineral forms of nitrogen, i.e. mineralization and immobilization, are described previously as a part of the soil organic matter model. In the present soil mineral nitrogen model transformation and transport processes of mineral nitrogen are described.

Processes involving inorganic nitrogen

The processes considered include nitrification and denitrification as well as the effects of soil temperature and soil water content. Furthermore the radial movement of $NH_4^+ - N$ and $NO_3^- - N$ to plant roots and the nitrogen uptake by plants are considered. Finally vertical movement of $NH_4^+ - N$ and $NO_3^- - N$ are described in terms of the convection dispersion equation to which an explicit nummerical solution is given by using the finite difference method.

7.2 Nitrification

Microbial oxidation of ammonium

The microbial process whereby $NH_4^+ - N$ is oxidized to $NO_3^- - N$ is referred to as nitrification. Ammonification, nitrification and denitrification, as well as possible interrelationships between the processes of nitrification and denitrification are illustrated in Fig. 7 – 1 from results collected by Knowles (1978) and Nicholas (1978).

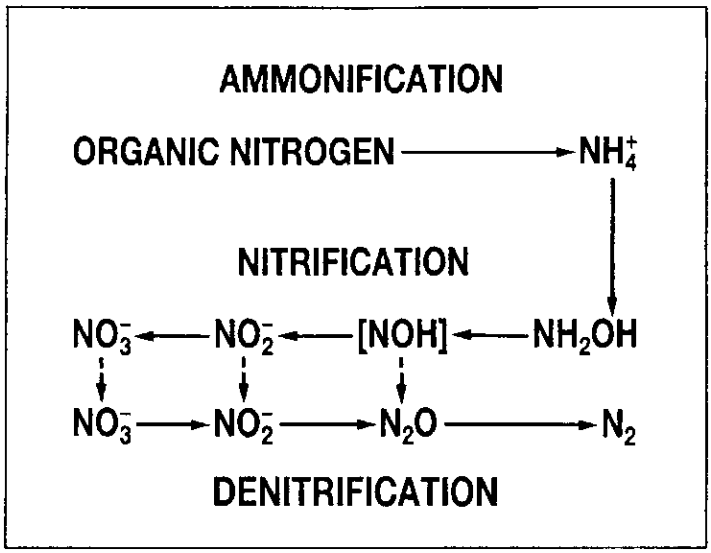

Fig. 7–1 Ammonification, nitrification, denitrification, and possible interrelationships.

First order kinetics

In well aerated arable soils, at relatively high water content ($1.5 < pF < 2.5$) pH in the range 4–8 soil temperature higher than 5°C, microbial activity is limited by the availability of organic carbon, and most $NH_4^+ - N$ is oxidized to $NO_3^- - N$ as rapidly as it is formed by the process of ammonification. Thus under such conditions $NO_2^- - N$ is rapidly oxidized to $NO_3^- - N$ and release of N_2O during oxidation of $NH_4^+ - N$ in all probability occurs only under conditions of reduced oxygen pressure. Under such conditions nitrification can be considered as a single step process which can be described by first order reaction kinetics, eq. (7–1).

$$\xi_n = k_n(T, \psi)\, N_{NH_4^+ - N} \qquad (7-1)$$

ξ_n = specific nitrification rate [kg $(NO_3^- - N)$ m^{-3} s^{-1}]
$k_n(T, \psi)$ = nitrification rate coefficient [s^{-1}]
$N_{NH_4^+ - N}$ = ammonium concentration in soil solution [kg $(NH_4^+ - N)$ m^{-3} (soil)]
T = soil temperature [°C]
ψ = pressure potential of soil water [m H_2O]

Abiotic functions

Abiotic factors affecting nitrification in soils are substrate (NH_4^+-N, O_2, CO_2) concentrations, pH, temperature and soil moisture content (Focht and Verstraete, 1977). In addition naturally occurring inhibitory substances may affect the nitrification. There is no evidence that pH in the range 5.5–8.0 and concentrations of CO_2 are ever limiting the nitrification process whereas the concentration of O_2 clearly can be limiting.

Effect of temperature

From data of Flowers and O'Callaghan (1983) temperature coefficients (Q_{10}-values) of nitrification of 2.0–2.9 in the temperature range 5–15°C were obtained. These findings are in accordance with earlier studies of Tyler et al. (1953) in which a Q_{10}-value of 2.1 was observed in the temperature range 7–24°C. Addiscott (1983) observed a sharp decrease in the rate of nitrification when the temperature decreased from 5.0 to 2.5°C. Thus it seems reasonable to assume that the rate of nitrification approaches zero at a temperature of 2°C.

Effect of soil water

At 30°C Miller and Johnson (1964) found the nitrification rate to be unlimited by soil moisture content in the pressure potential range from −0.15 to −0.50 bar. Similar results have been obtained by Sabey (1969). Results presented by Reichman et al. (1966) and Flowers and O'Callaghan (1983) show that the nitrification rate decreases from maximum to zero when the pressure potential decreases from −0.5 to −10 bars. From the present evidence the effects of temperature and soil moisture content on the nitrification rate coefficient can be expressed by eq. (7–2).

$$k_n(T, \psi) = k_n^{10} F_n^T(T) F_n^{\psi}(\psi) \qquad (7-2)$$

k_n^{10} = nitrification rate coefficient at 10°C and optimum soil water content conditions [s^{-1}]
$F_n^T(T)$ = soil temperature function given by eq. (7–3)
$F_n^{\psi}(\psi)$ = pressure potential function given by eq. (7–4)
T = soil temperature [°C]
ψ = pressure potential [m H_2O]

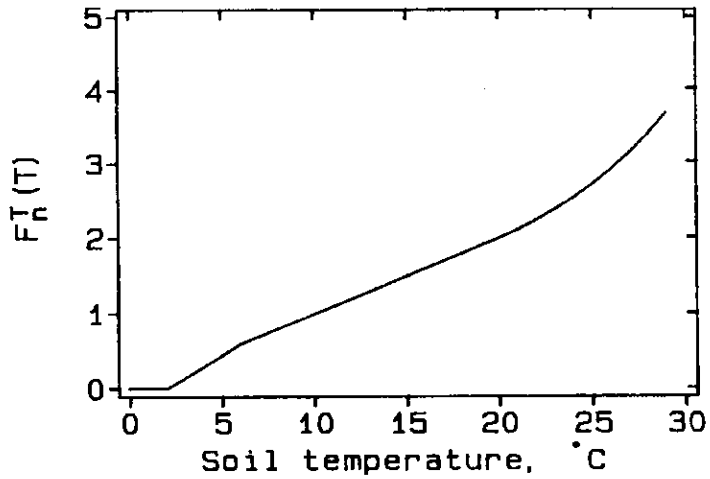

Fig. 7-2 Soil temperature function for adjustment of nitrification rate coefficient and denitrification rate to actual soil temperature.

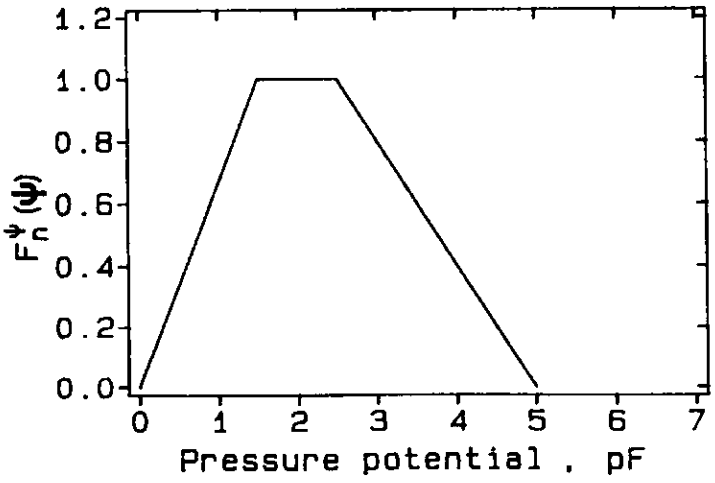

Fig. 7-3 Pressure potential function for adjustment of nitrification rate coefficient to actual soil water pressure potential.

$$F_n^T(T) = \begin{cases} 0 & T \leq 2 \\ 0.15\,(T-2) & 2 < T \leq 6 \\ 0.10\,T & 6 < T \leq 20 \\ e^{0.47-0.027T+0.00193T^2} & 20 < T < 40 \end{cases} \quad (7-3)$$

$$F_n^{\psi}(\psi) = \begin{cases} 0 & \psi \geq -10^{-2} \\ \log(-100\psi)/1.51 & -10^{-2} > \psi \geq -10^{-0.5} \\ 1 & -10^{-0.5} > \psi \geq -10^{0.5} \\ 1-\log(-100\psi)/2.5 & -10^{0.5} > \psi \geq -10^{-2} \\ 0 & -10^{-2} > \psi \end{cases} \quad (7-4)$$

Effect of oxygen

The effect of O_2 concentration on the nitrification rate is implicitly included in eq. (7-2) since O_2 concentration in solution is usually correlated with soil temperature and soil moisture content. Considering ammonification, eq. (6-19) and nitrification, eq. (7-1) it appears that NH_4^+-N accumulation may occur at low temperatures and at low and high soil water contents. The soil temperature function, eq. (7-3) and the pressure potential function, eq. (7-4) governing the nitrification rate coefficient are illustrated in Fig. 7-2 and Fig. 7-3, respectively.

7.3 Denitrification

Microbial reduction of nitrate

Biological denitrification has long been considered an important pathway by which nitrogen is lost in the form of gaseous nitrogen oxides or nitrogen gas, from the soil to the atmosphere. Although biological denitrification has been studied extensively during the recent two decades lack of knowledge still exists about the quantification of biological denitrification under field conditions from fundamental microbial processes. However, it is well established (Fillery, 1983) that the rate of denitrification is related to the amount of easily decomposeable organic matter, the volume of anaerobic microsites within an otherwise aerobic media, the soil temperature, and the concentration of NO_3^--N in the soil solution.

In the present model denitrification is simulated by means of a rather simple index type model taking into account the amount of easily available organic matter, volume of anaerobic microsites expressed simply in terms of soil water content, soil temperature, and the concentration of $NO_3^- - N$ in soil solution.

Potential denitrification

The evolution of CO_2 may be used as an index of the easily available organic matter. Thus in accordance with Lind (1980) the potential denitrification rate of the soil is expressed as a linear function of the CO_2 evolution rate, eq. (7–5).

$$\xi_d^* = F_d^T(T)\, \alpha_d^*\, \xi_{CO_2} \qquad (7-5)$$

ξ_d^* = potential denitrification rate of soil [kg N m^{-3} s^{-1}]
ξ_{CO_2} = CO_2 evolution rate [kg C m^{-3} s^{-1}]
α_d^* = empirical constant [kg C m^{-3} s^{-1}]
$F_d^T(T)$ = soil temperature function

In the present model the values of ξ_{CO_2} are derived from the organic matter model, as the evolution of CO_2 from the decomposition of organic matter.

For a soil with a potential denitrification rate given by eq. (7–5) it is assumed that the actual denitrification rate is determined either by the transport of $NO_3^- - N$ to the anaerobic microsites or the actual microbial activity at these sites.

Actual denitrification

Transport of $NO_3^- - N$ to the denitrifying microsites which are considered as zero sinks may be calculated from eq. (7–6).

$$\xi_t = \left[\sum_{i=1}^{n} \theta\, A_i\, D\, \frac{C_{NO_3^- - N}}{\Delta r_i} \right] V^{-1} = K_d\, N_{NO_3^- - N} \qquad (7-6)$$

ξ_t = denitrification rate determined by transport of $NO_3^- - N$ to anaerobic microsites [kg N m^{-3} s^{-1}]

θ = soil water content [m^3 m^{-3}]

D = diffusion coefficient [m^2 s^{-1}]

A_i = surface area of microsite i [m^2]

V = soil volume [m^3]

$C_{NO_3^- - N}$ = concentration of $NO_3^- - N$ in soil solution [kg N m^{-3}]

$N_{NO_3^- - N}$ = concentration of $NO_3^- - N$ in soil [kg N m^{-3}]

K_d = empirical constant [s^{-1}]

Δr_i = diffusion distance to microsite i [m]

n = number of microsites

The basic idea of the application of eq. (7–6) is that the transport of $NO_3^- - N$ to the anaerobic microsites is assumed to take place as diffusion. Thus (θ A_i) represents the area through which diffusion takes place toward microsite i within the soil volume V. In the present model the overall effect of D, A_i, and Δr_i is pooled in an emperial constant K_d.

In the case of ample supply of $NO_3^- - N$ to the microsites the actual denitrification rate is determined by the actual denitrification activity which is expressed by eq. (7–7).

$$\xi_a = F_d^{\theta}(\theta)\ \xi_d^{\star} \qquad (7-7)$$

ξ_a = denitrification rate determined by actual microbial activity at anaerobic microsites [kg N m^{-3} s^{-1}]

$F_d^{\theta}(\theta)$ = soil water content function

Effect of soil water

The soil water effect function is adopted from Rolston et al. (1984) and is expressed by eq. (7–8).

$$F_d^{\theta}(\theta) = \begin{cases} 0 & x_w \le x_1 \\ f\,\dfrac{x - x_1}{x_2 - x_1} & x_1 < x_w < x_2 \\ f + (1-f)\,\dfrac{x - x_2}{1 - x_2} & x_2 < x_w \le 1 \end{cases} \qquad (7-8)$$

x_w = degree of water saturation (θ/θ_s)
θ = soil water content [$m^3\ m^{-3}$]
θ_s = soil water content at saturation [$m^3\ m^{-3}$]
f, x_1, and x_2 are constants.

The soil water function is shown in Fig. 7–4. The temperature function is identical with the temperature function adopted for the nitrification process, eq. (7–3). The actual denitrification rate is then calculated from eq. (7–9).

$$\xi_d = \text{Min}\ \{\xi_t, \xi_a\} \qquad (7-9)$$

ξ_d = actual denitrification rate [kg N $m^{-3}\ s^{-1}$]

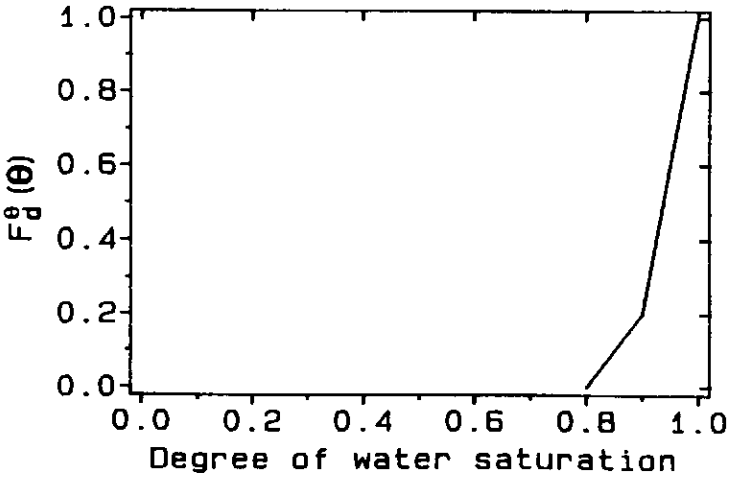

Fig. 7–4 Soil water content function for adjustment of denitrification rate to actual soil water content.

7.4 Nitrogen uptake by plants

Potential nitrogen uptake

The nitrogen uptake model can be considered as an analogy to the water uptake model. The upper limit for nitrogen uptake which may be designated as the potential nitrogen uptake is assumed to be solely determined by the crop.

The actual nitrogen uptake may be equal to the potential nitrogen uptake or it may be limited due to low availability of nitrogen in the soil.

It is assumed that a plant will take up nitrogen only until a certain nitrogen content in the plant is reached (Hansen and Aslyng, 1984; Greenwood, 1986). This maximum content of nitrogen is calculated from eq. (7 – 10).

$$N_c^* = \sum_{j=1}^{n} c_j^* W_j \qquad (7-10)$$

N_c^* = upper limit of nitrogen content in crop [kg (N) m^{-2}]
c_j^* = upper limit of nitrogen concentration in plant part j [kg (N) kg^{-1} (DM)]
W_j = dry matter in plant part j [kg (DM) m^{-2}]
n = number of plant parts constituting the plant.

Values of c_j^* and W_j are obtained from the crop model. In the present context a plant part may be e.g. the plant root system or the above ground part of wheat crop.

It is assumed that the crop will take up nitrogen until the upper limit (N_c^*) is reached if the nitrogen supply is ample and if the root density is sufficient. Thus the maximum nitrogen uptake rate can be calculated from eq. (7 – 11).

$$\zeta_u^* = \text{Min}\left\{(I^*_{NH_4^+-N} + I^*_{NO_3^--N}) \int_0^{dr} L\,dt,\ \frac{N_c^*(t+\Delta t) - N_c(t)}{\Delta t}\right\} \qquad (7-11)$$

ζ_u^* = maximum uptake rate of nitrogen [kg m^{-2} day^{-1}]

$I^*_{NH_4^+-N}$ = maximum uptake rate of NH_4^+ –N per unit length of root [kg (N) m^{-1} (root) day^{-1}]

$I^*_{NO_3^--N}$ = maximum uptake rate of NO_3^- –N per unit length of root [kg (N) m^{-1} (root) day^{-1}]

L = root density [m m^{-3}]

dr = root depth [m]

N_c = actual nitrogen content in the crop [kg (N) m^{-2}]

t = time

Δt = time step (1 day)

In eq. (7–11) it is assumed that $I^*_{NH_4^+-N}$ and $I^*_{NO_3^--N}$ are constants while values of L and dr are obtained from the crop model. If the soil is able to supply nitrogen to the root surface at a rate equal to or greater than the maximum uptake rate then the uptake rate is equal to the maximum uptake rate, otherwise the actual uptake rate is determined by the soil.

Nitrogen movement to root surfaces

In the calculation of nitrogen movement from the bulk soil to the root surfaces similar assumptions are made to those applied in the calculation of the movement of water from the bulk soil to the root surfaces. Thus it is assumed that only radial movement takes place and that the movement takes place only in the cylindrical soil volume surrounding the root. The radial transfer of nitrogen is approximated by a series of steady states. Assuming steady state the mass conservation equation in cylindrical coordinates takes the form of eq. (7–12)

$$\frac{1}{r}\frac{d}{dr}\left[r D_x^* \frac{dN_x}{dr} + r v_w C_x\right] = 0 \qquad (7-12)$$

r = distance from center of root [m]
v_w = water flux density [m s^{-1}]
N_x = concentration of substance x in soil [kg m^{-3}]
C_x = concentration of substance x in soil solution [kg m^{-3}]
D_x^* = dispersion coefficient for substance x [m^2 s^{-1}]

Considering uptake of nitrogen the x in eq. (7–12) may be either NH_4^+–N or NO_3^-–N. By introducing the buffer power with respect to substance x defined by eq. (7–13) into eq. (7–12) integration results in eq. (7–14).

$$b_x = \frac{dN_x}{dC_x} \qquad (7-13)$$

$$I_x = 2\pi r D_x \frac{dC_x}{dr} + q_w C_x \qquad (7-14)$$

I_x = flux of substance x towards the root [kg m^{-1} s^{-1}]
b_x = buffer power of soil with respect to substance x
$D_x = D_x^* \cdot b_x$
$q_w = 2\pi r v_w$, water flux towards the root [m^3 m^{-1} s^{-1}]

It is noted that the water flux towards the root is obtained from the soil water model. Eq. (7–14) may be rearranged to give eq. (7–15) the solution to which is eq. (7–16).

$$\frac{dC_x}{dr} = \frac{q_w}{2\pi D_x} \frac{C_x}{r} = \frac{I_x}{2\pi D_x} \frac{1}{r} \qquad (7-15)$$

$$C_x = \begin{cases} \dfrac{I_x}{2\pi D_x} \ln r + B & \alpha = 0 \\ \dfrac{I_x}{q_w} + B r^{-\alpha} & \alpha \neq 0 \end{cases} \qquad (7-16)$$

B = integration constant [kg m^{-3}]
$\alpha = q_w(2\pi D_x)^{-1}$

Assuming a concentration $C_x = C_{x,0}$ at the root surface at which $r = r_r$ the integration constant B is given by eq. (7-17) which introduced in eq. (7-16) results in eq. (7-18).

$$B = \begin{cases} C_{x,0} - \dfrac{I_x}{2\pi D_x} \ln r_r & \alpha = 0 \\ \left[(C_{x,0} - \dfrac{I_x}{q_w} \right] r_r^{\alpha} & \alpha \neq 0 \end{cases} \qquad (7-17)$$

$$C_x = \begin{cases} C_{x,0} + \dfrac{I_x}{2\pi D_x} \ln \left[\dfrac{r}{r_r} \right] & \alpha = 0 \\ \dfrac{I_x}{q_w} + \left[C_{x,0} \ \dfrac{I_x}{q_w} \right] \left[\dfrac{r}{r_r} \right]^{-\alpha} & \alpha \neq 0 \end{cases} \qquad (7-18)$$

The average concentration in solution within the considered cylindrical soil volume is given by eq. (7-19).

$$\bar{C}_x = \frac{2\pi}{\pi(r_c^2 - r_r^2)} \int_{r_r}^{r_c} r \, C_x \, d\, r \qquad (7-19)$$

$\bar{C}_x$ = average concentration in solution of substance x within cylindrical soil volume [kg m^{-3}]

r_c = $(\pi L)^{-½}$, radius of considered cylindrical soil volume [m].

Assuming a constant value of α or if $\alpha = 0$ that $I_x\, b_x\, (2\pi\, D_x)^{-1}$ is independent of r eq. (7-19) can be integrated which results in eq. (7-20).

$$\bar{C}_x = \begin{cases} C_{x,0} + \dfrac{I_x}{2\pi\, D_x}\left[\dfrac{\beta^2 \ln \beta}{\beta^2 - 1} - \tfrac{1}{2}\right] & \alpha = 0 \\ \dfrac{I_x}{q_w} + \left[C_{x,0} - \dfrac{I_x}{q_w}\right]\dfrac{\ln \beta^2}{\beta^2 - 1} & \alpha = 2 \\ \dfrac{I_x}{q_w} + \left[C_{x,0} - \dfrac{I_x}{q_w}\right]\dfrac{\beta^{2-\alpha} - 1}{(\beta^2 - 1)(1 - \tfrac{1}{2}\alpha)} & \text{else} \end{cases} \qquad (7-20)$$

$$\beta = r_c\, r_r^{-1} = r_r^{-1}\, (\pi\, L)^{-\frac{1}{2}}$$

Actual nitrogen uptake

Eq. (7-20) can be rearranged to give eq. (7-21) from which the uptake rate of substance x per unit length of root is calculated with the constraint that the uptake rate per unit root length can not exceed the uptake capacity of the root.

$$I_x = \begin{cases} 2\pi\, D_x\, (\bar{C}_x - C_{x,0})\left[\dfrac{\beta^2 \ln \beta}{\beta^2 - 1} - \tfrac{1}{2}\right]^{-1} & \alpha = 0 \\ q_w\, \dfrac{(\beta^2 - 1)\bar{C}_x - C_{x,0} \ln \beta^2}{(\beta^2 - 1) - \ln \beta^2} & \alpha = 2 \\ q_w\, \dfrac{(\beta^2 - 1)(1 - \tfrac{1}{2}\alpha)\bar{C}_x - (\beta^{2-\alpha} - 1)C_{x,0}}{(\beta^2 - 1)(1 - \tfrac{1}{2}\alpha) - (\beta^{2-\alpha} - 1)} & \text{else} \end{cases} \qquad (7-21)$$

The uptake rate of substance x from a unit layer of soil can be calculated from eq. (7-22) after which the total uptake rate of substance x from the entire root zone is calculated from eq. (7-23).

$$\xi_{u,x} = \text{Min}\ \{l_x^*, l_x\}L \qquad (7-22)$$

$$\zeta_{u,x} = \int_0^{d_r} \xi_{u,x}\, d\,z \qquad (7-23)$$

$\xi_{u,x}$ = uptake rate of substance x per unit layer of soil [kg m^{-3} day^{-1}]

$\zeta_{u,x}$ = uptake rate of substance x for entire root zone [kg m^{-2} day^{-1}]

d_r = rooting depth [m]

Thus the total nitrogen uptake rate from the entire root profile is found from eq. (7-24).

$$\zeta_u = \zeta_{u,NH_4^+-N} + \zeta_{u,NO_3^--N} \qquad (7-24)$$

ζ_u = total nitrogen uptake rate from root zone [kg (N) m^{-2} day^{-1}]

ζ_{u,NH_4^+-N} = uptake rate of NH_4-N from root zone [kg (N) m^{-2} day^{-1}]

ζ_{u,NO_3^--N} = uptake rate of NO_3-N from root zone [kg (N) m^{-2} day^{-1}]

Preferential uptake of ammonium

A basic assumption is that the uptake of NH_4^+-N has preference over the uptake of NO_3^--N. Consequently uptake of NO_3^--N only takes place if $\zeta_{u,NH_4^+-N} < \zeta_u^*$. Thus the potential uptake rate of NO_3^--N is given by eq. (7-25)

$$\zeta_{u,NO_3^--N}^* = \zeta_u^* - \zeta_{u,NH_4^+-N} \qquad (7-25)$$

$\zeta_{u,NO_3^--N}^*$ = potential uptake rate of NO_3^--N in root zone [kg (N) m^{-2} day^{-1}]

Mobility of nitrate and ammonium

In general the concentration of $NH_4^+ - N$ in soil solution in less that that of $NO_3^- - N$. Furthermore, the mobility of $NH_4^+ - N$ in soil is low and less than the mobility of $NO_3^- - N$. Consequently most of the nitrogen taken up by plants is in the form of $NO_3^- - N$.

In eq. (7–21) two unknown variables appear, viz. I_x and $C_{x,0}$. Thus when using eq. (7–21) it is assumed that $C_{x,0}$ is constant along the roots, while I_x may vary according to the variation in the other variables in the equation. Two situations may occur.

1. The nitrogen supply is ample and not limiting the uptake rate.
2. The nitrogen supply is limiting the uptake rate.

In the first situation a common value of $C_{x,0}$ along the root is used to give the distribution of the uptake. This common value of $C_{x,0}$ is obtained by applying an iterative procedure ensuring that the total uptake is equal to the potential uptake of nitrogen.

In the second situation a common fixed value of $C_{x,0}$ is used. In this case the calculation of I_x is straight forward. For $NH_4^+ - N$ as well as for $NO_3^- - N$ the fixed value of $C_{x,0}$ is assumed to be zero which means that the root acts as a zero-sink.

In order to calculate the nitrogen uptake by plants a number of crop, soil, and soil water parameters have to be known. The required crop parameters and variables are obtained from the crop model, while the soil water variables viz. the soil water content and the soil water uptake by roots are obtained from the soil water model.

Diffusion coefficient

The required soil properties are the dispersion coefficient and the buffer power. In the calculation of solute transfer to the root surfaces hydrodynamic dispersion is neglected. In that case the dispersion coefficient is replaced by the diffusion coefficient which is calculated from eq. (7-26).

$$D_x = D_{x,e}\,\theta\,f_l \qquad (7-26)$$

D_x = diffusion coefficient of substance x in soil [$m^2\ s^{-1}$]
$D_{x,e}$ = diffusion coefficient of substance x in free solution [$m^2\ s^{-1}$]
θ = volumetric soil water content [$m^3\ m^{-3}$]
f_l = tortuosity factor

Tortuosity factor

The tortuosity factor is assumed to be a soil characteristic depending on the soil water content, eq. (7-27).

$$f_l = \begin{cases} f_l^0 & \theta \le \theta_0 \\ f_l^0 + a(\theta - \theta_0) & \theta > \theta_0 \end{cases} \qquad (7-27)$$

In eq. (7-27) f_l^0, θ_0 and a are constants. A value of f_l^0 equal to 10^{-6} is selected arbitrarily, while a and θ_0 are parameters characterizing the soil.

Buffer power

In the case of $NO_3^- - N$ it is assumed that no adsorption or desorption takes place. Hence the buffer power with respect to $NO_3^- - N$ can be obtained from eq. (7-28) as being equal to the volumetric soil water content.

$$b_{NO_3^- - N} = \frac{d\,N_{NO_3^- - N}}{d\,C_{NO_3^- - N}} = \frac{d(\theta\,C_{NO_3^- - N})}{d\,C_{NO_3^-\ N}} = \theta \qquad (7-28)$$

Ammonium adsorption

In the case of $NH_4^+ - N$ adsorption and desorption processes are to be taken into account. It is assumed that the exchange capacity of the soil is determined by the clay content and that exchange processes take place at three different types of

Adsorption desorption equation for ammonium

exchange sites, viz. planar sites, edge sites and interlattice sites (van Schouwenburg and Schuffelen, 1963), the latter of which is considered insignificant in the present context and hence neglected. For an illitic clay van Schouwenburg and Schuffelen (1963) described potassium–calcium exchange by eq. (7–29).

$$\gamma_{K^+} = 0.4258 \frac{2.21\ R}{1 + 2.21\ R} + 0.020 \frac{102.3\ R}{1 + 102.3\ R} \qquad (7-29)$$

γ_{K^+} = potassium adsorbed [m.e. g^{-1} (clay)]
R = $C_{K^+} + /(C_{Ca^{++}})^{-½}$
C_{K^+} = concentration of potassium [mole l^{-1}]
$C_{Ca^{++}}$ = concentration of potassium [mole l^{-1}]

Potassium–ammonium exchange on a clay, eq. (7–30), may be quantitatively described by eq. (7–31).

$$\text{clay} - K^+ + NH_4^+ = \text{clay} - NH_4^+ + K^+ \qquad (7-30)$$

$$\frac{\gamma_{NH_4^+}}{\gamma_{K^+}} = K_{NH_4^+/K^+} \frac{C_{NH_4^+}}{C_{K^+}} \qquad (7-31)$$

$\gamma_{NH_4^+}$ = ammonium adsorbed [m.e. g^{-1} (clay)]
γ_{K^+} = potassium adsorbed [m.e. g^{-1} (clay)]
$C_{NH_4^+}$ = concentration of ammonium [mole l^{-1}]
C_{K^+} = concentration of potassium [mole l^{-1}]
$K_{NH_4^+/K^+}$ = exchange coefficient

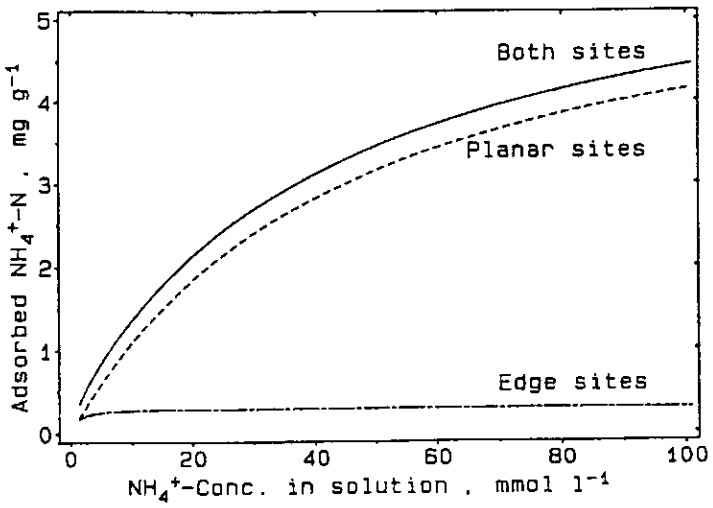

Fig. 7-5 Ammonium adsorption isotherms for various adsorption sites in the concentration range 0-100 mmol l^{-1}

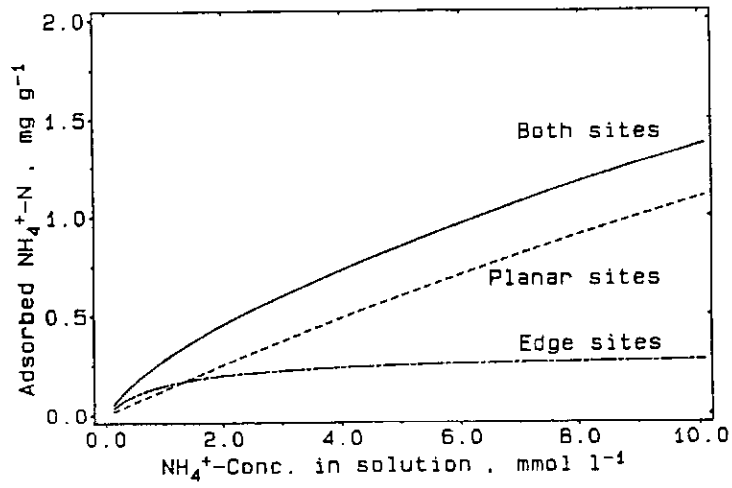

Fig. 7-6 Ammonium adsorption isotherms for various adsorption sites in the concentration range 0-10 mmol l^{-1}

Assuming calcium to be the dominant divalent cation, that $K_{NH_4^+/K^+} = 1.0$ and that $C_{Ca^{++}} = 0.01$ mole l^{-1} then eq. (7–29) and eq. (7–31) can be combined to give eq. (7–32) and eq. (7–33) in which V_p, K_p, V_e, and K_e are parameters depending on the exchange properties of the clay.

$$\gamma_{NH_4^+} = 6\ 10^{-3} \frac{C_{NH_4^+-N}}{0.64 + C_{NH_4^+-N}} + 0.3\ 10^{-3} \frac{C_{NH_4^+-N}}{0.014 + C_{NH_4^+-N}} \qquad (7-32)$$

$$\gamma_{NH_4^+} = V_p \frac{C_{NH_4^+-N}}{K_p + C_{NH_4^+-N}} + V_e \frac{C_{NH_4^+-N}}{K_e + C_{NH_4^+-N}} \qquad (7-33)$$

$\gamma_{NH_4^+}$ = adsorbed NH_4^+-N [kg N kg^{-1} (clay)
$C_{NH_4^+-N}$ = concentration of NH_4^+-N in soil solution [kg N m^{-3}]

The relationship expressed by eq. (7–32) is shown in Fig. 7–5 and Fig. 7–6. Assuming equilibrium conditions to exist, the relationship between the concentration of NH_4^+-N in the soil and in the soil solution can be expressed as eq. (7–34). Differentiation of eq. (7–34) results in eq. (7–35) from which the buffer power with respect to NH_4^+-N can be obtained.

$$N_{NH_4^+-N} = x_c \rho \left[V_p \frac{C_{NH_4^+-N}}{K_p + C_{NH_4^+-N}} + V_e \frac{C_{NH_4^+-N}}{K_e + C_{NH_4^+-N}} \right] + \theta\, C_{NH_4^+-N} \qquad (7-34)$$

$$b_{NH_4^+-N} = \frac{d\, N_{NH_4^+-N}}{d\, C_{NH_4^+-N}}$$

$$= \frac{x_c\, \rho\, V_p\, K_p}{(K_p + C_{NH_4^+-N})^2} + \frac{x_c\, \rho\, V_e\, K_e}{(K_e + C_{NH_4^+-N})^2} + \theta \quad (7-35)$$

$N_{NH_4^+-N}$ = concentration of NH_4^+-N in soil [kg N m^{-3} (soil)]
x_c = clay content of soil
ρ = soil dry bulk density [kg m^{-3}]

In calculations of diffusion coefficient and buffer power bulk values of the soil water content are used. Furthermore the average values of the concentration of NH_4^+-N and NO_3^-N, respectively, are assumed equal to the bulk values of the corresponding concentrations used in the solution of the convection dispersion equation.

7.5 Vertical movement of inorganic nitrogen

Convection dispersion equation

One dimensional vertical movement of a substance x takes place as a result of diffusion as well as convection which is described by eq. (7-36), while the principle of conservation of matter is expressed by eq. (7-37).

$$J_x = -D_x^* \frac{d\, N_x}{d\, z} + q_w\, C_x \quad (7-36)$$

$$\frac{\partial\, N_x}{\partial\, t} = -\frac{\partial\, J_x}{\partial\, z} + \phi_x \quad (7-37)$$

J_x = flux density of substance x [kg m^{-2} s^{-1}]
D_x^* = dispersion coefficient of substance x [m^2 s^{-1}]
N_x = concentration of substance x in soil [kg m^{-3}]
C_x = concentration of substance x in soil solution [kg m^{-3}]
q_w = water flux density [m^3 m^{-2} s^{-1}]

ϕ_x = sink-source term [kg m^{-3} s^{-1}]

By combining eq. (7-36) and eq. (7-37) and introducing the buffer power, eq. (7-13), the convection dispersion equation, eq. (7-38), is obtained.

$$\frac{\partial(A_x + \theta C_x)}{\partial t} = -\frac{\partial}{\partial z}\left[-\theta D_x \frac{\partial C_x}{\partial z} + q_w C_x\right] + \phi_x \qquad (7-38)$$

A_x = adsorbed amount of substance x [kg m^{-3}]

Dispersion coefficient

The dispersion coefficient is calculated from eq. (7-39).

$$D_x = \lambda \left|\frac{q_w}{\theta}\right| + D_{x,l} f_l \qquad (7-39)$$

D_x = dispersion coefficient [m^2 s^{-1}]
$D_{x,l}$ = diffusion coefficient of substance x in free solution [m^2 s^{-1}]
λ = dispersion length [m]
q_w = water flow [m^3 m^{-2} s^{-1}]
θ = volumetric water content
f_l = tortuosity factor

In the case of transfer of NH_4^+-N the adsorption term in eq. (7-38) is calculated as previously described, while in the case of transfer of NO_3^--N the adsorption term is assumed to be zero.

Source sink term

The sink source term in eq. (7-38) is calculated according to eq. (7-40) and eq. (7-41) for the transfer of NH_4^+-N and NO_3^--N, respectively.

$$\phi_{NH_4^+-N} = \xi_m + \xi_{f,NH_4^+-N} - \xi_{u,NH_4^+-N} - \xi_n \qquad (7-40)$$

$$\phi_{NO_3^--N} = \xi_n + \xi_{f,NO_3^--N} - \xi_{u,NO_3^--N} - \xi_d \qquad (7-41)$$

ξ_m = net mineralization rate [kg m^{-3} s^{-1}]
ξ_n = nitrification rate [kg m^{-3} s^{-1}]
ξ_d = denitrification rate [kg m^{-3} s^{-1}]
ξ_{f,NH_4^+-N} = NH_4^+ – N-fertilizer input rate [kg m^{-3} s^{-1}]
ξ_{f,NO_3^-N} = NO_3^- – N-fertilizer input rate [kg m^{-3} s^{-1}]
ξ_{u,NH_4^+-N} = NH_4^+ – N-uptake rate [kg m^{-3} s^{-1}]
ξ_{u,NO_3^-N} = NO_3^- – N-uptake rate [kg m^{-3} s^{-1}]

The fertilizer input rate for the substance x is given by Dirac's delta function, eq. (7–42).

$$\xi_{f,x} = \begin{cases} \frac{f_x}{\Delta} & t_f \le t \le t_f + \Delta \\ 0 & \text{else} \end{cases} \qquad (7-42)$$

f_x = fertilizer input of substance x [kg m^{-3}]
t_f = time of fertilizer input
f_x = $F_x/\Delta z$
F_x = applied fertilizer, substance x [kg m^{-2}]
Δz = depth to which the fertilizer is uniformly distributed [m]

Values of F_x and Δz are obtained from the system management model. In order to solve eq. (7–38) an upper boundary as well as a lower boundary condition have to be specified.

Upper boundary

The upper boundary condition is always a flux condition. The flux condition may be a zero flux or a positive flux, the latter when nitrogen dissolved in precipitation or irrigation water is entering the soil at the soil surface.

Lower boundary

The lower boundary condition constitutes a particular problem because the conditions at the bottom of the soil column under consideration are not known. Thus it is assumed that the concentration gradient is equal to zero at the bottom of the soil column, eq. (7–44).

$$\left[\frac{\partial C_x}{\partial z}\right]_{z = z_c} = 0 \qquad (7-44)$$

C_x = concentration of substance x in solution [kg m^{-3}]
z = soil depth [m]
z_c = depth of the bottom of the soil column considered [m]

This assumption is comparable with the assumption of gravity flow made as the lower boundary condition in the soil water model when the ground water level is well below the bottom of the soil column considered.

7.6 Numerical solution

The finite difference method

The finite difference scheme used in the nummerical approximation of the conversion dispersion equation, eq. (7-38), is illustrated in Fig. 7-7.

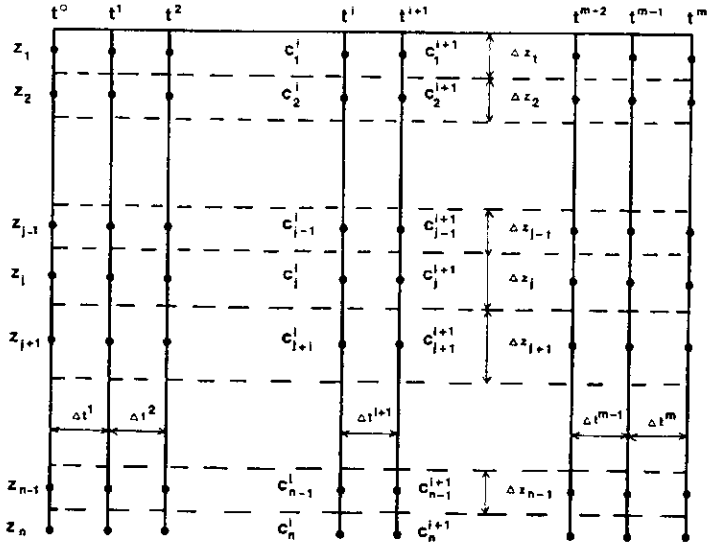

Fig. 7-7 Discretization after the finite difference method.

All nodes in the time-distance plan are numbered with the subscript j referring to the depth and with the subscript i referring to the time (i=0 is referring to the time of initialization). The time increments as well as the depth increments may vary. Thus the convection dispertion equation, eq. (7-38), may be approximated by means of eq. (7-45).

$$\frac{(\theta_j^{i+1} + \beta_j^{i+\frac{1}{2}})\, C_j^{i+1} - (\theta_j^{i} + \beta_j^{i+\frac{1}{2}})\, C_j^{i}}{\Delta z^{i+1}} =$$

$$\left[D_{j+\frac{1}{2}}^{i+\frac{1}{2}} \frac{C_{j+1}^{i+\frac{1}{2}} - C_j^{i+\frac{1}{2}}}{z_{j+1} - z_j} - D_{j-\frac{1}{2}}^{i+\frac{1}{2}} \frac{C_j^{i+\frac{1}{2}} - C_{j-1}^{i+\frac{1}{2}}}{z_j - z_{j-1}} - \right. \qquad (7-45)$$

$$q_{j+\frac{1}{2}}^{i+\frac{1}{2}} (\alpha_{j+\frac{1}{2}}^{i+\frac{1}{2}} C_j^{i+\frac{1}{2}} + (1 - \alpha_{j+\frac{1}{2}}^{i+\frac{1}{2}})\, C_{j+1}^{i+\frac{1}{2}}) +$$

$$\left. q_{j-\frac{1}{2}}^{i+\frac{1}{2}} (\alpha_{j-\frac{1}{2}}^{i+\frac{1}{2}} C_{j-1}^{i+\frac{1}{2}} + (1 - \alpha_{j-\frac{1}{2}}^{i+\frac{1}{2}})\, C_j^{i+\frac{1}{2}}) \right] / \Delta z_j + \phi_j^{i-\frac{1}{2}}$$

$$C_{j+1}^{i+\frac{1}{2}} = \tfrac{1}{2}(C_{j+1}^{i+1} + C_{j+1}^{i}) \qquad (7-46a)$$

$$C_j^{i+\frac{1}{2}} = \tfrac{1}{2}(C_j^{i+1} + C_j^{i}) \qquad (7-46b)$$

$$C_{j-1}^{i+\frac{1}{2}} = \tfrac{1}{2}(C_{j-1}^{i+1} + C_{j-1}^{i}) \qquad (7-46c)$$

α = weight factor

It is noted that the adsorption isotherm has been linearized by eq. (7-47). Furthermore the β-value is kept constant within the time step Δt. The value adopted for β is the value calculated at the beginning of the time step.

$$\Delta A = \beta\, \Delta c \qquad (7-47)$$

The values of θ_j^{i+1}, θ_j^{i}, $q_{j+\frac{1}{2}}^{i+\frac{1}{2}}$ and $q_{j-\frac{1}{2}}^{i+\frac{1}{2}}$ are obtained directly from the soil water model.

Values of D being dependent on θ and q_w are obtained from eq. (7-39).

The superscript i+½ refers to centering in time and the subscript j-½ and j+½ refer to centering in space.

The calculation of values of D is performed by using the corresponding values of q_w and θ, e.g. $\theta_{j+½}^{i+½} = ¼(\theta_{j+½}^{i+½} + \theta_j^{i+1} + \theta_{j+1}^{i} + \theta_j^{i})$.

The values of ϕ are calculated according to eq. (7-40) and eq. (7-41) for transfer of NH_4^+ and NO_3^-, respectively.

By combining eq. (7-45) and eq. (7-46) and rearranging eq. (7-48) is obtained.

$$a_j^{i+1} C_{j-1}^{i+1} + b_j^{i+1} C_j^{i+1} + c_j^{i+1} C_{j+1}^{i+1} = d_j^{i+1} \qquad (7-48)$$

$$a_j^{i+1} = - \frac{D_{j-½}^{i+½}}{2(z_j - z_{j-1})\,\Delta z_j} - \frac{\alpha_{j-½}^{i+½}\, q_{j-½}^{i+½}}{2\,\Delta z_j} \qquad (7-49)$$

$$b_j^{i+1} = \frac{\theta_j^{i+1} + \beta_j^{i+½}}{\Delta t^{i+1}} + \frac{D_{j-½}^{i+½}}{2(z_j - z_{j-1})\,\Delta z_j} + \frac{D_{j+½}^{i+½}}{2(z_{j+1} - z_j)\,\Delta z_j} - \frac{(1 - \alpha_{j-½}^{i+½})\, q_{j-½}^{i+½}}{2\,\Delta z_j} + \frac{\alpha_{j+½}^{i+½}\, q_{j+½}^{i+½}}{2\,\Delta z_j} \qquad (7-50)$$

$$c_j^{i+1} = - \frac{D_{j+½}^{i+½}}{2(z_{j+1} - z_j)\,\Delta z_j} - \frac{(1 - \alpha_{j+½}^{i+½})\, q_{j+½}^{i+½}}{2\,\Delta z_j} \qquad (7-51)$$

$$d_j^{i+1} = \frac{\theta_j^i + \beta_j^{i+\frac{1}{2}}}{\Delta t^{i+1}} C_j^i + \phi_j^{i+\frac{1}{2}} - \frac{D_{j-\frac{1}{2}}^{i+\frac{1}{2}} (C_j^i - C_{j-1}^i)}{2(z_j - z_{j-1}) \Delta z_j}$$

$$+ \frac{D_{j+\frac{1}{2}}^{i+\frac{1}{2}} (C_{j+1}^i - C_j^i)}{2(z_{j+1} - z_j) \Delta z_j} + \frac{q_{j-\frac{1}{2}}^{i+\frac{1}{2}} (\alpha_{j-\frac{1}{2}}^{i+\frac{1}{2}} C_{j-1}^i + (1 - \alpha_{j-\frac{1}{2}}^{i+\frac{1}{2}}) C_j^i)}{2 \Delta z_j}$$

$$- \frac{q_{j+\frac{1}{2}}^{i+\frac{1}{2}} (\alpha_{j+\frac{1}{2}}^{i+\frac{1}{2}} C_j^i + (1 - \alpha_{j+\frac{1}{2}}^{i+\frac{1}{2}}) C_{j+1}^i)}{2 \Delta z_j} \quad (7-52)$$

The upper boundary condition is always a prediscribed flux. In the numeric solution this flux is obtained by the introduction of a fictitious point, j=0 located at $z_0 = -z_1$. The flux across the upper boundary is given as an approximation by using eq. (7-53).

$$J_{\frac{1}{2}}^{i+\frac{1}{2}} = - D_1^{i+\frac{1}{2}} \frac{C_1^{i+\frac{1}{2}} - C_0^{i+\frac{1}{2}}}{z_1 - z_0}$$

$$+ q_{\frac{1}{2}}^{i+\frac{1}{2}} (\alpha_{\frac{1}{2}}^{i+\frac{1}{2}} C_0^{i+\frac{1}{2}} + (1 - \alpha_{\frac{1}{2}}^{i+\frac{1}{2}}) C_1^{i+\frac{1}{2}}) \quad (7-53)$$

Rearranging (7-53) results in eq. (7-54).

$$C_0^{i+\frac{1}{2}} = b_0^{i+1} C_1^{i+1} + d_0^{i+1} \quad (7-54)$$

$$d_0^{i+1} = \frac{J_{\frac{1}{2}}^{i+\frac{1}{2}} + \left[\frac{D_1^{i+\frac{1}{2}}}{z_1 - z_0} - q_{\frac{1}{2}}^{i+\frac{1}{2}} (1 - \alpha_{\frac{1}{2}}^{i+\frac{1}{2}}) \right] \frac{1}{2} C_1^{i+1}}{\left[\frac{D_1^{i+\frac{1}{2}}}{z_1 - z_0} + \alpha_{\frac{1}{2}}^{i+\frac{1}{2}} q_{\frac{1}{2}}^{i+\frac{1}{2}} \right]} \quad (7-55)$$

$$b_0^{i+1} = \frac{\left[\frac{D_1^{i+\frac{1}{2}}}{z_1 - z_0} - q_{\frac{1}{2}}^{i+\frac{1}{2}} (1 - \alpha_{\frac{1}{2}}^{i+\frac{1}{2}}) \right]}{2 \left[\frac{D_1^{i+\frac{1}{2}}}{z_1 - z_0} + \alpha_{\frac{1}{2}}^{i+\frac{1}{2}} q_{\frac{1}{2}}^{i+\frac{1}{2}} \right]} \quad (7-56)$$

By assuming that $C_0^i = C_0^{i+1} = C_0^{i+½}$ and introducing eq. (7–54) – eq. (7–56) in eq. (7–48) for j=1 eq. (7–57) is obtained.

$$a_1^{i+1} (b_0^{i+1} C_1^{i+1} + d_0^{i+1}) + b_1^{i+1} C_1^{i+1} + c_1^{i+1} C_2^{i+1} = d_1^{i+1}$$

or

$$(a_1^{i+1} b_0^{i+1} + b_1^{i+1}) C_1^{i+1} + c_1^{i+1} C_2^i =$$

$$d_1^{i+1} - a_1^{i+1} d_0^{i+1} \qquad (7-57)$$

The lower boundary condition is also a flux condition, eq. 7–44). This condition can be approximated by using eq. (7–48).

$$\frac{C_{N+1}^{i+1} - C_N^{i+1}}{z_{N+1} - z_N} = 0$$

or

$$C_{N+1}^{i+1} = C_N^{i+1} \qquad (7-58)$$

By introducing eq. (7–58) in eq. (7–48) for J = N eq. (7–59) is obtained.

$$a_N^{i+1} C_{N-1}^{i+1} + b_N^{i+1} C_N^{i+1} c_N^{i+1} + C_N^{i+1} = d_N^{i+1}$$

or

$$a_N^{i+1} C_{N-1}^{i+1} + (b_N^{i+1} + c_N^{i+1}) + C_N^{i+1} = d_N^{i+1} \qquad (7-59)$$

A matrix formulation of the solution now results in eq. (7-60).

$$\bar{H} \cdot \bar{C} = \bar{D} \tag{7-60}$$

$$\bar{H} = \begin{bmatrix} a_1^{i+1} b_0^{i+1} + b_1^{i+1} c^{i+1} & & & & & \\ a_2^{i+1} & b_2^{i+1} & c_2^{i+1} & & & \\ & a_3^{i+1} & b_3^{i+1} & c_3^{i+1} & & \\ & & & a_{N-1}^{i+1} & b_{N-1}^{i+1} & c_{N-1}^{i+1} \\ & & & & a_N^{i+1} & b_N^{i+1} + c_N^{i+1}) \end{bmatrix} \tag{7-61}$$

$$\bar{C} = \begin{bmatrix} C_1^{i+1} \\ C_2^{i+1} \\ C_3^{i+1} \\ \\ C_{N-1}^{i+1} \\ C_N^{i+1} \end{bmatrix} \quad (7-62), \qquad \bar{D} = \begin{bmatrix} d_1^{i+1} - a_1^{i-1} d_0^{i+1} \\ d_2^{i+1} \\ d_3^{i+1} \\ \\ d_{N-1}^{i+1} \\ d_N^{i+1} \end{bmatrix} \tag{7-63}$$

The coefficients of the matrixes eq. (7-61) and eq. (7-63) are calculated from eq. (7-50) – eq. (7-52), eq. (7-55), and eq. (7-56).

It appears that $\bar{H}$ constitutes a tridiagonal matrix hence the matrix eq. (7-60) can be solved by the double-sweep-method.

8. CROP MODEL

8.1 Introduction

Interactions in the soil plant atmosphere system

Crop production is a result of interactions in the soil plant atmosphere continuum involving physical, chemical, and biological processes. Incident solar radiation is intercepted by the crop canopy and CO_2 is assimilated from the atmosphere resulting in photosynthesis a process in which radiation energy is converted into chemical energy in terms of carbohydrates. Release of CO_2 in the crop takes place as a result of respiration processes associated with biochemical conversion of assimilates into structural dry matter and with production of energy used to maintain the biochemical and physiological state of the plants.

For a given crop a particular root system is developed in the soil profile depending on soil physical conditions including soil temperature and soil mechanical properties. Water and plant nutrients including nitrogen are taken up by the plant roots which at the same time release CO_2 from respiration processes to the soil atmosphere.

The concept of the crop as a sink source for carbon and nitrogen

In the present treatment of the soil plant atmosphere system the crop is mainly considered as a sink and source for energy and matter in particular carbon and nitrogen. During the growth season carbon and nitrogen are accumulated in the crop and at harvest partly removed from the system as harvested crop and partly allocated as plant residues to other pools of carbon in the system. The present crop model is developed as a conceptual model allowing calculation of crop production at three production levels, viz. potential crop production, water limited production, and nitrogen limited production.

8.2 Crop development

Crop emergence

For an annual crop the length of the period from sowing to emergence is assumed to be determined by soil temperature at sowing depth in terms of a temperature sum (Λ_1) calculated from the time of sowing.

Crop area index

The crop canopy is described in terms of total crop area index (C_{ai}) and green crop area index (L_{ai}), respectively, both of which are functional relationships of accumulated top dry matter (W_t) and temperature. After emergence the crop canopy expressed as green crop area is assumed to be described by eq. (8-1) for the period from emergence and until the top dry matter has reached a given value (W_t^0). From this point and until a certain temperature sum (Λ_2) calculated from the time of emergence is reached the green crop area index is calculated from eq. (8-2). For the remaining part of the growth period the green crop area index and the total crop area index are calculated from eq. (8-3) and eq. (8-4), respectively.

Crop thermal age

$$L_{ai} = 0.5(\exp(2.4\ \frac{\Sigma T_a}{\Lambda_i}) - 1) \qquad (8-1)$$

$$L_{ai} = S_{ai}\, W_t \qquad (8-2)$$

$$L_{ai} = (1 - \frac{\alpha_r^L(\Sigma T_a - \Lambda_2)}{(\Sigma T_a - \Lambda_2) + \Lambda_r^L})\, S_{ai}\, W_t \qquad (8-3)$$

$$C_{ai} = (1 - \frac{\alpha_r^C(\Sigma T_a - \Lambda_2)}{(\Sigma T_a - \Lambda_2) + \Lambda_r^C})\, S_{ai}\, W_t \qquad (8-4)$$

L_{ai} = green crop area index [m^2m^{-2}]
C_{ai} = total crop area index [m^2m^{-2}]
W_t = accumulated top dry matter [kg m^{-2}]
S_{ai} = specific green crop area [m^2kg^{-1}]
T_a = daily mean temperature [°C]
Λ_i = canopy development parameter [°C]

Λ_1 = canopy development parameter [°C]
Λ_2 = canopy development parameter [°C]
Λ_r^L = green crop area index damping parameter [°C]
Λ_r^C = total crop area index damping parameter [°C]
α_r^L = green crop index damping parameter [°C]
α_r^C = total crop index damping parameter [°C]

It is noted that for the period from emergence and until $\Sigma T_a = \Lambda_2$ green crop area index (L_{ai}) is equal to total crop area index (C_{ai}).

Harvest time

Time for harvest can either be predescribed by the system management model or simulated by the crop model except for the beet crop using a temperature sum (Λ_3) calculated from the time of crop emergence as a limit. For a beet crop an ultimative time for harvest is predescribed which is the latest date for harvesting the crop.

Root penetration

At crop emergence an initial root depth (d_r^0) is assumed. Root penetration rate is then described as a function of soil temperature (Jakobsen, 1976) at the actual root depth, eq. (8-5) whereas the root depth is calculated from eq. (8-6). If the amount of assimilates allocated to the roots is less than the root respiration, or if the soil depth at which the root density is halved exceeds a given limit (z_r^m), then no root penetration occurs. The maximum root depth is determined by the soil or the crop.

$$v_r = \begin{cases} 0 & T_s \leq T_c \\ a_r(T_s - T_c) & T_s > T_c \end{cases} \qquad (8-5)$$

$$d_r^{t+1} = \text{Min} \{ d_r^*, d_r^t + v_r \Delta t \} \qquad (8-6)$$

v_r = root penetration rate [m day^{-1}]
T_s = soil temperature at the root depth [°C]

T_c = minimum temperature for root growth [°C]
a_r = root penetration rate parameter [m day^{-1} °C^{-1}]
d_r^t = root depth at day number t [m]
d_r^* = maximum root depth [m]
t = day number from emergence

Root density

In accordance with Gerwitz and Page (1974) the root density profile is described by eq. (8–7) whereas the total root length is calculated from eq. (8–8) or by integration of eq. (8–7) resulting in eq. (8–9).

$$L_z = L_0 \, e^{-a_z z} \tag{8-7}$$

$$\ell_r = S_r \, W_r \tag{8-8}$$

$$\ell_r = \int_0^{d_r} L_z \, dz = \frac{L_0}{a_z} (1 - e^{-a_z d_r}) \tag{8-9}$$

L_z = root density at soil depth z (m m^{-3}]
L_0 = root density at soil surface [m m^{-3}]
L_d = root density at root depth d_r [m m^{-3}]
L_z^m = maximum root density (10^5m m^{-3})
ℓ_r = total root length [m m^{-2}]
W_r = root dry matter [kg m^{-2}]
S_r = specific root length [m kg^{-1}]
a_z = root density distribution parameter [m^{-1}]
d_r = root depth [m]
z = soil depth [m]

If the root density (L_{d_r}) at the root depth (d_r) is known ($L_{d_r} = L_0 \exp(-a_z d_r)$) then eq. (8–7), eq. (8–8) and eq. (8–9) can be combined to give an equation from which a_z can be obtained by iteration and L_0 subsequently calculated from eq. (8–7). If the root length is small, i.e. $(\ell/d_r) < 3 \, Ld_r$, then the root density is assumed to decrease linearly with depth in accordance with eq. (8–10).

$$L_z = L_0 - (L_0 - L_{dr})\frac{z}{d_r} \qquad (8-10)$$

$$L_0 = z\ \frac{\ell_r}{d_r} - L_{dr}$$

The root depth and the root density profile are calculated on a daily basis and they are used in the models for water and nitrogen uptake as input variables.
In the case of grass for cutting the crop canopy development until the first cut is described as in the case of annual crops, eg. (8-1) and eq. (8-2). After first cut the green leaf area index which in the case of grass is assumed to be equal to the total crop area index is calculated from eq. (8-11).

$$L_{ai} = S_{ai}\,(W_t - f_w\,W_t^c) \qquad (8-11)$$

W_t^c = amount of stubble left after cutting [kg m^{-2}]
f_w = fraction of stubble being inactive

Time for harvest of grass for cutting can either be predescribed by the system management model or simulated by the crop model. If simulated the time of cutting is determined by either criterion 1 or criterion 2 which is first fulfilled. Criterion 1 is fulfilled when a specified amount of accumulated top dry matter is reached while criterion 2 is fulfilled when a specified temperature sum (Λ_3) calculated from the time of the previous cut or in the case of first cut from the time of emergence is reached.

Furthermore in the case of grass for cutting an ultimate time for harvest is predescribed which is the latest date for harvesting the crop in the particular year. In addition a minimum amount of accumulated top dry matter is specified as a requirement for harvest of the crop to be performed. The calculations of root penetration and root density are performed for grass for cutting as described for annual crops.

8.3 Canopy gross photosynthesis

Intercepted radiation and conversion efficiency

Canopy gross photosynthesis of a crop is determined by the amount of photosynthetically active radiation (PAR) intercepted by the crop and by the efficiency by which the absorbed radiation energy is converted into chemical energy in terms of carbohydrates. In a natural environment the flux density of photosynthetically active radiation varies considerably in time and space within the crop canopy. Consequently the amount of energy in photosynthetically active radiation intercepted by the crop as well as the efficiency by which the intercepted radiation energy is converted to chemical energy also vary considerably in time and space within the crop canopy. In the present model such spatial variations in the crop canopy and temporal variations over a day are integrated to yield an integrated value of daily absorbed photosynthetically active radiation energy and an average daily value of the radiation conversion efficiency.

Photosynthetically active radiation

The photosynthetically active radiation is the radiation within the wavelength 400 – 700 nm. The energy in the radiation within this wave band constitutes a relatively constant fraction of the energy in global radiation (300 – 2500 nm) which can be expressed as eq. (8 – 12).

$$S_v = \alpha S_i \qquad (8-12)$$

S_v = photosynthetically active radiation [W m^{-2}]
S_i = global radiation [W m^{-2}]
α = constant

In accordance with results obtained by Hansen et al. (1981) a value of α equal to 0.48 has been used. Furthermore according to Hansen et al. (1981) the temporal variation in global radiation over an average day in a given month under Danish conditions can be described by eq. (8 – 13).

$$S_i(h) = A_0 + A_1 \cos(1\omega h) + B_1 \sin(1\omega h) + A_2 \cos(2\omega h) + B_2 \sin(2\omega h) \quad (8-13)$$

$\omega = 2\pi/24$ [rad h^{-1}]

h = hours

The values of A_0, A_1, A_2, B_1 and B_2 are given in Table 8-1.

Table 8-1 Values of parameters (W m^{-2}) in equation describing variation of global radiation during an average day.

Month	A_0	A_1	B_1	A_2	B_2
January	17	-31	-7	21	11
February	44	-74	-20	42	25
March	94	-148	-34	68	32
April	159	-232	-45	77	29
May	214	-291	-53	67	23
June	247	-320	-63	-	-
July	214	-279	-67	-	-
August	184	-261	-52	75	29
September	115	-177	-30	73	25
October	58	-96	-13	54	15
November	25	-45	-6	32	8
December	13	-24	-4	18	7

Interception of radiation

The distribution of photosynthetically active radiation within a crop canopy is described according to Beer's law. Hence the absorbed energy in photosynthetically active radiation can be esstimated eq. (8-14).

$$S_a(L) = (1 - A_v)\, S_v(0)\, (1 - \exp(-KL)) \quad (8-14)$$

$S_v(0)$ = photosynthetically active radiation at top of crop canopy [W m^{-2}]

$S_a(L)$ = absorbed photosynthetically active radiation by crop canopy [W m^{-2}]

L = green crop area index accumulated from top of crop canopy [$m^2 m^{-2}$]

K = extinction coefficient of crop canopy

A_v = reflection coefficient of crop canopy

Extinction coefficient

The value of K depends on solar altitude and in particular on the structure of the crop canopy. For crops of winter wheat, spring barley, fodder beet and grass Aslyng and Hansen (1985) found values of K in the range of 0.44 – 0.67. In accordance with results obtained by Hansen et al. (1981) a value of A_v equal to 0.06 has been used.

Leaf photosynthesis

In accordance with Goudriaan and Laar (1978) the relation between gross photosynthesis rate in a single leaf and the photosynthetically active radiation energy absorbed by the leaf is described by eq. (8 – 15).

$$F = F_m(1 - \exp(- S_a\, m^{-1})) \qquad (8-15)$$

F = gross photosynthesis rate [kg CO_2 $m^{-2}s^{-1}$]
F_m = constant [kg CO_2 $m^{-2}s^{-1}$]
S_a = absorbed photosynthetic active radiation [W m^{-2}]
m = constant [60 W m^{-2}]

The value of the constant F_m depends on leaf properties. For C_3-plants an average value of 8.3 10^{-7} kg CO_2 $m^{-2}s^{-1}$ can be used (Goudriaan and Laar, 1978).

Radiation absorption and gross photosynthesis in crop layer

In order to calculate gross photosynthesis of the entire crop the crop canopy is divided into distinct layers each having a green crop area index of ΔL. The absorption of photosynthetically active radiation in layer number j is then estimated by using eq. (8 – 16).

$$S_{a,j} = (1 - A_v)S_v(0)(\exp(- K(j - 1)\Delta L) - \exp(- Kj\Delta L)) \qquad (8-16)$$

$S_{a,j}$ = absorbed photosynthetically active radiation in layer j [W m^{-2}]
j = crop canopy layer number counted from top of canopy

Crop photosynthesis

Assuming the properties of each crop canopy layer to be equal to the properties of a single leaf with a green area index of ΔL the gross photosynthesis rate of crop canopy layer j can be estimated by eq. (8-17) after which the gross photosynthesis rate of the entire crop canopy can be calculated by using eq. (8-18).

$$F_j = \Delta L\, F_m\left(1 - \exp\left(-\frac{S_{a,j}}{\Delta L m}\right)\right) \qquad (8-17)$$

$$F_c = \sum_{j=1}^{n} F_j \qquad (8-18)$$

F_j = gross photosynthesis rate of crop canopy layer j [kg CO_2 $m^{-2}s^{-1}$]

F_c = gross photosynthesis rate of entire crop canopy [kg CO_2 $m^{-2}s^{-1}$]

Daily gross photosynthesis and absorption of radiation

The gross photosynthesis of a crop was calculated for each hour of the day after which the daily gross photosynthesis was calculated from eq. (8-19). Similarly the rate of absorbed energy in photosynthetically active radiation was calculated for each hour of the day by using eq. (8-14) after which the absorbed energy in photosynthetically active radiation was calculated from eq. (8-20).

$$F_{c,d} = k \sum_{h=1}^{24} F_c(h) \qquad (8-19)$$

$$S_{a,d} = k \sum_{h=1}^{24} S_a(h) \qquad (8-20)$$

$F_{c,d}$ = gross photosynthesis of crop [kg CO_2 $m^{-2}day^{-1}$]

$S_{a,d}$ = absorbed photosynthetically active radiation by crop [J m^{-2} day^{-1}]

k = constant (3600 s h^{-1})

Radiation conversion efficiency

After having obtained daily values of gross photosynthesis in terms of CO_2 assimilation and the corresponding values of energy in absorbed photosynthetically active radiation from eq. (8-19) and eq. (8-20), respectively, the efficiency by which absorbed radiation energy is converted into chemical energy was calculated from eq. (8-21).

$$\varepsilon = C \frac{M(CH_2O)}{M(CO_2)} \frac{F_{c,d}}{S_{a,d}} \qquad (8-21)$$

ε = radiation conversion efficiency
$M(CH_2O)$ = molecular weight of CH_2O (44 g $mole^{-1}$)
$M(CO_2)$ = molecular weight of CO_2 (30 g $mole^{-1}$)
C = energy in carbohydrate (15.7 M J $kg^{-1}(CH_2O)$)

For each month in the year the calculations to obtain ε have been performed using values of global radiation for the average day as given by eq. (8-13). Furthermore in order to obtain values of ε to represent the actual range of global radiation such calculations have been performed for the same values of global radiation, eq. (8-13), multiplied by 0.5, 0.6, 0.7, 0.8, 0.9, 1.2, 1.4, 1.6, and 1.8, respectively. In Fig. 8-1 the values of ε obtained are plotted against daily values of absorbed energy in photosynthetically active radiation ($S_{a,d}$) for all combinations of K = 0.4, 0.5, 0.6, 0.8 and L_{ai} = 1,2,3,5.

From Fig. 8-1 it appears that ε decreases with increasing $S_{a,d}$. Furthermore it appears that ε increases with increasing L_{ai}. In order to incorporate these effects in the calculations of gross photosynthesis the relationships shown in Fig. 8-1 have been parametericized resulting in eq. (8-22).

$$\varepsilon = 0.15 - (\beta_1 - \beta_2 \frac{L_{ai}}{L_{ai} + 3.0}) \frac{S_{a,d}}{S_{a,d} + 7.8\ 10^6} \qquad (8-22)$$

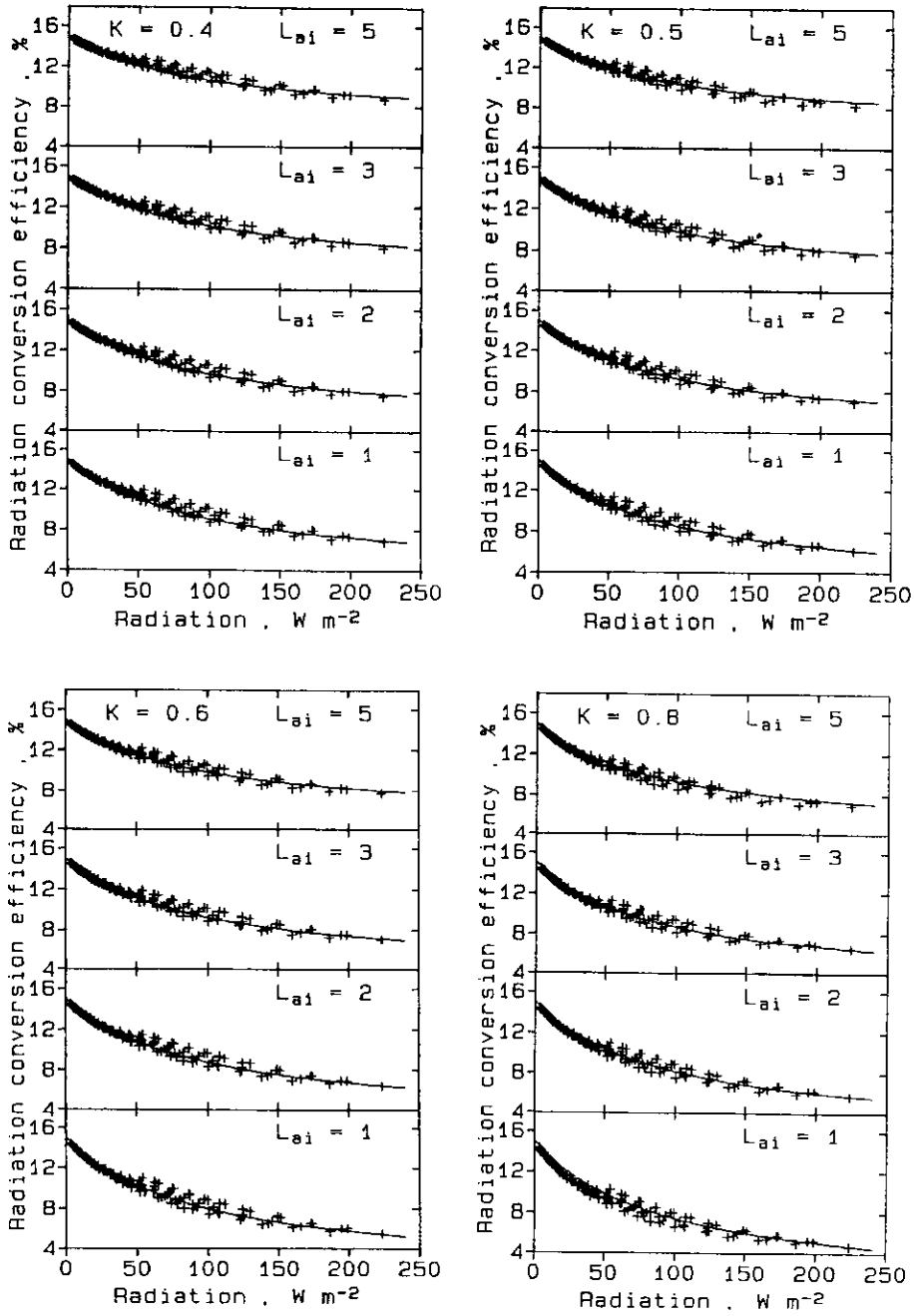

Fig. 8–1 Radiation conversion efficiency in relation to incident photosynthetically active radiation for various values of extinction coefficient (K) and green crop area index (L_{ai}).

The parameters β_1 and β_2 depend on the extinction coefficient of the crop canopy. In Table 8-2 the values of β_1 and β_2 are given for K = 0.4, 0.5, 0.6, and 0.8, respectively.

Table 8-2 Values of the parameters β_1 and β_2 in eq. (8-22) for various values of the extinction coefficient K.

K	β_1	β_2
0.4	0.133	0.078
0.5	0.148	0.094
0.6	0.158	0.094
0.8	0.168	0.094

Model calculation of daily gross photosynthesis

For a given value of daily global radiation, green crop area index and a selected value of the extinction coefficient the amount of daily absorbed energy in photosynthetically active radiation is calculated from eq. (8-23) after which daily gross photosynthesis for the crop is calculated from eq. (8-24).

$$S_{a,d} = (1 - A_v)(1 - \exp(-K L_{ai}))\alpha S_{i,d} \qquad (8-23)$$

$$F^*_{g,d} = \varepsilon S_{a,d} C^{-1} \qquad (8-24)$$

$S_{i,d}$ = global radiation [J $m^{-2}day^{-1}$]
$S_{a,d}$ = absorbed photosynthetically active radiation [J $m^{-2}day^{-1}$]
$F^*_{g,d}$ = gross photosynthesis of crop [kg (CH_2O) $m^{-2}day^{-1}$]
L_{ai} = green crop area index [m^2m^{-2}]
A_v = reflection coefficient of crop canopy
K = extinction coefficient of crop canopy
ε = radiation conversion efficiency
C = energy in carbohydrate [J kg^{-1}]
α = constant (0.48)

Effect of temperature

At low temperatures the gross photosynthesis may be restricted (Berry and Raison, 1981) which is taken into account by introducing a gross photosynthesis damping coefficient, eq. (8-25) which is of function of temperature, eq. (8-26).

$$F_{g,d} = f(T_a)\, F^{*}_{g,d} \qquad (8-25)$$

$$f(T_a) = \begin{cases} 0 & T_a \le T_{f,1} \\ \dfrac{T_a - T_{f,2}}{T_{f,2} - T_{f,1}} & T_{f,1} < T_a < T_{f,2} \\ 1 & T_{f,2} \le T_a \end{cases} \qquad (8-26)$$

$F_{g,d}$ = gross photosynthesis at actual temperature [kg (CH_2O) m^{-2} day^{-1}]
$f(T_a)$ = gross photosynthesis damping coefficient
T_a = daily mean temperature [°C]
$T_{f,1}$, $T_{f,2}$ = constants [°C]

8.4 Assimilate partitioning

Crop compartments

Assimilate partitioning is the process by which assimilates produced by gross photosynthesis are allocated to the various parts of the plant e.g. leaves, stems, roots, storage organs etc.

In the present model the various crops are divided into a number of compartments representing the various parts of the crop. Thus in the case of crops of cereals, rape and grass each crop is divided into two compartments only representing the above ground part and the roots, respectively, while in the case of crops of beet and potato each crop is divided into three compartments, viz. the above ground part, the roots and storage organs, i.e. tuber and beet, respectively. The assimilates are then allocated to the various compartments of the crop.

Top and roots

The annual crops of cereals, rape, beet and potato are assumed to follow a development pattern determined by physiological age which in the present model is expressed in terms of a temperature sum initiated at crop emergence. Consequently that temperature sum has been chosen as the variable governing the assimilate partitioning. In the case of cereals and rape the partitioning coefficients are given by eq. (8-27) and eq. (8-28).

$$\gamma_r = \begin{cases} \gamma_r^0 & \Sigma T_a \le \Lambda_r^0 \\ \gamma_r^0 + (\gamma_r' - \gamma_r^0)\ \dfrac{\Sigma T_a - \Lambda_r^0}{\Lambda_r' - \Lambda_r^0} & \Lambda_r^0 < \Sigma T_a < \Lambda_r' \\ \gamma_r' & \Lambda_r' \le \Sigma T_a \end{cases} \quad (8-27)$$

$$\gamma_t = 1 - \gamma_r \quad (8-28)$$

γ_r = assimilate fraction allocated to roots

γ_t = assimilate fraction allocated to top

T_a = daily mean temperature [°C]

Λ_r^0, Λ_r' = constants [°C]

γ_r^0, γ_r' = constants

Storage organs

In the case of beet and potato the partitioning coefficients for the roots are calculated from eq. (8-27) while the partitioning coefficients for storage organs and top are calculated from eq. (8-29) and eq. (8-30), respectively.

$$\gamma_s = \begin{cases} \gamma_s^0 & \Sigma T_a \le \Lambda_s^0 \\ \gamma_s^0 + (\gamma_s' - \gamma_s^0)\ \dfrac{\Sigma T_a - \Lambda_s^0}{\Lambda_s' - \Lambda_s^0} & \Lambda_s^0 < \Sigma T_a < \Lambda_s' \\ \gamma_s' & \Lambda_s' \le \Sigma T_a \end{cases} \quad (8-29)$$

$$\gamma_t = 1 - \gamma_r - \gamma_t \quad (8-30)$$

γ_s = assimilate fraction allocated to storage organs

Λ_s^0, Λ_s' = constants [°C]

γ_s^0, γ_s' = constants

In the case of a grass crop eq. (8-27) and eq. (8-28) are used and the temperature sum initiated at emergence.

8.5 Growth and respiration

Respiration concepts

Conceptually respiration can be divided into growth respiration and maintenance respiration. Growth respiration represents loss of CO_2 associated with biochemical conversion of assimilates into 'structural dry matter', while maintenance respiration represents loss of CO_2 associated with production of energy used to maintain the biochemical and physiological state of the plants.

In the present model in which the basic time step is one day it is assumed that any assimilate produced during a day is used for maintenance respiration and if the assimilate production is sufficient assimilate is also used for growth and growth respiration. Pools of reserve assimilates are neglected which however is adequate for a model of the present type (Penning de Vries et al., 1989). Thus net production of dry matter for any part of the crop is calculated from eq. (8-31).

$$P_{n,d} = Y(F_{g,d} - r_m W) \quad (8-31)$$

$P_{n,d}$ = net production [kg (DM) m^{-2} day^{-1}]

$F_{g,d}$ = assimilates allocated [kg (CH_2O) m^{-2} day^{-1}]

W = dry matter (DM) present [kg m^{-2}]

r_m = maintenance respiration coefficient [kg (CH_2O) kg^{-1} (DM) day^{-1}]

Y = asssimilate conversion efficiency [kg (DM) kg^{-1} (CH_2O)]

Growth respiration

The magnitude of the assimilate conversion efficiency (Y) varies with the composition of the end product. Fats and lignins are produced at high costs (low efficiency), structural carbohydrates and organic acids are relatively cheap, while proteins form an intermediate group (Penning de Vries et al., 1983; Penning de Vries et al., 1989). If the composition of the end product does not vary temperature and water stress are not likely to affect the conversion efficiency (Penning de Vries, 1983).

Maintenance respiration

The maintenance respiration is related to processes which maintain concentration gradients within the plant and to processes which provide energy for resynthesis of degraded proteins in particular enzymes which have a limited life time and furthermore the maintenance respiration is related to the intensity of the metabolism (Penning de Vries, 1975).

On a biochemical basis Penning de Vries et al. (1983) have computed the amount of substrate required for growth of seeds, fruits and other storage organs for 23 major crops. They stated that much of the proteins present in storage organs is inactive and that the requirements for their maintenance are almost zero.

In the assessment of maintenance respiration coefficients, it should be noted, that indications of significant differences in respiration rates between lines and cultivars of several crop species have been reported (Penning de Vries et al. 1989). It should also be noted, that due to the conceptual nature of the present model the values of Y and r_m in eq. (8-31) cannot be assessed individually.

Effect of temperature

Temperature has a strong influence on the rate of maintenance respiration corresponding to a doubling of the rate for each 10°C increment in temperature up to temperatures that kill the plant (McCree, 1974; Penning de Vries et al., 1979). In the present model the temperature effect function, eq. (6-13), used for biological processes in the soil organic matter model has been used to also account for the effect of temperature on the maintenance respiration.

8.6 Nitrogen in crops

The concept of ample nitrogen supply

In the present model it is assumed that at ample nitrogen supply the crop will take up nitrogen until an upper limit of the nitrogen concentration (c^*) in the dry matter is reached. If on the other hand the nitrogen supply is extremely low the nitrogen concentration in the dry matter is assumed to reach a lower limit (c^o) below which the crop ceases functioning. Between the upper and lower limit a concentration of nitrogen in dry matter (c^n) is assumed to exist below which the crop growth is limited due to lack of nitrogen and above which the crop growth is unlimited by nitrogen. The content of nitrogen in the crop at the three limits is expressed in eq. (8-32), eq. (8-33) and eq. (8-34), respectively.

$$N_c^* = \sum_{j=1}^{n} c_j^* W_j \qquad (8-32)$$

$$N_c^n = \sum_{j=1}^{n} c_j^n W_j \qquad (8-33)$$

$$N_c^0 = \sum_{j=1}^{n} c_j^0 W_j \qquad (8-34)$$

N_c^* = nitrogen content of a crop at ample nitrogen supply [kg m^{-2}]

N_c^n = nitrogen content of a crop at just ample nitrogen supply [kg m^{-2}]

N_c^0 = nitrogen content of a crop at extremely low nitrogen supply [kg m^{-2}]

c_j^* = nitrogen concentration in dry matter of part j of crop at ample nitrogen supply [kg (N) kg^{-1} (DM)]

c_j^n = nitrogen concentration in dry matter of part of crop at just ample nitrogen supply [kg (N) kg^{-1} (DM)]

c_j^0 = nitrogen concentration in dry matter of part j of crop at extremely low nitrogen supply [kg (N) kg^{-1} (DM)]

W_j = dry matter in part j of the crop [kg m^{-2}]

n = number of plant parts

It is noted that each part of the crop (top, roots, storage organs) is characterized by three particular nitrogen concentration limits each of which is assumed to vary with the development stage of the crop expressed in terms of a temperature sum initiated at crop emergence for annual crops and at the onset of growth for perennial crops, eq. (8-35), eq. (8-36), and eq. (8-37), respectively.

$$c_j^* = \begin{cases} c_{1,j}^* & \Sigma T_a \le \Lambda_{1,j}^* \\ c_{1,j}^* \exp(\alpha_j^*(\Sigma T_a - \Lambda_{1,j}^*)) & \Lambda_{1,j}^* < \Sigma T_a < \Lambda_{2,j}^* \\ c_{2,j}^* & \Lambda_{2,j}^* \le \Sigma T_a \end{cases} \quad (8-35)$$

$$c_j^n = \begin{cases} c_{1,j}^n & \Sigma T_a \le \Lambda_{1,j}^* \\ c_{1,j}^n \exp(\alpha_j^n(\Sigma T_a - \Lambda_{1,j}^*)) & \Lambda_{1,j}^* < \Sigma T_a < \Lambda_{2,j}^* \\ c_{2,j}^n & \Lambda_{2,j}^* \le \Sigma T_a \end{cases} \quad (8-36)$$

$$c_j^0 = \begin{cases} c_{1,j}^0 & \Sigma T_a \le \Lambda_{1,j}^* \\ c_{1,j}^0 \exp(\alpha_j^0(\Sigma T_a - \Lambda_{1,j}^*)) & \Lambda_{1,j}^* < \Sigma T_a < \Lambda_{2,j}^* \\ c_{2,j}^0 & \Lambda_{2,j}^* \le \Sigma T_a \end{cases} \quad (8-37)$$

$c_{1,j}^*$, $c_{2,j}^*$ = crop parameters, potential nitrogen uptake [kg kg^{-1}]

$c_{1,j}^n$, $c_{2,j}^n$ = crop parameters, limit for maximum production [kg kg^{-1}]

$c_{1,j}^0$, $c_{2,j}^0$ = crop parameters, limit for crop functioning [kg kg^{-1}]

$\Lambda_{1,j}^*$, $\Lambda_{2,j}^*$ = crop parameter [°C]

$$\alpha_j^* = \ln\left[\frac{c_{2,j}^*}{c_{1,j}^*}(\Lambda_{2,j}^* - \Lambda_{1,j}^*)\right]$$

$$\alpha_j^n = \ln\left[\frac{c_{2,j}^n}{c_{1,j}^n}(\Lambda_{2,j}^* - \Lambda_{1,j}^*)\right]$$

$$\alpha_j^0 = \ln\left[\frac{c_{2,j}^0}{c_{1,j}^0}(\Lambda_{2,j}^* - \Lambda_{1,j}^*)\right]$$

T_a = daily mean temperature [°C]

The nitrogen uptake by the crop is assumed to cease at a certain physiological age og the crop corresponding to a specified temperature sum (Λ_3^*). The values of N_c^n and N_c^0 are used in the calculation of nitrogen limited crop production.

8.7 Crop production

Production levels

A classification system based on growth limiting factors has been proposed and a number of levels of crop production have been destinguished (Penning de Vries and Van Laar, 1982). In the present model crop production level 1, 2 and 3 have been considered.

Crop production level 1

Potential crop production

The crop has ample water and nutrients and produces a higher yield than at any other crop production level. The growth rate depends only on the current state of the crop and on current weather, particular radiation and temperature. The crop production at this production level can be designated as potential crop production.

Crop production level 2

Water limited crop production

At crop production level 2 the crop growth rate is limited only by the availability of water for at least part of the growing season. Photosynthesis and transpiration take place simultaneously. In the photosynthesis proces CO_2 is assimilated from the ambient air through stomata, while H_2O in the transpiration process is lost from the crop through stomata to the ambient air. Thus CO_2 and H_2O follow the same pathway in opposite direction. In that pathway three resistances may be identified, viz. the stomata resistance, the boundary layer resistance, and the resistance to transport between air in the canopy and the air in the free atmosphere. However, in most situations the overall resistance is dominated by the stomata resistance which varies with the stomata aperture.

Most crops exhibit a regulation of stomata aperture which is related to plant water status and substomata CO_2 concentration. Furthermore the ratio of substomata CO_2 concentration to the CO_2 concentration in the ambient air tends to be constant (Raschke, 1979; Schulze and Hall, 1982). Thus the approximation expressed in eq. (8-38) is assumed to be valid.

$$\frac{A_2}{A_1} = \frac{E'_2}{E'_1} \qquad (8-38)$$

A = net CO_2 assimilation by single leaf [kg CO_2 m^{-2} day^{-1}]

E' = transpiration by single leaf [kg H_2O m^{-2} day^{-1}]

Subscript 1 and 2 refers to crop production level 1 and 2, respectively. Eq. (8-38) postulates that net CO_2 assimilation and transpiration are fully regulated by the stomata aperture. Furthermore it is assumed that the ratio between net CO_2 assimilation of a single leaf and gross photosynthesis of the entire crop is similar at crop production level 1 and 2 which is expressed by eq. (8-39). By combining eq. (8-38) and eq. (8-39) eq. (8-40) is obtained.

$$\frac{A_2}{A_1} = \frac{F_{g,d,2}}{F_{g,d,1}} \qquad (8-39)$$

$$F_{g,d,2} = \frac{E_2}{E_1} F_{g,d,1} \qquad (8-40)$$

$F_{g,d,1}$ = gross photosynthesis of crop at crop production level 1 [kg(CH_2O) m^{-2} day^{-1}]

$F_{g,d,2}$ = gross photosynthesis of crop at crop production level 2 [kg(CH_2O) m^{-2} day^{-1}]

E_1 = transpiration of crop at crop production level 1 [$kg(H_2O)\ m^{-2}\ day^{-1}$]

E_2 = transpiration of crop at crop production level 2 [$kg(H_2O)\ m^{-2}\ day^{-1}$]

Much experimental evidence substantiating the validity of eq. (8-39) has been reported (van Keulen and Seligman, 1987) and the relationship has been used in simulation studies with good results (Aslyng and Hansen, 1982, 1985). In the present model the transpiration term in eq. (8-40) has been modified to include evaporation of intercepted water thus postulating the stomata to be open for CO_2 assimilation when water is evaporating from its proximate surroundings.

Crop production level 3

Nitrogen limited crop production

At crop production level 3 the crop growth rate is limited by the availability of water as well as by shortage of nitrogen for at least parts of the growing season.

In the present model a simple procedure has been adopted in order to account for the effect of nitrogen shortage on the crop production. Thus it is assumed that if the nitrogen content of the crop is less than a certain limit (N_c^n) then crop growth is restricted and if the nitrogen content of the crop reaches a lower limit (N_c^0) then crop growth ceases. In situations between the two limits gross photosynthesis is reduced according to eq. (8-41).

$$F_{g,d,3} = \frac{N_c - N_c^0}{N_c^n - N_c^0} F_{g,d,2} \qquad (8-41)$$

$F_{g,d,3}$ = gross photosynthesis of crop at crop production level 3 [$kg(CH_2O)\ m^{-2}\ day^{-1}$]

$F_{g,d,2}$ = gross photosynthesis of crop at crop production level 2 [$kg(CH_2O)\ m^{-2}\ day^{-1}$]

N_c^n = nitrogen content of crop at just ample nitrogen supply [kg m^{-2}]

N_c^0 = nitrogen content of crop at extremely low nitrogen supply [kg m^{-2}]

N_c = nitrogen content of crop at actual nitrogen supply [kg m^{-2}]

Having obtained the gross photosynthesis at crop production level 1, 2 and 3 from eq. (8-25), eq. (8-40) and eq. (8-41) the corresponding values of net production are obtained from eq. (8-31) by using the appropriate values of gross photosynthesis.

8.8 Parameter assessment

Conceptual model

The present crop model is considered as a conceptual model parts of which may be described as descriptive, e.g. the assimilate partitioning, which imply that a number of parameters are required.

In order to assess parameters entering the crop model, litterature on several experimental studies has been considered. Furthermore the parameter assessment has been substantiated by including actual results of experimental studies.

For each crop considered the parameters to be assessed include particular parameters on crop canopy development, root development, assimilate partitioning, respiration, and nitrogen in the crop.

Assessment method

The parameters entering the crop model have been assessed for each crop by a trial and error method using pertinent information available in the literature. Thus using a qualified initial set of parameters simulations for the various crops were

performed for conditions of unlimited water supply combined with conditions of ample nitrogen supply as well as conditions of severe nitrogen deficiency. The simulated results were compared with pertinent available experimental results and the set of parameters adjusted until satisfactory agreement was obtained.

Parameters on root characteristics and root development were derived from data given by Jacobsen (1976), Jensen (1980), Madsen (1978, 1983), and Nielsen 1980 a, b), while crop canopy development parameters were derived from data given by Jensen (1980) Rab et al. (1984), Aslyng and Hansen (1985), and Penning de Vries et al. (1989). Regarding assimilate partitioning and respiration parameters were derived from data given by Aslyng and Hansen (1982), Hansen (1986), van Hemst (1986), and Penning de Vries et al. (1989). Assessment of crop nitrogen parameters was based primarily on data given by Hansen and Aslyng (1984) and Aslyng and Hansen (1985).

Resulting parameters

The resulting parameters are given in table 8-3, Table 8-4, Table 8-5, Table 8-6, and Table 8-7 for crop canopy development, root development, assimilate partitioning, respiration, and nitrogen in crop dry matter, respectively. Selected examples of simulation results by using the final sets of parameters are shown for winter wheat and spring barley, and spring rape and fodder beet in Fig. 8-2 and Fig. 8-3, respectively, together with corresponding experimental results given by Aslyng and Hansen (1985). In a similar way simulated results for potato were compared with experimental results given by Josefsen (1978). It should be noted, that due to the descriptive nature of various parts of the crop model several of the parameters assessed are closely related to the present model.

Table 8-3 Preliminary crop canopy development parameters.

Parameter	Unit	S.Barley	W.Wheat	S.Rape	Potato	F.Beet	Grass
Λ_i	°C	400	500	500	400	600	425
Λ_1	°C	200	100	125	500	400	125
Λ_2	°C	450	450	450	1200	1600	–
Λ_3	°C	1550	1800	1800	1700	–	–
Λ_r^L	°C	1450	1000	400	500	1500	–
Λ_r^C	°C	350	600	400	200	1500	–
α_r^L	$°C^{-1}$	3.00	1.80	1.25	0.30	1.00	–
α_r^C	$°C^{-1}$	1.20	1.25	1.20	1.00	1.00	–
W_t^0	kg m^{-2}	0.02	0.02	0.02	0.02	0.02	0.05
S_{ai}	m^2 kg^{-1}	20	14	18	17	11	17

Table 8-4 Preliminary root development parameters.

Parameter	Unit	S.Barley	W.Wheat	S.Rape	Potato	F.Beet	Grass
d_r^0	m	0.1	0.1	0.1	0.1	0.1	0.1
d_r^*	m	1.20	1.20	1.20	1.50	1.50	0.7
r_r	mm	0.1	0.1	0.1	0.1	0.1	0.1
S_r	$10^6 mkg^{-1}$	0.1	0.1	0.1	0.1	0.1	0.1
T_c	°C	4.0	4.0	4.0	4.0	4.0	4.0
a_r	$cmday^{-1}·C^{-1}$	0.25	0.25	0.25	0.20	0.20	0.20
L_{d_r}	m m^{-3}	100	100	100	100	100	100
L_Z^m	10^5m m^{-3}	1.0	1.0	1.0	1.0	1.0	1.0
z_r^m	m	0.15	0.15	0.15	0.15	0.15	0.15

Table 8-5 Preliminary assimilate partitioning parameters.

Parameter	Unit	S.Barley	W.Wheat	S.Rape	Potato	F.Beet	Grass
γ_r^o	-	0.60	0.60	0.60	0.50	0.60	0.25
γ_r'	-	0.15	0.10	0.15	0.05	0.10	0.25
Λ_r^o	°C	0	0	0	0	0	0
Λ_r'	°C	800	700	900	700	900	0
γ_s^o	-	-	-	-	0	0	-
γ_s'	-	-	-	-	0.85	0.60	-
Λ_s^o	°C	-	-	-	0	0	-
Λ_s'	°C	-	-	-	700	900	-

Table 8-6 Preliminary respiration parameters. For each parameter the values in first, second and third line are for shoots, roots and storage organs, respectively.

Parameter	Unit	S.Barley	W.Wheat	S.Rape	Potato	F.Beet	Grass
Y	kg kg^{-1}	0.72	0.72	0.65	0.72	0.83	0.70
		0.54	0.54	0.54	0.54	0.54	0.54
		-	-	-	0.85	0.85	-
r_m [1]	kgkg^{-1}day^{-1}	0.015	0.015	0.025	0.030	0.030	0.030
		0.065	0.065	0.065	0.065	0.065	0.065
		-	-	-	0.005	0.005	-
r_m [2]	kgkg^{-1}day^{-1}	0.010	0.005	0.015	-	-	-
		0.015	0.015	0.015	-	-	-
		-	-	-	-	-	-

[1] Respiration period 1 (S. Barley, W. Wheat, S. Rape)

[2] Respiration period 2 (S. Barley, W. Wheat, S. Rape)

Transition from respiration period 1 to respiration period 2 occurs at a temperature sum of 1200, 900 and 900 °C for S. Barley, W. Wheat and S. Rape, respectively.

Table 8-7 Preliminary crop nitrogen parameters. For each parameter the values in first, second and third line are for shoots, roots and storage organs, respectively.

Parameter	Unit	S.Barley	W.Wheat	S.Rape	Potato	F.Beet	Grass
$\Lambda^*_{1,j}$	°C	200	100	275	400	0	0[1]
		200	100	275	400	0	0[1]
		–	–	–	400	0	–
$\Lambda^*_{2,j}$	°C	900	1100	1300	1800	300	300[1]
		900	1100	1300	1800	300	300[1]
		–	–	–	1800	300	–
$c^*_{1,j}$	kg kg^{-1}	5.0	5.0	7.0	5.5	5.5	5.5
		1.8	1.8	2.0	2.0	2.0	2.0
		–	–	–	3.5	3.0	–
$c^*_{2,j}$	kg kg^{-1}	1.2	1.2	1.9	4.0	4.0	4.5
		1.0	1.0	1.0	1.5	1.5	1.5
		–	–	–	1.7	1.0	–
$c^n_{1,j}$	kg kg^{-1}	3.0	3.0	3.0	3.5	3.5	3.5
		1.3	1.3	1.3	1.2	1.2	1.0
		–	–	–	1.5	1.2	–
$c^n_{2,j}$	kg kg^{-1}	1.0	1.0	1.0	1.7	1.7	3.5
		0.8	0.8	0.8	0.8	0.8	0.8
		–	–	–	0.8	0.8	–
$c^o_{1,j}$	kg kg^{-1}	2.0	2.0	2.0	1.7	1.7	1.5
		1.0	1.0	1.0	1.0	1.0	0.8
		–	–	–	1.0	1.0	
$c^o_{2,j}$	kg kg^{-1}	0.7	0.7	0.7	1.0	1.0	1.5
		0.7	0.7	0.7	0.5	0.5	0.4
		–	–	–	0.5	0.5	
Λ^*_3	°C	1400	1700	1800	2200	–	

[1] Initiated at emergence or cut.

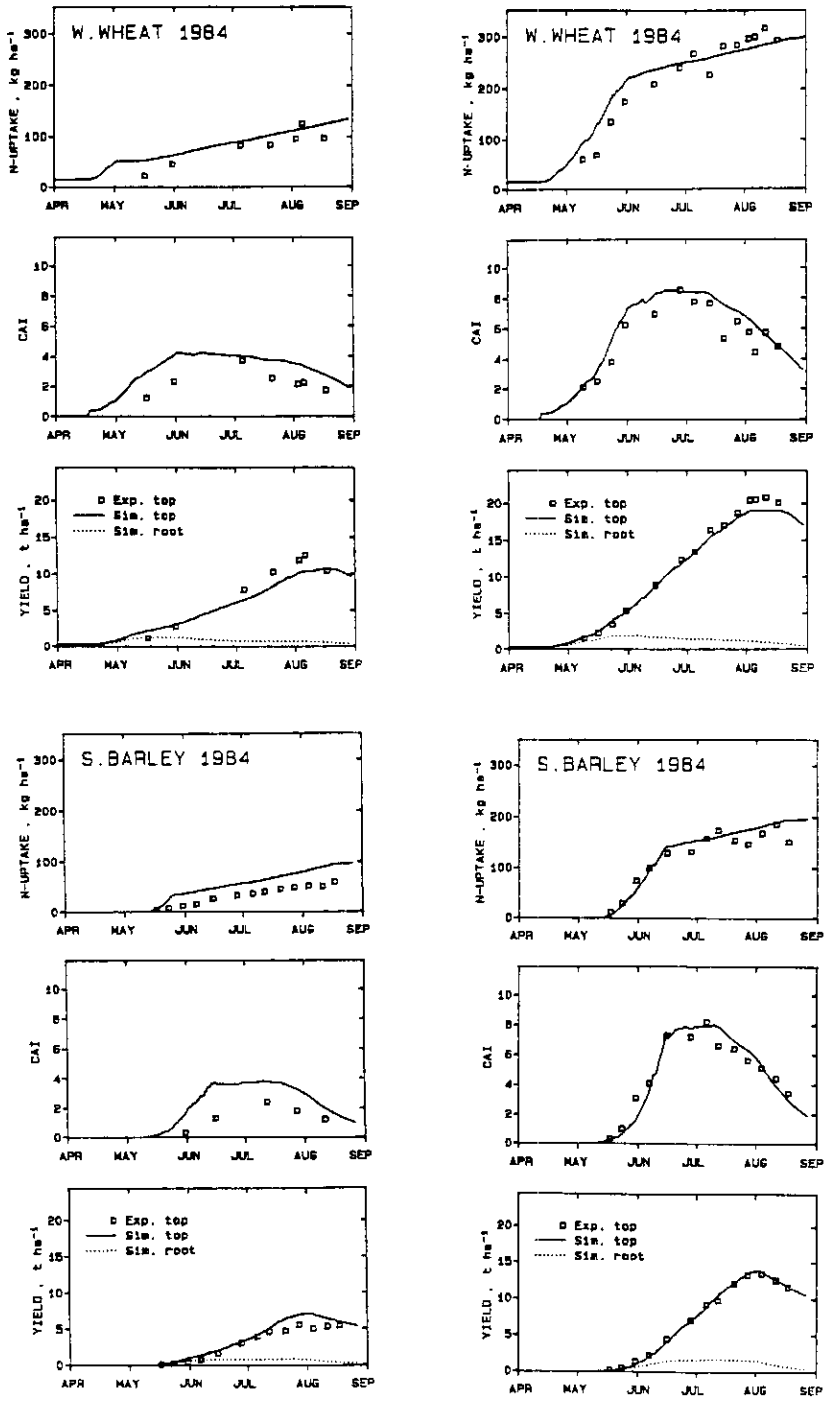

Fig. 8-2 Measured and simulated yield, crop area index, and nitrogen uptake in W. Wheat and S. Barley.

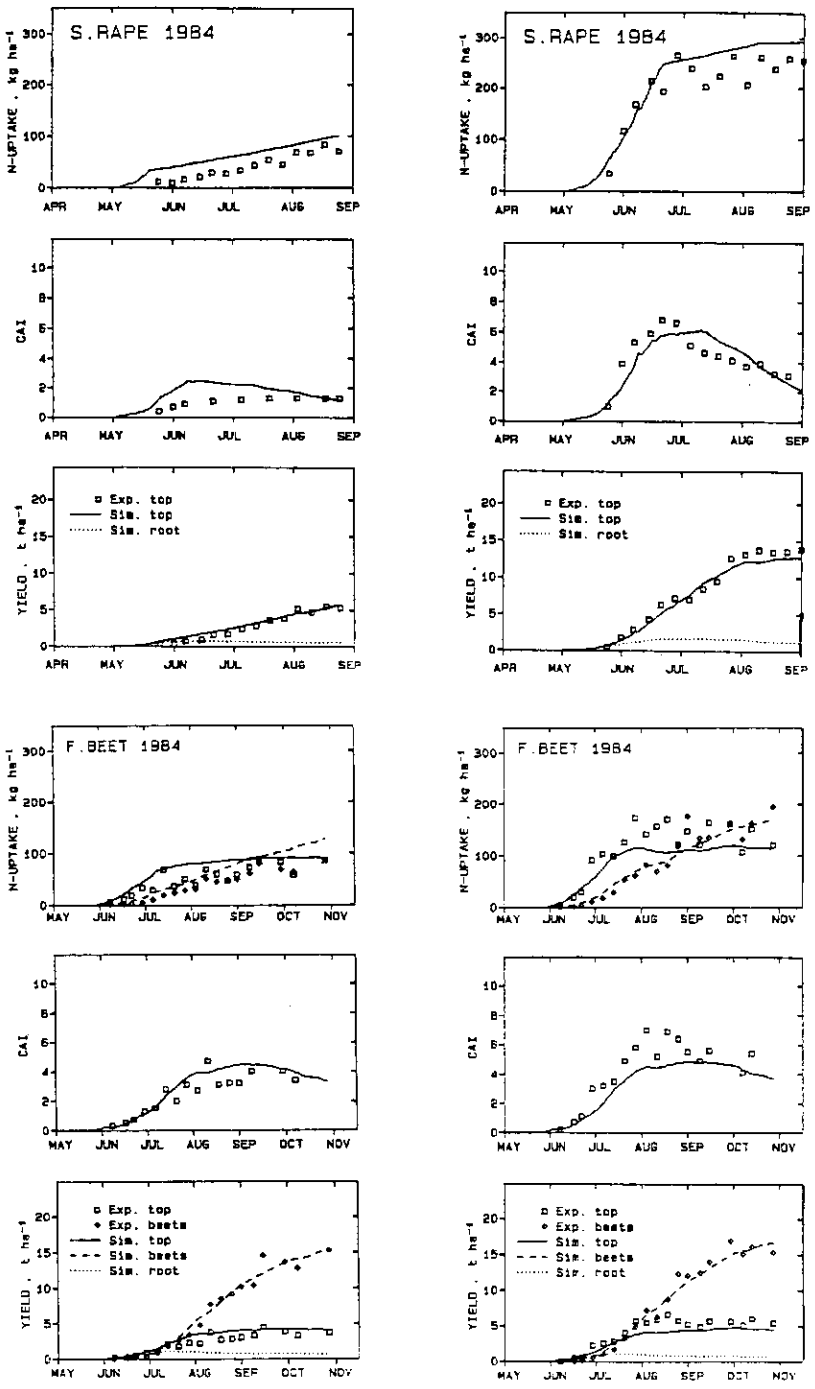

Fig. 8-3 Measured and simulated yield, crop area index, and introgen uptake in Rape and F. Beet.

9. SYSTEM MANAGEMENT MODEL

9.1 Introduction

Management operations

System management operations include soil tillage, crop sowing, fertilization, irrigation and crop harvest. In order to simulate different crop systems subject to various combinations of system management operations a system management model has been included in the DAISY model. Furthermore in order to make the model flexible and applicable to a range of combinations of system management operations a number of obtions have been included in each part of the system management model.

9.2 Soil trafficability

Trafficability concept

In order to carry out various system management operations the soil has to be trafficable. The trafficability of the soil in terms of the ability of the soil to withstand loads from tractors and implements is depending on the shear strength of the soil which increases with increasing soil bulk density and decreasing soil water content (Godwin and Spoor, 1977). Thus for a given soil the main criterion for soil trafficability is a maximum level of soil water content near the soil surface. In the present model the criterion used for soil trafficability is given in eq. (9 – 1).

$$\psi'_z \leq \psi_t \qquad (9-1)$$

ψ'_z = pressure potential of soil water at the soil depth z' [m H_2O]

z' = soil depth selected for application of soil trafficability criterion [m]

ψ_t = pressure potential of soil water selected as soil trafficability criterion [m H_2O]

For soils with a moderate clay content values of ψ_t and z' around -1.0 m H_2O and 0.1 m, respectively, may be appropriate. However, for soil with high clay content other values may be selected to ensure trafficability of the soil at the time of system management operations.

9.3 Crop sowing

In the present model a crop is sown at a date which must be specified. However, two criteria must be fulfilled viz. the trafficability criterion and that no ice is present in the soil. If the trafficability criterion is not fulfilled or if ice is present in the soil sowing is postponed untill both requirements are fulfilled. At sowing all crop parameters are allocated to the crop model.

9.4 Crop harvest

Date of harvest

The date of crop harvest can either be predescribed or simulated. In both cases time of harvest is postponed if the trafficability criteron is not fulfilled. At harvest predescribed fractions of the various parts of the crop are removed from the field. The remaining part of the crop is assumed to enter the soil as crop residue. The annual crops are assumed to follow a predescribed development scheme. In the case of the date of harvest being simulated it is assumed that the date of harvest is the time of termination of this predescribed development scheme. Above ground parts of a crop left at the field are assumed to enter the soil fully or partly when soil tillage is performed.

Crops of cereals and rape

Due to compartmentalization of crops of cereals and rape only total top dry matter and total root dry matter is simulated by the present model. At harvest the top dry matter is distributed between stubble, straw and grain or seed.

Stubble is assumed to be a fixed amount of dry matter e.g. predescribed to be 500 kg ha^{-1}. The rest of the top dry matter is then distributed between straw and grain or seed by using a specific harvest index. The carbon contents of roots, stubble, straw and seed or grain are calculted assuming a crop specific carbon concentration in each part.

The present model simulates the total nitrogen content of the entire crop during the growth season. Therefore at harvest the nitrogen content of the crop is distributed between roots, stubble, straw and grain or seed. Thus it is assumed that the relation between nitrogen concentration in the root and in the top dry matter can be described by eq. (9-2).

$$C_r = \beta C_t^{1/2} \qquad (9-2)$$

C_r = nitrogen concentration in root dry matter [kg kg^{-1}]
C_t = nitrogen concentration in top dry matter [kg kg^{-1}]
β = specific parameter for the particular crop [(kg $kg^{-1})^{1/2}$]

The concentration of nitrogen in the stubble and straw is assumed to be similar and related to the nitrogen concentration in grain or seed by eq. (9-3).

$$C_s = \begin{cases} C_{s,o} & C_g \le C_{g,o} \\ C_{s,o} + \alpha(C_g - C_{g,o}) & \text{else} \end{cases} \qquad (9-3)$$

C_s = nitrogen concentration in dry matter of straw or stubble [kg kg^{-1}]
C_g = nitrogen concentration in grain or seed dry matter [kg kg^{-1}]
$C_{s,o}$ = nitrogen concentration in dry matter of straw or stubble at low level of nitrogen supply [kg kg^{-1}]
$C_{g,o}$ = nitrogen concentration in grain or seed dry matter below which concentration of nitrogen in dry matter of straw or stubble is constant, $C_{s,o}$ [kg kg^{-1}]
α = parameter

When knowing the total nitrogen content of the entire crop and the amount of dry matter in roots, stubble, straw, and grain or seed the corresponding values of nitrogen in the various parts of the crop can be found by using eq. (9-2) and eq. (9-3). In the case of crops of cereals and rape, straw, and grain or seed may be fully or partly removed from the field while roots and stubble always remain in the field and enter the soil as crop residues.

Crops of beet and potato

In the case of beet and potato the dry matter in top and roots as well as in beets and tubers are simulated by the crop model. However, as in the case of cereals and rape the present model simulates the total nitrogen content of the entire crop during the growth season. Therefore at harvest the total nitrogen content of the crop is distributed between roots, top and beet or tubers. Thus it is assumed that eq. (9-2) holds true also for beet and potato. Furthermore it is assumed that the relation between the nitrogen concentration in the dry matter of storage organs (beet or tubers) and the nitrogen concentration in the top dry matter can be described by eq. (9-4).

$$C_{st} = a + b\,C_t \qquad (9-4)$$

C_{st} = nitrogen cencentration in dry matter of beet or tubers [kg kg^{-1}]
C_t = nitrogen concentration in top dry matter [kg kg^{-1}]
a = specific parameter for the particular crop
b = specific parameter for the particular crop

When knowing the total nitrogen content of the entire crop, the amount of dry matter in roots, top and beet or tubers the corresponding values of nitrogen in the various parts of the crop can be found by using eq. (9-2) and eq. (9-4).

In the case of a beet crop the top as well as the beet can be fully or partly removed from the field. In the case of a potato crop the tubers can be fully or partly removed from the field while the top always remains and enters the soil as crop residue. The carbon contents of top, roots and beet or tubers are calculated assuming a crop specific carbon concentration in each part. It is noted that in the case of a beet crop the date of harvest has to be predescribed. Furthermore an ultimative time for harvest has to be predescribed which is the latest date for harvesting the crop.

For all annual crops it is assumed that carbon and nitrogen in roots enter the soil at the day of harvest.

Grass crops

The grass considered is a perennial crop, and harvest or cut is normally performed several times during the growth season. If the harvest date is simulated, the time of cutting is determined either by a specified amount of accumulated top dry matter or a specified temperature sum calculated from the time of the previous cut or in the case of the first cut from the time of emergence. Thus when either the specified amount of top dry matter or the specified temperature sum is reached the system management model assumes that cutting is performed.

The present crop model simulates the amount of dry matter accumulated in top and roots. At harvest a predescribed amount of dry matter in stubble is left at the field and the rest of the top dry matter removed from the field. It is assumed that eq. (9–2) holds true for a grass crop and that the concentration of nitrogen in the stubble and top dry matter is similar. Thus knowing the total nitrogen content of the entire crop, the amount of dry matter in roots, stubble, and the top removed from the field the corresponding values of nitrogen in the various parts of the crop can be calculated.

For grass crops the harvested part is assumed fully removed from the field while the remaining parts continue to grow. In the case of grass crops for cutting an ultimative time for harvest is predescribed which is the latest date for harvesting the crop. Furthermore a minimum amount of accumulated top dry matter is specified as a requirement for harvest of the crop to be performed.

9.5 Irrigation

Irrigation models

Irrigation can be effectuated at a predescribed date or at a date simulated by an irrigation model. In the present version of the DAISY model three different irrigation models are included.

Irrigation model 1
Irrigation is effectuated when a predescribed fraction of the available soil water in the root zone is taken up by the crop.

Irrigation model 2
Irrigation is effectuated when the pressure potential of soil water at a predescribed depth deçreases to below a predescribed value.

Irrigation model 3
Irrigation is effectuated when a predescribed precipitation deficit is exceeded, eq. (9-5).

$$D_P = \Sigma (E_p - P - I) \qquad (9-5)$$

D_P = precipitation deficit [mm]
E_p = potential evapotranspiration [mm]
P = precipitation [mm]
I = irrigation [mm]

The summation in eq. (9-5) is initiated at the time of crop emergence or in the case of perennial crops at the time of on-

set of growth. An irrigation is characterized by the amount of water applied (mm of irrigation water) and the temperature of the irrigation water.

9.6 Soil tillage

Soil tillage operations

In the present model the date and type of soil tillage must be specified. Soil tillage operations are performed only if the trafficability criterion is fulfilled and if no ice is present in the soil. If the trafficability criterion is not fulfilled or if ice is present in the soil tillage operations are postponed untill both requirements are fulfilled. In the present model four types of soil tillage operation are included.

Seed bed preparation

Seed bed preparation is simulated by mixing the top soil layers to a depth corresponding to a specified seed bed preparation depth. The seed bed preparation which is always performed at the date of sowing results in homogeneous top soil layers, i.e. all soil layers within the depth of seed bed preparation assume an average value of soil water content, heat content and content of organic matter in the various pools of organic matter present in the soil, respectively.

Ploughing

Ploughing is characterized by ploughing depth, incorporation depth and incorporation fraction all of which have to be specified. The ploughing is simulated by a series of actions. 1. Soil layers from the top of soil to the incorporation depth are mixed. 2. A fraction, the incorporation fraction, of the organic material present at the soil surface, e.g. crop residues or organic fertilizers, is allocated to the appropriate pools of organic matter in the soil, after which each pool is mixed into the soil layers from the top of soil to the incorporation depth. 3. The soil layers from the incorporation depth to the ploughing depth are mixed. 4. The soil from top of soil to the ploughing depth is turned upside down.

Rotavation

Rotavation is characterized by a rotavation depth and an incorporation fraction both of which have to be specified. Rotavation is simulated by two different actions. 1. Soil layers from the top of soil to the incorporation depth which is equal to the rotavation depth are mixed. 2. A fraction, the incorporation fraction, of the organic material present at the soil surface, e.g. crop residues or organic fertilizers, is allocated to the appropriate pools of organic matter in the soil, after which each pool is mixed into the soil layers from top of soil to the rotavation depth.

Stubble cultivation

Stubble cultivation is simulated in a similar way as rotavation. All soil tillage operations are for a given field subject to the constraint that soil tillage must only affect one single soil type.

9.7 Fertilization

Type of fertilizer

In the present model the type of fertilizer as well as the date of fertilization must be specified. A fertilization operation is performed only if the soil trafficability criterion is fulfilled. If this is not the case the operation is postponed. Two methods of fertilizer application is included in the model viz. surface broadcasting and banding.

When surface broadcasting is selected then the inorganic part of the fertilizer is allocated to the uppermost node of the soil while the organic part of the fertilizer is assumed to enter the soil when a soil tillage operation is performed.

Application methods

When banding is selected then the fertilizer is mixed into the soil layers between two banding depths specified to characterize the banding fertilizer application.

Fertilization with an inorganic nitrogen fertilizer is characterized by the amounts of nitrogen applied as $NH_4^+ - N$ and $NO_3^- - N$, respectively. Liquid ammonia and urea are considered as $NH_4^+ - N$ fertilizers.

In the present model the application of organic fertilizer is stated in terms of the wet bulk amount of organic fertilizer applied. The organic fertilizer is characterized by dry matter content, carbon and nitrogen concentrations in dry matter and the fraction of nitrogen present as $NH_4^+ - N$, while the remaining part of the nitrogen is assumed to be present as $NO_3^- - N$. Furthermore the organic part of the fertilizer is characterized in terms of pools of organic matter with particular properties.

10. INTEGRATED MODEL

10.1 Introduction

Source code

In this chapter a general overview of the model is given in addition to information required to run the model. The source code of the model is written in FORTRAN 77 computer language and the program is compiled under Microsoft FORTRAN version 5.0 using a few extensions. The model can be run on a microcomputer under operation systems OS 2 or DOS version 3.3 or later versions. Additional utility programs have been written in PASCAL computer language and these programs are compiled under Borlands Turbo PASCAL version 5.5. The utility programs can be run under operation system DOS version 3.3 or later versions.

Modules

The source code of the model is divided into two modules. The first module comprises submodules for simulation of soil water dynamics, soil temperature, and crop production at production level 1 and 2. This module is designated the physical module. The second module of the model comprises submodules for simulation of the carbon and nitrogen dynamics and crop production at production level 3. This module is designated the chemical module. Information is transferred from the physical module to the nitrogen module by means of external files.

10.2 Main structure of physical module

Hierarchical structure

The main structure of the physical module of the present model is hierarchical. The upper level of the hierarchy is illustrated in Fig. 10 – 1. This structure allows the user to run a series of simulations. If the option serie run is selected, a file containing run files for each individual simulation has to be allocated. In Table 10 – 1 an example of a serie run file is shown.

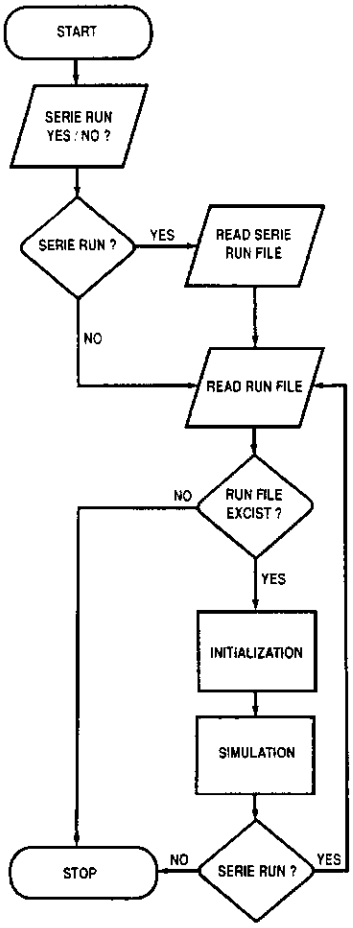

Fig. 10 – 1 Main structure of the physical module at the first hierarchical level.

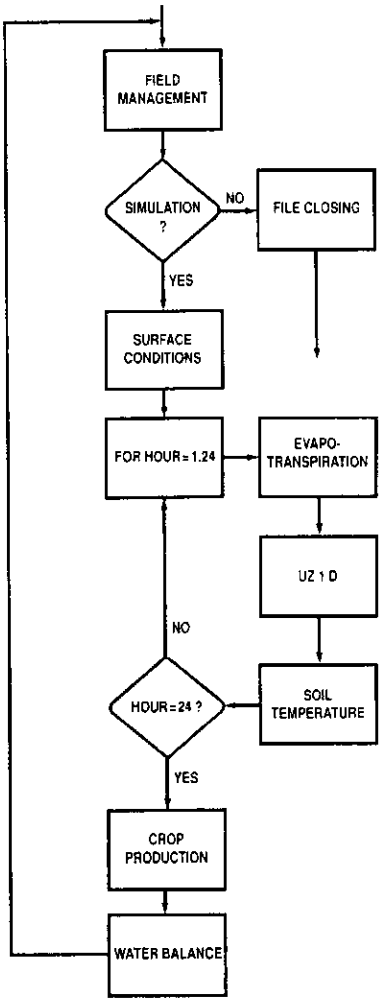

Fig. 10 – 2 Main structure of the simulation section of the physical module.

Run files

It is noted that each of the three run files is stored in a library called /RZ1/RUN on the C disk. Each of these run files contains the names of the files allocated to the physical module during an individual simulation. An example of a run file is shown in Table 10-2.

Sub modules

The first line in the run file is an identification line. The second line gives the name of the log file where messages from the simulation are printed. The next 4 files contain information to initialize the simulation whereas the remaining 7 files contain output from the simulation. The main structure of the simulation section of the physical module is illustrated in Fig. 10-2.

Submodule Field Management

The submodule Field Management simulates the impact of man on the system according to the principles given in chapter 9. The submodule Field Management reads the required information from a special external file given in Table 10-2 with the extention MAN. An example of this file is shown in Table 10-3. It is noted that the different management operations are determined by a special code, e.g. 2 for soil tillage, and that a special management code is 9 which corresponds to end of simulation.

Construction of such files which are governing the simulation of system management operations is rather complicated. Therefore a special utility program written in the PASCAL language has been developed. In an interactive fashion this program will guide the user through construction of such files as well as other initialization files.

Submodule Surface Conditions

The submodule Surface Conditions simulates processes at the soil crop surface. The driving variables are daily values of global radiation, air temperature, and precipitation. Accumulation and melting of snow, evaporation, sublimation, and percolation out of the snow pack are simulated according to the principles described in chapter 3.

The snow model requires information about soil heat flux at the soil surface, which is obtained as simulated values from the submodule Soil Temperature. Interception of precipitation in crop canopy and evaporation of water is simulated according to the principles described in chapter 3. This simulation requires information about total crop area index, which is obtained as simulated values from the submodule Crop Production.

The submodule Surface Conditions also simulates the upper boundary condition for the soil temperature model as a diurnal variation in soil surface temperature calculated according to the principles described in chapter 5. The submodule Surface Conditions simulates a potential infiltration rate of soil water to the soil system to be used in the submodule UZ 1 D. If the potential infiltration rate exceeds the intrafiltrability of the soil ponding occurs and in this way there is feed back between the submodule Surface Condition and the submodule UZ 1 D regarding simulation of the soil water dynamics. Finally the submodule Surface Conditions simulates a potential evapotranspiration rate allocated to the soil plant system. The potential evapotranspiration rate is distributed over the day according to the principles described in chapter 3 and used as input to the submodule Evapotranspiration.

Submodule Evapotranspiration

The submodule Evapotranspiration simulates evaporation from the soil surface, transpiration from the crop, and water extraction by plant roots according to the principles described in chapter 4. The driving variable in this simulation is the potential evapotranspiration rate obtained as simulated values from the submodule Surface Condition. Furthermore information about the total crop area index and root distribution is required which is obtained as simulated values from the submodule Crop Production, in addition to information about the status of the soil water, which is obtained as simulated values from the submodule UZ 1 D.

Submodule UZ 1 D

It is noted that the basic time step of the submodule Evapotranspiration is one hour. The submodule Evapotranspiration delivers information to submodule UZ 1 D as well as to submodule Crop Production.

The submodule UZ 1 D simulates the soil water dynamics according to the principles described in chapter 4. Simulated values of infiltration from submodule Surface Condition, and simulated values of surface evaporation and water extraction by plant roots from submodule Evapotranspiration act as driving variables. Furthermore if the lower boundary is a fluctuating ground water table also the ground water table acts as driving variable. Simulated water flow in the soil may also be influenced by freezing and thawing processes in the soil which is simulated by submodule Soil Temperature. The basic time step in submodule UZ 1 D is one hour. However, internal the time step in submodule UZ 1 D can be smaller depending on the flow conditions and prediscribed limitations.

Submodule Soil Temperature

The submodule Soil Temperature simulates the soil temperature, freezing and thawing in the soil according to the principles described in chapter 5. The driving variable is simulated values of surface temperature obtained from submodule Surface Conditions. Simulated soil temperature is influenced by the soil water status which is obtained as simulated values from submodule UZ 1 D. The Time step of submodule Soil temperature is one hour.

Submodule Crop Production

The submodule Crop Production simulates crop production at production level 1 and 2 as described in chapter 8. Driving variables are global radiation, air temperature, and soil temperature. Simulated crop production at producton level 2 is influenced by the evaporative conditions as simulated in submodule Surface Conditions and submodule Evapotranspiration.

Directly or indirectly most of the other parts of the system are influenced by submodule Crop Production.

Submodule Water Balance

The submodule Water Balance calculates a water balance of the considered soil profile to ensure that the conservation of mass regarding water is not violated.

Output files

The output of the physical module is indicated in Table 10-2. The file with the extention SWC contains hourly values of volumetric soil water content of each computational node in the considered soil profile. The file with the extention FUZ contains hourly values of the water flow between computational nodes in the unsaturated zone.

The file with the extention PWU contains hourly values of water uptake by plant roots for each computational node in the rooting zone. The file with the extention PF contains values of soil water pressure potential expressed as pF for each computational node. The values are written once a day. The file with the extention TMP contains daily values of the simulated soil temperature profile. The file with the extention W-C contains daily values of a number of water and crop variables which act as input to the chemical module.

Utility Programme

In addition to these files the physical module also writes a file with the extention ICE which contains values of the ice content of each computational node in the considered soil profile. A special utility program written in FORTRAN 77 has been developed to read these files.

The simulation continues until the decision variable Simulation assumes the value false, Fig. 10-2. This occurs either when the file with driving variables has terminated or when the submodule Field Management reads the special management operation with the code 9, Table 10-3.

10.3 Initialization of physical module

External files

In order to run the physical module of the present model the soil profile, the crop, and the system management operations have to be characterized which to a great extent is performed by alocating external files containing the required information to the program. This makes it possible for the user to select the initialization parameters for himself and consequently it also places the responsibility for the choice of the initialization parameter on the individual user.

In the example of the system management file, Table 10-3, the second line gives the name of the file containing data characterizing the selected soil profile. An example of such a file is shown in Table 10-4. It is noted that the soil profile is allowed to contain up to 40 computational nodes and that the soil profile may include up to 4 different soil horizons with individual hydraulic and thermal properties. The required hydraulic properties are allocated to the model by using an external file containing the required data in a large table, which in the example, Table 10-4, are the files with the extention TAB. As an example of such a file some lines of the file containing information for horizon 1 of the soil profile are shown as Table 10-5.

Utility programme

The first line in the file, Table 10-5, is an identification line, while the subsequent lines contain the required data, i.e. soil water pressure potential in terms of pF-values, volumetric soil water content ($m^3\ m^{-3}$), specific water capacity ($m^3\ m^{-3}\ (mH_2O)^{-1}$), and hydraulic conductivity ($m\ s^{-1}$). The value pF=0 indicates water saturation and the table contains data from water saturation to pF=5.0 in steps of 0.01 pF units. A special utility program written in the PASCAL language is developed to create the required table of soil hydraulic properties from single points of the soil water retention curve using the principles indicated in chapter 4. In some situations other methods may be more feasible.

The required thermal properties are also allocated to the model by using an external file containing the required data, which in the example, Table 10–4, are the files with the extention HCD. A file of this type contains a table with heat capacity of dry soil and with thermal conductivity of unfrozen as well as of frozen soil given as a function of the soil water content. The heat capacity and the thermal conductivity of the soil are assessed on the basis of principles described in chapter 5. A utility program written in PASCAL language is developed to create the thermal properties of the soil.

It is noted that the lower boundary conditions of water flow in the unsaturated zone in the example, Table 10–4, is a gravity flow condition as the pressure boundary is false. A Pressure boundary can also be selected but then an external file containing information about the ground water table is required. Such a file should contain date (year, month, day) and depth of the ground water table below the soil surface (m). The format of this file is expected to be (3I2, F6.2). If daily observations of the ground water table do not exist linear interpolation between the actual observations is performed. Initialization files of the type shown in Table 10–4 can be created by using an initialization program mentioned previously.

When the soil profile has been initialized information on the different system management operations is required, Table 10–3. After sowing date has been chosen the desired crop is indicated by allocating a file containing the necessary crop parameters. In the example, Table 10–3, this file is listed with the extention BAR indicating that spring barley has been selected. As an example this file is listed in Table 10–6. Not all the parameters listed in this file are used by the physical module of the present model. The remaining parameters are used in the chemical module of the model. A file of the type shown in Table 10–6 is required for each crop included in the system. However, the working out of the file may differ for different crops.

The soil tillage parameters are given in the file with extention TIL, Table 10-4. An example of such a file is given in Table 10-7.

Recalling Table 10-2 still three input files are necessary for running the physical module, viz. files containing control parameters, snow and interception parameters, and meteorological driving variables.

Control parameters

An example of the file containing control parameters is given in Table 10-8. The tolerance criteria refer to the criteria given in chapter 4. An example of the file containing the snow and interception parameters is given in Table 10-9.

Driving variables

Finally a file containing the meteorological driving variables is needed. This file should contain date (year, month, day), global radiation (W m^{-2}), air temperature (°C), precipitation (mm d^{-1}), and potential evapotranspiration (mm d^{-1}) if not calculated by the module Surface Conditions. The format of this file is expected to be (3I2, 4F6.1).

When all the input files mentioned are established it is possible to run the physical module of the present model. The required set up may seem to be quite complex. However, by using the initialization program the set up is straight forward. The problem is rather to obtain appropriate parameter values.

10.4 Main structure of chemical module

Hierarchical structure

The main structure of the chemical module of the present model is hierarchical. The structure of the upper level of the hierarchy is identical to the upper level of the structure of the physical module as shown in Fig. 10-1, which allows the user to run a series of simulations.

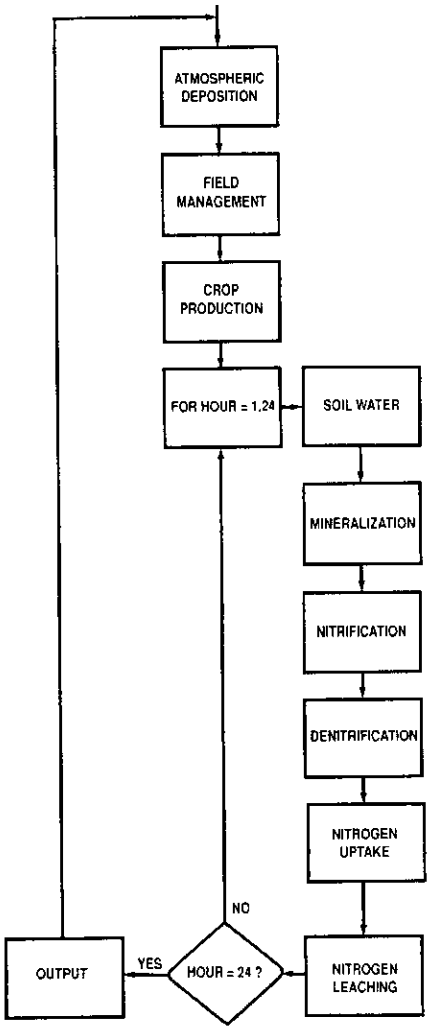

Fig. 10-3 Main structure of the simulation section of the chemical module.

Run files

An example of a serie run file used for running the chemical module is shown in Table 10-10. Each run file is constructed as shown in Table 10-11. The first line is a heading while the second line indicates the corresponding set up of the physical module of the model. The subsequent three files initiate the chemical module while the remaining four lines represent out files showing the simulation results.

Submodules

As in the case of the physical module the chemical module of the model comprises an initialization part and a simulation part the latter of which comprises a number of interacting submodules. The main structure of the simulation section of the chemical module is illustrated in Fig. 10-3.

Submodule Atmopspheric Deposition

The submodule Atmospheric Deposition simulates wet deposition of ammonium and nitrate as described in chapter 3. The required meteorological data are transferred from the physical module.

Submodule Field Management

The submodule Field Management simulates field management operations according to the principles described in chapter 9. Most of the required information is transferred from the physical module. However additional information on fertilizer practice is required which is obtained from a fertilizer management file indicated in Table 10-11.

The structure of the fertilization-management files appears in Table 10-12 and Table 10-13. In the first example, Table 10-12, only inorganic fertilizer is applied.

The submodule Field Management requires information on the date of fertilization, the application method, and the type of fertilizer applied. The additional information required depends on the type of fertilization. Two different application methods are allowed viz. surface broadcasting (code 1) and banding (code 2). Likewise two different types of fertilizer are allowed viz. inorganic fertilizer (code ≤ 9) and organic fertilizer (code ≥ 10).

In the case of application of inorganic fertilizer, as in the example shown in Table 10–12, the total amount of nitrogen applied and the relative amount being ammonium nitrogen have to be specified. The remaining part of the nitrogen applied is assumed to be nitrate nitrogen. In the case of application of organic fertilizer, as in the example shown in Table 10–13, the fertilizer has to be characterized in accordance with the soil organic matter model described in chapter 6. In the case of organic fertilizer all the inorganic nitrogen is assumed to be present as ammonium nitrogen.

Submodule Crop Production

In the chemical module the submodule Crop Production simulates crop production at production level 3 according to the principles concerning nitrogen limited production described in chapter 8. The submodule Crop Production also simulates maximum crop nitrogen content, actual crop nitrogen content, and root density of the crop. The information required by the submodule Crop Production is transferred from the physical module and from submodule Nitrogen Uptake. The basic time step of submodule Crop Production is one day.

Submodule Soil Water

The submodule Soil Water assesses information on soil water status which i transferred from the physical module.

Submodule Mineralization

The submodule Mineralization simulates the carbon turnover and the net mineralization according to the principles described in chapter 6. Information on soil water status and soil temperature is transferred from the physical module. Furthermore information and input to the system are transferred from the submodule Field Management.

Submodule Nitrification

The submodule Nitrification simulates nitrification according to the principles described in chapter 7. Soil water status expressed as pressure potential and soil temperature are transferred from the physical module.

Submodule Denitrification

The submodule Denitrification simulates the loss of nitrogen due to denitrification according to the principles described in chapter 7. The required information on CO_2 evolution is obtained as simulated values from submodule Mineralization. Furthermore information on soil water status and soil temperature is transferred from the physical module.

Submodule Nitrogen Uptake

The submodule Nitrogen Uptake simulates the nitrogen uptake (ammonium as well as nitrate) by the crop according to the principles described in chapter 7. Information on maximum crop nitrogen content, actual crop nitrogen content, and root density of the crop is transferred from submodule Crop Production. Furthermore information on soil temperature, water status, and soil water uptake by plant roots is transferred from the physical module.

Submodule Nitrogen Leaching

The submodule Nitrogen Leaching simulates the nitrogen status (ammonium as well as nitrate) of the soil profile which includes simulation of nitrogen leaching from the soil profile according to the principles described in chapter 7. Thus this submodule integrates the nitrogen processes taking place in the soil viz. net mineralization, nitrification, denitrification, nitrogen uptake by plant roots, and the input of nitrogen to the soil plant system due to fertilizer application and nitrogen deposition.

Basic time step

It is noted that the basic time step in the simulation of the nitrogen processes in the soil is one hour. The submodule Output writes simulated results to the output files described in Table 10 – 11.

10.5 Initialization of chemical module

External files

Several of the parameters and variables required to initialize the chemical module of the present model are transferred from the physical module while others are read from the same initialization files as read by the physical module. Files required in addition to those files are shown in Table 10-11.

The fertilization-management file has been discussed previously. An example of a file containing the parameters required by module Mineralization and values to initiate the different pools of organic matter as described in chapter 6 is shown in Table 10-14. The pools named ROM (Root Organic Matter) pools in Table 10-14 are pools containing root residuals and are in the context of chapter 6 to be considered as a special sort of AOM pools.

An example of a file containing the parameters required by module Nitrification and module Denitrification are shown in Table 10-15. The file also contains parameters characterizing the porous medium and parameters governing the adsorption and desorption of ammonium as required by module Nitrogen Leaching and module Nitrogen Uptake. Furthermore this file also contains values to initialize the soil profile considered regarding content of inorganic nitrogen. i.e. nitrate nitrogen and ammonium nitrogen.

Utility programme

As in the case of the physical module a utility program written in PASCAL language has been developed to establish the initialization files required by the chemical module.

When all the input files mentioned are established it is possible to run the chemical module of the present model. The required set up may seem to be quite complex. However, by using the initialization program the set up is straight forward. The problem is rather to obtain appropriate parameter values.

Table 10 – 1 Example of a serie run file for the physical module containing run files for 3 individual simulations.

```
C:\RZ1\RUN\ASKOV1.RUN
C:\RZ1\RUN\ASKOV4.RUN
C:\RZ1\RUN\ASKOV8.RUN
```

Table 10 – 2 Example of the content of a run file for the physical module for a single simulation.

Time of creation	1990 – 06 – 13:15.08.05
Print File	C:\RZ1\OUTPUT\ASKOV8.LOG
Field Management & Crop Rotation	C:\RZ1\MANAGEME\ASKOV8.MAN
Control Parameters	C:\RZ1\CNTR\ASKOV.PAR
Snow & Interception Parameters	C:\RZ1\SFLIB\ASKOV.INT
Meteorological Variables	C:\RZ1\METLIB\ASKOV8789.CLM
Volumetric Soil Water Content	C:\RZ1\OUTPUT\ASKOV8.SWC
Flow between UZ Nodes [mm/h]	C:\RZ1\OUTPUT\ASKOV8.FUZ
Water Uptake by Plants [mm/h]	C:\RZ1\OUTPUT\ASKOV8.PWU
Soil Pressure potential [pF]	C:\RZ1\OUTPUT\ASKOV8.PF
Soil Temperature [°C]	C:\RZ1\OUTPUT\ASKOV8.TMP
Water & Crop Variables	C:\RZ1\OUTPUT\ASKOV8.W – C
Ice Content in the soil [%]	C:\RZ1\OUTPUT\ASKOV8.ICE

Table 10 – 3 Example of a system management file.

```
ASKOV 8 1987-89
 Soil Profile Initialization .....> C:\RZ1\SOILDEF\ASKOV.INI
 Date of Initialization or Sowing [yy.mm.dd]                1 87  4 29
 Crop Parameters (Data File).....> C:\DAISY\CRPLIB\SBARLEY.BAR
 Date of latest or end Harvest [yy.mm.dd]                  87  9 30
 ------------------------------------- Tillage ----------------------------------------
 Soil Tillage Parameters (Data File).....>C:\RZ1\TILLAGE\ASKOV.TIL
 ------------------------------------- Irrigation -------------------------------------
 Irrigation Criteria :                                              0
 ------------------------------------- Harvest ----------------------------------------
 Harvest Simulation - Default Harvest Simulation                .FALSE.
   STUBBLE DRY MATTER                                             1.3
   HARVINDEX                                                     0.45
   PRIMARY YIELD, HARVESTED PART [%]                            100.0
   SECUNDARY YIELD, HARVESTED PART [%]                          100.0
 ---------------------- Field Managements Operations ------------------------------
 SOIL TILLAGE                                                2 87  4 28
 5 SEED BED PREPARATION                                             5
 SOIL TILLAGE                                                2 87 12  3
 1 PLOWING                                                          1
 SOIL TILLAGE                                                2 88  4 15
 5 SEED BED PREPARATION                                             5
 Date of Initialization or Sowing [yy.mm.dd]                 1 88  4 19
 Crop Parameters (Data File).....>C:\DAISY\CRPLIB\SBARLEY.BAR
 Date of latest or end Harvest [yy.mm.dd]                   88  8 18
```

Table 10-3 continued

Tillage	
Soil Tillage Parameters (Data File).....	>C:\RZ1\TILLAGE\ASKOV.TIL
Irrigation	
Irrigation Criteria :	0
Harvest	
Harvest Simulation - Default Harvest Simulation	.FALSE.
STUBBLE DRY MATTER	0.65
HARVINDEX	0.45
PRIMARY YIELD, HARVESTED PART [%]	100.0
SECUNDARY YIELD, HARVESTED PART [%]	100.0
Field Managements Operations	
SOIL TILLAGE	2 88 12 6
1 PLOWING	1
END OF SIMULATION	9 89 03 31

Table 10-4 Example of file containing data for characterization and initialization of soil profile.

ASKOV 1987-89	
Number of Nodes in the UZ-Column (max. 40)	19
Number of Horizons in the UZ-column (max. 4)	3
Hydraulic Soil Properties	
Horizon 1 : C:\RZ1\RETENT\ASKOVTOP.TAB	
Hydraulic Conductivity Matching	
- pF	2.0
- Hydraulic Conductivity [m/s]	1.57800E-08
Horizon 2 : C:\RZ1\RETENT\ASKOVINT.TAB	
Hydraulic Conductivity Matching	
- pF	2.0
- Hydraulic Conductivity [m/s]	5.17800E-09
Horizon 3 : C:\RZ1\RETENT\ASKOVSUB.TAB	
Hydraulic Conductivity Matching	
- pF	2.0
- Hydraulic Conductivity [m/s]	5.00000E-10
Thermic Soil Properties	
Horizon 1 : C:\RZ1\THERMAL\AS_TOP.HCD	
Horizon 2 : C:\RZ1\THERMAL\AS_INT.HCD	
Horizon 3 : C:\RZ1\THERMAL\AS_SUB.HCD	
Clay Content [%]	
Horizon 1 :	11.0
Horizon 2 :	13.0
Horizon 3 :	16.0
Maximum Allowed Root Depth in Profile [m]	1.00

Table 10-4 continued

Initialization of soil profile, Date of initialization : 87 4 1

Node	Z [m]	Hori-zon	Psi [m H_2O]	Theta [m^3/m^3]	Ice	Tsoil [°C]
1	0.0200	1	-1.00	0.30	0.00	5.2
2	0.0500	1	-1.00	0.30	0.00	5.2
3	0.1000	1	-1.00	0.30	0.00	5.1
4	0.2000	1	-1.00	0.30	0.00	4.9
5	0.3000	2	-1.00	0.26	0.00	4.8
6	0.4000	2	-1.00	0.26	0.00	4.6
7	0.5000	2	-1.00	0.26	0.00	4.5
8	0.6000	2	-0.80	0.26	0.00	4.4
9	0.7000	3	-0.30	0.21	0.00	4.3
10	0.8000	3	-0.20	0.21	0.00	4.3
11	0.9000	3	-0.20	0.21	0.00	4.2
12	1.0000	3	-0.20	0.21	0.00	4.2
13	1.1000	3	-0.20	0.21	0.00	4.1
14	1.2000	3	-0.20	0.21	0.00	4.1
15	1.3000	3	-0.20	0.21	0.00	4.1
16	1.4000	3	-0.20	0.21	0.00	4.1
17	1.6000	3	-0.20	0.21	0.00	4.1
18	1.8000	3	-0.20	0.21	0.00	4.1
19	2.0000	3	-0.20	0.21	0.00	4.2

Boundary Conditions at Lower Limit

- Water flow :	
- Pressure Boundary (ground Water Table):	.FALSE.
- Heat Flow:	
- Forced Annual Sinusidal Variation at node:	Nz+1
- Top Boundary Condition _ Sinusidal Variation	
- Average Annual Temperature [°C]:	7.8
- Amplitude of Annual Variation [°C]:	8.5
- Lag - Annual Sinusidal:	200
- Damping Depth [m]:	

Table 10-5 Example of part of file containing hydraulic properties for a selected soil profile.

ASKOV TOP SOIL RETENTION CURVE

0.00	0.387000	1.681E-0005	4.005E-0006
0.01	0.386991	6.895E-0002	3.902E-0006
0.02	0.386967	1.328E-0001	3.803E-0006
0.03	0.386928	1.919E-0001	3.706E-0006
.	.	.	.
.	.	.	.
.	.	.	.
4.96	0.049674	1.316E-0004	7.453E-0014
4.97	0.049268	1.316E-0004	6.923E-0014
4.98	0.048863	1.316E-0004	6.543E-0014
4.99	0.048460	1.316E-0004	6.185E-0014
5.00	0.048057	1.316E-0004	5.846E-0014

Table 10-6 Example of crop parameter file.

S. Barley	
Crop Parameters	S. Barley
Model Type	2
Spring Crop	.True.
Photosynthesis - Gross Assimilation Rate	
Max Efficiency at low radiation	0.150
Formfactor in efficiency equation (8-22) [W/m^2]	90.0
Constant in efficiency eguation (8-22) beta 1	0.158
Constant in efficiency eguation (8-22) beta 2	0.094
Formfactor in efficiency equation (8-22) [LAI]	3.0
Max. efficient LAI [LAI]	5.0
Lower Temperature Limit for photosynthesis [°C]	4.0
Upper Limit for Temperature influence on photosynthesis [°C]	10.0
Extinction coefficient - P.A.R. -	0.6
Percentage of P.A.R. in the Global Radiation	48.0
Crop reflectance - P.A.R. - [%]	6.0
Partitioning of Assimilate between Root and Shoot	
Initial Fraction Allocated to Roots [%]	60.0
Ultimate Fraction Allocated to Roots [%]	15.0
Transition Time - Thermal Time [°C days]	800.
Respiration	
Thermal Time [°C days] at Transition between Period I and II	1200.
Root Respiration - Period I	
Conversion efficiency	0.540
Maintenance Respiration Coefficient at 20 °C	0.065
Root Respiration - Period II	
Conversion efficiency	0.540
Maintenance Respiration Coefficient at 20 °C	0.015
Shoot Respiration - Period I	
Conversion efficiency	0.720
Maintenance Respiration Coefficient at 20 °C	0.015
Shoot Respiration - Period II	
Conversion efficiency	0.720
Maintenance Respiration Coefficient at 20 °C	0.010
CAI and LAI Development	
Temperature Sum at Emergence	200.
Governed by Temperature	Fase I
Development Rate Thermal Time Constant [°C days]	400.
Transition to Fase II - Accumulated Top Dry Matter [t/ha]	0.2
Governed by Dry Matter Production & Age (Thermal Time)	FASE II
Specific Leaf Area [(m^2/m^2)/(t DM/ha)]	2.0
Temperature Sum - Start of LAI reduction periode	450.
LAI-Reduction parameter 1	3.0
LAI-Reduction parameter 2 [°C days]	1450.
CAI-Reduction parameter 1	1.2
CAI-Reduction parameter 2 [°C days]	350.
Temperature Sum at Harvest	1550.

Table 10-6 continued

Root-Development	
Root Penetration Parameters	
Penetration Rate Parameter [cm/day/°C]	0.25
Soil Temperature Penetration Limit [°C]	4.0
Root Depth at Emergence [cm]	10.0
Maximum Effective Root Depth [m]	1.2
Logaritmic Root Density Profile	
Root Density at Effective Root Depth [cm/cm^3]	0.01
Maximum Root Density [cm/cm^3]	10.0
Maximum Damping Depth (Halfing root density) [m]	0.15
Total Root Length per Mass Unit [km/g]	0.1
Root Diameter [mm]	0.1
Max. Matrix Potential at Root Surface [mH_2O]	150.0
Extinction Coefficient of a mature crop	0.5
Energy (Ep) Extinction Coefficient - Distributing Ep	0.5
Harvest Parameter (Default Harvest)	
Stubble DM left in the field [t DM/ha]	0.5
Harvest Index	0.45
Crop Thermal Age at the Beginning of the Irrigation Period	300.
Crop Thermal Age at the End of the Irrigation Period	1000.
Nitrogen Parameters	
Nitrogen content in the seed [kg/ha]	4.0
Length of uptake periode (Thermal Age)	1400.
End of part one of the uptake period (Thermal Age)	200.
End of part two of the uptake period (Thermal Age)	900.
Potential N concentrations in the crop	
Initial concentration in Shoot	0.058
End concentration in Shoot	0.014
Initial concentration in Root	0.018
End concentration in Root	0.010
N concentrations governing the DM production at level 3	
Initial concentration in Shoot (Optimum Limit)	0.030
End concentration in Shoot (Optimum Limit)	0.010
Initial concentration in Shoot (Function Limit)	0.020
End concentration in Shoot (Function Limit)	0.007
Initial concentration in Root (Optimum Limit)	0.013
End concentration in Root (Optimum Limit)	0.008
Initial concentration in Root (Function Limit)	0.010
End concentration in Root (Function Limit)	0.007
Max NH_4-Uptake per unit root length [mg/m/day]	60.00
Max NO_3-Uptake per unit root length [mg/m/day]	0.10

Table 10-6 continued

Parameters governing the partitioning of N at harvest	
Constant in the root/top concentration relation	0.90
Constants in the grain/straw concentration relation	
Normal straw concentration	0.0065
Grain concentration at the end of the normal range	0.0215
Relative increase in straw conc. above the normal range	0.80
Decompostion of residual plant material	
Straw Material	
C-concentration	0.490
Partitioning of C between organic matter pools	2
Pool 1, slowly decomposable material	0.800
Pool 2, easily decomposable material	0.200
C/N ratios of organic pools	
Pool 1, slowly decomposable material	100.0
Turnover Rate coefficients [d**-1]	
Pool 1, slowly decomposable material	0.700E-02
Pool 2, easily decomposable material	0.700E-01
Partition Constant, Transfer to BioA	
Pool 1, slowly decomposable material	0.50
Pool 2, easily decomposable material	0.00
Grain Material	
C-concentration	0.470
Partitioning of C between organic matter pools	2
Pool 1, slowly decomposable material	0.000
Pool 2, easily decomposable material	1.000
C/N ratios of organic pools	
Pool 1, slowly decomposable material	100.0
Turnover Rate coefficients [d**-1]	
Pool 1, slowly decomposable material	0.700E 02
Pool 2, easily decomposable material	0.700E-01
Partition Constant, Transfer to BioA	
Pool 1, slowly decomposable material	0.50
Pool 2, easily decomposable material	0.00
Root Material	
C-concentration	0.460
Partitioning of C between organic matter pools	2
Pool 1, slowly decomposable material	0.800
Pool 2, easily decomposable material	0.200
C/N ratios of organic pools	
Pool 1, slowly decomposable material	100.0

Table 10-6 continued

Turnover Rate coefficients [d**-1]	
Pool 1, slowly decomposable material	0.700E-02
Pool 2, easily decomposable material	0.700E-01
Partition Constant, Transfer to BioA	
Pool 1, slowly decomposable material	0.50
Pool 2, easily decomposable material	0.00

Table 10-7 Example of soil tillage parameter file.

Tillage File C:\RZ1\TILLAGE\ASKOV.TIL	
Trafficability Criterium (Potential Criterium)	
Depth of Critical Pressure Potential [m]	0.10
Critical Pressure Potential [m H_2O]	-0.5
PLOWING	1
Tillage Depth [m]	0.18
Depth of Incorporation of Surface Applyed Matter [m]	0.09
Fraction of Surface Applyed Matter Incorporated	1.00
ROTAVATION	2
Tillage Depth [m]	0.15
Depth of Incorporation of Surface Applyed Matter [m]	0.15
Fraction of Surface Applyed Matter Incorporated	1.00
DISK HARROWING	3
Tillage Depth [m]	0.10
Depth of Incorporation of Surface Applyed Matter [m]	0.10
Fraction of Surface Applyed Matter Incorporated	0.80
STUBBLE CULTIVATION	4
Tillage Depth [m]	0.12
Depth of Incorporation of Surface Applyed Matter [m]	0.12
Fraction of Surface Applyed Matter Incorporated	0.60
SEED BED PREPARATION	5
Tillage Depth [m]	0.08
Depth of Incorporation of Surface Applyed Matter [m]	0.08
Fraction of Surface Applyed Matter Incorporated	1.00

Table 10-8 Example of control parameter file.

Control Parameters	
Date of Temperature Zero-setting	3 1
Control of UZ Model	
Tolerance Criteria for Convergense (Relative Measure) 0.001	
Tolerance Criteria for Convergense (Absolute Measure [m H_2O])	0.002
Max. Number of Iterations	25
Max. Number of Times the Timestep is reduced	4
Control of the Water Balance of the Root Zone	
Lower Limit of the Root Zone [m]	1.00
Output from UZ , Node 1 to Node	19

Table 10–9 Example of file containing snow and interception parameters.

Potential Evapotranspiration, E_p [mm/d]
- Supplied by the meteorological variables : .TRUE.
- Makkink Equation : .FALSE.

- Distribution
$E_p(h) = E_p*[1 + A*\cos(2*Pi/24*h) + B*\sin(2*Pi/24*h)]$,

Month	A	B
1	-0.916667	-0.166667
2	-1.687500	-0.437500
3	-1.681818	-0.454545
4	-1.468085	-0.382979
5	-1.387324	-0.338028
6	-1.377246	-0.335329
7	-1.389937	-0.389937
8	-1.518519	-0.407407
9	-1.629630	-0.358025
10	-1.631579	-0.236842
11	-1.333333	-0.166667
12	-0.900000	-0.200000

Snow Model
- Distribution betweeb liquid (rain) and solid (snow) precipitation
  Upper limit for snow °C, mean daily air temperature] : 2.0
  Lower limit for rain °C, mean daily air temperature] : -2.0
  Linear distribution between the Limits

- The ability of the snowpack to retain fluid water
  Fluid Water Retention Capasity Coefficient of the Snowpack : 0.07

- Freezing or Melting in the snowpack
  - Temperature Effect Parameters

Mt1 [mm/d/C]	Mt2 [m**-1]
2.00	10.00

  - Radiative Effect Parameters

Mr1 [kg/J]	Mr2	Mr2 [d**-1]
1.500E-7	2.00	0.10

  - Age of surface of snowpack [d], conditions for zero-setting
    Minimum amount of solid precipitation (snow) [mm] : 5.0
    Minimum thermal quality of the snow : 0.9

- Density of newly fallen snow [kg/m^3] : 100.0
- Density of snowpack [kg/m3] Parameters

Rho1 [kg/m^3]	Rho2 [m**-1]
200.00	0.50

- Thermal Conductivity Coefficient of snow [$W*m^4/kg^2$] : 2.86E-6

Interception Model
- Interception Storage Capacity Coefficient [mm] : 0.50

Table 10-10 Example of a serie run file for the chemical module containing run files for three individual simulations.

C:\RZ2\RUN\ASKOV1.RUN
C:\RZ2\RUN\ASKOV4.RUN
C:\RZ2\RUN\ASKOV8.RUN

Table 10-11 Example of the content of a run file for the chemical module for a single simulation.

DAISY /RZ2-Setup/ : ASKOV PLOT 8 1987-89	
Setup RZ1	C:\RZ1\RUN\ASKOV8.RUN
Setup & init. Soil Org. C & N	C:\RZ2\ORG\ASKOV8.Org
Setup & init. Soil Inorg. N	C:\RZ2\INORG\ASKOV8.InO
Fertilization / Management	C:\RZ2\FERT\ASKOV8.FRT
---------- Output Files ----------	
Log-List	C:\RZ2\OUTPUT\ASKOV8.Log
N Balance	C:\RZ2\OUTPUT\ASKOV8.NBl
NH_4 & NO_3 Profiles	C:\RZ2\OUTPUT\ASKOV8.NPr
Organic Matter	C:\RZ2\OUTPUT\ASKOV8.OM
Output frequency - Organic Matter (Output every n th day)	n = 5

Table 10-12 Example of a fertilization management file.

Fertilization Date	87 05 05
Application Method - Surface Broadcasting	1
Type of Fertilizer - Inorganic	1
Applied Amount [kg N/ha]	133.0
NH_4-Content [%]	50.0
Fertilization Date	88 04 15
Application Method - Surface Broadcasting	1
Type of Fertilizer - Inorganic	1
Applied Amount [kg N/ha]	133.0
NH_4-Content [%]	50.0

Table 10-13 Example opf a fertilization management file.

Fertilization Date	87 04 28
Application Method - Surface Broadcasting	1
Type of Fertilizer - Pig Slurry	10
Applied Amount [kg/ha] wet weigth	28000.0
Dry Matter, per cent of wet weight	5.06
C content, per cent of dry matter	45.00
N content, per cent of dry matter	9.56
NH_4-N cont. per cent of N content	70.70
Number of AOM-pools	2
C-Distribution, pool 1	0.80
C-Distribution, pool 2	0.20
C/N - ratio in pool 1	100.0
Turnover rate coefficient, pool 1	5.0E-3
Turnover rate coefficient, pool 2	5.0E-2
Number of Biomass pools	2
Fraction of AOM 1 allocated to BOM 1	0.50
Fraction of AOM 2 allocated to BOM 2	0.00

Table 10-13 continued

Fertilization Date	88 04 15
Application Method - Surface Broadcasting	1
Type of Fertilizer - Pig Slurry	10
Applied Amount [kg/ha] wet weigth	28600.0
Dry Matter, per cent of wet weight	7.64
C content, per cent of dry matter	45.00
N content, per cent of dry matter	7.03
NH_4-N cont. per cent of N content	61.80
Number of AOM-pools	2
C-Distribution, pool 1	0.80
C-Distribution, pool 2	0.20
C/N - ratio in pool 1	100.0
Turnover rate coefficient, pool 1	5.0E-3
Turnover rate coefficient, pool 2	5.0E-2
Number of Biomass pools	2
Fraction of AOM 1 allocated to BOM 1	0.50
Fraction of AOM 2 allocated to BOM 2	0.00

Table 10-14 Example of a file containing parameters and values to initiate pools of organic matter in soil.

Profile identification : ASKOV 1987-89 PLOT 8	
SOM-Pools	Nsom 2
Partitioning of C between organic pools	
SOM-Pool 1 (slowly decomposable material)	0.80
SOM-Pool 2 (easily decomposable material)	0.20
C/N ratios of organic pools	
SOM-Pool 1 (slowly decomposable material)	11.0
Turnover rate coefficients [d**-1]	
SOM-Pool 1 (slowly decomposable material)	2.7E-6
SOM-Pool 2 (easily decomposable material)	1.4E-4
Transfer Constants	
SOM-Pool 2 to SOM-Pool 1	0.10
Microbial Biomass	
Per cent of total soil C (SOM) in BioA	0.45
C/N ratios of BioA	6.0
Turnover rate coefficient of BioA [d**-1]	1.0E-3
Per cent of total soil C (SOM) in BioB	0.15
C/N ratios of BioB	10.0
Turnover rate coefficient of BioB [d**-1]	1.0E-2
Transfer to SOM-Pool 2, Decomposition of Biomass	0.40
Efficiency, utilizing organic matter	0.60
Maintenance respiration [10 °C, optimum water]	0.01
Immobilization rate coefficient, NH_4 [d**-1]	5.0E-1
Immobilization rate coefficient, NO_3 [d**-1]	5.0E-1

Table 10-14 continued

SOM & Biomass initialization	
Number of soil layers (initialization)	6
Depth of layer 1 [m]	0.20
C-content in layer 1 [%]	1.40
C/N in layer 1	11.0
Depth of layer 2 [m]	0.20
C-content in layer 2 [%]	1.09
C/N in layer 2	11.0
Depth of layer 3 [m]	0.20
C-content in layer 3 [%]	0.53
C/N in layer 3	11.0
Depth of layer 4 [m]	0.20
C-content in layer 4 [%]	0.23
C/N in layer 4	11.0
Depth of layer 5 [m]	0.20
C-content in layer 5 [%]	0.14
C/N in layer 5	11.0
Depth of layer 6 [m]	0.30
C-content in layer 6 [%]	0.01
C/N in layer 6	11.0

ROM initialization	
Number of different root residuals present in the field	1
Root type number = Crop model type number	2
Root depth [m]	0.90
Root distribution parameter	0.07
Root dry matter [t DM/ha]	0.80
C-Per cent in root dry matter	46.0
Partitioning of C between organic pools	
ROM-Pool 1 (slowly decomposable material)	1.00
ROM-Pool 2 (easily decomposable material)	0.00
C/N ratios of organic pools	
ROM-Pool 1 (slowly decomposable material)	100.0
ROM-Pool 2 (easily decomposable material)	12.0
Turnover rate coefficients [d** -1]	
SOM-Pool 1 (slowly decomposable material)	7.0E-3
SOM-Pool 2 (easily decomposable material)	7.0E-2
Partitioning constants	
ROM-Pool 1 to BioA	0.50
ROM-Pool 2 to BioA	0.50

Table 10-14 continued

AOM initialization		
Number of different type of AOM material present in the field	0	1
Partitioning of C between organic pools		
AOM-Pool 1 (slowly decomposable material)		0.80
AOM-Pool 2 (easily decomposable material)		0.20
C/N ratios of organic pools		
AOM-Pool 1 (slowly decomposable material)		90.0
AOM-Pool 2 (easily decomposable material)		15.0
Turnover rate coefficients [d**-1]		
SOM-Pool 1 (slowly decomposable material)		7.0E-3
SOM-Pool 2 (easily decomposable material)		7.0E-2
Partitioning constants		
AOM-Pool 1 to BioA		0.50
AOM-Pool 2 to BioA		0.50
Number of soil layers (initialization)		2
Depth of layer 1 [m]		0.10
C-content in layer 1 [kg C/ha]		500.0
Depth of layer 2 [m]		0.10
C-content in layer 2 [kg C/ha]		1500.0

Table 10-15 Example of file containing parameters and values to initiate inorganic nitrogen in soil.

Inorganic Nitrogen Profile : ASKOV 1987		
Number of horizons in profile		3
Nitrification Parameter		
1st order rate constant at 10 degrees C [d-1]	1.0E-01	
Denitrification Parameters		
Transport Rate Coefficient (Transport to microsites) [d-1]		1.0E-01
Specific anaerobic denitrification [g Gas-N/g CO_2-C]		0.10
Characterization of the porous medium		
Impedance Factor Parameters { f = b*(Theta-a) }		
Horizon 1 - Impedance Factor Parameter a :		0.10
- Impedance Factor Parameter b :		2.20
Horizon 2 - Impedance Factor Parameter a :		0.10
- Impedance Factor Parameter b :		2.00
Horizon 3 - Impedance Factor Parameter a :		0.10
- Impedance Factor Parameter b :		2.00
Longitudinal Dispersivity - Horizon 1 [cm]		4.0
Longitudinal Dispersivity - Horizon 2 [cm]		4.0
Longitudinal Dispersivity - Horizon 3 [cm]		4.0

Table 10-15 continued

NH_4 adsorption isoterm		
Planer Sites		
Maximum specific adsorption	[m.e./g of clay]	0.4258
Half saturation constant	[mol/l]	4.5E-3
Edge Sites		
Maximum specific adsorption	[m.e./g of clay]	0.022
Half saturation constant	[mol/l]	9.8E-4

Initialization of Soil Mineral N Content		
Initialization Date		87.04.13
Number of initialization compartments		6
Compartment 1	- Size [m]	0.10
	- NH_4 Content [g/m^3]	1.80
	- NO_3 Content [g/m^3]	1.90
Compartment 2	- Size [m]	0.10
	- NH_4 Content [g/m$_3$]	3.00
	- NO_3 Content [g/m^3]	4.50
Compartment 3	- Size [m]	0.20
	- NH_4 Content [g/m^3]	1.70
	- NO_3 Content [g/m^3]	3.40
Compartment 4	- Size [m]	0.20
	- NH_4 Content [g/m^3]	0.50
	- NO_3 Content [g/m^3]	2.65
Compartment 5	- Size [m]	0.20
	- NH_4 Content [g/m^3]	0.15
	- NO_3 Content [g/m^3]	2.50
Compartment 6	- Size [m]	1.20
	- NH_4 Content [g/m^3]	0.20
	- NO_3 Content [g/m^3]	2.70

Atmospheric Deposition Parameters	
NH_4 "concentration in precipitation" [ppm]	2.00
NH_4 "dry deposition" [kg/ha/d]	0.015
NO_3 "concentration in precipitation" [ppm]	1.50
NO_3 "dry deposition" [kg/ha/d]	0.005

Control Parameters	
Leaching Depth [m]	1.00

11. MODEL VALIDATION

11.1 Introduction

Validation

Validation of a model is the process by which the behaviour of the model is compared with that of the real system, i.e. modelled and real phenomena of the system are compared. If the behaviour of the model matches qualitatively with that of the real system a quantitative comparison and the predictive performance of the model is to be made.

Repeatable systems

It is realized that only models of systems that are repeatable or recur can be validated. Only then may the model be derived from the analysis of some systems and validated on others. Repeatable systems can always be analyzed by experimentation, but recurring systems sometimes only by observations. Models of unique systems are concepts that cannot be validated experimentally but only more or less verified by observations of the behaviour of the real system over time. They remain therefore speculative models.

Overall performance

Considering the present comprehensive model developed for transformation and transport processes involving heat, water, carbon, and nitrogen in the soil plant system it is obvious that within the framework of the present research project it has not been possible to perform a throughout validation of the model. Thus emphasis has been placed on validation regarding the overall performance of the model for some major processes in systems for which independent comprehensive esperimental data have been available.

11.2 Characterization and initialization of system

Experimental data

Validation of the model has been performed by using experimental data obtained from field experiments described by Lind et al. (1990). Thus in the present context only necessary information regarding characterization and initialization of the various systems for running the simulation model are briefly described.

Soil types

Two soil types were considered viz. Jyndevad which is a Coarse Sand and Askov which is a Sandy Loam. Spring barley was grown in 1987 and 1988 at various fertilizer treatments including application of inorganic fertilizers as well as pig slurry. The plots considered are listed in Table 11-1. Pig slurry was applied at a rate corresponding to an application rate of approximately 100 kg N ha^{-1} as ammonium. The application rate of nitrogen in mineral fertilizer was approximately 120 and 133 kg N ha^{-1} to Jyndevad and Askov soil, respectively, in the form of equal amounts of ammonium and nitrate nitrogen.

Table 11-1 Field experimental plots considered for model validation.

Soil	Jyndevad	Askov
No fertilizer	Plot 6	Plot 1
Pig slurry, autumn[1)]	Plot 5	-
Pig slurry, autumn	Plot 4	-
Pig slurry, spring	Plot 3	Plot 4
Pig slury, spring[2)]	Plot 2	-
Mineral fertilizer	Plot 1	Plot 8

1) With undersown catch crop; 2) Half application rate

Retention curves

Soil water retention curves were established from experimental data using the method described in chapter 4. The results are shown in Fig. 11-1 and Fig. 11-2.

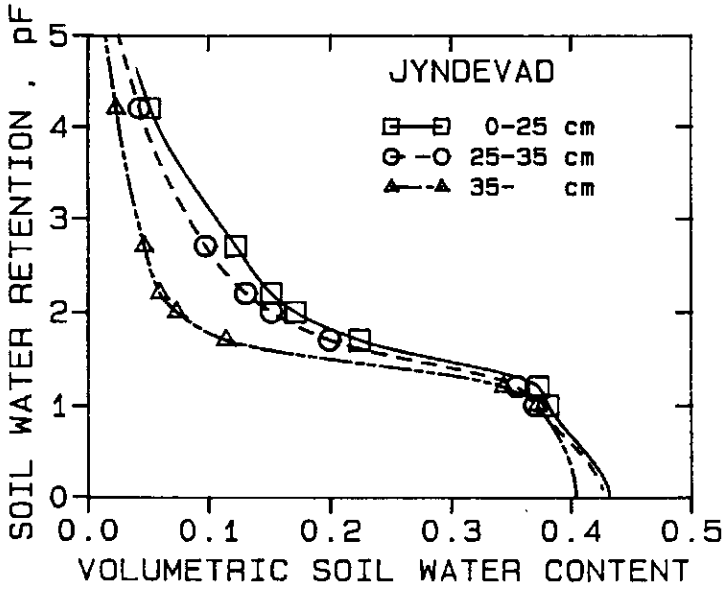

Fig. 11-1 Retention curves for Jyndevad soil.

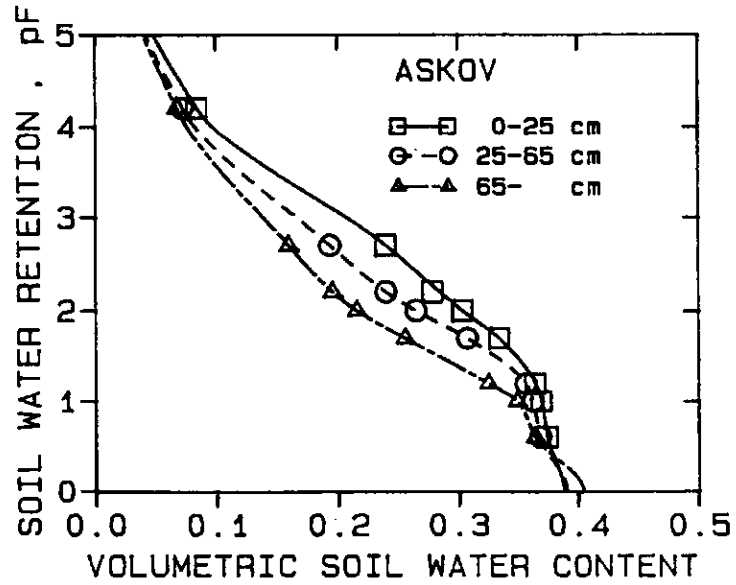

Fig. 11-2 Retention curves for Askov soil.

Hydraulic conductivity

In a similar way hydraulic conductivity functions were established from experimental data. The results are shown in Fig. 11-3 and Fig. 11-4, respectively. Regarding soil water content initial values were derived from the first set of measurements.

Nitrogen parameters

Parameters used for inorganic nitrogen in soil were as listed in Table 10-15 except for the impedans factor, parameter a, which was assumed to be 0.04 and 0.10 for Jyndevad and Askov soil, respectively. Regarding content of inorganic nitrogen initial values were derived from the first set of measurements.

Crop parameters

Parameters used for crop and residual plant material were as listed in Table 10-14. Thermal properties of the soils were calculated according to the methods described in chapter 5. Initial values of soil temperature were derived from a forced sinusidal variation.

Organic matter pools

The initialization of pools of organic matter in soil was based on experimental values of total content of carbon which was allocated as SOM 1 and SOM 2 by using coefficients shown in Table 10-14. Per cent of total C allocated to BOM 1 and BOM 2 was assumed to be 0.30 and 0.05, respectively, which resulted in a stable biomass. The initial value of AOM 1 was assumed to be 370 kg C ha^{-1} with C/N = 100, consisting of root residues from previous crop, while the initial value of AOM 2 was assumed to be zero.

Pig slurry

The characterization of pig slurry was based on experimental data available regarding applied amounts, dry matter content, carbon content in dry matter, total nitrogen content of dry matter, and per cent nitrogen as ammonium. The additional parameters used for the pig slurry were as listed in Table 10-13.

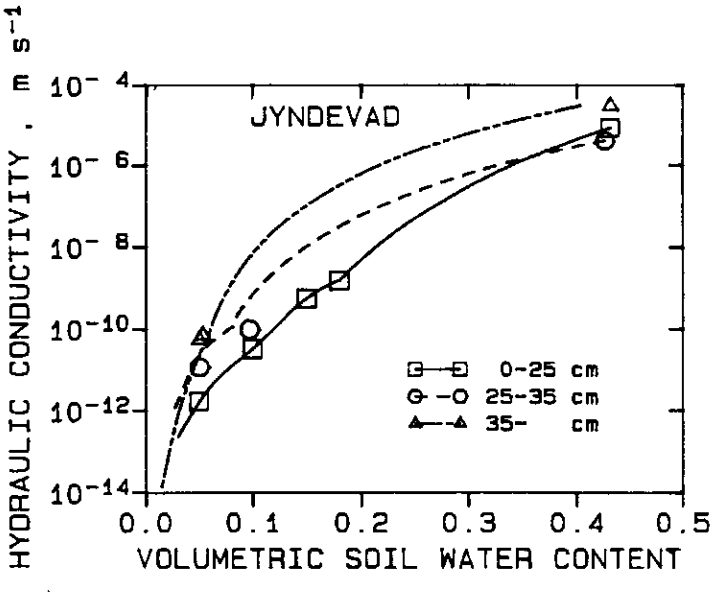

Fig. 11-3 Hydraulic conductivity functions for Jyndevad soil.

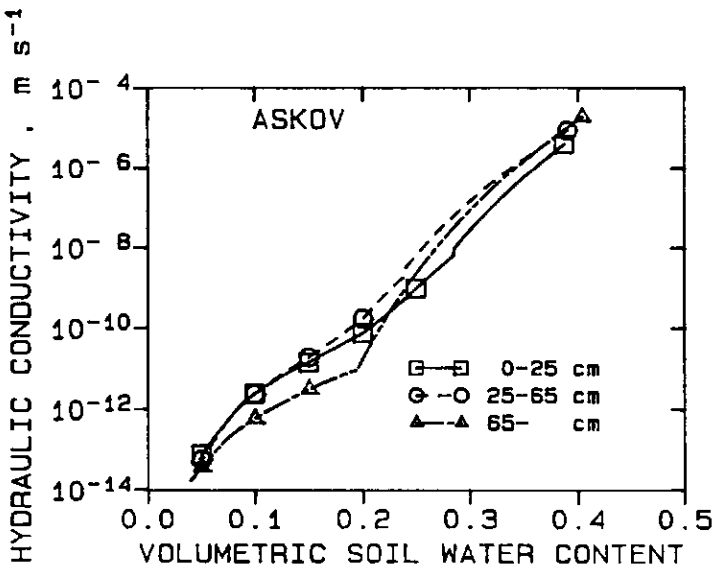

Fig. 11-4 Hydraulic conductivity functions for Askov soil.

11.3 Simulated and experimental results

The field experimental plots considered for model validation are listed in Table 11 – 1. Experimental data on soil water content, soil content of nitrate nitrogen, soil content of ammonium nitrogen, crop yield, nitrogen uptake in crop top dry matter, and leaching for 1987 and 1988, and denitrification for Askov soil in 1988 were available for model validation (Lind et al. 1990).

Soil water profiles

Measured and simulated examples of soil water content profiles are shown in Fig. 11 – 5 for Jyndevad and Askov soil. Qualitatively the agreement between measured and simulated soil water content is satisfactory for both soils. Furthermore quantitatively the agreement is satisfactory for both soils, except for the 20 – 30 cm soil layer in the case of Jyndevad soil where the simulated values in general are greater than the measured values of soil water content.

Regarding soil water retention and hydraulic conductivity big spatial variability is known to exist in the Jyndevad soil (Hansen et al., 1986) as well as in the Askov soil (Lind et al., 1990). For such soils a particular sampling scheme is required in order to establish representative hydraulic functions as well as representative measurements of soil water content profiles.

Soil water balance

Simulated soil water balances of Jyndevad soil (0 – 85 cm) and Askov soil (0 – 95 cm) profiles are shown in Table 11 – 2. The two locations are situated in areas generally rich in annual precipitation. Thus the precipitation is relatively high for both locations in both simulation periods considered, resulting in high values of percolation.

It is noted that in all cases the evapotranspiration is close to the potential evapotranspiration, indicating that crop production presumably has been unlimited by soil water except for short periods in the growth season.

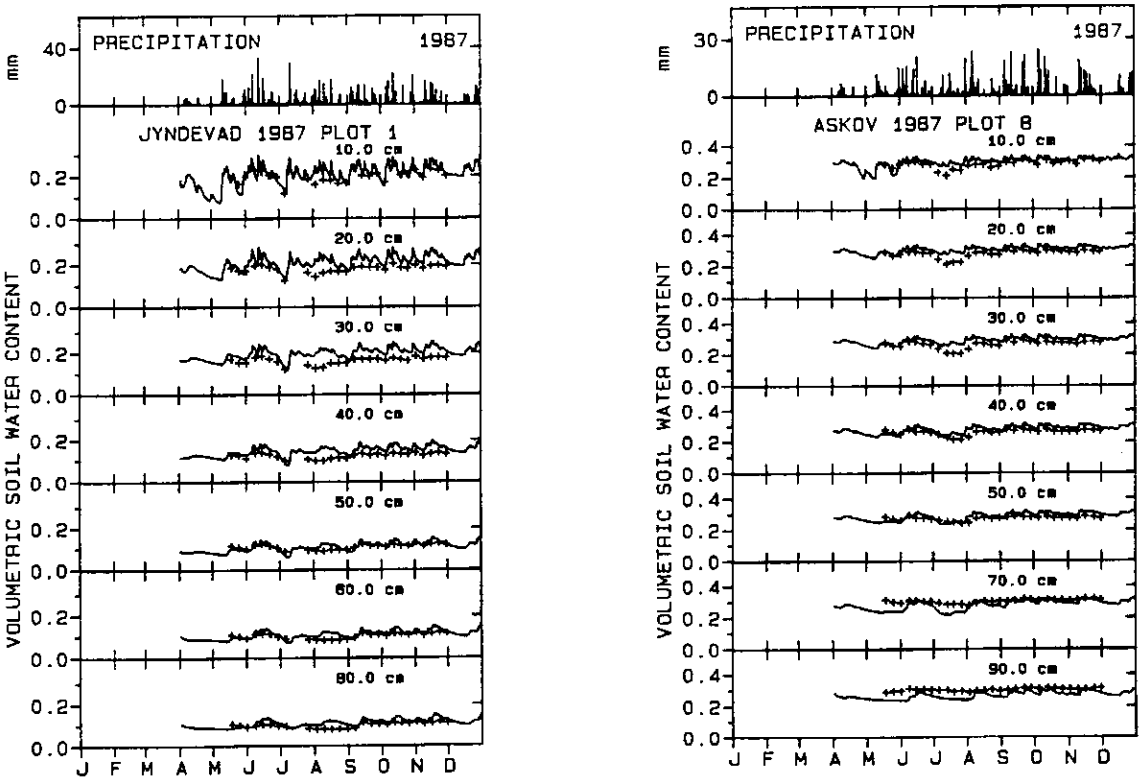

Fig. 11-5 Measured and simulated profiles of soil water content.

Table 11-2 Measured precipitation and simulatd evapotranspiration, percolation and change of soil water storage, mm.

Period	1987-04-01 - 1988-03-31		1988-04-01 - 1989-03-31	
Location	Jyndevad	Askov	Jyndevad	Askov
Precipitation[1]	1262[2]	1189	1027[3]	1109
Evapotranspiration	448	435	555	540
Percolation	780	717	500	591
Soil water storage	34	37	-28	-22
Pot. evapotranspiration	465	473	571	573

1) Corrected to soil surface according to Allerup and Madsen (1979).

2) Incl. 23 mm applied by irrigation.

3) Incl. 30 mm applied by irrigation.

Nitrate profiles

Measured and simulated examples of profiles of nitrate nitrogen concentrations in the soil are shown in Fig. 11-6 for Jyndevad soil plot 1, and for Askov soil plot 8. The measured nitrate nitrogen concentrations were obtained by analyzing soil samples.

The simulated profiles of nitrate nitrogen concentrations show characteristic peaks occurring in the upper soil layer as a consequense of fertilizer application or high rates of net mineralization. The concentration peaks are recognized to deeper soil layers with some phase displacement as compared to the upper soil layers. Furthermore, considering the lower soil layers, the peak values are smaller and less distinct. Thus the general pattern of the simulated profiles of nitrate nitrogen concentrations indicates that some downward movement of nitrate nitrogen has taken place even during the growth season. This is due to high values of net precipitation which occurred also in part of the growth season.

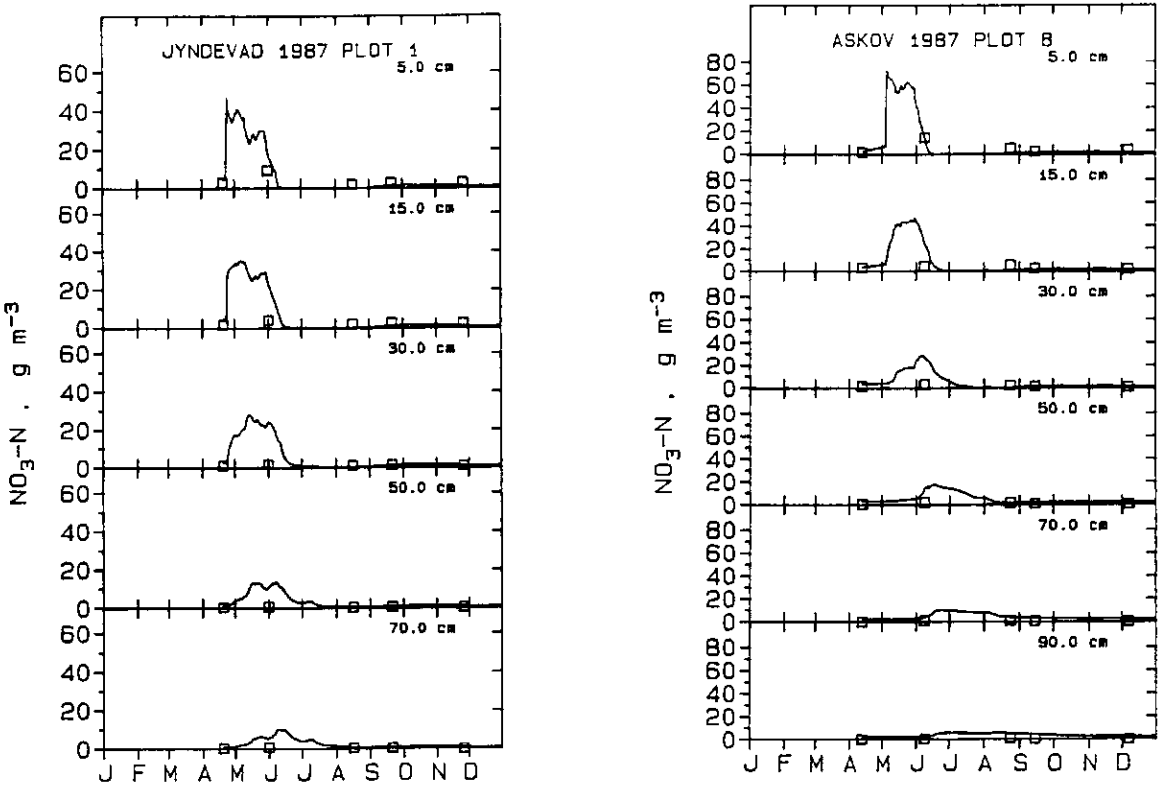

Fig. 11-6 Measured and simulated profiles of nitrate nitrogen in soil; plots receiving mineral fertilizer.

When comparing the measured and simulated nitrate nitrogen concentrations, unfortunately no experimental data cover periods with relatively high concentration values, i.e. periods immediatly after fertilizer application and periods with high rates of net mineralization. However, the level of simulated concentrations in these periods seems reasonable when compared to experimental data obtained in other experiments under comparable conditions (Nørlund et al., 1985; Schjørring et al. 1988a, 1988b; Nielsen and Jensen, 1990). Regarding lower levels of nitrate nitrogen concentrations the qualitative as well as the quantitative agreement between measured and simulated values appears to be quite satisfactory in most cases.

Measured and simulated values of nitrate nitrogen concentration in soil water at 80 and 100 cm soil depth at Jyndevad and Askov, respectively, are shown in Fig. 11 – 7 for all plots listed in Table 11 – 1. The measured nitrate nitrogen concentrations were obtained by analyzing soil water samples obtained from ceramic cups installed in the soil.

In general the temporal variation of measured and simulated values of the nitrate nitrogen concentration is much bigger at Jyndevad than at Askov which may be ascribed mainly to differences in hydraulic properties of the soils.

It appears that satisfactory qualitative and quantitative agreement between measured and simulated values of the nitrate nitrogen concentration in soil water has been obtained for the Askov soil and in most cases also for the Jyndevad soil. However, in the case of Jyndevad plot 1 in particular, which received mineral nitrogen fertilizer, big differences were observed in 1987.

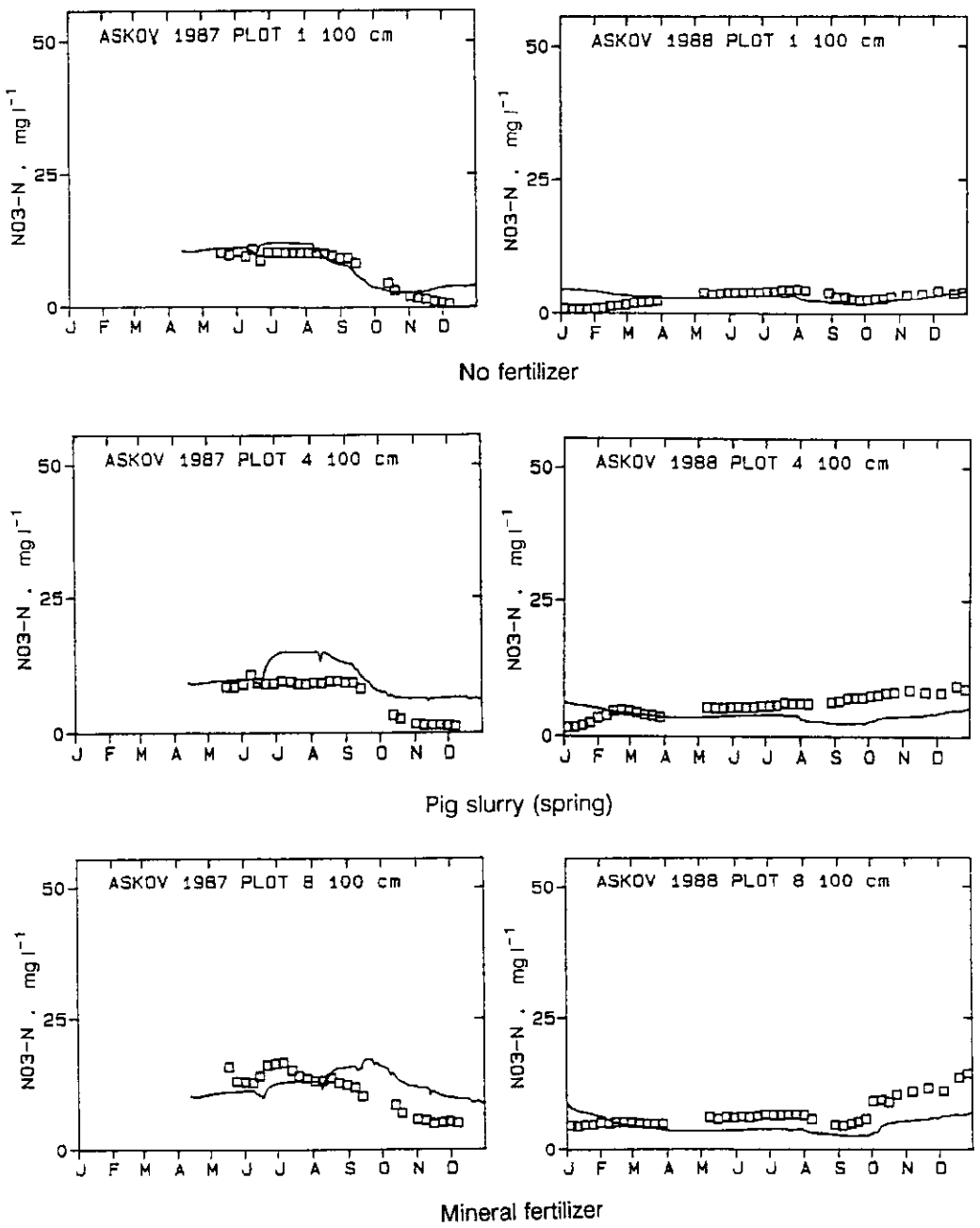

Fig. 11-7 Measured and simulated values of nitrate nitrogen concentration in soil solution.

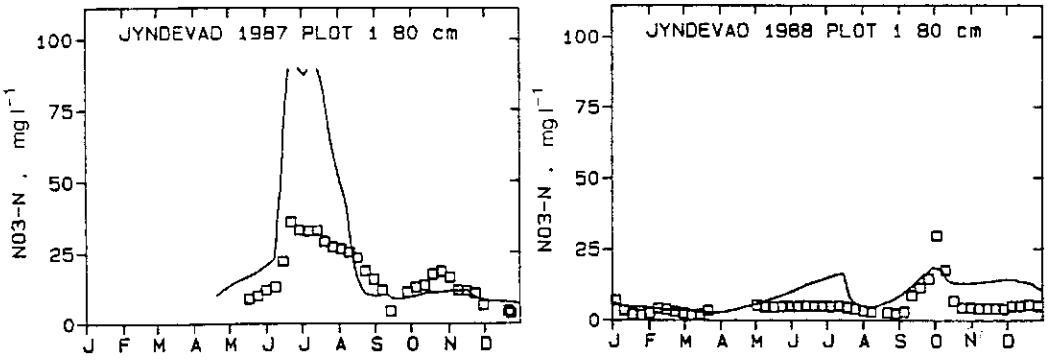

Mineral fertilizer

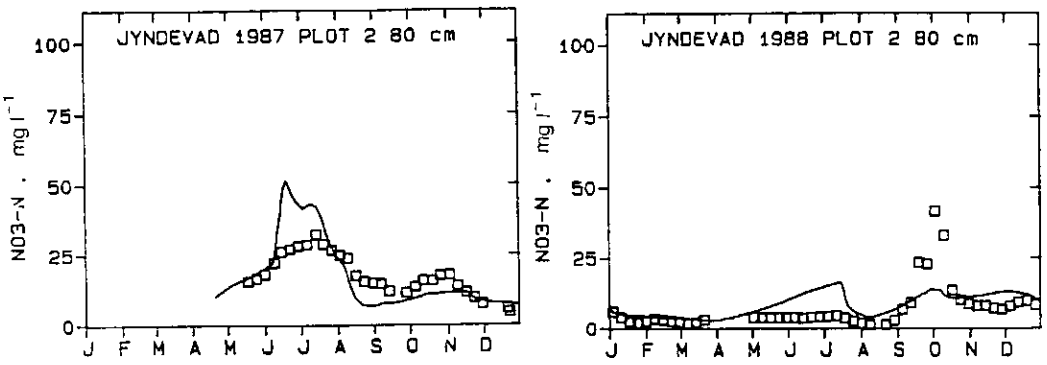

Pig slurry (spring), half application rate

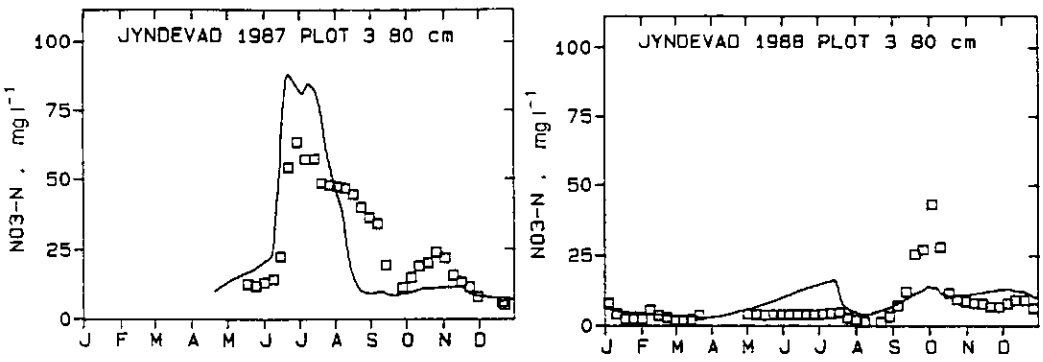

Pig slurry (spring)

Fig. 11–7 Continued.

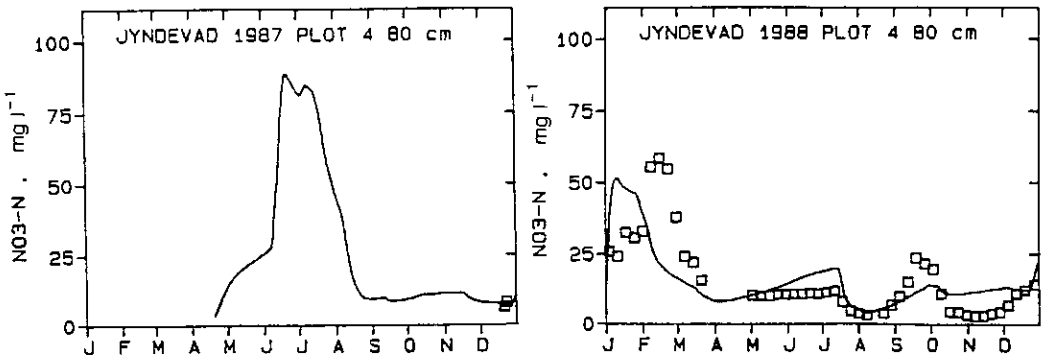

Pig slurry (autumn)

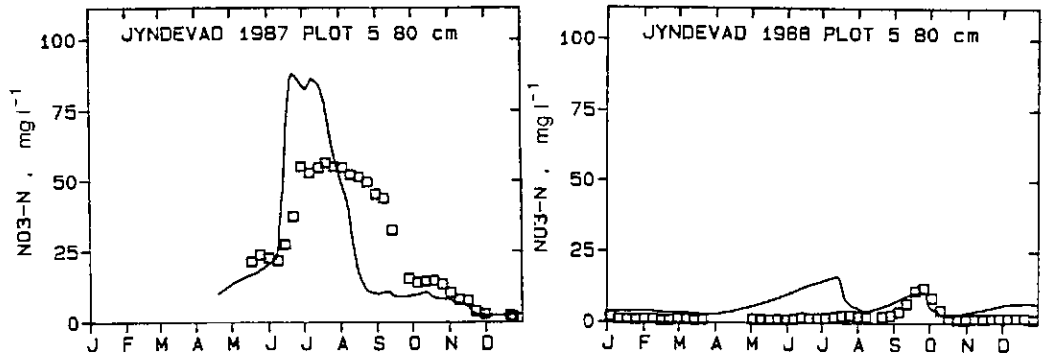

Pig slurry (autumn), catch crop

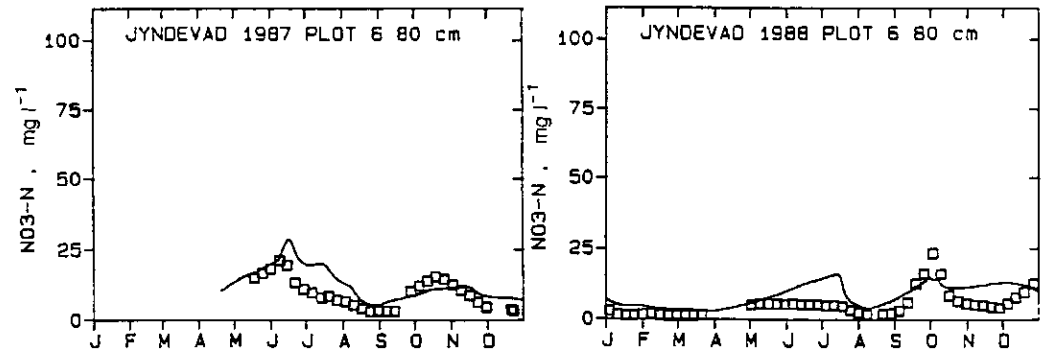

No fertilizer

Fig. 11 – 7 Continued.

It is noted that the relatively big differences between simulated and measured values of the nitrate nitrogen concentrations occur in situations in which nitrogen fertilizer application is followed by a period with high values of percolation. Schjørring et al. (1988) reported that some of the fertilizer nitrogen disappeared from the soil solution shortly after fertilizer application, and reappeared later on in the growth season. This may be explained by a quasi-equilibrium between soil solution and microbial biomass with respect to ammonium, as suggested by Nielsen et al. (1988), which is not taken into account in the present model. At high concentrations of ammonium in the soil solution the simulated nitrification is expected to be overestimated due to detrimental effects by the ammonium on the microbial biomass.

These effects may partly explain the too high values of simulated nitrate nitrogen concentration in periods after nitrogen fertilizer application.

Ammonium profiles

Measured and simulated examples of profiles of ammonium nitrogen concentrations in the soil are shown in Fig. 11-8 for Jyndevad soil plot 6 and Askov soil plot 8. The measured ammonium nitrogen concentrations were obtained by analyzing soil samples.

The simulated profiles of ammonium nitrogen concentrations show distinct peaks in the uppermost soil layer (5 cm depth) in all plots receiving ammonium fertilizer or pig slurry. The peaks appear immediately after application of fertilizer and pig slurry, respectively. In the case of application of pig slurry the concentration peaks were recognized to 15 cm soil depth in the Jyndevad soil, whereas in the Askov soil no concentration peaks were simulated in that soil depth. It appears that the ammonium applied was nitrified within a short period of time after which the ammonium nitrogen concentrations in the upper soil layers were quite low and similar to the concentrations in the lower soil layers.

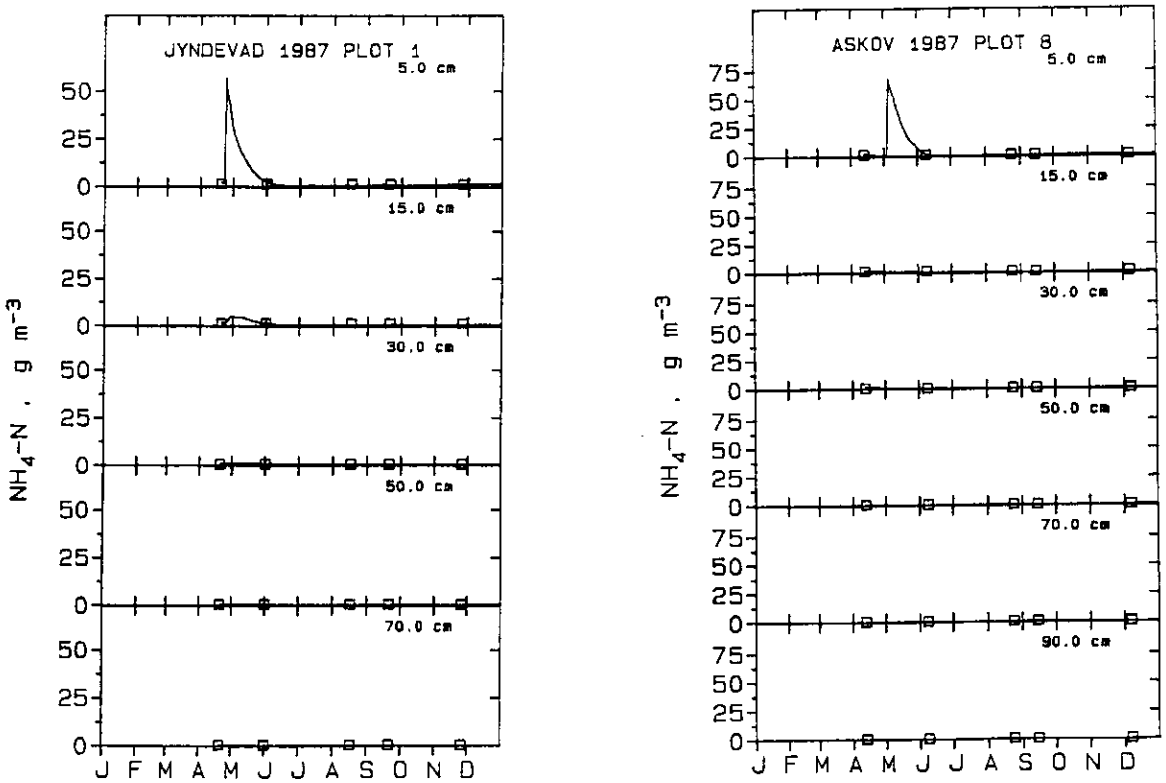

Fig. 11-8 Measured and simulated profiles of ammonium nitrogen concentration in soil; plots receiving mineral fertilizer.

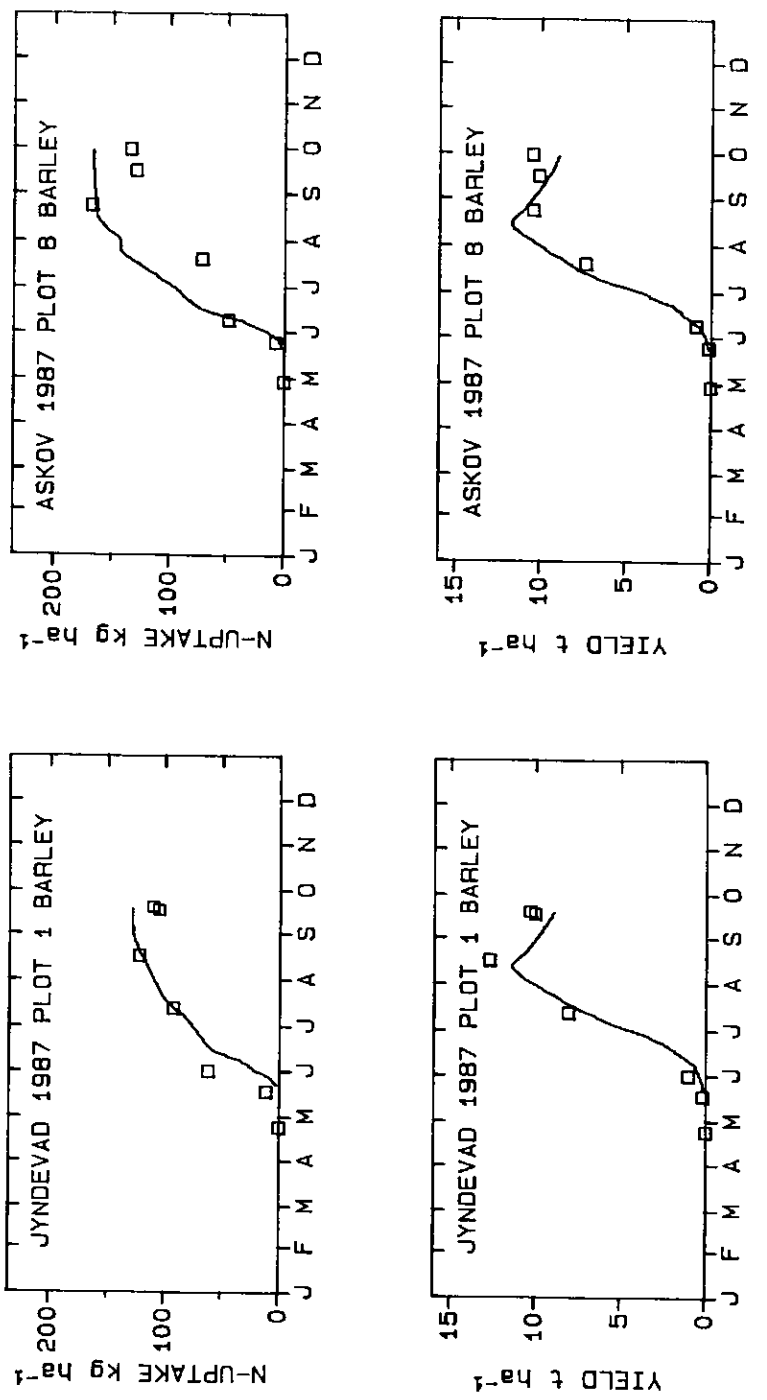

Fig. 11-9 Measured and simulated courses of crop yield and nitrogen uptake; plots receiving mineral fertilizer.

As in the case of profiles of nitrate nitrogen concentrations no experimental data cover periods with relatively high values of ammonium nitrogen concentrations, which in fact have occurred as a result of application of ammmonium nitrogen. Regarding lower levels of ammonium nitrogen concentrations which occurred most of the time the qualitative as well as the quantitative agreement between measured and simulated values appears to be quite satisfactory in most cases.

Nitrogen uptake

Measured and simulated examples of courses of nitrogen uptake by crop and crop yield are shown in Fig. 11 – 9 for Jyndevad soil plot 1 and for Askov soil plot 8.

The qualitative as well as the quantitative agreement between measured and simulated values appears to be reasonable in most cases in 1988.

Crop yield

Considering the growth season 1988 the agreement was exellent for Jyndevad soil plot 6. However, for the other plots considered the simulated values were in general somewhat greater than the measured values of nitrogen uptake and crop yield. The measured values of nitrogen uptake and crop yield were less in 1988 as compared to 1987. Furthermore, the values for Askov were less than those for Jyndevad. Probably factors other than water and nitrogen may have been limiting crop growth in particular at Askov resulting in differences between simulated and measured values of nitrogen uptake and crop yield.

Considering in particular the case of application of pig slurry, the agreement between measured and simulated values was satisfactory in 1987, whereas in 1988 some differences occur in particular in the case of Askov soil plot 4. For both locations the simulated values of nitrogen uptake and crop yield were greater than the corresponding experimental values.

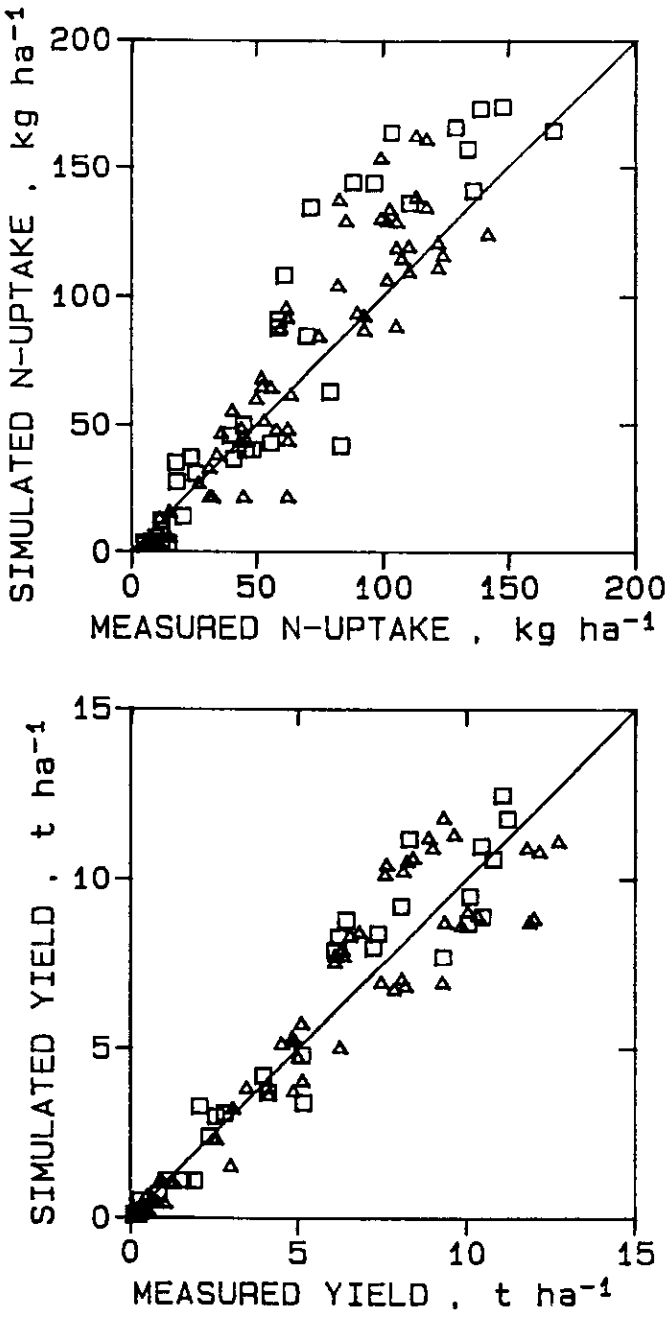

Fig. 11 – 10 Measured and simulated nitrogen uptake and total dry matter yield in spring barley. Jyndevad: Δ; Askov: □.

As the pig slurry was applied in spring some loss of ammonia is likely to have occurred resulting in a smaller real fertilizer input than that assumed in the simulation.

Furthermore, in the case of Jyndevad the pig slurry was incorporated in the soil by ploughing immediately after the application, whereas in the case of Askov the pig slurry was incorporated in the soil by harrowing and disc ploughing in 1987 and 1988, respectively, which was performed some hours after the application (Lind et al., 1990). It is likely that the loss of ammonia has been much bigger at Askov than at Jyndevad, particularly in 1988. Thus by reducing the input of ammonia nitrogen by pig slurry used in the simulation for Askov soil plot 4, 1988, the agreement between simulated and measured values of nitrogen uptake and crop yield could be made satisfactory.

In Fig. 11 – 10 all measured values of nitrogen uptake and crop yield are plotted against the corresponding simulated values. In the case of crop yield the data are evenly distributed relatively close around the 1:1 line.

In the case on nitrogen uptake the data points are more scattered and in some cases showing relatively big differences between measured and simulated values.

These differences may be real and indicate weaknesses in the model, e.g. regarding distribution of nitrogen between top dry matter and root dry matter. However, it should be noted that the experimental data for the most part are based on harvest of very small subplots, less than one square meter, the results of which then are transformed to one hectar. This may imply relatively great uncertainties in the final result.

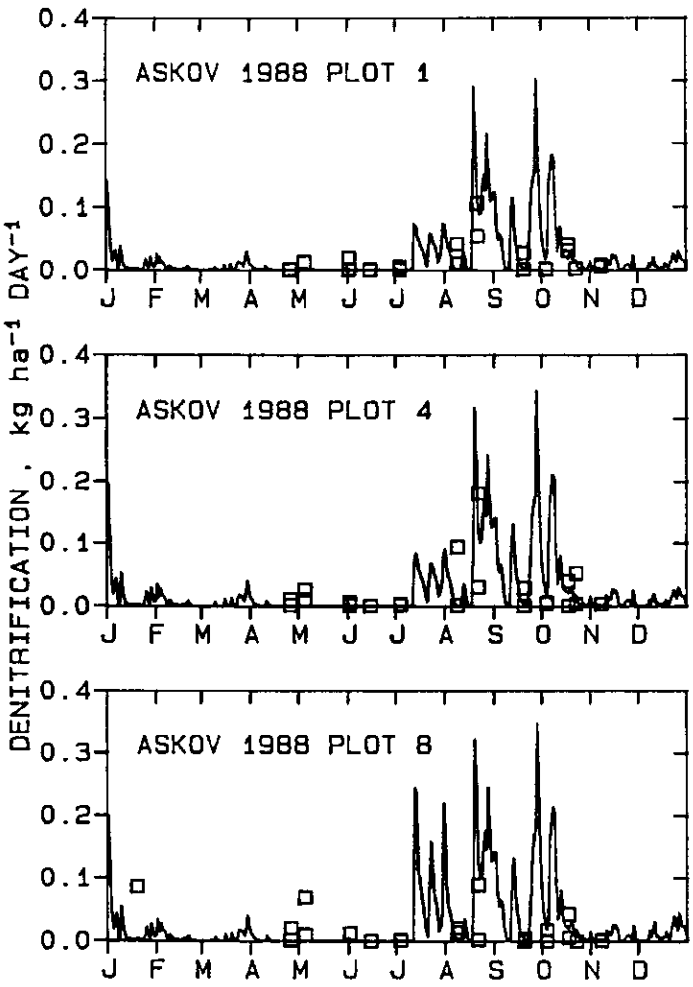

Fig. 11 – 11 Measured and simulated denitrification rate.

Denitrification

Measured and simulated values of denitrification during 1988 are shown in Fig. 11-11 for Askov soil plots 1, 4, and 8. Considering simulated denitrification the values are quite small during most of the year. During the periods January - March and April - July the simulated denitrification most probably was limited due to soil temperature and soil aeration conditions, respectively. However, during the period from medio July to medio October the level of simulated denitrification increased and several peak values almost coinciding with precipitation events occurred. Thus most of the simulated denitrification took place in a period after harvest during which the soil was rewetting after a relatively dry period stimulating microbial activity in terms of net mineralization from plant residues left at harvest and subsequent denitrification.

From medio October and during the remaining part of the year the simulated denitrification rate was again quite low probably due to low soil temperature. Integration of daily rates of denitrification over the entire year resulted in denitrification values of 7, 8, and 9 kg N ha^{-1} $year^{-1}$ for Askov soil plots 1, 4, and 8, respectively, which are in agreement with corresponding values estimated experimentally by Lind et al. (1990).

In comparing simulated and measured values of denitrification quantitatively the agreement is satisfactory. The order of magnitude of measured and simulated values is similar and within the range of 0-0.4 kg N ha^{-1} day^{-1}. Furthermore, in the period in which simulated denitrification increased also the measured values increased and in some cases peak values of simulated and measured denitrification coincided. In the case of Jyndevad the measured denitrification (Lind et al., 1990) as well as the simulated denitrification was almost zero in all plots considered. Thus based on comparison using the present limited experimental evidence the performance of the model regarding denitrification is considered satisfactory.

Table 11-3 Simulated annual balances of inorganic nitrogen, kg N ha^{-1} $år^{-1}$, for Jyndevad soil plots 1, 3, and 6.

Period	1987-04-01 - 1988-03-31			1988-04-01 - 1989-03-31		
Plot	6	3	1	6	3	1
Fertilizer	0	111	123	0	92	125
Net mineralization	82	81	81	95	95	97
Atm. deposition	22	22	22	19	19	19
Plant uptake	53	122	131	55	147	174
Leaching	66	108	111	55	54	62
Denitrification	0	0	0	0	0	0
Storage	-15	-16	-16	4	5	5

Table 11-4 Simulated annual balances of inorganic nitrogen, kg N ha^{-1} $år^{-1}$, for Jyndevad plots 2,4, and 5.

Period	1987-04-01 - 1988-03-31			1988-04-01 - 1989-03-31		
Plot	5	4	2	5	4	2
Fertilizer	111	215	55	89	101	46
Net mineralization	81	81	81	100	95	94
Atm. deposition	22	22	22	19	19	19
Plant uptake	137	122	92	168	66	101
Leaching	94	201	83	35	124	54
Denitrification	0	0	0	0	0	0
Storage	-17	-5	-17	5	25	4

Table 11-5 Simulated annual balances of inorganic nitrogen, kg N ha^{-1} $år^{-1}$, for Askov soil plots 1, 4, and 8.

Period	1987-04-01 - 1988-03-31			1988-04-01 - 1989-03-31		
Plot	1	4	8	1	4	8
Fertilizer	0	96	133	0	96	133
Net mineralization	49	60	62	59	74	74
Atm. deposition	21	21	21	20	20	20
Plant uptake	55	150	173	46	147	182
Leaching	27	40	59	19	25	29
Denitrification	6	7	7	7	8	9
Storage	-18	-20	-23	7	10	7

Simulated balances of inorganic nitrogen are shown in Table 11-3, Table 11-4, and Table 11-5.

Net mineralization

The simulated net mineralization includes mineralization from crop residues and soil organic matter the latter of which is affected by clay content of the soil. It is noted that the simulated net mineralization is higher for Jyndevad soil than for Askov soil which is due to higher content of soil organic matter and lower content of clay in the Jyndevad soil. The simulated differences in the net mineralization between treatments are caused by differences in nitrogen content of crop residues. The magnitude of the simulated annual net mineralization seems reasonable.

The order of magnitude of simulated annual denitrification was 10 kg N ha^{-1} $year^{-1}$ for Askov soil, whereas for Jyndevad soil the simulated annual denitrification was zero. These results which reflect differences in aeration properties of the soils are in agreement with the experimental results reported by Lind et al. (1990).

The simulated plant uptake of nitrogen was lower for Jyndevad than for the Askov soil which is mainly due to differences in soil water properties of the two soils. Thus as a result of differences in net mineralization, plant uptake of nitrogen, and soil water properties the level of simulated nitrogen leaching was higher at Jyndevad as compared to Askov. Furthermore, the application rate of mineral fertilizer probably was higher than optimum for Jyndevad soil. It is noted that Jyndevad plot 4 received normal application rate of pig slurry in the spring as well as in the autumn 1987. This caused considerable nitrogen leaching, Table 11-4.

Nitrogen leaching

In Fig 11-12 simulated values of nitrogen leaching are plotted against corresponding estimated values of leaching obtained from field experiments (Lind et al., 1990). The symbols used are explained in Table 11-6.

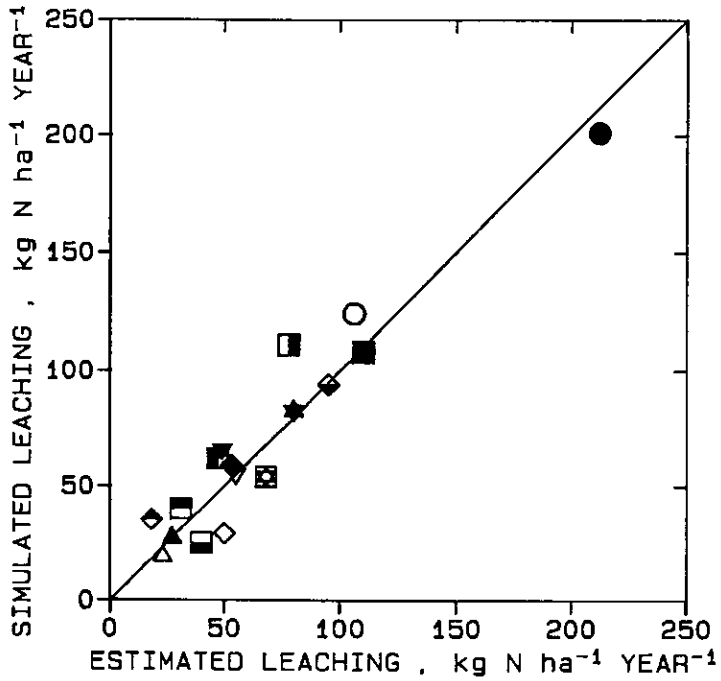

Fig. 11 – 12 Estimated and simulated nitrogen leaching from Jyndevad and Askov soils.

The estimated values of leaching were obtained as accumulated values of the product of estimated water discharge and nitrate nitrogen concentration at the lower boundary of the soil profile considered (Lind et al., 1990). This method is most reliable at low concentration gradients in the soil profile and at low rates of water discharge. Considering Fig. 11 – 12 the agreement between simulated and estimated values of nitrogen leaching is satisfactory in most cases. However, in some cases relatively big differences occur. In the case of Askov soil plot 4 and 8 the estimated values of leaching were somewhat higher than the simulated values of leaching in the second year. These differences were expected as the measured values of plant uptake of nitrogen were less than the simulated values in that particular year for reasons which are previously discussed.

Table 11-6 Symbols used in Fig. 11-12.

Plot	1987-1988	1988-1989
Jyndevad 1	◨	◧
Jyndevad 2	✸	✡
Jyndevad 3	■	□
Jyndevad 4	●	○
Jyndevad 5	◆	◆
Jyndevad 6	▼	▽
Askov 1	▲	△
Askov 4	⬒	⬓
Askov 8	◆	◇

In the case of Jyndevad soil plot 1 the simulated value of leaching was higher than the estimated value in particular in the first year. This difference was accumulated mainly during June 1987 in which period big concentration gradients occurred in the soil profile. During that period the simulated nitrate nitrogen concentration in soil solution most likely was overestimated, Fig 11-7, as previously discussed. For Jyndevad plot 4 which received pig slurry in autumn the simulated value of leaching was also somewhat higher than the value estimated from the field experiment.

For Jyndevad plot 5 which had an undersown catch crop of ryegrass the agreement was excellent in the first year, whereas in the second year the simulated value of leaching was somewhat higher than the value estimated from field experiment. This was probably due to the fact that the simulated amount of dry matter and nitrogen uptake by the catch crop was less than actual measured in the experiment. However, in agreement with the experimental results the simulations clearly demonstrated the reducing effect of the catch crop on the nitrogen leaching.

The present model validation has included experimental data from one main crop grown on two soil types in two years at various rates of application of mineral fertilizer and pig slurry. The simulated and experimentally determined data have included soil water content, concentration of nitrate nitrogen in soil, concentration of ammonium nitrogen in soil, crop yield, nitrogen harvested in crop top dry matter, denitrification, and leaching of nitrogen from soil.

Based on the present validation it can be concluded that basicly the overall performance of the model is satisfactory, although some minor adjustments may prove to be necessary. Before extensive predictive application of the model further validation including data from other combinations of soil, crop, climate, and management would be usefull.

12. MODEL APPLICATION

12.1 Introduction

Model application

The potential areas of application of the present soil plant system model are numerous. In general the simulation model can be used to explore and predict how various system management practices and strategies will affect the course and outcome of various processes in the system in particular transformation and transport processes involving water, heat, carbon, and nitrogen.

More specifically the model can be used to simulate the effect of various crop systems, and various irrigation and fertilization strategies, and management operations including soil tillage and crop residue management, on crop production and the dynamics of carbon and nitrogen in the soil including loss of nitrogen by leaching processes.

Application example

In the present chapter an example of model application is given in the form of results of simulation of effects of straw incorporation in soil during twenty consecutive years of barley crop production as compared to removal of straw from the field. Two soil types and three levels of nitrogen fertilizer application were considered, viz. JB 1 (Coarse Sand) and JB 6 (Sandy Loam) corresponding to the two soil types Jyndevad and Askov, respectively, previously considered for model validation, while levels of annual fertilization considered were 60, 90, and 120 kg N ha^{-1}, respectively.

Characterization of the system including model parameters were as in the case of model validation except hydraulic functions for JB 6 , which were taken from Hansen et al. (1986). The period considered was 1966 - 1986 for which driving variables measured at Askov were kindly provided by Olesen (1990).

12.2 Simulated results

Dry matter production

Simulated annual values of total dry matter production are illustrated in Fig. 12–1. In the case of the JB 6 soil only small variations in dry matter production from year to year occur, which is a consequence of a relatively high content of available water in that soil making the crop less dependent on precipitation. On the other hand the JB 1 soil has only a small content of available water making the crop very dependent on precipitation and resulting in a big variation in dry matter production from year to year due mainly to limited water supply in several of the years considered.

The increase in dry matter production was higher between annual application of 60 and 90 kg N ha^{-1} than between application of 90 and 120 kg N ha^{-1} indicating a nitrogen deficiency in the barley crop in particular at application of 60 kg N ha^{-1}. In the JB 6 soil straw incorporation reduced dry matter production the first year at the application of 60 and 90 kg N ha^{-1}, whereas in most other cases straw incorporation in soil increased the dry matter production.

Added organic matter

The most frequently simulated values of the annual amounts of dry matter and nitrogen in crop residues added to the soil during twenty years are shown in Table 12–1.

Added nitrogen

The annual amounts of dry matter and nitrogen in roots and stubble added to the soil in the cases of straw being removed from the field were 1.1–1.5 t DM ha^{-1} and 10–14 kg N ha^{-1} respectively, whereas the annual amounts of dry matter and nitrogen in straw, roots and stubble added to the soil in the case of straw incorporation in soil were 4.5–7.3 t DM ha^{-1} and 39–70 kg N ha^{-1} respectively.

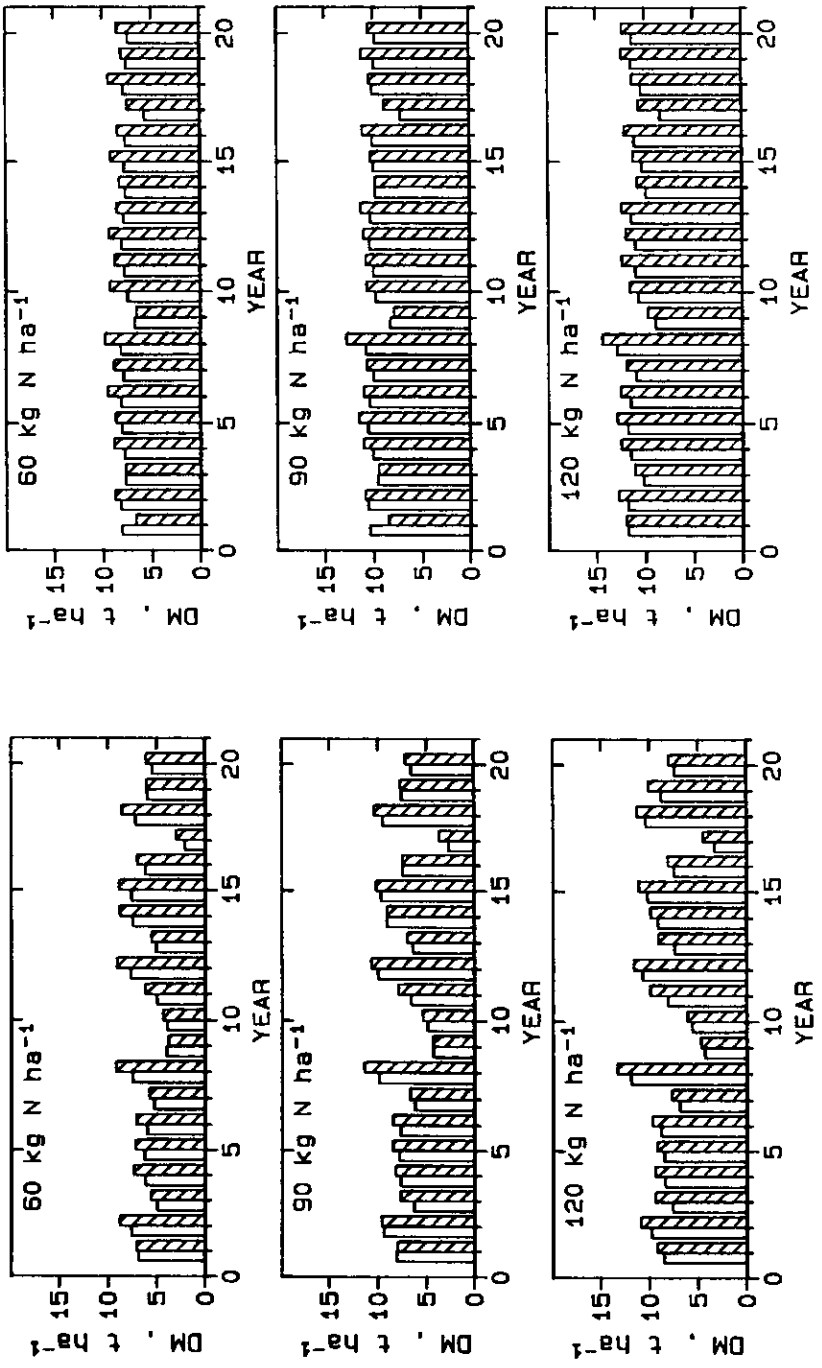

Fig. 12–1 Simulated annual values of dry matter production during twenty consecutive years of barley crop production in Jyndevad soil (left) and Askov soil (right). Straw incorporated (hatched columns), straw removed (open columns). Simulation period 1966–1986, Askov climate.

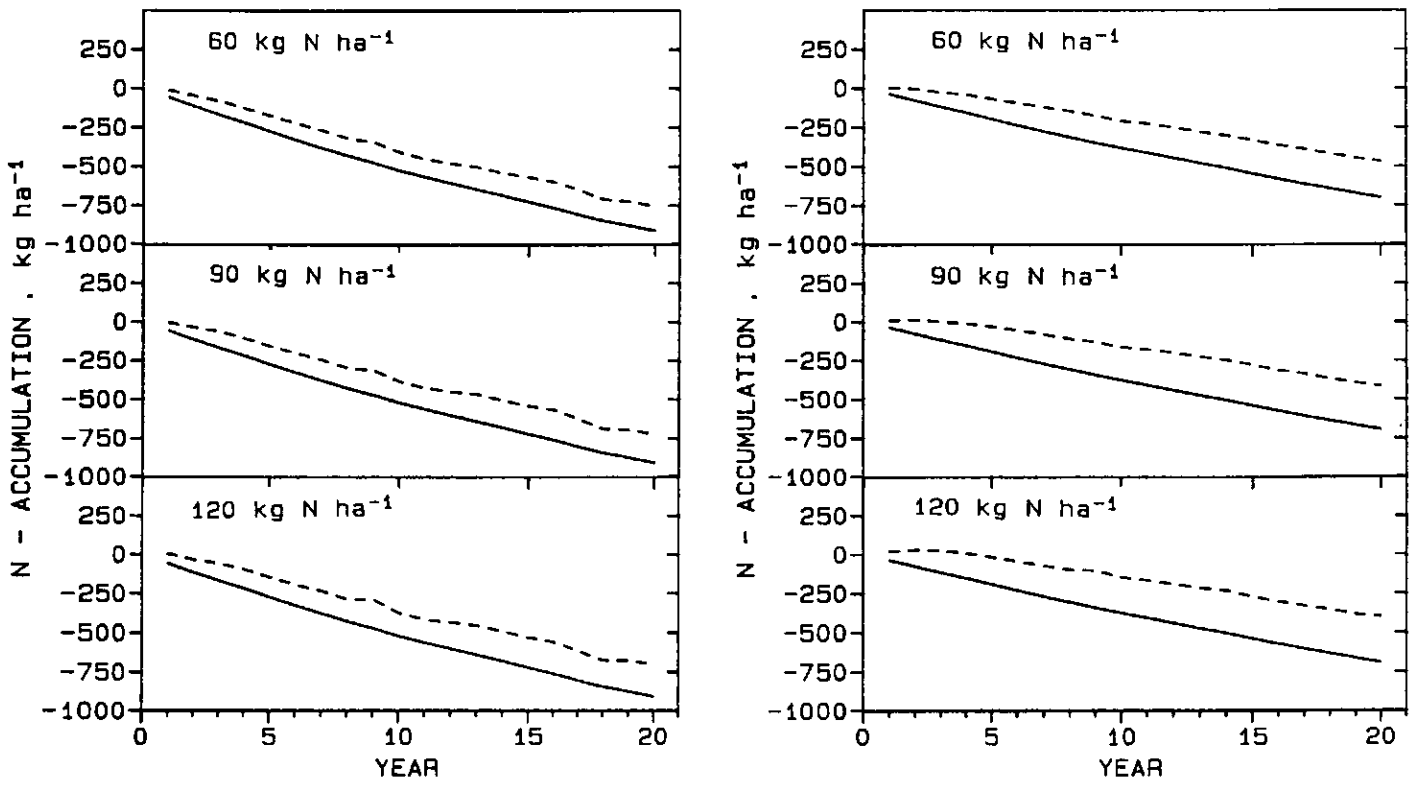

Fig. 12–2 Nitrogen accumulation during twenty consecutive years of barley crop production in Jyndevad soil (left) and Askov soil (right). Straw incorporated (dashed lines), straw removed (solid lines). Simulation period 1966–1986. Askov climate.

Table 12–1 Simulated most frequent amounts of dry matter and nitrogen added to the soil during twenty consecutive years of barley crop production on two soil types at three levels of nitrogen fertilizer application.

Fertilizer	Soil	Straw removed		Straw incorporated	
kg N ha^{-1}	JB No.	t DM ha^{-1}	kg N ha^{-1}	t DM ha^{-1}	kg N ha^{-1}
60	1	1.1	10	4.5	39
90	1	1.2	11	5.2	49
120	1	1.2	12	5.4	59
60	6	1.4	12	5.9	43
90	6	1.5	13	7.0	56
120	6	1.5	14	7.3	70

In the case of the straw being removed from the field the amounts of dry matter and nitrogen in roots and stubble added to the soil are only slightly affected by nitrogen fertilizer application, while in the case of straw incorporation the amounts of dry matter and nitrogen in straw, roots, and stubble added to the soil increase considerably with increasing nitrogen fertilizer application.

Nitrogen exhaustion

The nitrogen accumulation in the soil during twenty years is shown in Fig. 12–2 for both soils at all three levels of nitrogen fertilizer application. The solid lines represent straw removed from the field while dashed lines represent straw incorporation. In all cases the nitrogen accumulation is negative which means nitrogen exhaustion of the soils. In all cases the straw incorporation delayed the nitrogen exhaustion and most in the case of the JB 6 soil. For the JB 6 soil the average annual nitrogen exhaustion of the soil was 20 and 34 kg N ha^{-1} with straw incorporation and straw removal, respectively. These results are in good agreement with experimental results obtained by Christensen (1990). The corresponding values for the JB 1 soil were 38 and 46 kg N ha^{-1} with straw incorporation and straw removal, respectively. Nitrogen fertilizer application appeared to have only a minor effect on nitrogen exhaustion of the soil.

Net mineralization

The simulated annual values of net mineralization of nitrogen are shown in Fig. 12–3.

For both soils at all levels of nitrogen fertilizer application it appears that net mineralization in the first year after straw incorporation is highest when the straw is removed from the field which is due to an initial immobilization effect of straw incorporation.

From the second year the annual net mineralization is highest in all cases when the straw is incorporated. In the case of the JB 6 soil the annual net mineralization of nitrogen was almost doubled after 5 years of straw incorporation.

The simulated increases in net mineralization of nitrogen in the period of nitrogen uptake by the barley crop (April 1. – July 15.) due to straw incorporation are shown in Table 12–2.

For the JB 1 soil it appears that the increase in net mineralization during this particular period due to straw incorporation increases from ca. 10 kg N ha^{-1} in year 1 to about 20 kg N ha^{-1} in year 20. The corresponding values for the JB 6 soil are about 4 and about 25 kg N ha^{-1}, respectively.

The results imply that after 5 years, straw incorporation would decrease the demand of nitrogen fertilizer application with about 20 kg N in a continuous spring barley cropping system.

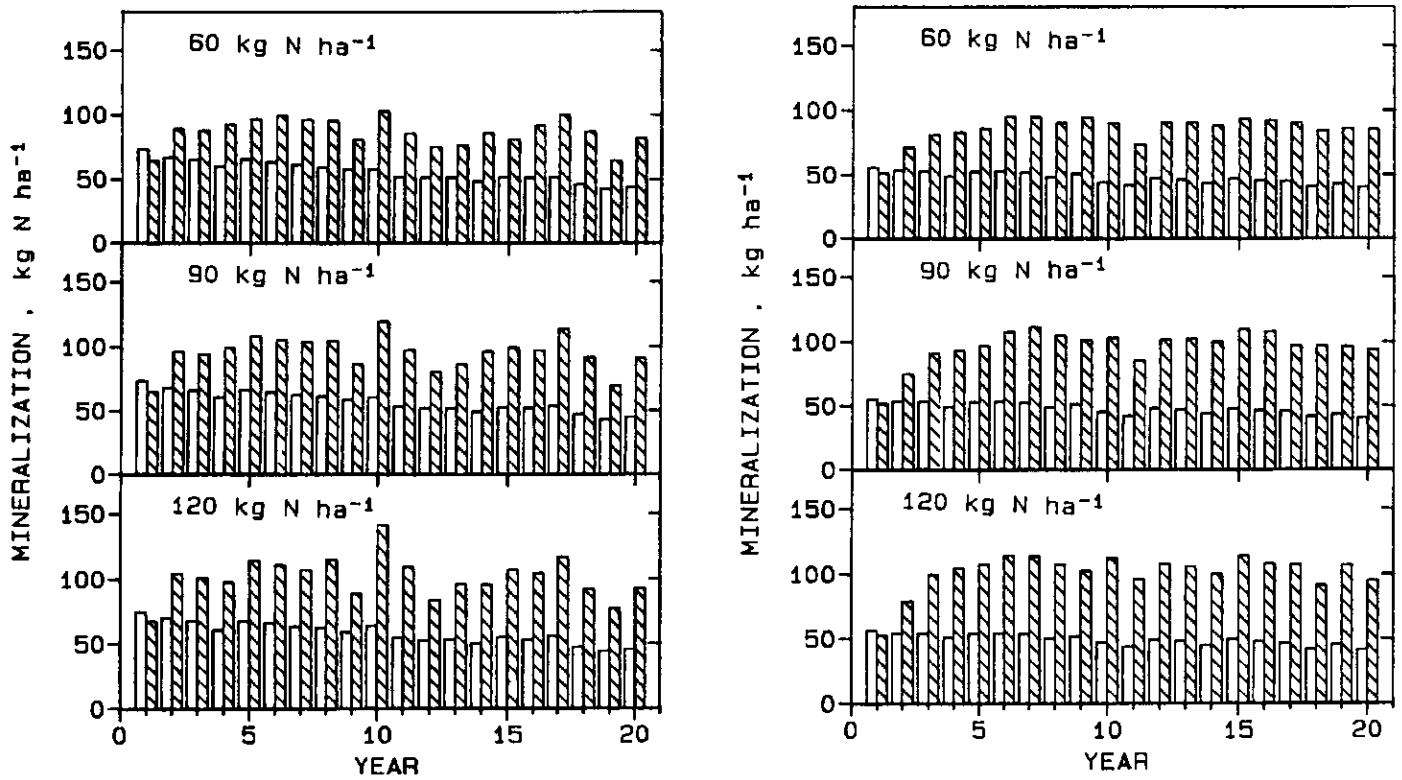

Fig. 12–3 Simulated annual values of net mineralization during twenty consecutive years of barley crop production in Jyndevad soil (left) and Askov soil (right). Straw incorporated (hatched columns), straw removed (open columns). Simulation period 1966–1986. Askov climate.

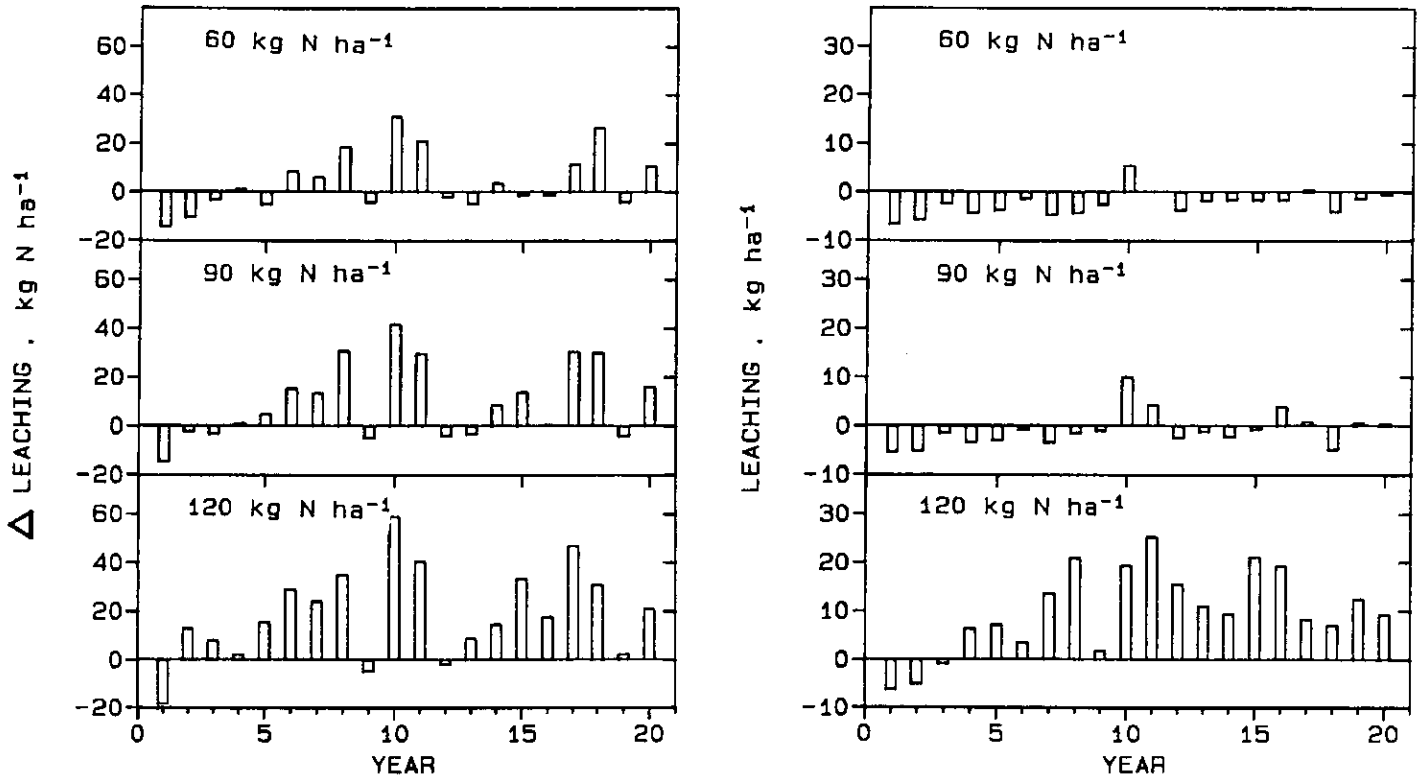

Fig. 12-4 Simulated effects of straw incorporation as compared to straw removal on nitrogen leaching during twenty consecutive years of barley crop production in Jyndevad soil (left) and Askov soil (right). Simulation period 1966-1986. Askov climate.

Table 12–2 Simulated increases in net mineralization of nitrogen, kg N ha^{-1}, in the period April 1.–July 15. due to straw incorporation during twenty years of barley crop production on two soil types at three levels of nitrogen fertilizer application.

Year No.	Soil JB No.	Nitrogen fertilizer, kg N ha^{-1} 60	90	120
Year 1	1	10	9	16
Year 2	1	15	17	17
Year 10	1	14	18	18
Year 20	1	18	22	24
Year 1	6	4	4	5
Year 2	6	10	18	24
Year 10	6	20	26	28
Year 20	6	21	25	28

Nitrogen leaching

The simulated effects of straw incorporation on leaching of nitrogen are shown in Fig. 12–4 for both soils at all three levels of nitrogen fertilizer application. It appears that leaching of nitrogen during the first year after straw incorporation may be reduced by up to 10 and 20 kg N ha^{-1} in the sandy loam (JB 6) and coarse sandy soil (JB 1), respectively, due to straw incorporation. After some years depending on soil type and level of nitrogen fertilizer application this decrease is changed to an increase in nitrogen leaching due to the increased net mineralization resulting from incorporation of straw.

Taking into consideration the implied decrease in nitrogen fertilizer demand it seems likely that a long term reduction in annual nitrogen leaching is possible by straw incorporation in particular on the sandy loam soil. For the coarse sand on which the crop production is very much dependent on precipitation in the growth season the long term effect of straw incorporation on nitrogen leaching appears to be very much dependent on actual weather conditions.

From the present simulation it may be stated that

- the soil nitrogen balance is negative in nitrogen fertilizer based long term grain crop production

- the nitrogen exhaustion of the soil is decreased by straw incorporation

- the annual net mineralization of nitrogen is increased considerably after some years of straw incorporation

- the net mineralization in the growth season is increased by up to 20 kg N ha^{-1} after some years of straw incorporation

- the nitrogen leaching during the first year after straw incorporation may by decreased by up to 20 kg N ha^{-1} as a result of straw incorporation

- depending on soil type and nitrogen fertilizer application the annual nitrogen leaching may increase after some years of straw incorporation

- taking a decrease in the demand for nitrogen fertilizer application into consideration it seems likely that a long term reduction of nitrogen leaching is possible by straw incorporation.

13. DANSK SAMMENDRAG

Formål

Formålet med det foreliggende forskningsprojekt har været at udvikle og validere en matematisk model for simulering af planteproduktion, jordvandets dynamik og kvælstoffets dynamik ved planteproduktion under forskellige kulturtekniske betingelser og strategier. Sigtet har været en omfattende dynamisk forklarende simuleringsmodel for jord plante systemet. De særlige processer, som er behandlet, vedrører transformations- og transportprocesser for vand, varme, kulstof og kvælstof. For nogle processer foreligger velkendte teorier og mekanismer, medens foreliggende viden om andre processer er begrænset. De behandlede processer er beskrevet og modelleret i overensstemmelse med eksisterende viden.

Hydrologiske processer

De behandlede hydrologiske processer i modellen omfatter sneakkumulering, interception af nedbør i afgrøden, fordampning fra jordoverfladen, infiltration, vandoptagelse i planterødder, transpiration og vertikal vandbevægelse i jordprofilen. I modellen influeres snesmeltning af indstråling, jord- og lufttemperatur. Interception er bestemt af enten nedbøren eller afgrøden. Beskrivelse af evapotranspiration er baseret på en klimatisk bestemt potentiel evapotranspiration og vandets tilgængelighed. Modellering af vandoptagelse i planterødder er baseret på en kvasi stationær løsning af differentialligningen for radiær vandstrømning til rodoverfladerne, og af rodtætheden i jordprofilen. Vertikal strømning i jordprofilen er modelleret i form af en numerisk løsning til Richards ligning.

Jordtemperatur

Jordtemperatur er modelleret ved løsning af varmestrømningsligningen, idet varmetransport ved konduktion og konvektion såvel som ændringer i varmeindhold som følge af frysning og smeltning er taget i betragtning. Frysningsprocessen inducerer vandbevægelse i jorden mod frysningszonen, idet isdannelse antages at finde sted i store porer, hvorved der ekstraheres vand fra de små porer i jorden.

Puljer af organisk stof

Omsætning af organisk stof er modelleret ved begrebsmæssig opdeling af det organiske stof i tre hovedpuljer, nemlig tilført organisk stof omfattende organisk stof i planterester og i organisk gødning, mikrobiel biomasse omfattende organisk stof i levende mikroorganismer, og organisk stof i jord omfattende ikke levende oprindeligt organisk stof i jord. Hver hovedpulje af organisk stof er underopdelt i to subpuljer, der hver især er karakteriseret ved et særskilt kulstof kvælstof forhold og en særskilt omsætningshastighed. For hver subpulje af organisk stof i jord og tilført organisk stof er kulstofomsætningen modelleret ved anvendelse af første ordens kinetik, idet hastighedskoefficienterne antages at være influeret af jordtemperatur og vandindholdet i jorden. For subpuljer af organisk stof i jord antages hastighedskoefficienterne endvidere at være influeret af lerindholdet i jorden.

Biomassens vækst og henfald

Den mikrobielle biomasse udnytter organisk stof som vækstsubstrat. Hver subpulje af mikrobiel biomasse er karakteriseret ved en vækstsubstrat udnyttelseskoefficient, en koefficient for vedligeholdelsesrespiration og en koefficient for dødsrate. Vedligeholdelsesrespiration og mikrobiel dødsrate antages at være influeret af jordtemperatur og vandindholdet i jorden, og for subpuljen af resistent mikrobiel biomasse endvidere af lerindholdet i jorden. Kulstof tabes i form af kuldioxid som følge af respirationsprocesser i den mikrobielle biomåsse.

Kvælstofmineralisering

Ved biomassens vækst og henfald translokeres kulstof mellem de forskellige subpuljer af organisk stof, hvorved uorganisk kvælstof mobiliseres eller immobiliseres afhængig af kulstof kvælstof forholdet i det organiske stof, som udnyttes som vækstsubstrat, og kulstof kvælstof forholdet i de mikroorganismer, der syntetiseres. Det samlede resultat af alle processer, hvorved organisk stof omsættes, er enten nettomineralisering af kvælstof, som kan være positiv, hvorved ammonium frigøres, eller negativ, hvorved ammonium eller nitrat immobiliseres.

Nitrification	Processer i modellen vedrørende uorganisk kvælstof omfatter nitrifikation, denitrifikation, kvælstofoptagelse i planterødder og vertikal transport i jordprofilen. Nitrifikation simuleres ved anvendelse af første ordens kinetik, idet hastighedskoefficienten antages at være influeret af jordtemperatur og vandindholdet i jorden.
Denitrification	Denitrifikation simuleres ved at definere en potentiel denitrifikationshastighed, der antages at være relateret til frigivelseshastigheden af kuldioxid og jordtemperaturen. Den potentielle denitrifikationshastighed reduceres i henhold til jordens oxygen status udtrykt som en funktion af jordens vandindhold. Den aktuelle denitrifikationshastighed er bestemt ved enten den reducerede potentielle denitrifikationshastighed eller den hastighed, hvormed nitrat er tilgængelig for denitrifikation.
Kvælstofoptagelse	Modellen for kvælstofoptagelse er begrebsmæssigt baseret på et potentielt kvælstofbehov for afgrøden, som simuleres i afgrødemodellen, og tilgængeligheden af kvælstof i jorden for optagelse i planterne. Modellen for kvælstofoptagelse i planter er aktuelt baseret på en kvasi stationær løsning af differentialligningen for diffusiv og konvektiv radiær transport af kvælstof til overfladen af planterødderne, og rodtætheden i jordprofilen. Planterne antages at optage ammonium præferentielt i forhold til nitrat.
Kvælstoftransport	Mobiliteten af ammonium i jorden antages at være mindre end mobiliteten af nitrat, hvilket skyldes adsorption af ammonium til jordkolloiderne, som beskrives ved en adsorptions desorptions isoterm. Den vertikale transport af kvælstof er modelleret i form af en numerisk løsning til konvektions dispersionsligningen for såvel ammonium som nitrat. Source sink termen i konvektions dispersionsligningen integrerer transformationsprocesser for såvel ammonium som for nitrat.

Topudvikling

Afgrødemodellen er begrebsmæssigt baseret på at afgrødens fysiologiske alder, der beskrives som afgrødens termiske alder i form af en temperatursum. Afgrødens overjordiske del beskrives ved total afgrøde areal index og grøn afgrødeareal index, der simuleres som funktioner af afgrødens termiske alder og mængden af akkumuleret top tørstof.

Rodudvikling

Rodnedtrængningshastigheden i jorden simuleres som en funktion af jordtemperaturen ved rodspidsen, medens rodtætheden simuleres som en funktion af mængden af akkumuleret rodtørstof og roddybden.

Planteproduktion

Simulering af planteproduktion er baseret på beregning af brutto fotosyntese i afgrødens top og fordeling af assimilater til afgrødens forskellige dele. Bruttofotosyntese er bestemt af mængden af fotosynteseaktiv stråling absorberet i afgrøden og den effektivitet, hvormed absorberet stråling konverteres til kulhydrater. Fordeling af assimilater fra bruttofotosyntesen mellem afgrødens dele, i.e. top, rødder og for nogle afgrøder oplagsorganer, simuleres som en funktion af afgrødens termiske alder. Respiration omfatter vækstrespiration og en temperaturafhængig vedligeholdelsesrespiration.

Produktionsniveauer

Bruttofotosyntesen i afgrødens top kan være begrænset af vand- eller kvælstofmangel. I tilfælde af vandmangel reduceres bruttofotosyntesen med forholdet mellem aktuel og potentiel evapotranspiration. Ved høj og ekstrem lav kvælstofforsyning antages kvælstofkoncentrationen i tørstoffet at nå henholdsvis en øvre og en nedre grænseværdi, der i begge tilfælde er afhængig af afgrødens termiske alder. Mellem disse grænseværdier eksisterer en kvælstofkoncentration i tørstoffet, der også afhænger af afgrødens termiske alder, hvor kvælstofforsyningen netop er tilstrækkelig. Begrænsningen af bruttofotosyntesen som følge af kvælstofmangel antages at være proportional med afvigelsen af den aktuelle kvælstofkoncentration i tørstoffet fra den kvælstofkoncentration i tørstoffet, hvor kvælstofforsyningen netop er tilstrækkelig.

Management strategier	Modellen for management tillader forskellige kulturtekniske metoder og strategier, herunder forskellig jordbehandling, såning, gødskning, vanding og afgrødehøst.
Drivvariable	Meteorologiske variable, der kræves for at anvende modellen, omfatter daglige værdier af globalstråling, lufttemperatur og nedbør. Derudover er et antal parametre nødvendige for karakterisering af systemet.
Modelvalidering	Modelvalidering har inkluderet eksperimentelle data for jordens vandindhold, koncentation af nitrat i jord, koncentration af ammonium i jord, afgrødeudbytte, kvælstof i toptørstof, denitrifikation og kvælstofudvaskning fra jorden. Det konkluderes at modellens præstation som hedhed er tilfredsstillende, omend nogle justeringer kan vise sig at være nødvendige.
Modelanvendelse	Der er givet eksempel på prædiktiv anvendelse af modellen i form af simulering af effekten af halmnedmulding igennem tyve år. Før ekstensiv prædiktiv anvendelse af modellen vil yderligere validering omfattende flere kombinationer af jord, afgrøde, klima og management være nyttig.

14. REFERENCES

Addiscott, T.M. (1983): Kinetics and temperature relationships of mineralization and nitrification in Rothamsted soils with different histories. J. Soil Science 34, 343-353.

Alexander, L. and R.W. Skaggs (1986): Predicting unsaturated hydraulic conductivity from the soil water characteristic. Trans. Amer. Soc. Agric. Eng. 29, 176-184.

Anderson, D.W. (1979): Processes of humus formation and transformation in soils of the Canadian Great Plains. J. Soil Sci. 30: 77-84.

Aslyng, H.C. and S. Hansen (1982): Water balance and crop production simulation. Model WATCROS for local and regional application. The Royal Veterinary and Agricultural University, Copenhagen 1982.

Aslyng, H.C. and S. Hansen (1985): Radiation, water and nitrogen balance in crop production. Field experiments and simulation models. The Royal Veterinary and Agricultural University, Copenhagen 1985.

Berry, J.A. and J.K. Raison (1981): Response of macrophytes to temperature. Encyclopedia of Plant Physiology, New Series Volume 12 A. Springer Verlag, 1981.

Burger, H.C. (1919): Das Leitvermögen verdünter mischkristallfreier Legirungen. Physikalische Zeitscrift 20, 73–75.

Butland, J. (1980): A review of methods for curve and function drawings (K.W. Brodlie). In: Mathematical methods in computer graphics and design. Academic Press 1980.

Cambell, C.A., R.J.K. Meyers and K.L. Weier (1981): Potential mineralizable nitrogen, decomposition rates and their relationships to temperature for five Quensland soils. Austr. J. Soil Res. 19, 323-332.

Childs, E.C. and N. Collis-George (1950): The permeability of porous materials. Proc. Royal Soc. London, Series A 201, 392-405.

Christensen, B.T. (1990): Sædskiftets indflydelse på jordens indhold af organisk stof. II. Markforsøg på grov sandblandet lerjord (JB 5), 1956-1985. Tidsskrift for Planteavl 94, 161-169.

Corps of Engineers (1956): Snow hydrology. North Pacific Division, U.S. Army Corps of Engineers, Portland, Oregon, U.S.A.

Dexter, A.R. (1988): Advances in characterization of soil structure. Soil and Tillage Research 11, 199-238.

Emerson, E.W. (1959): The structure of soil crumbs. J. Soil Sci. 10, 235.

Fillery, I.R.P. (1983): Biological denitrification. In: Gaseous loss of nitrogen from plant-soil systems. Martinus Nijhoff/Dr W. Junk Publishers. The Hague.

Flowers, H. and J.R. O'Callaghan (1983): Nitrification in soils incubated with pig slurry or ammonium sulphate. Soil Biol. Biochem. 15, 337-342.

Focht, D.D. and W. Verstraete (1977): Biochemical ecology of nitrification and denitrification. In: Advances in Microbiol Ecology, vol. 1. Plenum Press, New York.

Gerwitz, S. and E.R. Page (1974): An empirical mathematical model to describe plant root systems. J. Appl. Ecol. 11, 773-781.

Godwin, R.J. and G. Spoor (1977): Soil factors influencing workdays. The Agric. Eng. 32, 87-92.

Goudrian, J. and H.H. van Laar (1978): Calculation of daily totals of the gross CO_2 assimilation of leaf canopies. Neth. J. Agric. Sci. 26, 373 – 382.

Greenwood, D.J. (1986): Prediction of nitrogen fertilizer needs of arable crops. In: Advances in Plant Nutrition 1B. Prager Sci. Pub.

Grundahl, L. and J. Grønbeck Hansen (1990): Atmosfærisk nedfald af næringssalte i Danmark. NPO-forskning fra Miljøstyrelsen. Rapport Nr. A6, 1990.

Hansen, G.K. (1986): Hejmdal. Analyser og simulering af afgrøders vækst, vand- og kvælstofbalance. Disputats. Den Kgl. Veterinær- og Landbohøjskole, København.

Hansen, S. and H.C. Aslyng (1984): Nitrogen balance in crop production. Simulation model NITCROS. The Royal Veterinary and Agricultural University, Copenhagen 1984.

Hansen, S., S.E. Jensen og H.C. Aslyng (1981): Jordbrugsmeteorologiske observationer, statistisk analyse og vurdering 1955 – 1979. Hydroteknisk Laboratorium, Den Kgl. Veterinær- og Landbohøjskole, København 1981.

Hansen, S., B. Storm and H.E. Jensen (1986): Spatial variability of soil physical properties. Theoretical and experimental analysis. I. Soil sampling, experimental analysis and basic statistics of soil physical properties. Research Report No. 1201. Department of Soil and Water and Plant Nutrition. The Royal Veterinary and Agricultural University, Copenhagen.

Harris, R.F, G. Chester and O.N. Allen (1965): Dynamics of soil aggregation. Adv. Agron. 18, 107-160.

Heemst, H.D.J. van (1986): The distribution of dry matter during growth of a potato crop. Potato Research 29, 55–66.

Hopmans, J.W. and J.H. Dane (1986): Thermal conductivity of two porous media as a function of water content temperature, and density. Soil Sci. 142, 187-195.

Jakobsen, B.F. (1976): Jord, rodvækst og stofoptagelse. In: Simuleret planteproduktion. Hydroteknisk Laboratorium, Den Kgl. Veterinær- og Landbohøjskole, København.

Jansson, P.-E. and S. Halldin (1980): Soil water and heat model. Technical description. Technical Report 26, 1980. Swedish Coniferous Forest Project. Dept. of Ecology and Environment Research. Swedish University of Agricultural Sciences, Uppsala, Sweden.

Jenkinson, D.S. (1981): The fate of plant and animal residues in soil. In: The chemistry of Soil Processes. John Wiley and Sons, Ltd.

Jenkinson, D.S. and J.H. Rayner (1977): The turnover of soil organic matter in some of the Rothamsted classical experiments. Soil Sci. 123, 298-305.

Jenkinson, D.S., P.B.S. Hart, J.H. Rayner and L.C. Parry (1987): Modelling the turnover of organic matter in long-term experiments at Rothamsted. Intecol Bulletin 15, 1–18.

Jensen, H.E. (1980): Afgrødeproduktion og -kvalitet, lysenergi- og vandudnyttelse, nitrogenbalance og -transport i relation til nitrogen- og vandstatus. Eksperimentale studier med lolium perenne. Doktordisputats. D.S.R. Forlag, København, 1980.

Jensen, J. (1962): Undersøgelser over nedbørens indhold af plantenæringsstoffer. Tidsskrift for Planteavl 65, 894–906.

Jensen, K.H. (1983): Simulation of water flow in the unsaturated zone including the root zone. Series Paper No. 33. Institute of Hydrodynamics and Hydraulic Engineering, Technical University of Denmark.

Jensen, O. (1988a): Kvælstof i jord–plante–systemet. Denitrification i jord – et litteraturstudium. Rapport Nr. 1204. Institut for Kulturteknik og Planteernæring. Den Kgl. Veterinær- og Landbohøjskole, København 1988.

Jensen, O. (1988b): Kvælstof i jord–plante–systemet. Kulstof– og kvælstof omsætning ved nedbrydning af plantemateriale og husdyrgødning i jord – et litteraturstudium. Rapport Nr. 1206. Institut for Kulturteknik og Planteernæring, Den Kgl. Veterinær- og Landbohøjskole, København 1988.

Jensen, O. (1988c): Kvælstof i jord–plante–systemet. Abiotiske faktorer – et litteraturstudium. Rapport Nr. 1207. Institut for Kulturteknik og Planteernæring, Den Kgl. Veterinær- og Landbohøjskole, København 1988.

Jensen, O. (1988d): Kvælstof i jord – plante – systemet. Respiration og assimilat fordeling i planter – et litteraturstudium. Rapport Nr. 1211. Institut for Kulturteknik og Planteernæring, Den Kgl. Veterinær- og Landbohøjskole, København 1988.

Jensen, S.E. (1979): Model ETFOREST for calculating actual evapotranspiration. In: Comparison of forest water and energy exchange models. Proc. IUFRO (Int. Un. Forestry Res. Org.) Workshop, Uppsala 1978. Publ. Int. Soc. for Ecol. Modelling, Copenhagen 1979, 165-172.

Josefsen, A.B. (1979): Vandpotential og -balance, afgrødeproduktion og kvalitet reguleret af vandforsyning ved forskelligt udviklingstrin af kartoffel. Licentialtafhandling. Den Kgl. Veterinær- og Landbohøjskole, 1979.

Jørgensen, V. (1979): Luftens og nedbørens kemiske sammensætning i danske landområder. Tidsskrift for Planteavl 82, 633 – 656.

Kempner, W. (1937): The effect of oxygen tensions on cellular metabolism. J. Cellular and Comp. Physiol. 10, 339-363.

Keulen, H. van and N.G. Seligman (1987): Simulation of water use, nitrogen nutrition and growth of a spring wheat crop. Pudoc, Wageningen.

Kimball, B.A., R.D. Jackson, R.J. Reginato, F.S. Nakayama and S.B. Idso (1976): Comparison of field-measured and calculated soil-heat fluxes. Soil Sci. Soc. Amer. J. 40, 18-24.

Knowles, R. (1978): Common intermediates of nitrification and denitrification, and the metabolism of nitrous oxides. In: Microbiology. Amer. Soc. Microbiol., Washington D.C.

Kunze, R.J., G. Uehara and K. Graham (1968): Factors important in the calculation of hydraulic conductivity. Soil Sci. Soc. Amer. Proc. 32, 760-765.

Lind, A.-M. (1980): Denitrification in the root zone. Tidsskrift for Planteavl 84, 101-110.

Lind, A.-M., K. Debosz, J. Djurhuus og M. Maag (1990): Kvælstofomsætning og -transport i to dyrkede jorde. NPO-forskning fra Miljøstyrelsen. Rapport Nr. A9, 1990.

Madsen, H.B. (1978): Bygs rodudvikling i relation til fysiske parametre i naturligt lejret jord. Tidsskrift for Planteavl 82, 335-342.

Madsen, H.B. (1983): Himmerlands jordbundsforhold. Et regionalt studie omhandlende jordbundsudvikling, -klassifikation, afgrøders rodudvikling og jordens plantetilgængelige vandmængde. Disputats. C.A. Reitzels Forlag, København.

McCree, K.J. (1974): Equation for the rate of dark respiration of white clover and grain sorghum, as a function of dry weight, photosynthesis rate and temperature. Crop Science 14, 509-514.

Makkink, G.F. (1957): Ekzameno de la formula de Penman. Neth. J. Agric. Sci. 5, 290-305

Marshall, T.J. (1958): A relationship between permeability and size distribution of pores. J. Soil Sci. 9, 1-8.

Miller, R.D. (1980): Freezing phenomena in soils. In: Application of soil physics. Academic Press 1980.

Miller, R.D. and D.D. Johnson (1964): The effect of soil moisture tension on carbon dioxide evolution, nitrification and nitrogen mineralization. Soil Sci. Soc. Amer. Proc. 24, 644-647.

Millington, R.J. and J.P. Quirk (1960): Transport in porous media. Int. Congr. Soil Sci. Trans. 7th (Madison, Wisconsin), 3, 97-106.

Mogensen, V.O. (1969): Varmeledningsevne i jorden og kalibreringsfaktorer for heat flux metre på Klimastationen. Hydroteknisk Laboratorium. Den Kgl. Veterinær- og Landbohøjskole, København 1969.

Nicholas, D.J.D. (1978): Intermediary metabolism of nitrifying bacteria, with particular reference to nitrogen, carbon, and sulphur compounds. In: Microbiology. Amer. Soc. Microbiol. Washington D.C.

Nielsen, H. (1988): Kvælstof i jord – plante-systemet. Omsætning af organisk stof i jord – et litteraturstudium. Rapport Nr. 1205. Institut for Kulturteknik og Planteernæring, Den Kgl. Veterinær- og Landbohøjskole, København 1988.

Nielsen, N.E. (1980a): Forløbet af rodudvikling, næringsstofoptagelse og stofproduktion hos byg, dyrket ved moderat mangel på phosphor og kalium. Meddelelse Nr. 1180. Afd. for Planternes Ernæring, Den Kgl. Veterinær- og Landbohøjskole, København 1980.

Nielsen, N.E. (1980b): Forløbet af rodudvikling, næringsstofoptagelse og stofproduktion hos byg, dyrket på frugtpart morænejord. Meddelelse Nr. 1119. Afd. for Planternes Ernæring, Den Kgl. Veterinær- og Landbohøjskole, København, 1980.

Nielsen, N.E. and H.E. Jensen (1990): Nitrate leaching from loamy soils as affected by crop rotation and nitrogen fertilizer application. Fertilizer Research, 1990 (In print).

Nielsen, N.E., Schjørring, J.K. and Jensen, H.E. (1988): Efficiency of fertilizer nitrogen uptake by spring barley. In: Nitrogen efficiency in agricultural soils. Elsevier Applied Science, London.

Nordmeyer, H. and J. Richter (1985): Incubation experiments on nitrogen mineralization in loess and sandy soils. Plant and Soil 83, 433–445.

Nørlund, T., A. Gottschau, K. Thorhauge, N.E. Nielsen, and H.E. Jensen (1985): The dynamics of nitrogen under field grown spring barley as affected by nitrogen application, irrigation and undersown catch crops, Dept. of Soil and Water and Plant Nutrition. Report No. 1129, Department of Soil and Water and Plant Nutrition. The Royal Veterinary and Agricultural University, Copenhagen.

Olesen, J. (1990): Personal communication.

Orchard, V.A. and F.J. Cook (1983): Relationships between soil respiration and soil moisture. Soil Biol. Biochem. 15, 447–453.

Parr, J.F. and H.W. Reuszer (1959): Organic matter decomposition as influenced by oxygen level and method of application to soil. Soil Sci. Soc. Amer. Proc. 23, 214-216.

Penman, H.L. (1948): Natural evaporation from open water, bare soil and grass. Proc. Royal Soc. A 193, 120–146.

Penning de Vries, F.W.T. (1975): The cost of maintenance processes in plant cells. Annals of Botany 39, 77–92.

Penning de Vries, F.W.T. (1983): Modelling of growth and production. In: Encyclopedia of Plant Physiology. New Series Volume 12 D. Springer Verlag, 1983.

Penning de Vries, F.W.T., D.M. Jansen, H.F.M. ten Berge and A Bakema (1989): Simulation of ecophysiological processes of growth in several annual crops. Pudoc Wageningen, 1989.

Penning de Vries, F.W.T. and H.H. van Laar (Eds) (1982): Simulation of plant growth and crop production, Puduc, Wageningen, 1982.

Penning de Vries, F.W.T., H.H. van Laar and M.C.M Chardon (1983): Bioenergetics of growth of seeds, fruits and storage organs. In: Potential productivity of field crops under different environments. International Rice Research Institute, Los Banos, pp., 38 – 59.

Penning de Vries, F.W.T., J.M. Witlage and D. Kremer (1979: Rates of respiration and increase in structural dry matter in young wheat, ryegrass and maize plants in relation to temperature, to water stress and to their sugar content. Annals of Botany 44, 595 – 609.

Rab, A., H.E. Jensen and V.O. Mogensen (1984): Dry matter production of spring wheat subjected to water stress at various growth stages. Cereal Research Communications vol. 12 No. 1 – 2.

Rasche, K. (1979): Movements of stomata. In: Encyclopedia of Plant Physiology, New Series, Volume 6. Springer Verlag, 1979.

Reichman G.A., D.L. Grunes and F.G. Viets (1966): Effect of soil moisture on ammonification and nitrification in two northern plain soils. Soil Sci. Soc. Amer. Proc. 30, 363-366.

Richard, L.A. (1931): Capillary conductivity of liquids in porous mediums. Physics 1, 318-333.

Rolston, D.E., P.S.C. Rao, J.M. Davidson and R.E. Jessup (1984): Simulation of denitrification losses of nitrate fertilizer applied to uncropped, cropped and manure-amended field plots. Soil Science 13, 270-279.

Sabey, B.R. (1969): Influence of soil moisture tension on nitrate accumulation in soils. Soil Sci. Soc. Amer. Proc. 33, 263-266.

Schjørring, J.K. Nørlund, T., Gottschau, A., Nielsen, N.E. and Jensen, H.E. (1988a): The dynamics of nitrogen in the root zone of field grown spring barley as affected by nitrogen application, irrigation, and undersown catch crops. Experimental results 1983. - Research Report No. 1208, Department of Soil and Water and Plant Nutrition. The Royal Veterinary and Agricultural University, Copenhagen.

Schjørring, J.K. Nørlund, T., Gottschau, A., Nielsen, N.E. and Jensen, H.E. (1988b): The dynamics of nitrogen in the root zone of field grown spring barley as affected by nitrogen application, irrigation, and undersown catch crops. Experimental results 1984. - Research Report No. 1213, Department of Soil and Water and Plant Nutrition. The Royal Veterinary and Agricultural University, Copenhagen.

Schouwenburg, J. Ch. van and A.C. Schuffelen (1963): Potassium-exchange behaviour of an illite. Neth. J. Agric. Sci. 11, 13-22.

Schulze, E.-D. and A.E. Hall (1982): Stomatal responses, water loss and CO_2 assimilation rates of plants in contrasting environments. In: Encyclopedia of Plant Physiology. New Series Volume 12 B. Springer Verlag, 1982.

Sepaskhah, A.R. and L. Boersma (1979): Thermal conductivity of soils as function of temperature and water content. Soil Sci. Soc. Am. J. 43, 439-443.

Stanford, G., M.H. Frere and D.H. Schwaninger (1973): Temperature coefficient of soil nitrogen mineralization. Soil Science 115, 321-323.

Stanford, G. and E. Epstein (1974): Nitrogen mineralization – water relations in soils. Soil Sci. Soc. Amer. Proc. 38, 103-107.

Stott, D.E., L.F. Elliot, R.I. Papendick and G.S. Campbell (1986): Low temperature or low water potential effects on the microbial decomposition of wheat residue. Soil Biol. Biochem. 18, 577-582.

Sørensen, L.H. (1975): The influence of clay on the rate of decay of amino acid metabolites synthesized in soils during decomposition of cellulose. Soil Biol. Biochem. 7: 171-177.

Tyler, K.B., F.E. Broadbent and G.N. Hill (1959): Low-temperature effects on nitrification in four California soils. Soil Science 87, 123-129.

Veen, J.A. van and E.A. Paul (1981): Organic carbon dynamics
in grassland soils. 1. Background information and computer simulation. Can. J. Soil Sci. 61, 185-201.

Veen, J.A. van, J.N. Lodd and M.J. Frissel (1984): Modelling C and N turnover through the microbial biomass in soil. Plant and Soil 76: 257-274.

Veen, J.A. van, J.N. Lodd and M. Amato (1985): The turnover of carbon nitrogen through the microbial biomass in a sandy loam and a clay soil incubated with C^{14}-Glucose and ^{15}N-$(NH_4)_2$ SO_4 under different moisture regimes. Soil Biol. Biochem. 17: 747-756.

Vries, D.A. de (1952): The thermal conductivity of soil. Mededelingen van Landbouwhogeschool, Wageningen, 52, 1-73.

Vries, D.A. de (1963): Thermal properties of soils. In: Physics of plant environment. North-Holland Publishing Co., Amsterdam.

Wit, C.T. de (1959): Potential photosynthesis of crop surfaces. Neth. J. Agric. Res. 7, 141 – 149

Wit, C.T. de (1965): Photosynthesis of leaf canopies. Agric. Res. Rep. 663, Pudoc, Wageningen, 57 p.

Wit, C.T. de (1982): Simulation of living systems. In: Simulation of plant growth and crop production. Pudoc Wageningen, 1982.

Data Sheet

Publisher: Ministry of the Environment, National Agency of Environmental Protection, Strandgade 29, DK-1401 København K.

Serial title and no.: NPo-forskning fra Miljøstyrelsen, A10

Year of publication: 1990

Title:
DAISY - Soil Plant Atmosphere System Model

Subtitle:

Author(s):
Hansen, Søren; Jensen, Henry E.; Nielsen, Niels Erik; Svendsen, Henrik

Performing organization(s):
Section of Soil, Water and Plant Nutrition, Department of Agricultural Sciences, Royal Veterinary and Agricultural University, Thorvaldsensvej 40, DK-1871 Frederiksberg C

Abstract:
DAISY is a dynamic soil plant system simulation model. Modelled processes include transformation and transport of water, heat, carbon, and nitrogen. Model predictions include yield, nitrogen uptake, and evapotranspiration for a number of agricultural crops, mineralization and immobilization, nitrification and denitrification, and nitrogen leaching from the root zone. The model allows for various management practices. Validation against some experimental data showed satisfactory results.

Terms:
crops; nitrification; denitrification; leaching; transformation; hydrology: biomass; temperature; soil; mathematical models; nitrogen CAS 7727-37-9

ISBN: 87-503-8790-1

ISSN:

Price: (incl. 22 % VAT): 250 DKK

Format: AS5

Number of pages: 272 p.

Edition closed (month/year): October 1990

Circulation: 550

Supplementary notes:
Report from coordination group A for soil and air

Printed by: Luna-Tryk ApS, Copenhagen

Registreringsblad

Udgiver: Miljøstyrelsen, Strandgade 29, 1401 København K.

Serietitel, nr.: NPo-forskning fra Miljøstyrelsen, A10

Udgivelsesår: 1990

Titel:
DAISY – Soil Plant Atmosphere System Model

Undertitel:

Forfatter(e):
Hansen, Søren; Jensen, Henry E.; Nielsen, Niels Erik;
Svendsen, Henrik

Udførende institution(er):
Kongelige Veterinær- og Landbohøjskole. Sektion for
Kulturteknik og Planteernæring

Resumè:
DAISY er en dynamisk simuleringsmodel af jord-plantesystemet. Procesbeskrivelsen omfatter transformation og transport af vand, varme, kulstof og kvælstof i systemet. Modellen simulerer udbytte, kvælstofoptagelse og evapotranspiration for et antal landbrugsafgrøder samt mineralisering-immobilisering, nitrifikation, denitrifikation og kvælstofudvaskning fra rodzonen. Modellen kan simulere forskellige jordbrugssystemer. Modellen er valideret mod eksperimentelle data.

Emneord:
afgrøder; nitrifikation; denitrifikation; udvaskning; omsætning; hydrologi; biomasse; temperatur; jord; matematiske modeller; nitrogen CAS 7727-37-9

ISBN: 87-503-8790-1

ISSN:

Pris: 190,- **(inkl. 22 % moms)**

Format: AS5

Sideantal: 272 s.

Md./år for redaktionens afslutning: oktober 1990

Oplag: 550

Andre oplysninger:
Rapport fra koordinationsgruppe A for jord og luft

Tryk: Luna-Tryk ApS, København

NPo-forskning fra Miljøstyrelsen

Rapporter fra koordinationsgruppe A for jord og luft

Nr. A 1 : Kvælstof- og fosforbalancer ved kvæg- og svinehold
Nr. A 2 : Kortlægning af landbrugsdriften i to områder i Danmark
Nr. A 3 : Temperatur og denitrifikation
Nr. A 4 : Ammoniakafsætning omkring et landbrug med malkekvæg
Nr. A 5 : Ammoniakmonitering
Nr. A 6 : Atmosfærisk nedfald af næringssalte i Danmark
Nr. A 7 : NH_3-fordampning fra handels- og husdyrgødning
Nr. A 8 : Næringsstofudvaskning fra arealer i landbrugsdrift
* Nr. A 9 : Kvælstofomsætning og -transport i to dyrkede jorder
Nr. A10 : DAISY – Soil Plant Atmosphere System Model
Nr. A11 : Bestemmelse af NH_3-fordampning med passive fluxmålere
* Nr. A12 : NH_3-fordampning fra gyllebeholdere
* Nr. A13 : Næringsstofomsætning i marginaliseret landbrugsjord
* Nr. A14 : Regionale beregninger af N-udvaskningen
* Nr. A15 : Ammoniakfordampning fra bygplanter
* Nr. A16 : Den mikrobielle biomasses variation i jordbunden
* Nr. A17 : Analyse af jordvands sammensætning - metodesammenligning
* Nr. A18 : Atmosfærisk ammoniak og ammonium i Danmark
* Nr. A19 : N-transformation in Soil, Amended with Digested Pig Slurry
* Nr. A20 : Simulering af kvælstoftab med SOIL-N-modellen
* Nr. A21 : Landbrugets gødnings- og arealanvendelse i 1983 og 1989

De med * mærkede titler er ikke trykt på udgivelsesdagen for denne rapport, men forventes trykt i løbet af 1990.

Nr. A19 er tidligere annonceret med titlen:
Afgasset gylles indflydelse på N-omsætning i jorden.

DAISY - Soil Plant Atmosphere System Model

DAISY is a dynamic soil plant system simulation model. Modelled processes include transformation and transport of water, heat, carbon, and nitrogen. Model predictions include yield, nitrogen uptake, and evapotranspiration for a number of agricultural crops, mineralization and immobilization, nitrification and denitrification, and nitrogen leaching from the root zone. The model allows for various management practices. Validation against some experimental data showed satisfactory results.

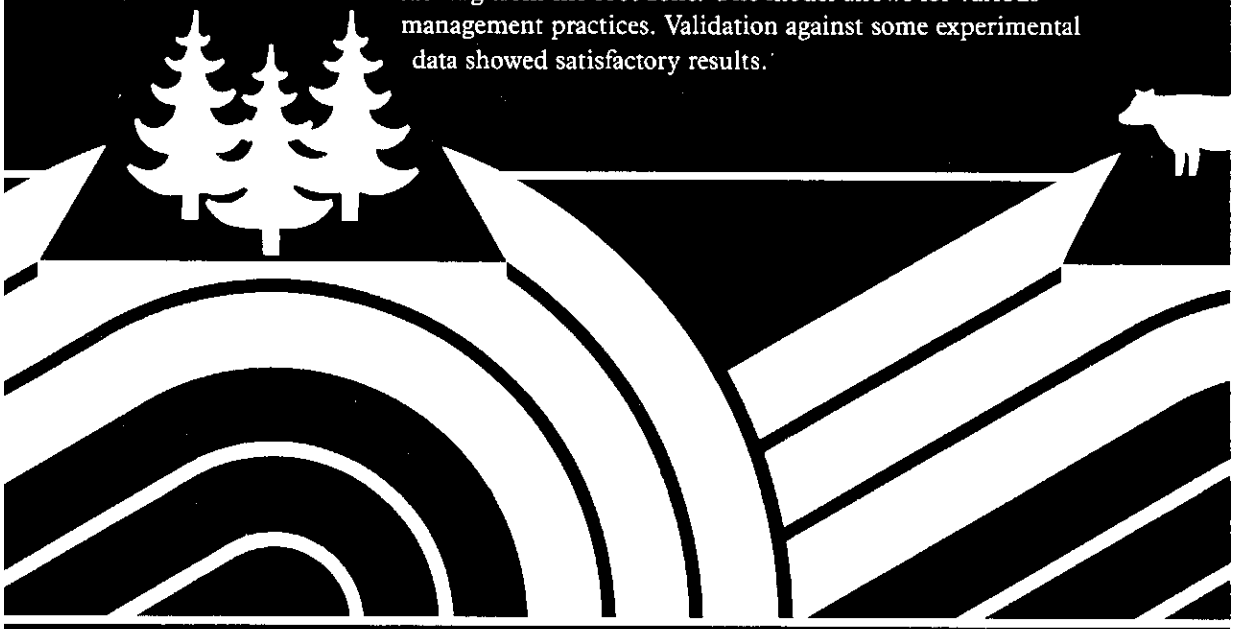

Miljøministeriet **Miljøstyrelsen**

Strandgade 29, 1401 København K, tlf. 31 57 83 10

Pris kr. 190.- inkl. 22% moms

ISBN nr. 87-503-8790-1